SPECTRAL STUDIES ON GROUP VIB METAL CHALCOCARBONYLS

Ann Marie English

A Thesis Submitted to the Faculty of
Graduate Studies and Research at
McGill University in Partial Fulfillment
of the Requirements for the
Degree of Doctor of Philosophy

From the Inorganic Chemistry Laboratory
under the Supervision of
Dr. I.S. Butler

McGill University
Montreal, P.Q.

October, 1979

SPECTRAL STUDIES ON GROUP VIB METAL CHALCOCARBONYLS

Ph.D. Chemistry Department

Ann Marie English

ABSTRACT

Reaction of $BzCr(CO)_2(CX)$ ($Bz = \eta^6-C_6H_6$; X = S,Se) with CO under pressure affords $Cr(CO)_5(CX)$ in high yield. The selenocarbonyl complexes are among the first examples of complexes containing metal-CSe linkages ever to be prepared. The new ^{13}C-labelled complexes, $BzCr(^{13}CO)_3$, $BzCr(^{13}CO)_2(CX)$, $Cr(^{13}CO)_5(CX)$ and $Cr(CO)_5(^{13}CS)$, have been synthesized and their vibrational spectra, as well as those of the unlabelled and perdeuterated species, have been analyzed in detail. The proposed assignments have been verified by normal coordinate calculations employing compliance constants. Similar calculations have been performed for $W(CO)_5(CS)$ and trans-$W(CO)_4(^{13}CO)(CS)$. The trends observed in certain of the potential constants have been rationalized in terms of the different bonding behaviour of the CO, CS and CSe ligands. These studies show definitively that interaction constants can be transferred between complexes of similar geometries. A comparison of the CX general quadratic (F) and energy-factored force constants reveals that the latter are an increasingly poor approximation for F as X descends the chalcogen group. Finally, photoelectron spectra have been obtained for $Cr(CO)_5(CSe)$ and $BzCr(CO)_2(CX)$, and the results substantiate the bonding trends predicted for the CX ligands on the basis of the vibrational analyses.

SPECTRAL STUDIES ON GROUP VIB METAL CHALCOCARBONYLS

Ph.D. Département de Chimie

Ann Marie English

RESUME

La réaction de $BzCr(CO)_2(CX)$ ($Bz = \eta^6-C_6H_6$; X = S,Se) sous pression de CO donne $Cr(CO)_5(CX)$ avec un bon rendement. Les complexes sélénocarbonylés sont parmi les premiers contenant des liaisons métal-CSe qui aient jamais été préparés. Les nouveaux dérivés isotopiques, marqués au ^{13}C, $BzCr(^{13}CO)_3$, $BzCr(^{13}CO)_2(CX)$, $Cr(^{13}CO)_5(CX)$ et $Cr(CO)_5(^{13}CS)$ ont été synthétisés. Des analyses détaillées des spectres de vibration de ces complexes, ainsi que des complexes non marqués et des dérivés deutériés, ont été effectuées. L'attribution des fréquences observées a été vérifiée par analyse en coordonnées normales, en employant des constantes de compliance. Les mêmes calculs ont été faits pour $W(CO)_5(CS)$ et <u>trans</u>-$W(CO)_4(^{13}CO)(CS)$. Les variations de certaines des constantes potentielles ont été interpretées en fonction des différences entre les liens joignant les ligands CO, CS et CSe avec le métal. Ces études démontrent définitivement que les constantes d'intéraction sont transposables entre complexes de pareille géométrie. Une comparaison entre les constantes de force calculées suivant un champ de force quadratique général et celles déterminées en isolant les vibrateurs CX montre que l'approximation de l'isolement des vibrateurs CX se détériore lorsque X progresse de l'oxygène au sélénium. Finalement, les spectres photoélectroniques de $Cr(CO)_5(CSe)$ et de $BzCr(CO)_2(CX)$ ont été mesurés et les résultats obtenus, concernant les différents comportements des ligands CX, sont en accord avec les conclusions tirées des analyses vibrationnelles.

ACKNOWLEDGEMENTS

I would like to express my sincere gratitude to my supervisor, Ian Butler, to Keith Plowman and to Jacqueline Sedman, for their guidance and patience during the course of this work.

Drs. O. Mamer and A. Müller are thanked for the mass and photoelectron spectra, respectively.

As well, I would like to thank Geraldine Bazuin and Renée Charron who spent long hours carefully typing this manuscript.

The financial support of McGill University and NSERC is acknowledged.

NOTE ON UNITS

Stretching force and compliance constants are expressed in mdyn A^{-1}(millidynes per Angstrom) and A^{-1} mdyn, respectively, as these are the units generally employed for potential constants. The S.I. equivalents are N m^{-1} (Newtons per meter) and m^{-1} N. In these units the force constants would be 100 times larger and the compliance constants 100 times smaller than the values reported here.

TABLE OF CONTENTS

PART I. SYNTHESIS OF CHROMIUM(0) CHALCOCARBONYL COMPLEXES

PART III. NORMAL COORDINATE ANALYSES OF
(η^6-BENZENE)TRICARBONYLCHROMIUM(0),
(η^6-BENZENE)DICARBONYL(THIOCARBONYL)-
CHROMIUM(0) AND (η^6-BENZENE)DICARBONYL-
(SELENOCARBONYL)CHROMIUM(0)

PART IV. CORRELATION OF THE POTENTIAL CONSTANTS OF GROUP VIB METAL CHALCOCARBONYLS WITH SOME NON-VIBRATIONAL DATA

LIST OF FIGURES

LIST OF TABLES

INTRODUCTION

Introduction

Infrared spectroscopy is the most commonly used technique in the elucidation of the structure of metal carbonyls. The bands arising from CO stretching vibrations are sharp, intense and usually well-isolated from other features in the spectrum. The number and intensity pattern of these bands provide information on molecular geometry and symmetry, while their actual positions are related to the bonding in the molecule. For example, the extent of M-CO multiple bonding can be estimated from the position of a ν(CO) band since it moves to lower energy as the MC bond order increases.

Interpretation of the complete vibrational spectrum of a metal carbonyl complex through normal mode calculations leads to an evaluation of the potential constants and interaction coordinates, which provide even more information on the bonding and electronic structure of the molecule. During the last decade, complete normal coordinate analyses have been performed on a number of metal carbonyl derivatives, e.g., $M(CO)_6$, ($M=Cr,Mo,W$[1]), $Fe(CO)_5$[2], $Ni(CO)_4$[3], $Co(CO)_3(NO)$[4] and $Mn(CO)_5Br$[5], and the potential constants thus obtained are among the few quantitative measurements of the differences in bonding in these molecules. The results of these analyses are discussed in some detail in Part II of this thesis.

At the outset of the work presented here, one of the main objectives of the research in our laboratory was an investigation of the physical properties of the numerous thio- and selenocarbonyl complexes that we and other researchers had recently prepared[6]. We were particularly interested in comparing the relative bonding properties of the CO, CS and CSe ligands in related series of complexes by both vibrational and nmr spectroscopy. The ^{13}C and ^{17}O nmr data obtained for many of these series, e.g., $CpM(CO)_2(CX)$ ($Cp = \eta^5-C_5H_5$; $M = Mn,Re$; $X = O,S,Se$) and $(\eta^6-CH_3CO_2C_6H_5)Cr(CO)_2(CX)$, have since appeared in the literature[7].

The $BzCr(CO)_2(CX)$ ($Bz = \eta^6-C_6H_6$; $X = O,S,Se$) series was initially chosen for normal coordinate analysis because several analyses of the tricarbonyl complex had already been reported using various approximations (Part III). However, our preliminary potential constant data indicated that the strength of the Bz-Cr interaction decreases significantly when O is replaced by S or Se. This prompted us to investigate the possibility of displacing the benzene ring with CO in the thio- and selenocarbonyl complexes. The success of this investigation led to the preparation of both $Cr(CO)_5(CS)$ and the hitherto unknown complex, $Cr(CO)_5(CSe)$, in high yields (Part I). With the discovery of this relatively simple selenocarbonyl complex we now had the best opportunity to date to study the comparative bonding properties of the isoelectronic ligands, CO, CS and CSe, especially since the potential constants of the parent $Cr(CO)_6$ molecule were so well-established[1].

In order to have sufficient vibrational data to produce reliable potential fields for the pentacarbonylchromium(0) chalcocarbonyl complexes, the all-^{13}CO- and mono-^{13}CS-labelled derivatives were also prepared and their spectra analyzed. Anharmonicity corrections were determined for the CO, CS and CSe stretching modes, and the normal mode calculations were performed using compliance constants rather than the more familiar force constants for the reasons explained in detail in Part II. A compliant field was also determined for $W(CO)_5(CS)$ using the vibrational data reported previously for this complex and its trans-mono ^{13}CO derivative[8]. It should be mentioned, however, that although compliance constants were used in the calculations, the final potential fields are expressed in both force and compliance constants. Valence force fields had already been obtained in this laboratory for $Cr(CO)_5(CS)$ and $W(CO)_5(CS)$[8], but the wavenumber fit of many of the observed bands was not totally satisfactory. The only additional isotopic species examined was <u>trans</u>-$W(CO)_4(^{13}CO)(CS)$ which supplied relatively few extra frequencies for the vibrational analysis and the $\nu(CO)$ and $\nu(CS)$ modes were not corrected for anharmonicity. Furthermore, the use of force rather than compliance constants prevented the direct transfer of the angle bending constants from $M(CO)_6$ to $M(CO)_5(CS)$ due to the redundancy in the CMC coordinates (Part II).

Following the successful completion of the analyses on the pentacarbonyl derivatives, we returned to our normal coordinate calculations on the benzenechromium(0) series (Part III). With the availability of reliable potential constants for the CrCS and CrCSe fragments, those obtained for $BzCr(CO)_2(CX)$ are more meaningful than would otherwise have been the case. In addition, a comparison of these constants for both series provides useful information on the relative behaviour of the CX ligands in two quite different chemical environments.

In Part IV of this thesis, the results of the He(I) photoelectron measurements on $Cr(CO)_5(CSe)$ and $BzCr(CO)_2(CX)$ are presented and analyzed. Similar measurements had been reported previously for $Cr(CO)_6$[9], $Cr(CO)_5(CS)$[10] and $BzCr(CO)_3$[11], and these have proven to be quite valuable probes into the structure of the valence electrons in these molecules. Similarly, some predictions on the electronic structures of the $Cr(CO)_5(CSe)$ and $BzCr(CO)_2(CX)$ complexes can be made from their photoelectron spectra.

Also in Part IV, the vibrational data are interpreted in terms of the molecular orbitals of the chalcocarbonyl complexes. This provides a better understanding of what features of the electronic structure are important in determining the trends in the potential constants. Furthermore, the potential constants are correlated with other physicochemical properties of the complexes (e.g. ^{13}C and ^{17}O nmr chemical shifts, crystallographic bond lengths, chemical reactivities, etc.) to determine if data from different sources offer a consistent interpretation for the bonding properties of the CX ligands.

Finally, a summary of the contributions to knowledge and a list of publications to date pertaining to this work are given.

References (Introduction)

1. L.H. Jones, R.S. McDowell and M. Goldblatt, Inorg. Chem., 8, 2349 (1969).

2. L.H. Jones, R.S. McDowell, M. Goldblatt and B.I. Swanson, J. Chem. Phys., 57, 2050 (1972).

3. L.H. Jones, R.S. McDowell and M. Goldblatt, ibid., 48, 2663 (1968).

4. L.H. Jones, R.S. McDowell and B.I. Swanson, ibid., 58, 3757 (1973).

5. D.K. Ottesen, H.B. Gray, L.H. Jones and M. Goldblatt, Inorg. Chem., 12, 1051 (1973).

6. I.S. Butler, Accounts Chem. Res., 10, 359 (1977).

7. J.P. Hickey, I.M. Baibich, I.S. Butler and L.J. Todd, Spectrosc. Lett., 11, 671 (1978), and references therein.

8. I.S. Butler, A. Garcia-Rodriguez, K.R. Plowman and C.F. Shaw III, Inorg. Chem., 15, 2602 (1976).

9. D.R. Higginson, D.R. Lloyd, P. Burroughs, D.M. Gibson and A.F. Orchard, J. Chem. Soc., Faraday Trans. II, 69, 1659 (1973).

10. D.L. Lichtenberger and R.F. Fenske, Inorg. Chem., 15, 2015 (1976).

11. M.F. Guest, I.H. Hillier, B.R. Higginson and D.R. Lloyd, Mol. Phys., 29, 113 (1975).

PART I

SYNTHESIS OF CHROMIUM(0) CHALCOCARBONYL COMPLEXES

Chapter 1

Introduction

The paucity of transition-metal complexes containing M-CS and M-CSe linkages in comparison with those having M-CO linkages cannot be ascribed to the relative strengths of these bonding interactions. The various physical measurements on metal chalcocarbonyls discussed in later sections of this thesis clearly indicate that MC bond strengths increase in the order MC(O) < MC(S) < MC(Se). The key to the abundance of metal carbonyls is the relative ease with which they can be prepared from gaseous carbon monoxide. Most syntheses simply involve the reduction of a transition metal compound in the presence of carbon monoxide under various conditions of pressure and temperature (reductive carbonylation)[1].

Carbon monosulphide, which can be produced in several gram quantities by the decomposition of CS_2 in a high-voltage ac discharge[2], polymerizes (often explosively) at temperatures above -160°C. Carbon monoselenide is apparently more unstable as it has not yet been isolated, even at low temperatures[3]. Thus, to date*, virtually all metal chalcocarbonyls have been prepared by the activation of small organic molecules which contain a $\rangle C=X$ (X=S,Se) group. For X=S, suitable reagents include CS_2, Cl_2CS and ClC(S)OR (R=Me,Et) while CSe_2 is the only direct source of the $\rangle C=Se$ group used thus far. Several examples of metal thio- and selenocarbonyl syntheses using these reagents are described in two comprehensive reviews[5,6].

Direct reaction with the appropriate carbon dichalcogenide[6] was the method used to prepare the compounds under investigation in this thesis. The monothio- and monoselenocarbonyl derivatives of $BzCr(CO)_3$ were prepared via a *cis*-cyclooctene intermediate

$$BzCr(CO)_2(C_8H_{14}) \xrightarrow{CX_2} BzCr(CO)_2(CX).$$

The fate of the second chalcogen atom in these reactions is

---

*The synthesis of $Ni(CS)_4$[4] by the co-condensation of Ni atoms and CS (produced by passing a microwave discharge through CS_2 vapour) in an Ar matrix at 10K is the only example of the direct reaction of CS with a metal to yield a metal thiocarbonyl. Furthermore, $Ni(CS)_4$, which is unstable, is the only known binary transition-metal thiocarbonyl complex.

not known but the possibility of the formation of cis-cyclooctene-episulphide ($C_8H_{14}S$) cannot be discounted[7]. In the analogous reactions of $CpMn(CO)_2(C_8H_{14})$, the presence of a chalcogen-acceptor, such as PPh_3, is crucial for the high-yield syntheses of the chalcocarbonyls[6].

The pentacarbonyl complexes, $Cr(CO)_5(CX)$, were prepared by the displacement of the arene ligand from $BzCr(CO)_2(CX)$ with CO under pressure:

$$BzCr(CO)_2(CX) + 3CO \xrightarrow[20\ atm]{\sim 60°C} Cr(CO)_5(CX) + Bz$$

The yields are typically 30-50% based on $Cr(CO)_6$ [50-95% based on $BzCr(CO)_2(CX)$] which is far superior to the 3-6% yield obtained for $Cr(CO)_5(CS)$ by the literature method[8]. This latter method involves the reduction of $Cr(CO)_6$ and the treatment of the resulting anions with excess Cl_2CS as follows:

$$Cr(CO)_6 \xrightarrow[THF]{Na/Hg} \underset{\text{and other anions}}{[Cr_2(CO)_{10}]^{2-}} \xrightarrow{Cl_2CS} Cr(CO)_5(CS) + Cr(CO)_6 + 2Cl^-$$

In addition to the poor yields obtained, the thiophosgene route requires the tedious separation of the thiocarbonyl from the large quantity of $Cr(CO)_6$ regenerated during the reaction [up to eight times as much $Cr(CO)_6$ as $Cr(CO)_5(CS)$ is produced] which is an extremely difficult process because of the closely similar physical properties of the complexes[8]. The new preparative method described here does not suffer from this drawback and, furthermore, it offers a simple route to $Cr(CO)_5(CSe)$ which cannot be synthesized using the literature approach owing to the nonexistence of Cl_2CSe.

To furnish extra frequency data for the normal coordinate analyses, approximately 90 atom % ^{13}C-enrichment of the CO groups in the various complexes was desired. This high level of enrichment is necessary since large concentrations of partially-labelled species would complicate the vibrational spectra, especially in the low-energy region (700-300 cm^{-1}) where weak and overlapping bands are usually present. The easiest way to label metal carbonyls is through CO-exchange reactions using ^{13}CO which is readily available in high-isotopic enrichment. In many complexes, the CO groups undergo both thermal and photochemical CO exchange. In $BzCr(CO)_3$, however, thermal reactions lead only to arene group replacement with no loss of CO[9]. Thus, the most convenient route to $BzCr(^{13}CO)_3$ is the photochemically-induced exchange of the three CO groups in the unlabelled molecule with ^{13}CO. The best method to prepare the $BzCr(^{13}CO)_2(CX)$ derivatives is by replacement of one of the ^{13}CO groups in $BzCr(^{13}CO)_3$ with

CX since direct uv irradiation of the $BzCr(CO)_2(CX)$ complexes in the presence of ^{13}CO leads to extensive decomposition. Displacement of the arene ring in $BzCr(^{13}CO)_2(CX)$ with ^{13}CO is the most facile route to $Cr(^{13}CO)_5(CX)$ of high-isotopic enrichment.

Thus, since $BzCr(^{13}CO)_3$ was needed as a precursor for further syntheses, as well as for vibrational analysis, we estimated that we would require approximately 1 g of this ^{13}C-labelled complex. To obtain such a quantity with 90 atom % ^{13}C-enrichment from a single-step exchange reaction would take about 6 ℓ of 95 atom % ^{13}CO [at a current cost of ca. $160. (U.S.) per liter], and 6 ℓ of 90 atom % ^{13}CO would be left over after the exchange. A much less expensive method is to enrich the starting material in several steps. The multistep enrichment procedure described below allows a theoretical yield of 1.5 g of $BzCr(^{13}CO)_3$ with 90 atom % ^{13}C-enrichment from 1 ℓ of 95 atom % ^{13}CO while the recovered CO is reduced to about 50 atom % ^{13}C-enrichment.

As a final comment, it should be emphasized that the selenocarbonyl complexes prepared in this thesis had not been synthesized previously.

Chapter 2

Synthesis of Benzenechromium(0) Chalcocarbonyl Complexes

2.1. Sources of Materials

All chemicals used were obtained from the sources listed below.

Chemical	Source
Benzene	Anachemica Chemicals Ltd.
Carbon Disulphide	"
Diethyl Ether	"
Hexanes	"
Tetrahydrofuran (THF)	"
Carbon Diselenide	Strem Chemicals Inc.
Hexacarbonylchromium(0)	"
cis-Cyclooctene (C_8H_{14})	Eastman Kodak Co.
2-Picolene ($CH_3C_5H_4N$)	Aldrich Chemical Co.

Chemical	Source
Deuterobenzene (d_6-C_6H_6)	Merck, Sharp and Dohme Ltd.
^{13}CO 95 atom % ^{13}C-enriched	Prochem
^{13}CO 97 atom % ^{13}C-enriched	Prochem
$^{13}CS_2$ 90 atom % ^{13}C-enriched	Prochem

2.2. Physical Measurements

Infrared spectra were recorded on a Perkin-Elmer model 337 spectrophotometer coupled to a Texas Instruments Servo-Riter model II expanded-scale recorder. The solution spectra were obtained using a pair of matched 0.1-mm NaCl cells. Mass spectra were obtained on an LKB 9000 mass spectrometer and typical operating conditions were 20°C and an ion source energy of 70 eV. Melting points were taken on a Gallenkamp Melting Point apparatus and are uncorrected. Elemental analyses of the new selenocarbonyl complexes were performed by the Schwarzkopf Microanalytical Laboratory, Inc., Woodside, New York, USA.

2.3. General

All procedures were performed routinely under a nitrogen atmosphere. Benzene, THF, diethyl ether, hexanes, carbon disulphide and 2-picolene were refluxed under nitrogen over suitable drying agents (sodium metal strips in the presence of benzophenone, and phosphorous pentoxide for 2-picolene) and distilled immediately prior to use. Deuterobenzene and cis-cyclooctene were stored over molecular sieves (Linde 3A) and used without further purification. Carbon diselenide was purchased in 1 g quantities in sealed ampoules which were broken directly into the reaction mixtures.

The uv-irradiation source was a 100-W "Hanovia" (No. 6515-30) high-pressure, quartz mercury-vapour lamp (Ace Glass Inc., Vineland, N.J., USA). A Pyrex irradiation vessel (capacity 350 ml) fitted with a water-cooled quartz finger to house the uv lamp was used in the photochemical step of the chalcogen-exchange reactions. The design of similar vessels has been described in detail previously[10,11].

Chromatographic separation of the products was performed by preparative thin-layer chromatography (TLC). Five 20x20-cm TLC plates (1 mm thick) were prepared from a slurry of 80 g silica gel G (Macherey, Nagel & Co., 516 Düren, West Germany) and 170 ml water. The plates were activated before use by heating them at 110°C for 1 h. A maximum of 100 mg of product was spotted on to each plate.

2.4. Preparation of the All-^{12}CO and Perdeuterated Complexes

2.4.1. (η^6-Benzene)tricarbonylchromium(0)

The $BzCr(CO)_3$ complex was prepared by Rausch's method[12]. $Cr(CO)_6$ (12 g, 54 mmol) was dissolved in a mixture of benzene (120 ml) and 2-picolene (75 ml) in a 250-ml round-bottomed flask. After refluxing this mixture under nitrogen for 1 week, the tricarbonyl product was extracted with diethyl ether and recrystallized from diethyl ether/hexanes. The reaction afforded 8.8 g (41 mmol, 76% yield) of the yellow compound (mp 163-164°C, lit.[12] 162-163°C).

2.4.2. (η^6-Benzene)dicarbonyl(thiocarbonyl)chromium(0) and (η^6-Benzene)dicarbonyl(selenocarbonyl)chromium(0)

$BzCr(CO)_3$ (350 mg, 1.64 mmol) and excess *cis*-cyclooctene (20 ml) were added to 300 ml of benzene in the uv reaction vessel. The reaction mixture was well agitated with a stream of nitrogen and, after wrapping the vessel in aluminum foil and placing it in an ice-water bath, the uv lamp was turned on. The colour of the solution gradually turned dark wine-red owing to the formation of $BzCr(CO)_2(C_8H_{14})$. The progress of the reaction was conveniently monitored by diluting a small sample of the reaction mixture with an equal volume of hexanes and following changes in the CO stretching region (2150-1800 cm^{-1}) of the ir spectrum of this mixture. The bands observed were: $BzCr(CO)_3$, 1970 (a_1) and 1900 (e) cm^{-1}; $BzCr(CO)_2(C_8H_{14})$, 1900 (a') and 1850 (a") cm^{-1}. After ∿50 min, the a_1 mode of the tricarbonyl had disappeared and the irradiation was terminated. The reaction mixture was allowed to stand for 30 min with a steady stream of nitrogen bubbling through it in order to flush out any CO remaining.

Carbon disulphide (25 ml) or carbon diselenide (1 g, 6 mmol) was added to the reaction mixture and the ice-water bath was removed. The solution slowly turned dark yellow and some brown-black decomposition product was evident. After standing for 2-3 h, the reaction mixture was filtered under nitrogen through a medium-porosity, sintered glass filter to remove the decomposition product. The benzene solvent and excess cis-cyclooctene were removed from the clear orange filtrate at room temperature on a rotary evaporator using a mechanical vacuum pump protected by a liquid-nitrogen trap. The residue remaining contained $BzCr(CO)_2(CX)$ mixed with about 10% $BzCr(CO)_3$. The desired complex was isolated by TLC. The crude product was dissolved in a minimum quantity of diethyl ether and spotted on to three TLC plates and eluted with a hexanes/diethyl ether mixture (3/1 for the thiocarbonyl and 2/1 for the selenocarbonyl). The trailing dark yellow band of product was quickly scraped off with a spatula. The scrapings were placed in a medium-porosity, sintered-glass filter and washed with diethyl ether. The filtrate was reduced to dryness at room temperature on a rotary evaporator when orange crystals formed. The thio- and selenocarbonyl products were further purified by recrystallization from hexanes/diethyl ether mixtures: $BzCr(CO)_2(CS)$ [200 mg, 0.870 mmol, 53% yield; mp 123°C (dec.), lit.[11] 120°C]; $BzCr(CO)_2(CSe)$ [150 mg, 0.542 mmol, 33% yield; mp 99°C (dec.). Anal. Calcd. for $C_9H_6O_2SeCr$: C, 39.0; H, 2.18; Se, 28.5; mol. wt. 278. Found: C, 39.2; H, 2.26; Se, 28.1; mol. wt., 278 (mass spectrum)].

2.4.3. [η^6-(d_6-Benzene)]tricarbonylchromium(0), [η^6(d_6-Benzene)]dicarbonyl(thiocarbonyl)chromium(0) and [η^6-(d_6-Benzene)]dicarbonyl(selenocarbonyl)chromium(0)

The perdeuterated tricarbonyl complex was prepared by using d_6-deuterobenzene instead of benzene in the procedure outlined in Section 2.4.1. The scale of the reaction was reduced by half. The perdeuterated thio- and selenocarbonyl preparations were identical to those described for the normal species.

2.5. Preparation of the All-^{13}CO and ^{13}CS Complexes

2.5.1. (η^6-Benzene)[tri(^{13}C-carbonyl)]chromium(0)

A sketch of a typical reaction vessel used is shown in Figure I.1. Five such vessels were constructed and attached to a calibrated vacuum manifold; the capacity of each vessel was ∿100 ml. Supply and recovery vessels (capacity ∿250 ml) for the ^{13}CO gas were also connected to the vacuum line. Several grams of activated charcoal were placed in each vessel to allow quantitative transfer of ^{13}CO from vessel to vessel. The volume of gas transferred each time was completely adsorbed onto the charcoal at -196°C; in the absence of charcoal the quantitative transfer of ^{13}CO is not possible because its vapor pressure at -196°C is 400 torr[13]. The uv source used for the irradiations was the 100-W mercury-vapour lamp described above.

Approximately 300 mg (∿1.40 mmol) of BzCr(CO)$_3$ was dissolved in 90 ml of THF and the solution was placed in reaction vessel #1. This vessel was reconnected to the vacuum line and the solution was degassed twice at -196°C

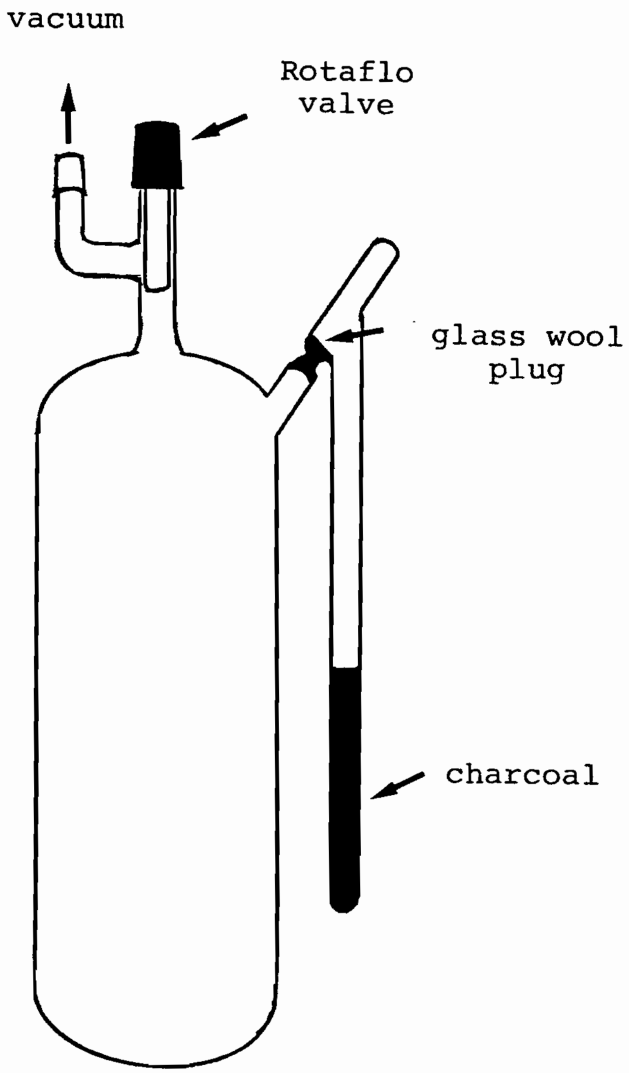

Figure I.1. Typical reaction vessel for the CO exchange reactions.

by the usual freeze-thaw method. A 5-molar excess of ^{13}CO (7 mmol; 95 atom % ^{13}C-enriched) was introduced into the reaction vessel at -196°C from the supply vessel and, after thermal equilibration, the reaction mixture was irradiated for 8 h*. Following the irradiation, the ^{13}CO gas of reduced enrichment was transferred to reaction vessel #2 which contained a further 300-mg quantity of $BzCr(CO)_3$, while a fresh supply of 95 atom % ^{13}CO was introduced into vessel #1. Both vessels were then subjected to irradiation until the exchange reactions reached equilibrium. This procedure was continued until the exchanges in all five reaction vessels were completed. Table I.1 presents the statistical equilibration expected after each step for the five vessels using a 5:1 molar ratio of ^{13}CO to $BzCr(CO)_3$. The arrows in this table indicate the pathways of ^{13}CO transfer from vessel to vessel. Since the final percent enrichment in each reaction vessel was not the same, the $BzCr(^{13}CO)_3$ formed was recovered from each vessel separately by the following

---

*Prior to the preparative-scale reaction, the time necessary for statistical equilibration to occur was determined by irradiating small amounts of $BzCr(CO)_3$ dissolved in THF (2 ml) in the presence of a 5-molar excess of ^{13}CO. The exchange reactions were monitored by observing changes in the ν(CO) region (2000-1800 cm^{-1}) of the ir spectrum of the reaction mixture. Since no further changes occurred in this region after 8 h irradiation, it was assumed that a statistical distribution of ^{13}CO had been established.

TABLE I.1: Atom Fraction of ^{13}CO in Reaction Vessels #1-5 after Statistical Equilibration for a 5:1 Molar Ratio of ^{13}CO to $(\eta^6\text{-}C_6H_6)Cr(CO)_3$[a]

Reaction Step (1 step = 8 h irradiation)	Reaction Vessel				
	1	2	3	4	5
1	S → 0.594	-	-	-	-
2	S → 0.816	↘ 0.371	-	-	-
3	S → 0.900	↘ 0.649	↘ 0.232	-	-
4		↘ 0.806	↘ 0.493	↘ 0.145	-
5		S → 0.896	↘ 0.689	↘ 0.362	↘ 0.091 → R
6			↘ 0.816	↘ 0.566	↘ 0.260 → R
7			S → 0.900	↘ 0.722	↘ 0.451 → R
8				↘ 0.833	↘ 0.620 → R
9				S → 0.906	↘ 0.753 → R
10					↘ 0.849 → R

---

[a] Arrows indicate pathways of ^{13}CO transfer from vessel to vessel; S = supply vessel; R = recovery vessel.

procedure. The contents of each vessel were syringed into a 250-ml round-bottomed flask and the THF solvent was removed at room temperature on a rotary evaporator. Small quantities of $Cr(CO)_6$, which had formed during the irradiations, were removed by high-vacuum sublimation (0.01 torr/25°C) and the remaining $BzCr(^{13}CO)_3$ was recrystallized from hexanes/diethyl ether to give a yellow crystalline solid [total yield 0.83 g, 39 mmol, 53% based on unlabelled $BzCr(CO)_3$; mp 164-165°C, lit.[12] 162-163°C. Mol. wt: calcd. for $C_6{}^{13}C_3H_6O_3Cr$, 217; found, 217 (mass spectrum)].

2.5.2. (η^6-Benzene)[di(^{13}C-carbonyl)](thiocarbonyl)chromium(0) and (η^6-Benzene)[di(^{13}C-carbonyl)](selenocarbonyl)chromium(0)

These complexes were prepared from $BzCr(^{13}CO)_3$ following the procedure given in Section 2.4.2. which produced optimum yields in trial runs with unlabelled $BzCr(CO)_3$. $BzCr(^{13}CO)_2(CS)$ [mol. wt: calcd. for $C_7{}^{13}C_2H_6O_2SCr$, 232; found 232 (mass spectrum)]; $BzCr(^{13}CO)_2(CSe)$ [mol. wt: calcd. for $C_7{}^{13}C_2H_6O_2SeCr$, 279; found, 279 (mass spectrum)].

2.5.3. (η^6-Benzene)dicarbonyl(^{13}C-thiocarbonyl)chromium(0)

Again the procedure given above was used except the quantities were adjusted as follows: $BzCr(CO)_3$ (1.5 g, 7.0 mmol) was added to benzene (700 ml) and C_8H_{14} (40 ml). After formation of the cis-cyclooctene intermediate, $^{13}CS_2$ (0.5 ml, 8 mmol; 90 atom % ^{13}C-enriched) was added to the reaction vessel. Yield, 0.70 g, 3.0 mmol, 43% based on $BzCr(CO)_3$. Mol. wt: calcd. for $C_8{}^{13}CH_6O_2SCr$, 231; found, 231 (mass spectrum).

2.6. Determination of the Percent ^{13}C-Enrichment of (η^6-Benzene)[tri(^{13}C-carbonyl)]chromium(0)

The percent ^{13}C-enrichment of $BzCr(^{13}CO)_3$ was determined by ir spectroscopy in the following manner. The absolute integrated intensity (A) of a fundamental absorption band is directly proportional to the square of the partial derivative of the dipole moment with respect to the normal coordinate, $(\partial\mu/\partial Q)^2$. Assuming that the normal coordinates for CO stretching vibrations are identical to the CO symmetry coordinates (method of local oscillating dipoles[14]), the intensity of the a_1 CO stretching vibration of $BzCr(CO)_3$ is directly proportional to $(\partial\mu/\partial r)^2$, where r is the CO bond coordinate. If equal concentrations and equal pathlengths are employed, the ratio of the absolute intensity of the a_1 modes in the labelled (A_{13}) and unlabelled (A_{12}) tricarbonyl is given by

$$\frac{A_{13}}{A_{12}} = \frac{(\partial\mu/\partial r)^2_{13}}{(\partial\mu/\partial r)^2_{12}}$$

Since $\partial\mu/\partial r$ is independent of isotopic substitution, then $A_{13} = A_{12}$. The intensity of the a_1 mode was measured for hexanes solutions of both complexes and the ratio $A_{13}/A_{12} = 0.804$. This indicates that the labelled sample contains 80.4% of the all-^{13}CO species and the percent ^{13}C-enrichment is therefore ($\sqrt[3]{0.804}$ x 100) = 93%, which is in good agreement with the predicted value of ∿90% (Table I.1). The ^{13}C-enrichments of the $BzCr(^{13}CO)_2(CX)$ derivatives are similarly expected to be about 90%.

Chapter 3

Synthesis of Pentacarbonylchromium(0) Chalcocarbonyl Complexes

3.1. General

The chemical sources, preparation of solvents, etc. given in Chapter 2 also apply here. Furthermore, it should be emphasized that the crude products obtained in the syntheses of $BzCr(CO)_2(CX)$ can be used in the pentacarbonyl syntheses. Removal of traces of $BzCr(CO)_3$ is not necessary because $Cr(CO)_6$ is not formed under the mild reaction conditions used and the low volatility of the tricarbonyl complex prevents it from co-subliming with the volatile pentacarbonyls complexes.

3.2. Preparation of Pentacarbonyl(thiocarbonyl)chromium(0) and Pentacarbonyl(selenocarbonyl)chromium(0)

A solution of $BzCr(CO)_2(CX)$ (0.50 g; 2.2 mmol, X=S; 1.8 mmol, X=Se) in THF (50 ml) was syringed into a 75-ml stainless-steel bomb (Matheson Ltd., Whitby, Ontario, Canada) fitted with a valve. The valve was securely tightened to the bomb and, after degassing the solution by repeated freeze-thaw cycles, CO gas (22 mmol) was added to the bomb from a calibrated vacuum manifold at liquid nitrogen temperature. The valve was closed and the bomb was placed in an oil bath at 70°C for 72 h in the case of the thiocarbonyl complex. A 50° oil bath was used for the selenocarbonyl complex and the formation of $Cr(CO)_5(CSe)$ was complete in 3-4 h. Under these conditions, the pressure in the bomb, assuming that no CO gas dissolves, is approximately 20 atm. The bomb was again cooled to liquid nitrogen temperature before opening the valve, and the CO gas remaining was slowly pumped off on a vacuum line in a well-ventilated area. The bomb was then allowed to warm up to room temperature before the reaction mixture was syringed into a 250-ml round-bottomed flask. The flask was shielded from light as much as possible because the products (especially the selenocarbonyl) are photosensitive. The THF solvent was removed at -25 to -15°C (C_6H_5Cl/dry-ice slush bath) on a rotary evaporator using a mechanical pump protected by a liquid nitrogen trap [the temperature was kept close to the lower limit during solvent removal from $Cr(CO)_5(CSe)$ while the upper limit was maintained for the much less volatile $Cr(CO)_5(CS)$ complex]. Sublimation of the residue under vacuum onto an ice-water cooled finger inserted into the flask gave analytically pure samples of the deep-yellow complexes. $Cr(CO)_5(CSe)$ [0.23 g, 0.81 mmol, 45% yield based on $BzCr(CO)_2(CSe)$. Anal. Calcd. for C_6O_5SeCr: C, 25.5; Se, 27.9; mol. wt., 284. Found: C, 25.6; Se, 27.8; mol. wt., 284 (mass spectrum)]. $Cr(CO)_5(CS)$ [0.45 g, 1.9 mmol, 87% yield based on $BzCr(CO)_2(CS)$; mp = 87-88°C. Mol. wt: calcd. for C_6O_5SCr, 236; found, 236 (mass spectrum)]. The extremely volatile $Cr(CO)_5(CSe)$ sublimes before melting.

3.3. Preparation of the All-^{13}CO and ^{13}CS Complexes

3.3.1. Penta(^{13}C-carbonyl)(thiocarbonyl)chromium(0) and Penta(^{13}C-carbonyl)(selenocarbonyl)chromium(0)

The arene ring was displaced from $BzCr(^{13}CO)_2(CX)$ with ^{13}CO (97 atom % ^{13}C-enriched) to produce the desired highly-enriched $Cr(^{13}CO)_5(CX)$ complexes. The procedure followed was identical to that given above for the unlabelled complexes except that more dilute reaction conditions

(0.15 - 0.20 g of the starting material) were employed. One liter of 97 atom % ^{13}CO was necessary to produce a sufficiently high pressure of ^{13}CO in the bomb (∿13 atm at room temperature); since no CO exchange was expected to occur[9], the recovered ^{13}CO should also be 97 atom % ^{13}C-enriched. Furthermore, the overall isotopic enrichment of the pentacarbonyls should exceed that of the benzene complexes since three of the CO groups are 97 atom % ^{13}CO-enriched compared to the 90% enrichment estimated for BzCr(^{13}CO)$_2$(CX). The weak intensity of the bands due to the partially-labelled species in the ν(CO) region of the ir spectrum of Cr(CO)$_5$(CX) vapour bears this prediction out (Part II). Mol. wt: calcd. for ^{13}C$_5$CO$_5$SCr, 241; found, 241 (mass spectrum). Mol. wt: calcd. for ^{13}C$_5$CO$_5$SeCr, 289; found, 289 (mass spectrum).

3.3.2. Pentacarbonyl(^{13}C-thiocarbonyl)chromium(0)

This complex was obtained by displacement of the benzene ring from the appropriate arene complex [BzCr(CO)$_2$(^{13}CS)] under an atmosphere of CO. Owing to the large quantity of BzCr(CO)$_2$(^{13}CS) obtained above (700 mg), the procedure followed for this displacement reaction was identical to that given for the ^{12}CS preparation. Mol. wt: calcd. for C$_5$^{13}CO$_5$SCr, 237; found, 237 (mass spectrum).

References (Part I)

1. E.W. Abel and F.G.A. Stone, Quart. Rev., 24, 498 (1970), and references therein.

2. K.J. Klabunde, C.M. White and H.F. Efner, Inorg. Chem., 13, 1778 (1974).

3. R. Steudel, Angew. Chem., Int. Ed. Engl., 6, 635 (1967).

4. G.V. Calder, J.G. Verkade and L.W. Yarbrough II, J. Chem. Soc., Chem. Commun., 705 (1973).

5. P.V. Yaneff, Coord. Chem. Rev., 23, 183 (1977).

6. I.S. Butler, Accounts Chem. Res., 10, 359 (1977).

7. A.E. Fenster, Ph.D. Thesis, McGill University, Montreal, Quebec, Canada, 1972.

8. B.D. Dombek and R.J. Angelici, Inorg. Chem., 15, 1089 (1976).

9. G. Natta, R. Ercoli, F. Calderazzo and E. Santambrozio, Chem. Ind. (Milan), 40, 1003 (1958).

10. G. Jaouen and G. Simonneaux, Inorg. Syn., 19, 197 (1979).

11. D. Cozak, Ph.D. Thesis, McGill University, Montreal, Quebec, Canada, 1977.

12. M.D. Rausch, J. Org. Chem., 39, 1787 (1974).

13. "Handbook of Chemistry and Physics", 48th ed., The Chemical Rubber Co., Columbus, Ohio, USA, 1967-68.

14. S.F.A. Kettle and I. Paul, Adv. Organometal. Chem., 10, 199 (1972).

PART II

NORMAL COORDINATE ANALYSES OF PENTACARBONYL(THIOCARBONYL)CHROMIUM(0), PENTACARBONYL(SELENOCARBONYL)CHROMIUM(0) AND PENTACARBONYL(THIOCARBONYL)TUNGSTEN(0)

Chapter 4

Infrared and Raman Spectra of $Cr(CO)_5(CS)$, $Cr(CO)_5(CSe)$ and $W(CO)_5(CS)$

4.1. Introduction

The vibrational spectra of $Cr(CO)_5(CS)$, $W(CO)_5(CS)$ and the mono-^{13}CO substituted derivative, trans-$W(CO)_4(^{13}CO)(CS)$ (90% ^{13}C-enriched), have been analyzed previously in this laboratory[1]. Assignments were proposed for the fundamental modes largely on the basis of the frequencies calculated using force fields transferred from the corresponding metal hexacarbonyls. The assignments in all cases were consistent with C_{4v} molecular symmetry.

A re-examination of the vibrational spectra of $Cr(CO)_5(CS)$, together with data from the isotopically-labelled species $Cr(^{13}CO)_5(CS)$ and $Cr(CO)_5(^{13}CS)$, leads to some changes in the original assignments, especially in the 700-250 cm^{-1} region.

In addition, this work involves a study of the ir overtone and combination spectra of $Cr(CO)_5(CS)$ including the binary and ternary $\nu(CO)$ regions; these data permit the calculation of harmonic frequencies for the CO and CS stretching modes which are necessary for the calculation of general-quadratic compliance and force constants.

The complete vibrational spectra of $Cr(CO)_5(CSe)$ and $Cr(^{13}CO)_5(CSe)$ are reported here for the first time. Again, harmonic frequencies are calculated for the CO and CSe stretching modes. Since no additional vibrational data were observed for the tungsten thiocarbonyl complexes, the previously proposed assignments[1] are adopted without change. A detailed discussion of the assignments for the chromium chalcocarbonyls and their ^{13}C-labelled derivatives is presented in the following sections.

4.2. Assignment of the CO and CX (X = S, Se) Stretching Regions

The bands observed in the CO and CX stretching regions of the ir and Raman spectra of $Cr(CO)_5(CX)$, $Cr(^{13}CO)_5(CX)$, $Cr(CO)_5(^{13}CX)$, $W(CO)_5(CS)$ and trans-$W(CO)_4(^{13}CO)(CS)$ are listed in Table II.1. From the correlation diagram given in Figure II.1, three ir-active ($2a_1 + e$) and four Raman-active

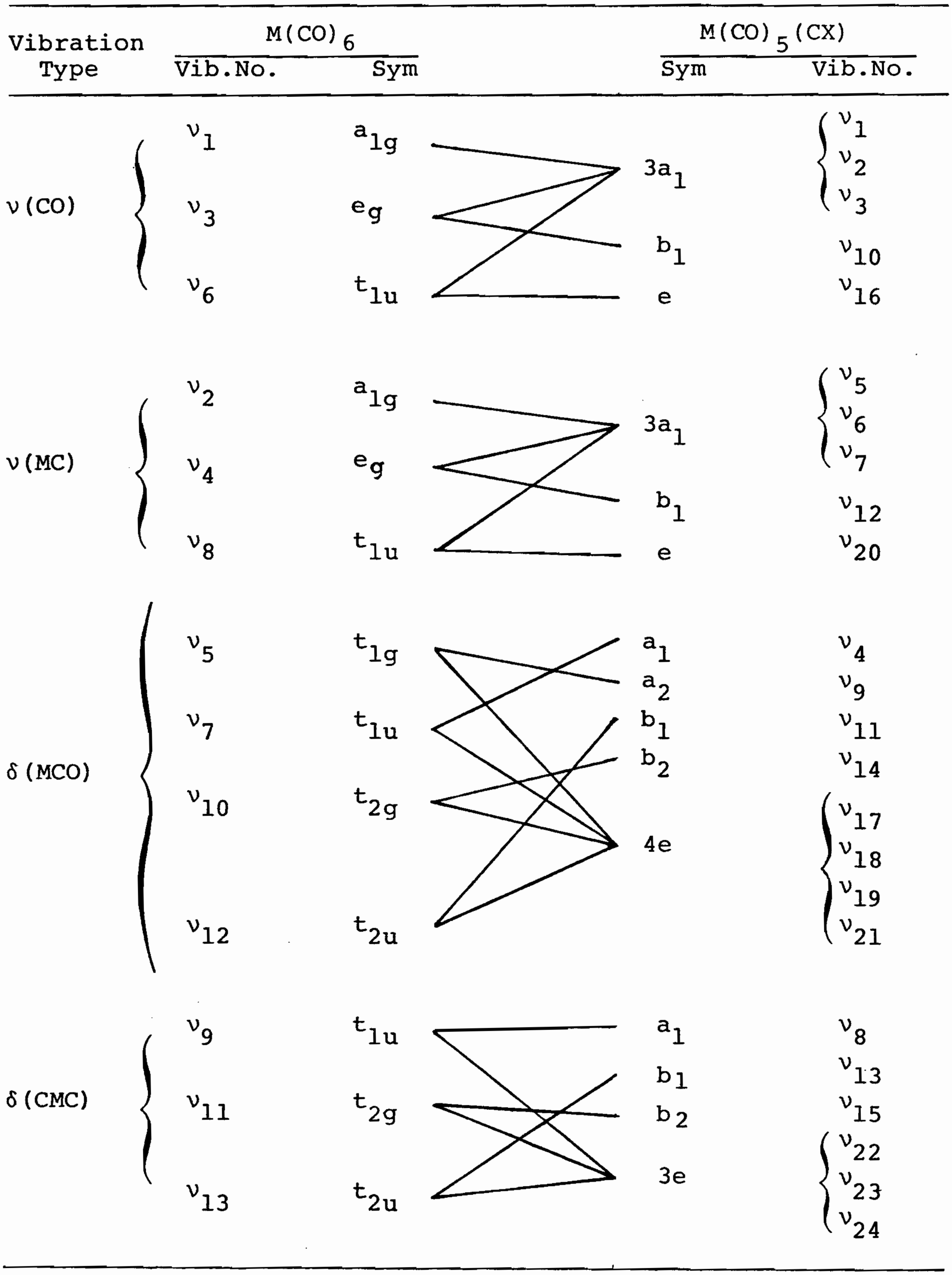

FIGURE II.1: Correlation diagram between $M(CO)_6$ (O_h symmetry) and $M(CO)_5(CX)$ (C_{4v} symmetry).

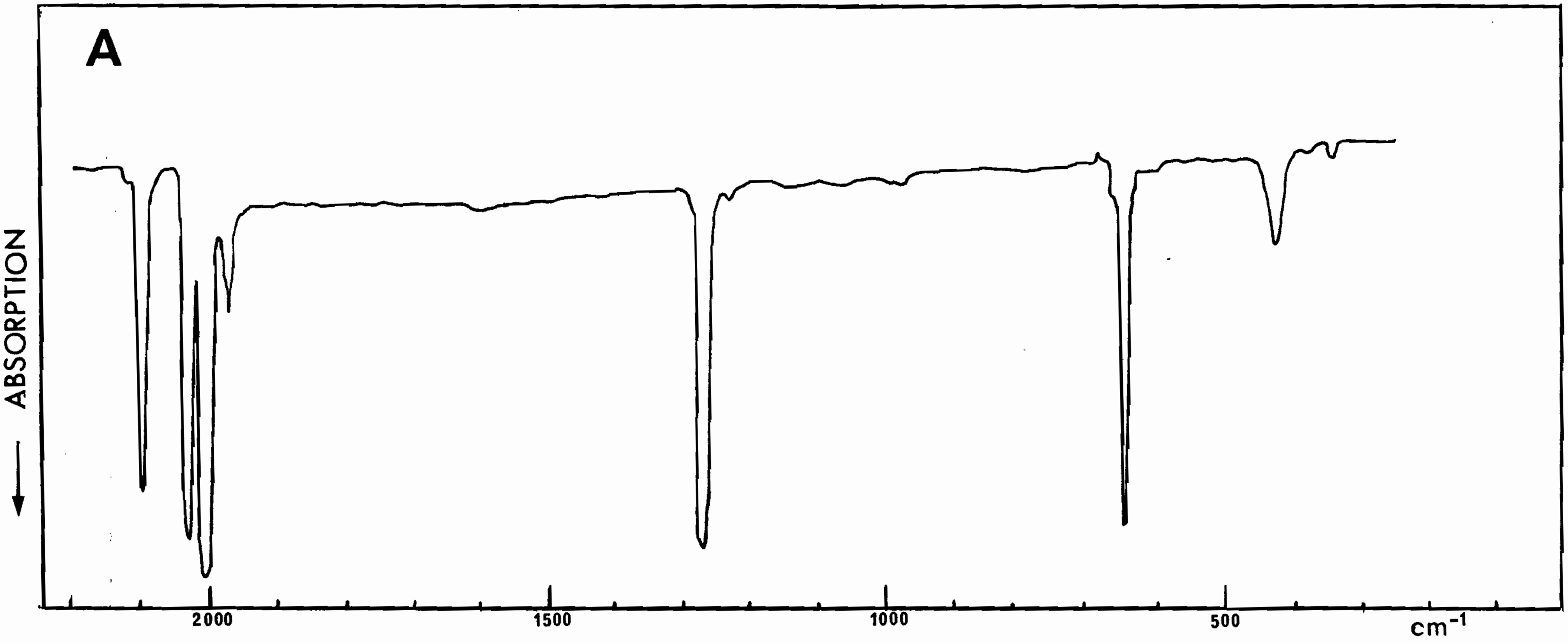

Figure II.2. Vibrational spectra of $Cr(CO)_5(CS)$ in the fundamental regions. (A) Infrared spectrum of the vapour at ∿38°C; 10-cm gas cell with CsI windows.

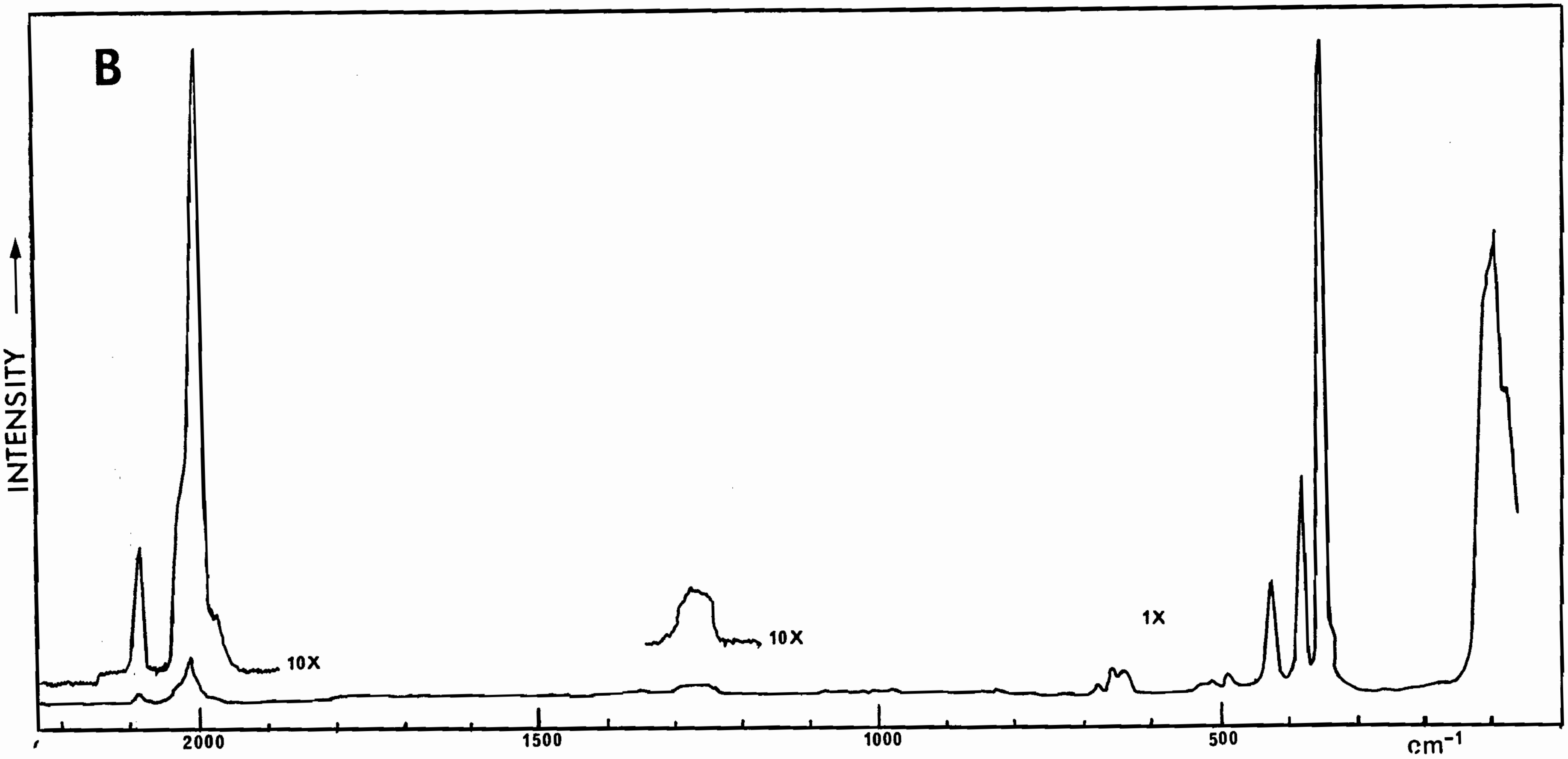

(B) Raman spectrum of the solid at ∿25°C. Conditions: sensitivity 10^4 counts s^{-1}, slit widths 5 cm^{-1}, time constant 2 s, scan speed 50 cm^{-1} min^{-1}, Kr^+ 568.1 nm excitation, 50 mW.

TABLE II.1: Observed Fundamental Modes (cm^{-1}) for $M(CO)_5(CX)$ in the CO and CX Stretching Regions

	Vib. No. and Sym.	$Cr(CO)_5(CS)$	$Cr(^{13}CO)_5(CS)$	$Cr(CO)_5(^{13}CS)$	$Cr(CO)_5(CSe)$	$Cr(^{13}CO)_5(CSe)$	$W(CO)_5(CS)$[a]	trans-$W(CO)_4(^{13}CO)(CS)$
IR GAS PHASE	ν_1 : a_1	2097.5 ms	2049.9 ms	2097.2 ms	2097.8 ms	2050.3 ms	2102 ms	2102 ms
	ν_2 : a_1	2032.7 s	1987.5 s	2032.9 s	2037.8 s	1991.7 s	2017 s	1979 s
	ν_{16} : e	2007.6 vs	1964.0 vs	2008.2 vs	2010.5 vs	1965.5 vs	2002 vs	2006 vs
	ν_3 : a_1	1279.7 s	1279.2 s	1240.1 s	1095.4 s	1093.6 s	1286 s	1284 s
IR AND RAMAN CH_2Cl_2 SOLN[b]	ν_1 : a_1	2092 m (2092 p)	2044 m (2046 p)	2091 m (2093 p)	2092 m	2044 m	2099 m (2097 p)	
	ν_2 : a_1	2021 s (2025 dp)	1975 s (1978 dp)	2020 s (2024 dp)	2028 s	1983 s	2007 s (2015 p)	
	ν_{16} : e	1988 vs	1944 vs	1988 vs	1992 vs	1948 vs	1994 vs	
	ν_3 : a_1	1257 s	1257 s	1226 s	1082 s	1080 s	1272 s (1269 p)	
IR CS_2 SOLN	ν_1 : a_1	2088.4 m			2087.6 m		2095 m	
	ν_2 : a_1	2017.3 s			2023.4 s		1965 m	
	ν_{16} : e	1989.0 vs			1991.8 vs		1983 s	
	ν_3 : a_1	1261.0 s			1077.4 s		1265 s	

TABLE II.1: (cont'd)

	Vib. No. and Sym.	$Cr(CO)_5(CS)$	$Cr(^{13}CO)_5(CS)$	$Cr(CO)_5(^{13}CS)$	$Cr(CO)_5(CSe)$	$Cr(^{13}CO)_5(CSe)$	$W(CO)_5(CS)$[a]	trans-$W(CO)_4(^{13}CO)(CS)$
IR CCl_4 SOLN	ν_1 : a_1	2091 m	2091 m		2090.5 m	2042.4 m		
	ν_2 : a_1	2022 s	2022 s		2028 s	1982 s		
	ν_{16} : e				1996.6 vs	1952 vs		
	ν_3 : a_1	1266.8 s	1228.3 s		1983.4 s	1081.5 s		
RAMAN[d] SOLID					2095.4 w	2058.8 w		
	ν_1 : a_1	2089.0 w	2040.6 w	2089.0 w	2087.8 w	2047.5 w	2102 m	2091 w
					2084.0 w, sh	2040.1 w,sh		
					2041.3 ms	1995.2 ms		
	ν_{10} : b_1	2031 w,sh[c]	1986 w,sh	2032 w,sh	2028 m,sh	1982.7 m,sh	2025 vw	2022 vw
					2023.5 s	1980.8 s		
	ν_2 : a_1	2014 m	1968 m	2014 m	2014.3 s	1970.0 s	2003 w	1954 w
	ν_{16} : e	2014 m	1968 m	2014 m	2006.0 ms	1962.0 ms	2003 w	2008 mw
					1994.3 m	1951.1 m		
					1971.1 w	1929.2 w		
	ν_3 : a_1	1266 w	1268 w	1228 w	1100 w	1098 w	1261 vw	1264 vw

[a] Data for tungsten complexes from Ref. 1.

[b] Raman data in brackets.

[c] Sh = shoulder.

[d] In the Raman spectrum of solid $Cr(CO)_5(CSe)$ at 15 K two additional bands are observed at 2044 and 1973 cm^{-1}.

TABLE II.1(a): Observed and Calculated[a] Wavenumbers for ν(CO) Fundamental Modes of $Cr(^{13}CO)_n(CO)_{5-n}(CX)$ Vapour

Obs	Calc	Sym (C_{4v})	Obs	Calc	Sym (C_s)	Obs	Calc	Sym (C_{4v})	Obs	Calc	Sym (C_s)	Obs	Calc	Sym (C_{4v})
$Cr(CO)_5(CS)$			*cis*-$Cr(CO)_4(^{13}CO)(CS)$			$Cr(^{13}CO)_5(CS)$			*cis*-$Cr(^{13}CO)_4(CO)(CS)$			*trans*-$Cr(^{13}CO)_4(CO)(CS)$		
2097.5	2096.9	a_1		2090.8	a'	2049.9	2050.2	a_1	2065.0	2065.3	a'		2067.9	a_1
2032.7	2032.8	a_1		2032.2	a'	1987.5	1987.4	a_1	2004.5	2004.6	a'		2015.4	a_1
	2028.1	b_1		2022.9	a'		1982.8	b_1		1986.6	a'		1982.8	b_1
2007.6	2008.3	e		2008.3	a"	1964.0	1963.6	e		1972.8	a'		1963.6	e
			1976.0	1974.9	a'					1963.6	a"			
$Cr(CO)_5(CSe)$			*cis*-$Cr(CO)_4(^{13}CO)(CSe)$			$Cr(^{13}CO)_5(CSe)$			*cis*-$Cr(^{13}CO)_4(CO)(CSe)$			*trans*-$Cr(^{13}CO)_4(CO)(CSe)$		
2097.8	2097.4	a_1		2091.3	a'	2050.3	2050.7	a_1	2065.9	2065.9	a'		2069.1	a_1
2037.8	2037.5	a_1		2036.7	a'	1991.7	1992.0	a_1	2006.8	2006.8	a'		2019.3	a_1
	2029.7	b_1		2024.6	a'		1984.5	b_1		1990.5	a'		1984.5	b_1
2010.0	2010.1	e		2010.1	a"	1965.5	1965.3	e		1974.6	a'		1965.3	e
			1976.0	1976.7	a'					1965.3	a"			

---

[a] Details of CO energy-factored calculations are given in Section 7.4.

TABLE II.1(b): Observed and Calculated[a] Wavenumbers for ν(CO) Fundamental Modes of $Cr(CO)_5(CX)$ and *cis*-$Cr(CO)_4(^{13}CO)(CX)$ in CS_2 Solution

Obs	Calc	Sym	Obs	Calc	Sym
	$Cr(CO)_5(CS)$	(C_{4v})	*cis*-$Cr(CO)_4(^{13}CO)(CS)$		(C_s)
2088.4	2088.5	a_1		2081.8	a'
2017.3	2017.4	a_1		2017.1	a'
	2017.1	b_1		2010.5	a'
1989.0	1989.3	e		1989.3	a"
			1957.8	1957.8	a'
	$Cr(CO)_5(CSe)$	(C_{4v})	*cis*-$Cr(CO)_4(^{13}CO)(CSe)$		(C_s)
2087.6	2087.8	a_1		2081.3	a'
2023.4	2023.3	a_1		2023.1	a'
	2021.7	b_1		2014.8	a'
1991.8	1992.3	e		1992.3	a"
			1962.0	1960.9	a'

[a] Details of CO energy-factored calculations are given in Section 7.4.

$(2a_1 + b_1 + e)$ modes are expected in the CO region under the C_{4v} symmetry of the $M(CO)_5(CX)$ molecules. The ir gas-phase and solution spectra are readily assigned on this basis and the assignments given previously for the thiocarbonyl complexes (see Ref. 1 and references therein) are adopted here. The CO stretching region of $Cr(CO)_5(CSe)$ is similar to that observed for $Cr(CO)_5(CS)$ (Figure II.2) and so the assignments for the selenocarbonyl complex follow directly from those for the thiocarbonyl complex. The weaker peaks due to partially-labelled species which appear in the ir gas-phase spectra of the enriched species were assigned by means of energy-factored force fields. The results of these calculations are given in Table II.1(a) while the computational details are given in Chapter 6.

Assignment of the Raman spectra in this region is not so straightforward. For example, re-examination of the CH_2Cl_2 solution spectrum of $Cr(CO)_5(CS)$ reveals a strongly polarized band at 2092 cm^{-1} and a depolarized band ($\rho \sim 0.8$) at 2025 cm^{-1}. The results of the energy-factored calculations, which place the a_1 axial (ν_2) and b_1 (ν_{10}) modes about 5 cm^{-1} apart in the ir gas-phase spectra [Table II.1(a)], suggest that the depolarized Raman band arises from a superposition of these two modes. If one of the component peaks is due to a totally symmetric mode, the resultant envelope should at least be weakly polarized. However, Bigorgne[2] has shown that if the ratio of the amplitudes of S_1 to S_2 (equatorial and axial CO symmetry coordinates, respectively) is $-\frac{1}{2}$ in ν_1 and $+\frac{1}{2}$ in ν_2, and if the molecular polarizability derivatives with respect to the equatorial and axial CO internal coordinates are equal, a highly polarized band will be observed for ν_1 and an essentially depolarized band for ν_2. The amplitudes of S_1 and S_2 have the above ratios if the equatorial and axial CO stretching force constants are equal[2]. No peak attributable to the e ν(CO) mode (ν_{16}) was observed.

Similar results were reported by Edgell[3] for the Raman spectrum of $Mn(CO)_5Br$ in solution. However, he proposed that the deviation from strict C_{4v} symmetry is a consequence of the "hidden" or "dual" symmetry which exists in the molecule. This hidden symmetry arises because of the near equivalence of the five CO groups. If all five were strictly equivalent, they would transform as P_5, but in the absence of such strict equivalence, the CO groups show the symmetry of both C_{4v} and P_5 groups. Under C_{4v}/P_5 dual symmetry, three ir- and three Raman-active bands are expected in the ν(CO) region. Two of the bands should be coincident in the ir and Raman, and only one polarized Raman band should be observed[3]. Although these predictions are in agreement with our data for the vibrational spectra of $Cr(CO)_5(CS)$ (Table II.1, CH_2Cl_2 soln.), the non-appearance of ν_{16} in the Raman spectrum does not violate the C_{4v} selection rules. Thus, the introduction of dual symmetry is unnecessary since the polarization data can be explained by Bigorgne's predictions.

Attempts to obtain Raman solution data for $Cr(CO)_5(CSe)$ in the $\nu(CO)$ region failed because the complex decomposed rapidly in the laser beam. The spectra of the tungsten thiocarbonyl complex were not re-investigated but the Raman solution data previously reported[1] indicated the existence of two polarized $\nu(CO)$ bands. This suggests that the mixing of S_1 and S_2 in the CO stretching modes is somewhat different for the chromium and tungsten thiocarbonyls. After presentation of the eigenvectors in Chapter 7, this point will be discussed further. Unfortunately, no solution Raman data were recorded for trans-$W(CO)_4(^{13}CO)(CS)$[1]; in this complex, the a_1 axial mode (ν_2) should be shifted considerably to lower energy, thus allowing a more precise measurement of its depolarization ratio.

The solid-state Raman spectra in the $\nu(CO)$ region also show some interesting features. As previously reported[1], both solid $Cr(CO)_5(CS)$ and $W(CO)_5(CS)$ exhibit a broad, unsymmetric feature at ∿2010 cm^{-1} and a weak band around 2100 cm^{-1} in their Raman spectra. The weak band can be readily assigned to the a_1 equatorial CO stretch (ν_1) by comparison with the solution and gas-phase spectra, while the second, broader peak, which possesses a shoulder on its high energy side, is assigned to the remaining CO modes (Table II.1).

In contrast to the thiocarbonyl complexes, the Raman spectrum of solid $Cr(CO)_5(CSe)$ displays a multitude of bands in its $\nu(CO)$ region (at 15K a total of twelve peaks are observed; Figure II.3). To correlate the modes of the solid with those of the isolated molecule the perturbations due to the crystal lattice must be known. The crystal structure of $Cr(CO)_5(CSe)$ has not been studied but both $Cr(CO)_6$[4] and $Cr(CO)_5(CS)$[5] crystallize in the centrosymmetric space group P_{nma} (D_{2h}^{16}) with four molecules (on C_s sites) per unit cell. If $Cr(CO)_5(CSe)$ were isostructural with $Cr(CO)_6$ and $Cr(CO)_5(CS)$, the correlation given in Figure II.4 between C_{4v} molecular symmetry, C_s site symmetry and D_{2h} factor group symmetry indicates that the non-degenerate modes of $Cr(CO)_5(CSe)$ could theoretically be split into two ir-active and two Raman-active components [$a_g(R) + b_{1g}(R) + b_{2u}(ir) + b_{3u}(ir)$] in the crystal. The doublet centered at $\sim$2080 cm^{-1} in the room temperature Raman spectrum almost certainly corresponds to the a_1 equatorial $\nu(CO)$ mode (ν_1) in the free molecule. Closer examination of this doublet reveals a shoulder at 2084.0 cm^{-1} on the low-energy peak and at 15K three bands are clearly

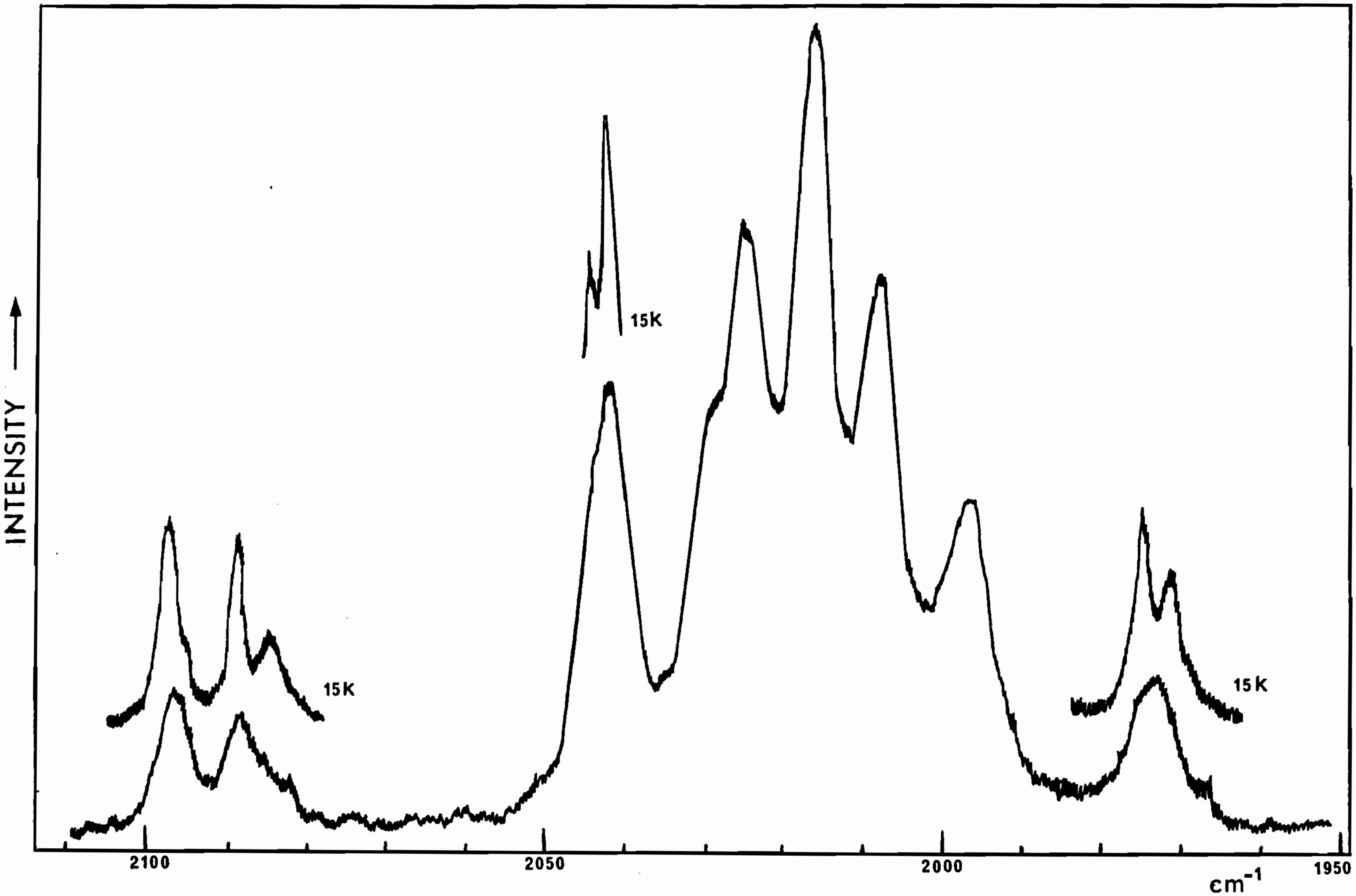

Figure II.3. Raman spectra of $Cr(CO)_5(CSe)$ at 15 and 300 K in the CO fundamental stretching region Conditions: sensitivity 5×10^2 counts s^{-1}, slit widths 1 cm^{-1}, time constant 2 s, scan speed 5 cm^{-1} min^{-1}, Kr^+ 568.1 nm excitation, 50 mW.

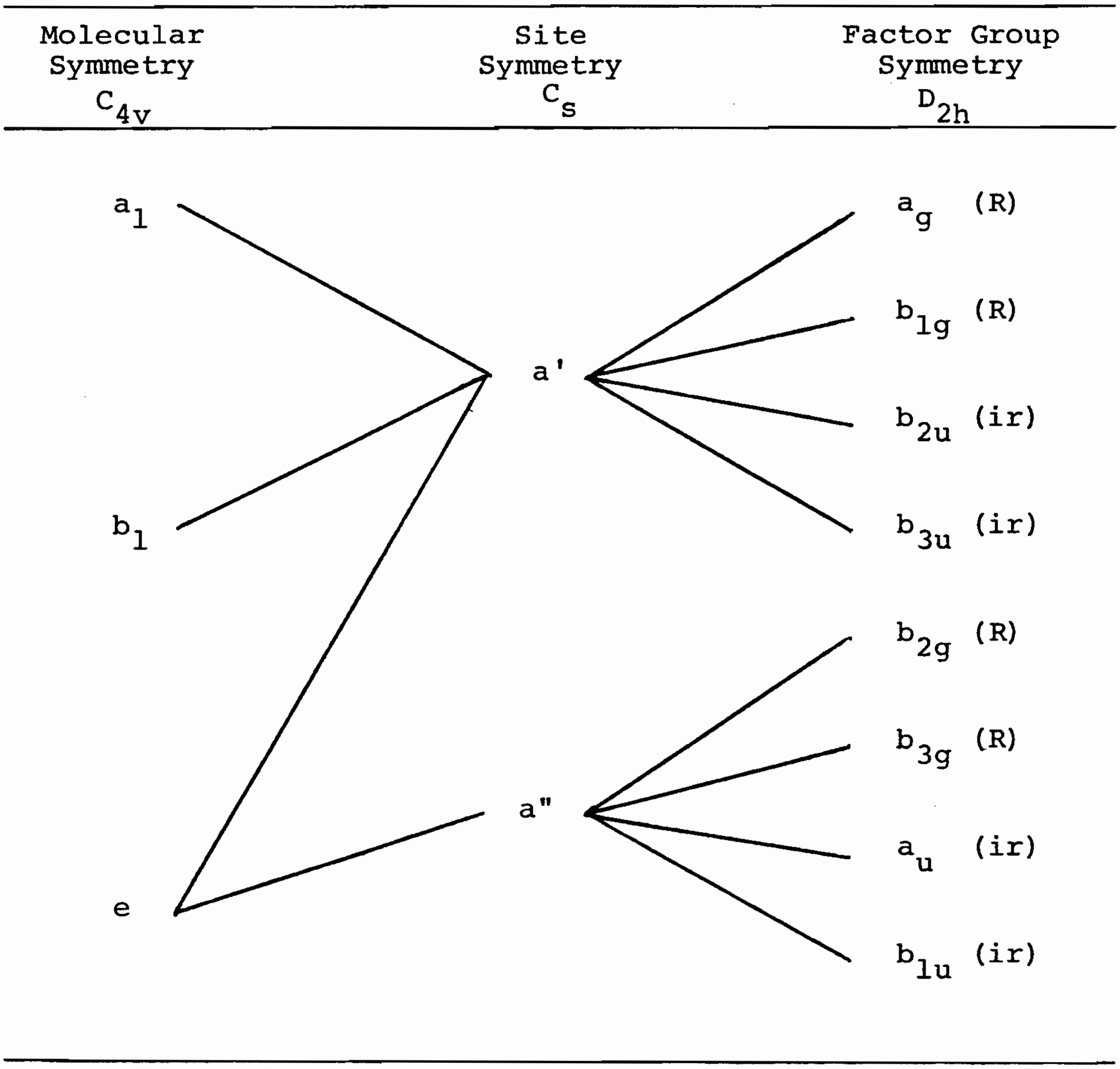

FIGURE II.4. Correlation diagram between C_{4v} molecular symmetry, C_s site symmetry and D_{2h} factor group symmetry for the ν(CO) symmetry species of $M(CO)_5(CX)$.

resolved in this region (Figure II.3). This suggests that, unless the third peak is due to a combination mode involving a CO stretch and a CMC bend, $Cr(CO)_5(CSe)$ may not be isostructural with $Cr(CO)_5(CS)$ and $Cr(CO)_6$. An attempt to supplement the Raman data for solid $Cr(CO)_5(CSe)$ by recording its ir spectrum in a KBr disc failed because of rapid sublimation of the complex out of the disc.

The observed $\nu(CX)$ $(X = S, Se)$ values from the ir and Raman spectra of all the complexes studied are also presented in Table II.1. As observed previously for the thiocarbonyl complexes[1], the only prominent feature in the ir spectrum of $Cr(CO)_5(CSe)$ in the 1900-700 cm^{-1} region is the peak attributable to $\nu(CSe)$ at 1095.4 cm^{-1}. Furthermore, the weak Raman activity found for $\nu(CS)$[1] extends to $\nu(CSe)$. On the basis of molecular orbital calculations, Lichtenberger and Fenske[6] have accounted for the weak Raman activity of $\nu(CS)$ in metal thiocarbonyls. Similar arguments are expected to apply to $Cr(CO)_5(CSe)$ and these will discussed, together with the electronic structure of these complexes, in Part IV of this thesis.

4.3. Assignment of the 700-40 cm^{-1} Region

In addition to CO and CX stretching vibrations, metal chalcocarbonyls give rise to bands at 700-250 cm^{-1} due to MC(X) stretching and MCX (X=O,S,Se) linear bending modes, while in the 150-40 cm^{-1} region peaks due to CMC deformations are observed. The 700-250 cm^{-1} region is always the most difficult to assign because of the large number of weak and overlapping bands which are present. Although δ(MCO) and ν[MC(O)] modes of the same symmetry interact strongly, it is still necessary to know which frequency is due predominantly to which kind of vibration since a wrong assignment will lead to incorrect values for the potential constants of the symmetry block in question. Fortunately, isotopic substitution at either the carbon or oxygen positions of the carbonyl groups allows one to distinguish between bending and stretching modes[7,8]. On ^{13}CO substitution, ν[MC(O)] modes exhibit only a slight downward shift while δ(MCO) modes show a significant decrease in energy; for $C^{18}O$ substitition, the opposite is true. Also, the shifts observed on changing S to Se help to isolate those peaks involving the MCX (X=S,Se) moiety.

From the correlation diagram in Figure II.1, the vibrations expected in the 700-250 cm^{-1} region for $M(CO)_5(CX)$ are: ν[MC(O)] ($2a_1 + b_1 + e$), ν[MC(X)] (a_1), δ(MCO) ($a_1 + a_2 + b_1 + b_2 + 3e$) and δ(MCX) (e). This region has been assigned previously for $Cr(CO)_5(CS)$, $W(CO)_5(CS)$ and <u>trans</u>-

$W(CO)_4(^{13}CO)(CS)$[1]. The previous assignments are adopted here for the tungsten complexes since no additional data are available. In the case of the chromium thiocarbonyl complex, the extra data obtained from the spectra of the ^{13}C-labelled species, $Cr(^{13}CO)_5(CS)$ and $Cr(CO)_5(^{13}CS)$, as well as the observation of some extra bands for the parent complex lead to some changes in the assignments. Table II.2 contains the data obtained for all the complexes in this region and some of the assignments presented there will now be discussed.

The strong band at 650.4 cm^{-1} in the ir spectrum of $Cr(CO)_5(CS)$ vapour [and at 643.1 cm^{-1} in that of $Cr(CO)_5(CSe)$ vapour] is assigned to both the $a_1(\nu_4)$ and $e(\nu_{17})$ in-plane equatorial $\delta(MCO)$ modes (β). The CH_2Cl_2 solution spectra of the thiocarbonyl complex support this assignment since an ir and a polarized Raman band are observed approximately 2 cm^{-1} apart suggesting that these two modes are almost degenerate. A peak at 669 cm^{-1} in the ir spectrum of the thiocarbonyl complex was previously assigned to the a_1 mode[1] but this peak is most probably due to a small amount of $Cr(CO)_6$ impurity; it appears in the spectra of both the chalcocarbonyls and its intensity, relative to the other modes, varies for different samples of the complexes.

TABLE II.2: Observed Fundamental Modes for $Cr(CO)_5(CX)$, $Cr(^{13}CO)_5(CX)$ (X=S,Se) and $Cr(CO)_5(^{13}CS)$ in the 700-250 cm^{-1} Region

	Vib. No. and Sym.	$Cr(CO)_5(CS)$	$Cr(CO)_5(^{13}CS)$	$Cr(^{13}CO)_5(CS)$	$Cr(CO)_5(CSe)$	$Cr(^{13}CO)_5(CSe)$
IR GAS PHASE	ν_4 : a_1 ν_{17} : e	650.4 s	649.6 s	639.6 s	643.1 s	631.4 s
	ν_{18} : e	512 vw	510 vw	497 vw	509 vw	489 vw
	ν_{19} : e	488 vw	487 vw	475 vw	481 vw	472 vw
	ν_{20} : e	424.6 w	423.2 w	417.8 w	419.8 w	413.9 w
	ν_5 : a_1	421.2 w	420.8 w	415.0 w	406.4 w	400.4 w
	ν_6 : a_1	376.0 w	376.1 w	370 w	370.2 w	363.2 w
	ν_{21} : e	340.7 vw	335.3 vw	335.8 vw	328.3 w	323.8 vw
IR CH_2Cl_2 SOLN	ν_{17} : e	647.2 s	646.4 s	636.4 s	639.1 s	629.2 s
	ν_{18} : e	513 vw	510.5 w	498.6 w	505.4 w	490 vw
	ν_{19} : e	-	485.8 w	475.4 w	480.1 w	467.6 w
	ν_{20} : e	430.4 m	427.4 m	424.3 m	423.1 m	416.8 m
	ν_5 : e	422 mw	422 mw	415.7 mw	408.0 mw	399.8 w
	ν_6 : a_1	378.4 w	377.9 w	372.7 w	372.0 w	365.4 w
	ν_{21} : e	340.5 vw	334.4 vw	333.3 vw	-	-

TABLE II.2: (cont'd)

	Vib. No. and Sym.	$Cr(CO)_5(CS)$	$Cr(CO)_5(^{13}CS)$	$Cr(^{13}CO)_5(CS)$	$Cr(CO)_5(CSe)$	$Cr(^{13}CO)_5(CSe)$
	ν_4 : a_1	649 p	648.4 p	634.8 p	-	626 p ?
	ν_{11} : b_1	512 dp ?	-	499 dp ?	-	-
RAMAN	ν_{19} : e	487 dp ?	-	475 dp ?	-	-
CH_2Cl_2	ν_5 : a_1	421 p	421.1 p	415 p	404 p	398 p
SOLN.	ν_6 : a_1	378.8 p	377.9 p	373.9 p	376.8 p	366.7 p
	ν_7 : a_1	346.6 p	345.9 p	343.7 p	a	a
	ν_4 : a_1	658.2 w	656.2 w	645.4 w	640.2 w	631.4 w
	ν_{17} : e	643.0 w	640.9 w	628.6 w	630.2 w	618.5 w
	ν_{14} : b_2	525 vw	524.7 vw	507.6 vw	528 vw	508 vw
	ν_{11} : b_1	511 w	510 w	495.6 w	505.5 w	490 w
RAMAN	ν_{19} : e	487.6 w	484.7 w	475.0 w	480.5 w	468.4 w
SOLID	ν_{20} : e	-	-	-	425.5 w	419.4 w
	ν_5 : a_1	423.6 ms	423.6 ms	416.9 ms	407.8 ms	401.6 ms
	ν_6 : a_1	380.1 s	380.5 s	373.9 s	379 s	375.8 s
	ν_7 : a_1	351.1 vs	348.2 vs	347.1 vs	280.1 vs	378.4 vs
	ν_{21} : e	339.5 w, sh	334 w, sh	334 w, sh	327.1 m	327.2 m

[a] Solvent absorption.

[b] Sh = shoulder.

From the correlation diagram in Figure II.1 and the assignments of Jones *et al.*[7] for $M(CO)_6$, four modes ($b_1 + b_2 + 2e$) are expected around 500 cm^{-1} for $M(CO)_5(CX)$. All of these should exhibit $\delta(MCO)$ isotopic behaviour and the b_1 and b_2 modes should be Raman-active only. The Raman spectra of the solid chromium chalcocarbonyls and the ir spectra of their vapours exhibit three and two very weak peaks, respectively, in this region. All peaks show $\delta(MCO)$ isotopic behaviour but the two ir bands are coincident with two of the Raman bands. Based on the calculated frequencies for $Cr(CO)_5(CS)$[1], the 488 cm^{-1} peak in the ir and Raman spectra of this complex is assigned to an e $\delta(MCO)$ mode and the Raman band at 525 cm^{-1} is assigned to the b_2 in-plane bend (ν_{14}). The two remaining MCO modes of e and $b_1(\nu_{11})$ symmetries are assumed to be accidently degenerate, and are assigned to a 512 cm^{-1} band in the ir and Raman spectra, respectively. An alternative assignment of this band to a combination mode is precluded by its isotopic behaviour since a combination band in this region would most probably arise from an MC stretching plus a CMC deformation mode; this combination would exhibit $\nu(MC)$ isotopic behaviour because CMC deformations show less than a wavenumber shift on isotopic substitution at the carbon atom[7].

The assignments for the selenocarbonyl complex follow from the thiocarbonyl. The e δ(MCX) mode (ν_{21}) is assigned to the weak peaks at 340.7 and 328.3 cm^{-1} in the ir vapour-phase spectra of the thiocarbonyl and selenocarbonyl complexes, respectively, largely because of the mass effect observed on replacing S by Se.

Assignment of the ν(MC) modes is somewhat simplified by their characteristic Raman intensity in addition to their isotopic behaviour. The three intense bands observed in the Raman spectra of solid $Cr(CO)_5(CS)$ (at 423.6, 380.1 and 351.1 cm^{-1}) and solid $Cr(CO)_5(CSe)$ (at 407.8, 379.0 and 280.1 cm^{-1}) are assigned to the three a_1 ν(MC) modes. The shifts observed in the first and third peaks on changing S to Se suggest that these be assigned to the a_1 axial ν[MC(O)] (ν_5) and the a_1 ν[MC(X)] (ν_7) modes, respectively. The a_1 equatorial ν[MC(O)] mode (ν_6) is expected to be the least perturbed on substitution of an axial ligand and is, therefore, assigned to the middle band. The Raman spectrum of solid $Cr(CO)_5(CSe)$ shows a fourth, weaker band at 425.5 cm^{-1} which is assigned to the e equatorial ν[MC(O)] mode (ν_{20}); in the thiocarbonyl complex, this mode is apparently buried beneath the intense a_1 mode (ν_5). However, in the ir solution spectrum (CH_2Cl_2) of $Cr(CO)_5(CS)$, $\nu_5(a_1)$ and ν_{20}(e) appear as a poorly resolved doublet. The lower-energy component of this doublet is coincident with a polarized Raman band and is, therefore, assigned to $\nu_5(a_1)$.

The previously calculated wavenumbers for $Cr(CO)_5(CS)$[1] predict that the b_1 $\nu[MC(O)]$ mode (ν_{12}) should occur at 390 cm^{-1} yet no band was observed in the Raman spectrum at this position. Assignment of this mode is based, instead, on a binary combination observed in the CS_2 solution ir spectra of $Cr(CO)_5(CS)$ and $Cr(CO)_5(CSe)$ (Table II.4) at 2379 and 2381 cm^{-1}, respectively. Attributing these peaks to binary combinations of the e $\nu(CO)$ mode (ν_{16}) and ν_{12} predicts values of 390 and 389 cm^{-1} for the latter. The previous assignment of the first overtone of the inactive a_2 $\delta(MCO)$ mode (ν_9) to a peak at 728 cm^{-1} in the solid-state Raman spectrum of $Cr(CO)_5(CS)$[1] is substantiated by the observation of a corresponding peak in the spectrum of $Cr(^{13}CO)_5(CS)$ at 706.5 cm^{-1} thus yielding fundamentals possessing the isotopic behaviour characteristic of $\delta(MCO)$ modes; $Cr(CO)_5(CSe)$ and $Cr(^{13}CO)_5(CSe)$ exhibit analogous peaks (Table II.4).

Correlation with $M(CO)_6$ (Figure II.1) reveals that six ($a_1 + b_1 + b_2 + 3e$) CMC deformation modes are expected for the $M(CO)_5(CX)$ molecules. The wavenumbers calculated for these modes using the $Cr(CO)_6$ compliant field[9] are given in Table II.3 together with the observed values. The lack of vapour phase data necessitates the use of data

TABLE II.3: Calculated[a] and Observed Wavenumbers for CMC Deformation Modes

Vib. No. and Sym.	$Cr(CO)_5(CS)$			$Cr(CO)_5(^{13}CS)$			$Cr(^{13}CO)_5(CS)$			$Cr(CO)_5(CSe)$			$Cr(^{13}CO)_5(CSe)$		
	Calc	Raman Solid	IR Comb[d]	Calc	Raman Solid	IR Comb	Calc	Raman Solid	IR Comb	Calc	Raman Solid	IR Comb	Calc	Raman Solid	IR Comb
ν_8 : a_1	93.8	185	98	93.6	104.5	98	93.5	104		86.4	109	86	86.2	109	
ν_{13} : b_1	67.9			67.9			67.4			67.9	68		67.4	67	
ν_{15} : b_2	89.4			84.4			89.1			89			89.1		
ν_{22} : e	94.8	95	98	94.8	95	98	94.4	95		94.7		95.5	94.2		95.6
ν_{23} : e	80.0			80.0			79.6			78.3			77.9		
ν_{24} : e	57.0	56	56.7	57.0		56.9	56.7			48.4	45.5[b]		48.0	45.2[c]	

[a] Details of CO energy-factored force field calculations are given in Section 7.4.

[b,c] Average values for doublets with peaks at 40.0 and 51.0 cm^{-1} and 39.3 and 51.2 cm^{-1}.

[d] These wavenumbers were determined from ir combination bands, see Table II.4.

from solid-state Raman and ir combination spectra, and the assignments are based on the calculated wavenumbers which, as Table II.3 shows, are in close agreement with those observed.

4.4 Overtone and Combination Spectra in the 3000-500 cm^{-1} Region

The proposed assignments for the overtone and combination spectra in the 3000-500 cm^{-1} region of $Cr(CO)_5(CS)$ and $Cr(CO)_5(CSe)$ are given in Tables II.4(a) and (b), respectively. The selection rules for binary overtones and combinations under C_{4v} symmetry are presented in Table II.5. All first overtones are ir allowed, although they are expected to be only weakly ir-active. The ir-inactive modes (a_2, b_1 and b_2) can become allowed only by combining with e modes. All combinations are Raman allowed except for a_2 with a_1. However, combinations and overtones are usually too weak to be observed in Raman solution spectra.

Most of the data reported are from the ir solution (CS_2) spectra of the normal species since insufficient quantities of the labelled compounds were available. As previously observed for the metal hexacarbonyls[10], combinations involving only one CO stretching vibration give rise to bands which are within a few wavenumbers of the sum of the fundamentals.

TABLE II.4(a): Overtone and Combination Spectra of $Cr(CO)_5(CS)$ and its ^{13}C-Labelled Derivatives in the 3000-500 cm^{-1} Region

$Cr(CO)_5(CS)$			$Cr(CO)_5(^{13}CS)$		$Cr(^{13}CO)_5(CS)$	
IR soln.		Raman	IR soln	Raman	Raman	Assignments
CS_2	CCl_4	solid	CCl_4	solid	solid	
2733	2735		2733			$\nu_1+\nu_{17}$; $\nu_1+\nu_4$
2663	2668		2666			$\nu_2+\nu_{17}$; $\nu_2+\nu_4$
			2575			
2515	2523		2518			$\nu_1+\nu_5$; $2\nu_3$; $\nu_1+\nu_{20}$
2445	2448		2448			$2\nu_3(^{13}CS)$; $\nu_2+\nu_5$; $\nu_2+\nu_{20}$
2379	2377		2376			$\nu_{16}+\nu_{12}$
			2352			$\nu_2+\nu_{21}$
	2336		2336			$\nu_7+\nu_{16}$; $\nu_{21}+\nu_{16}$
	2189		2189			$\nu_1+\nu_8$; $\nu_1+\nu_{22}$
1958.5		1976[a]		1976[a]	1928[a]	$\nu_2-\nu_{24}$; a'ν(CO) $Cr(CO)_4(^{13}CO)(CS)$
1904.5						
1157						$\nu_4+\nu_{18}$; $\nu_{17}+\nu_{18}$; $\nu_{17}+\nu_{11}$
		1058±5		1060±5		$2\nu_{14}$

TABLE II.4(a): (cont'd)

$Cr(CO)_5(CS)$			$Cr(CO)_5(^{13}CS)$		$Cr(^{13}CO)_5(CS)$	
IR soln.		Raman	IR soln	Raman	Raman	Assignments
CS_2	CCl_4	solid	CCl_4	solid	solid	
1003						$\nu_{19}+\nu_{18}$; $\nu_{19}+\nu_{14}$
984						$\nu_4+\nu_{21}$; $\nu_{17}+\nu_{21}$
		976.5		971.2	953±5	$2\nu_{19}$
848						$2\nu_5$; $2\nu_{20}$; $\nu_5+\nu_{20}$
824		826		817	808±2	$\nu_{19}+\nu_{21}$
766						$\nu_5+\nu_{21}$; $\nu_{20}+\nu_{21}$
		728		728	706.5	$2\nu_9$
		680.6		669.3	667.8	$2\nu_{21}$
535±5[b]			531±5[b]		529±5[b]	$\nu_{19}+\nu_{24}$

---

[a] From ir gas-phase spectra.

[b] From ir CH_2Cl_2 solution spectra.

TABLE II.4(b): Overtone and Combination Spectra of $Cr(CO)_5(CSe)$ and $Cr(^{13}CO)_5(CSe)$ in the 3000-500 cm^{-1} Region

$Cr(CO)_5(CSe)$			$Cr(^{13}CO)_5(CSe)$		Assignments
IR soln.		Raman solid	IR soln.	Raman solid	
CS_2	CCl_4		CCl_4		
2724					$\nu_1+\nu_4$; $\nu_1+\nu_{17}$
2659					$\nu_2+\nu_4$; $\nu_2+\nu_{17}$
2508.7					$\nu_1+\nu_{20}$; $\nu_2+\nu_{19}$
2462					$\nu_1+\nu_6$
2445					$\nu_2+\nu_{20}$
2432					$\nu_2+\nu_5$
2381					$\nu_{16}+\nu_{12}$
2351					$\nu_2+\nu_{21}$
			2160±2		$2\nu(CSe)$
	2186		2138		$\nu_1+\nu_{22}$
1962	1952	1976^a		1931^a	$\nu_2+\nu_{24}$; a'$\nu(CO)$ $Cr(CO)_4(^{13}CO)CSe$
1353					$\nu_3+\nu_7$
		1181.5			$\nu_3+\nu_8$

TABLE II.4(b): (cont'd)

$Cr(CO)_5(CSe)$			$Cr(^{13}CO)_5(CSe)$		
IR soln.		Raman solid	IR soln	Raman solid	Assignments
CS_2	CCl_4		CCl_4		
1042		1059.9			$\nu_3(^{13}CSe)$
		1008.6			$2\nu_{11}$; $\nu_{19}+\nu_{18}$; $\nu_{19}+\nu_{14}$; $\nu_4+\nu_6$; $\nu_3-\nu_8$
996		990±5			
965	965±2	969			$2\nu_{19}$; $\nu_4+\nu_{21}$
		932			$\nu_5+\nu_{18}$; $\nu_{20}+\nu_{11}$
857					$\nu_{18}+\nu_{21}$
843					$2\nu_{20}$
803	803±3	803±5			$\nu_{21}+\nu_{19}$; $\nu_7+\nu_{18}$; $\nu_{20}+\nu_{12}$
		754		742	$\nu_{20}+\nu_{21}$
739		738			$2\nu_6$; $\nu_4+\nu_{22}$; $\nu_5+\nu_{21}$
		726		704	$2\nu_9$
		651.5		641.7	$2\nu_{21}$

[a,b] See Footnotes to Table II.4(a).

TABLE II.5: Selection Rules for Binary Overtones and Combinations Under C_{4v} Symmetry[a,b]

	a_1	a_2	b_1	b_2	e
a_1	A_1	A_2	B_1	B_2	E
a_2		A_1	B_2	B_1	E
b_1			A_1	A_2	E
b_2				A_1	E
e					$A_1+A_2+B_1+B_2$

[a] The activities are: a_1, e, ir allowed: a_1, b_1, b_2, e, Raman allowed.

[b] For e^2 the symmetry species is $A_1+B_1+B_2$.

This means that reasonable values can be predicted for inactive, or otherwise unobtainable, fundamental modes from the combination spectra.

Most of the combinations in the 3000-2000 cm^{-1} region can be fitted to within ±5 cm^{-1} by allowed combinations of a $\nu(CO)$ and a low-energy mode. Some exceptions are the bands attributed to $2\nu(CX)$ and two bands at 2378 and 2189 cm^{-1} in the CS_2 ir solution spectrum of $Cr(CO)_5(CS)$ and a corresponding pair at 2381 and 2186 cm^{-1} in the spectrum of $Cr(CO)_5(CSe)$. The combination bands near 2380 cm^{-1} can only be satisfactorily accounted for by a combination of the e $\nu(CO)$ mode (ν_{16}) and a low-energy mode; combinations involving other CO stretching modes give rise to values which do not correspond to either calculated[1] or observed fundamentals. Therefore, attributing these peaks to $\nu_{16} + \nu_{12}$ predicts ν_{12} at ∿390 cm^{-1} which is in agreement with the value calculated for this b_1 MC stretching mode[1]. Assigning the combinations at ∿2190 cm^{-1} to ν_1 and a CMC deformation mode leads to a value of ∿98 cm^{-1} for the latter which corresponds to the calculated values for ν_8 and ν_{22} (Table II.3). The assignments for $2\nu(CX)$ will be discussed in the next section.

Most of the combinations in the 2000-500 cm^{-1} region are again readily assigned except those at 1976 and 1928 cm^{-1}

in the ir vapour spectra of $Cr(CO)_5(CS)$ and $Cr(^{13}CO)_5(CS)$, respectively, and at 1976 and 1931 cm^{-1} in the analogous selenocarbonyl derivatives. The close similarity of these bands in the labelled and unlabelled species suggests that they arise from the same sum or difference modes. Ascribing these bands to a difference mode between the a_1 axial $\nu(CO)$ mode (ν_2) and a CMC deformation mode predicts a value of ∿60 cm^{-1} for the latter which, as can be seen from Table II.3, is not in agreement with any of the calculated or observed frequencies for $\delta(CMC)$. Alternative assignments for the labelled complexes are not apparent at the present time, but the peaks in the normal species can be attributed to the low-energy a' mode of cis-$Cr(CO)_4(^{13}CO)(CX)$ [see Table II.1(a)].

4.5. Overtones and Combinations of the CO and CX (X = S, Se) Stretching Modes

Anharmonicity corrections for vibrations involving changes in two or more CO stretching modes are considerably greater than those involving only one CO mode[10]. Consequently, the observed frequencies are a poor approximation to the true harmonic values required in the determination of a general quadratic force field. To calculate harmonic $\nu(CO)$ frequencies, all the anharmonicity constants, $X_{i,j}$, where both i and j refer to CO stretching modes, must be known. All

$X_{i,j}$ values, where i or j refer to a mode other than a CO stretching mode, are considered zero; this approximation is considered reasonable because of the small non-additivity errors found for the combinations in the previous section.

To determine the required $X_{i,j}$ values, it is necessary to observe the associated overtone and combinations bands; for example, $X_{a,b}$ is determined from the combination band, $\nu_a + \nu_b$, and the fundamentals, ν_a and ν_b. For $Cr(CO)_5(CX)$, ten such $X_{i,j}$ exist; thus, a minimum of ten overtones and combinations are required, many of which are ir-inactive and too weak to be observed in the Raman spectra. Fortunately, additional bands were detected in the ternary CO stretching region which allow an almost complete set of $X_{i,j}$ values to be determined for $Cr(CO)_5(CX)$.

Table II.6 lists the bands observed in the binary and ternary CO regions of the ir solution (CS_2) spectra of $Cr(CO)_5(CX)$. Typical survey spectra of these regions are shown for the thiocarbonyl complex in Figures II.5 and II.6. The positions of the ir-inactive fundamentals, ν_{10} (b_1), given in Table II.6 were calculated from CO energy-factored force fields using CS_2 solution data as input. The results of these calculations are given in Table II.1(b) (calculated wavenumbers) and Table II.19 (final force constants). The values obtained for the b_1 modes are considered accurate

TABLE II.6: Observed Wavenumbers in the ν(CO) and ν(CX) Fundamental, Combination and Overtone Regions of $Cr(CO)_5(CX)$ (X=S,Se) from the IR CS_2 Solution Spectra

Assignments	$Cr(CO)_5(CS)$	$Cr(CO)_5(CSe)$
ν_3 : a_1	1261.7 s	1077.4 s
ν_{16} : e	1989.0 vs	1991.8 vs
ν_2 : a_1	2017.0 s	2023.4 s
ν_{10} : b_1	2017.3 (calc)	2021.7 (calc)
ν_1 : a_1	2088.4 ms	2087.6 ms
$2\nu_3$: a_1	2515.6 w	2160 ± 2 vw, sh
$a'(e) + a'(b_1)^a$	3946 ± 4 w, sh	
$2\nu_{16}$: a_1	3966 w, sh	3971 w, sh
$\nu_{10} + \nu_{16}$: e	3991.0 s	3998.1 s
$2\nu_2$: a_1	4011 m, sh	4024 m, sh
$2\nu_{10}$: a_1	4032 w, sh	4039 w, sh
$\nu_1 + \nu_{16}$: e	4068.4 s	4072.1 s
$a'(a_1^{eq}) + a'(a_1^{ax})^a$	4082.7 w, sh	
$\nu_1 + \nu_2$: a_1	4099.5 mw	4105.1 s
$2a'(a_1^{eq})^a$	4158.2 m, sh	4157.8 w, sh
$2\nu_1$: a_1	4172.5 m	4171.2 w
	5694.0 w, br	5685 w, br
	5787.0 w, br	5757 w, br
	5839.2 w, br	5864.1 w, br
$3\nu_{16}$: e	5917.2 w, br	5929 w, br
$2\nu_{10} + \nu_{16}$: e	5989.8 ms	6001 w

TABLE II.6: (cont'd)

Assignments	$Cr(CO)_5(CS)$	$Cr(CO)_5(CSe)$
$2\nu_{10}+\nu_2$: a_1	6043.1 m	
$2\nu_{10}+\nu_1$: a_1	6101.3 w	
$2\nu_1+\nu_{16}$: e	6141.5 s	6145 w
$2\nu_1+\nu_2$: a_1	6176.6 m	
$3\nu_1$: a_1	6250 m	6246.1 w

[a] *cis*-$Cr(CO)_4(^{13}CO)(CX)$ peak [see Table II.1(a)].

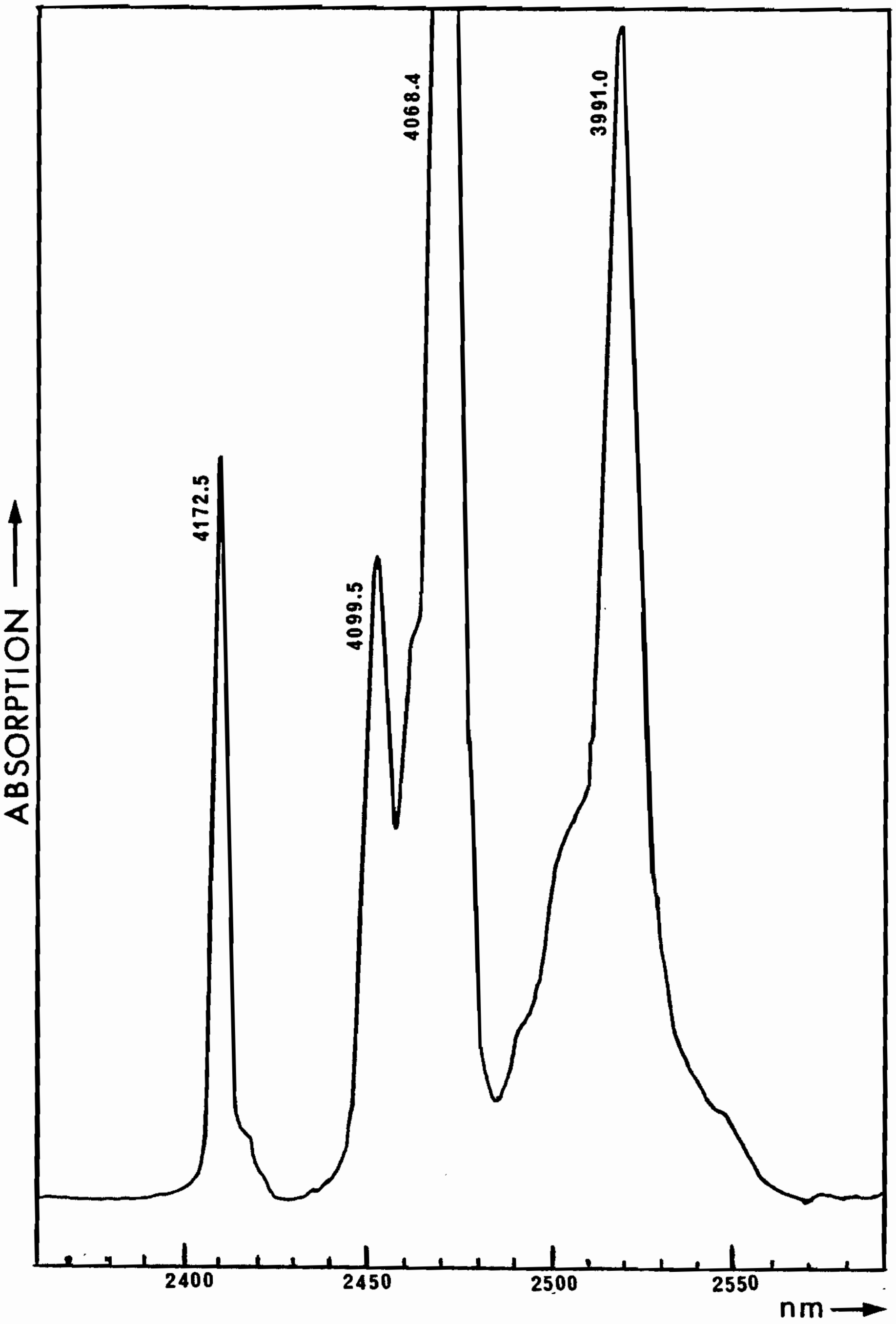

Figure II.5. CO binary stretching region of the ir spectrum of $Cr(CO)_5(CS)$ in CS_2 solution (5-cm solution cells). Positions of the major peaks are given in wavenumbers.

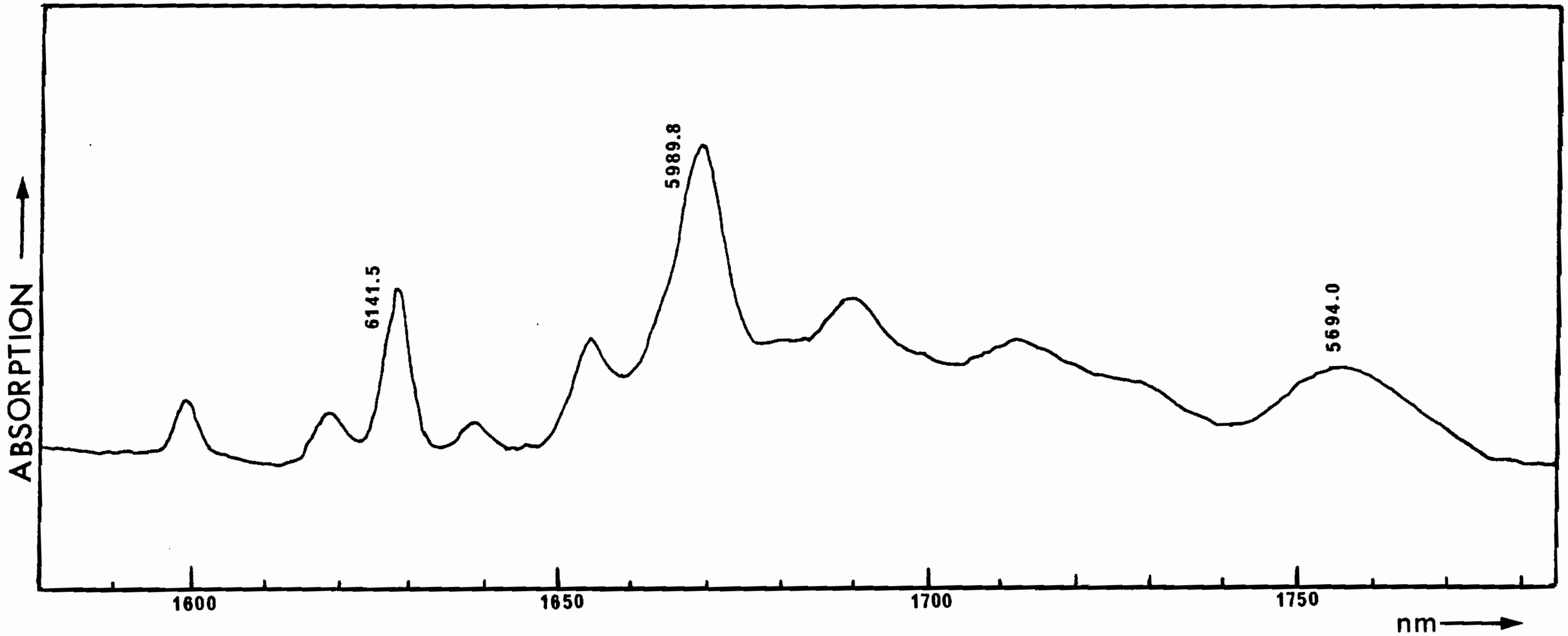

Figure II.6. CO ternary stretching region of the near-ir spectrum of $Cr(CO)_5(CS)$ in CS_2 solution (10-cm solution cells). Positions of the major peaks are given in wavenumbers.

to ±1 cm^{-1} since Cotton et al.[11] have shown that the position of these modes can be accurately predicted for a series of $Mn(CO)_5L$ molecules using CO energy-factored force fields even when the observed frequencies for b_1 are not input into the calculations.

From the proposed assignments (Table II.6) and the survey spectrum of the binary ν(CO) region (Figure II.5), it is apparent that the intensity pattern of $2\nu_1$, $\nu_1 + \nu_2$ and $\nu_1 + \nu_{16}$ closely resembles that of the fundamental ν(CO) region (Figure II.2). This similarity in intensity between the two regions has also been noted for some $Mn(CO)_5L$ complexes[11]. In the ternary region (Figure II.6), the same intensity pattern is again repeated for the three highest-energy bands, and assignment of these bands to $3\nu_1$, $2\nu_1 + \nu_2$ and $2\nu_1 + \nu_{16}$ leads to anharmonicity corrections similar to those obtained from the binary region (Table II.7). The assignments given for the remaining peaks in the binary and ternary spectra are based largely on obtaining reasonable and consistent values for the anharmonicity constants. Also, similar corrections are expected for the thio- and selenocarbonyl complexes because of their similar structures as was shown to be the case for the metal hexacarbonyls[10].

The anharmonicity constants are determined from the relationship[10]:

$$[\sum_i v_i \nu_i]^{obs} - \sum_i v_i[(\nu_i)^{obs}] = \sum_i X_{i,i}(v_2^2 - v_i) + \sum_{i<j} X_{i,j} v_i v_j + \sum_{i<j} g_{i,j} \ell_i \ell_j \qquad \text{(II.1)}$$

where v_i is the vibrational quantum number, $(\nu_i)^{obs}$ the observed fundamental, $X_{i,j}$ the anharmonicity constants and $g_{i,j}$ a function of the internal angular momentum quantum numbers ℓ_i, ℓ_j which can have values equal to v_i, v_{i-2}, ...0 or 1; $g_{i,j}$ is zero if either i or j represents a non-degenerate vibration. If $v_i \geq 2$ for a degenerate mode, the non-zero values possible for $g_{i,j}$ can give rise to splitting of the overtones. However, in the present calculation all $g_{i,j}$ values are considered zero since no splitting of the binary or ternary overtones of ν_{16}(e) is observed, although $3\nu_{16}$ in the thiocarbonyl is very broad indicating some lifting of degeneracy. All the $X_{i,j}$ values calculated using Eq. II.1 are listed in Table II.7. The $X_{i,j}$ values for the isotopic molecules were calculated from an empirical relationship which has been shown to hold for the few cases where sufficient isotopic data are available[12]:

$$X^k_{i,j} = X^\ell_{i,j}\omega^k_i\omega^k_j/\omega^\ell_i\omega^\ell_j \qquad \text{(II.2)}$$

The k and ℓ superscripts refer to labelled and unlabelled species, respectively, and the harmonic frequency, ω_i, is approximated by ν_i, the observed frequency.

Table II.7 also includes the anharmonicity constants

TABLE II.7: Anharmonicity Constants for $Cr(CO)_5(CX)$ (X=O,S,Se) and $Mn(CO)_5Br$

$X_{i,j}$	$Cr(CO)_5(CS)$	$Cr(CO)_5(CSe)$	$X_{i,j}$	$Mn(CO)_5Br^a$	$X_{i,j}$	$Cr(CO)_6^b$
$X_{1,1}$	-2.2	-2.0	$X_{1,1}$	-2.7	$X_{1,1}$	-1.5
$X_{2,2}$	-11.8	-11.4	$X_{2,2}$	-10.4		
$X_{3,3}$	-3.9	-1.5±1				
$X_{10,10}$	-2	-2^d	$X_{9,9}$	7^e	$X_{3,3}$	9
$X_{16,16}$	-8.3	-7.7	$X_{15,15}$	-7.3	$X_{6,6}$	-7
$X_{1,2}$	-6.2	-6.0	$X_{1,2}$	-4.6		
$X_{1,10}$	-8.6	-8.6^d	$X_{1,9}$	-10^e	$X_{1,3}$	-8
$X_{1,16}$	-9.0	-7.3	$X_{1,15}$	-8.2	$X_{1,6}$	-8
$X_{2,10}$	-2	-2^d	$X_{2,9}$	0^e		
$X_{2,16}$	-0.4^c	-0.4^c	$X_{2,15}$	-0.4		
$X_{10,16}$	-15.0	-15.3	$X_{9,15}$	-14.7	$X_{3,6}$	-19

[a] From Ref. 13.

[b] From Ref. 10.

[c] Value transferred from $Mn(CO)_5Br$.

[d] Value transferred from $Cr(CO)_5(CS)$.

[e] Estimated values only, see Ref. 13.

calculated for $Mn(CO)_5Br$[13] and $Cr(CO)_6$[10] to allow a comparison of constants obtained for similar systems. In $Cr(CO)_5(CX)$, ν_1, ν_{10} and ν_{16} involve motions similar to ν_1, ν_9 and ν_{15} of $Mn(CO)_5Br$ and ν_1, ν_3 and ν_6 of $Cr(CO)_6$; thus, the $X_{i,j}$ values reveal that similar types of stretching motion yield similar anharmonicity corrections. For example, $X_{1,1}$ in all four compounds has a value in the neighbourhood of -2. However, one obvious exception stands out; $X_{10,10}$ for $Cr(CO)_5(CX)$ and $X_{3,3}$ for $Cr(CO)_6$ [$X_{9,9}$ for $Mn(CO)_5Br$ is the average of $X_{3,3}$ for $M(CO)_6$[10,13]] have values of -2 and 9, respectively. The $X_{3,3}$ value for $Cr(CO)_6$ was determined from a band observed in the ternary $\nu(CO)$ region of its ir spectrum[10]. Jones and Smith[10] also report combination bands of ν_3 at 4094 ($2\nu_3 + \nu_7$) and 4484 cm^{-1} ($2\nu_3 + \nu_8$). Assuming that $X_{3,7}$, $X_{3,8}$ and $g_{3,3}$ are all zero, values of -1.5 and -4 are calculated for $X_{3,3}$ from these two bands. Hence, the average value of $X_{3,3}$ calculated using these approximations is close to the values assigned to $X_{10,10}$ for the chromium pentacarbonyls. The consistencies observed suggest that anharmonicity constants may be transferred between similar systems with a reasonable degree of certainty, considering the experimental errors possible in estimating peak maxima of weak and oftentimes broad bands.

No previous data on anharmonicity corrections for CS and CSe stretching modes have been reported. Figure II.7 shows the bands observed in the ir CCl_4 solution spectra of $Cr(CO)_5(CS)$ and $Cr(CO)_5(^{13}CS)$ in the region of $2\nu(CS)$. The peak maxima occur at 2523 and 2448 cm^{-1} in the normal species and at 2518 and 2448 cm^{-1} in the labelled species. Although both bands can be accounted for by $\nu(CO)$ and $\nu(MC)$ combination modes [Table II.4(a)], the difference in the relative intensities of the peaks depicted in Figure II.7, together with the observed fundamental frequencies of the $\nu(CS)$ modes [1266.8 and 1228.8 cm^{-1} for $\nu(CS)$ and $\nu(^{13}CS)$, respectively], suggest that the peak at 2523 cm^{-1} in $Cr(CO)_5(CS)$ and at 2448 cm^{-1} in $Cr(CO)_5(^{13}CS)$ should be assigned to the $\nu(CS)$ overtones coincident with the $\nu(CO)$ combination bands. This assignment would give reasonable and consistent values for $X_{3,3}$: -5.3 for the normal complex and -4.8 and -5.0 for the observed and calculated (Eq. II.2) values, respectively, for the labelled species.

The $\nu(CS)$ fundamental and proposed overtone modes were also observed in the CS_2 solution spectrum of the normal species [$2\nu(^{13}CS)$ is obscured by solvent absorption in CS_2] and the value obtained for $X_{3,3}$ (-3.9) was used in the determination of the harmonic frequency, $\omega(CS)$, since all $X_{i,j}$ values for the $\nu(CO)$ modes were determined using CS_2 data.

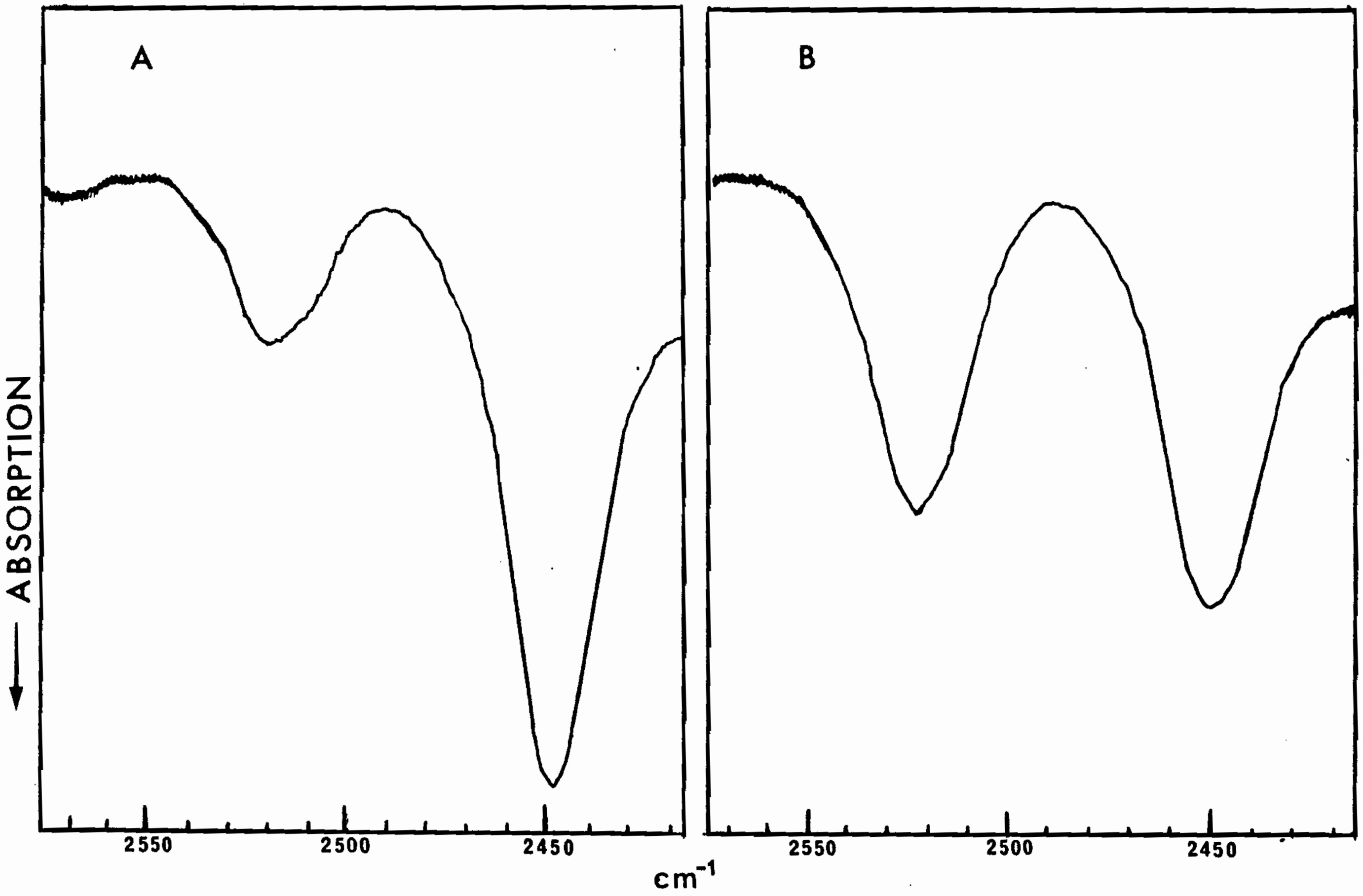

Figure II.7. CS binary stretching regions of the ir spectra of (A) $Cr(CO)_5(^{13}CS)$ and (B) $Cr(CO)_5(CS)$ in CCl_4 solutions (0.2-mm solution cells).

Observation of $2\nu(CSe)$ is more difficult. The fundamental occurs at 1081.5 cm^{-1} in the ir spectrum (CCl_4 solution) of $Cr(CO)_5(CSe)$ indicating that the overtone should be observed at $\sim$2163 cm^{-1}. However, for a concentrated solution of $Cr(CO)_5(CSe)$ this region is dominated by ν_1 whose maximum occurs at 2090.5 cm^{-1}. In $Cr(^{13}CO)_5(CSe)$, ν_1 shifts to 2042.4 cm^{-1} so some features can be discerned in the $2\nu(CSe)$ region as shown in Figure II.8. The well-defined shoulder (at $\sim$2138 cm^{-1}) on ν_1 is assigned to a combination of ν_1 and a CMC deformation mode [Table II.4(b)]; a second, weak and poorly resolved shoulder, barely visible on the high-energy side of the first shoulder, occurs at about 2160±2 cm^{-1}. Ascribing this value to $2\nu(CSe)$ gives $X_{3,3} = -1.5 \pm 1$.

All $X_{i,j}$ values (where $i \neq j$) for $\nu(CX)$ are considered zero since no combinations involving $\nu(CX)$ and $\nu(CO)$ modes are observed and only one band can be attributed to $\nu(CX)$ and a low-energy combination.

The vibrational energy of any level can be determined from[10]:

$$G(v_1, v_2 \ldots.) = \sum_i \omega_i (v_i + \frac{d_i}{2}) + \sum_{i \geq j} X_{i,j} (v_i + \frac{d_i}{2})(v_j + \frac{d_j}{2}) + \sum_{i \geq j} g_{i,j} \ell_i \ell_j \qquad (II.3)$$

where $G(v_1, v_2 \ldots.)$ gives the energy of a vibrational level

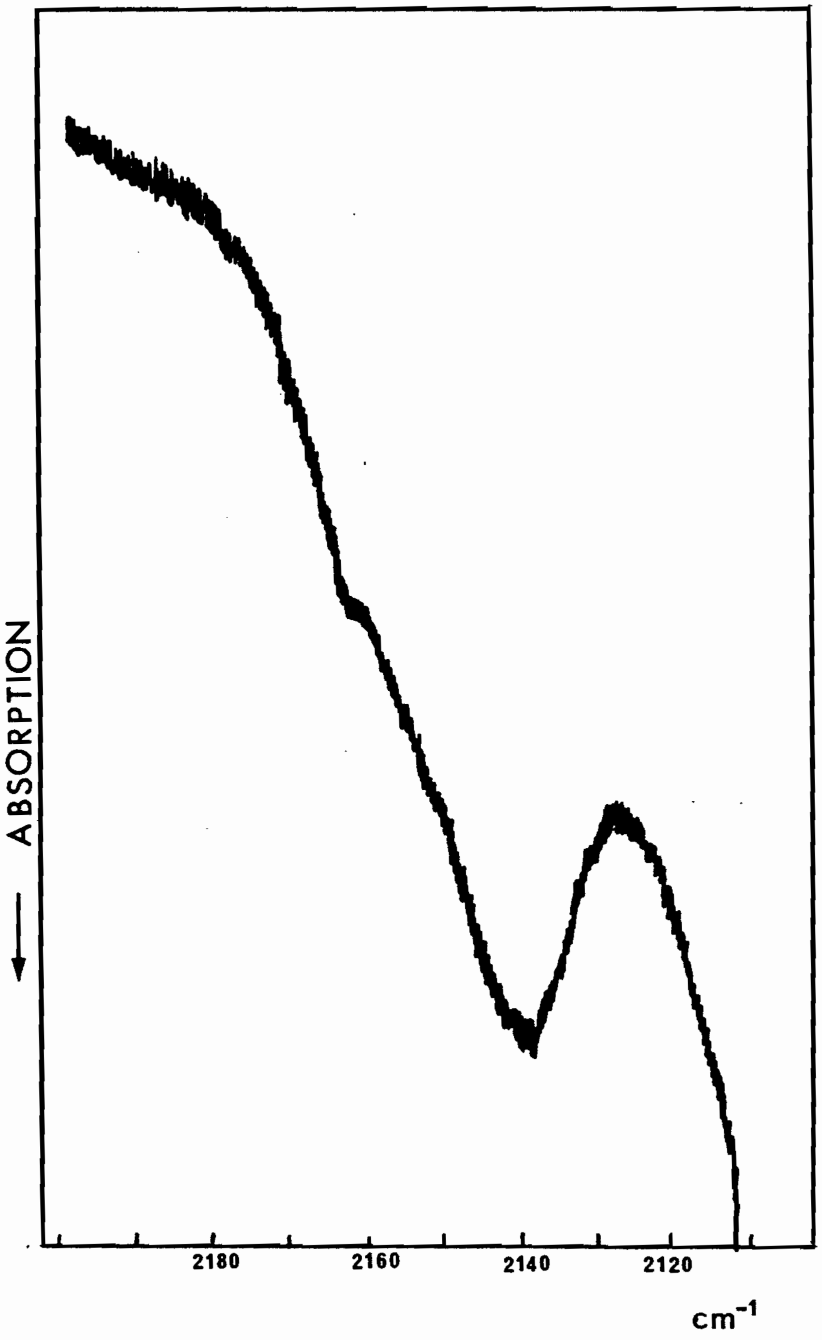

Figure II.8. The CSe binary stretching region of the ir spectrum of $Cr(^{13}CO)_5(CSe)$ in CCl_4 solution (0.2-mm solution cells).

TABLE II.8: Harmonic and Anharmonic ν(CO) and ν(CX) Wavenumbers for $M(CO)_5(CX)$ Vapour

Sym. and Vib. No.	Har.	Anhar.	Har.	Anhar.	Har.	Anhar.
	$Cr(CO)_5(CS)$[a]		$Cr(^{13}CO)_5(CS)$		$Cr(CO)_5(^{13}CS)$	
a_1, ν_1	2118.1	2097.4	2069.6	2050.0	2117.9	2097.2
a_1, ν_2	2060.7	2032.6	2014.4	1987.5	2060.8	2032.7
b_1, ν_{10}	2052.4	2028.1	2006.0	1982.8	-	-
e, ν_{16}	2044.9	2007.8	1999.4	1964.0	2044.8	2007.7
a_1, ν_3	1287.3	1279.5	1287.0	1279.2	1247.4	1240.1
	$Cr(CO)_5(CSe)$		$Cr(^{13}CO)_5(CSe)$			
a_1, ν_1	2116.0	2097.3	2068.0	2050.3		
a_1, ν_2	2064.6	2037.3	2017.7	1991.7		
b_1, ν_{10}	2054.3	2029.7	2008.0	1984.5		
e, ν_{16}	2044.6	2010.0	1998.7	1965.5		
a_1 ν_3	1098.4	1095.4	1096.6	1093.6		
	$W(CO)_5(CS)$[b]		*trans*-$W(CO)_4(^{13}CO)(CS)$			
a_1, ν_1	2123	2102	2118	2102		
a_1, ν_2	2045	2017	2006	1979		
b_1, ν_{10}	2054	2030	2054	2030		
e, ν_{16}	2039	2002	2039	2006		
a_1, ν_3	1294	1286	1292	1284		

[a] Anharmonic b_1 ν(CO) modes (ν_{10}) for all species determined by CO energy-factored force fields (see text).

[b] Anharmonic ν(CO) frequencies for tungsten complexes from Ref. 1.

with vibrational quantum numbers, v_1, v_2 ....; d_i is the degeneracy of fundamental mode with quantum number v_i; $g_{i,j}$ and ℓ_i were defined previously (Eq. II.1). Therefore, the harmonic frequency, ω_i, for any of the four ν(CO) modes of $Cr(CO)_5(CX)$ can be obtained from the equation: $(\nu_i)^{obs} = G(0,0,0,0) - G(1,0,0,0)$, where $(\nu_i)^{obs}$ is the fundamental frequency observed for ν_i. The harmonic frequencies obtained for all the $M(CO)_5(CX)$ molecules are collected in Table II.8. The $X_{i,j}$ values for $Cr(CO)_5(CS)$ were also used for $W(CO)_5(CS)$ since these constants are expected to have similar values in the two complexes as little change occurred in going from Cr to W in $M(CO)_6$[10].

4.6. Experimental

The $Cr(CO)_5(CX)$ (X = S, Se) complexes studied were prepared as outlined in Part I and sublimed prior to use. Small traces of $Cr(CO)_6$ were found in some samples and the extent of this impurity was estimated from the intensity of a band at 668 cm^{-1} in the ir spectrum of the vapour which can be attributed to the t_{1u} δ(MCO) mode (ν_7) of the hexacarbonyl. The presence or absence of $Cr(CO)_6$ impurity cannot be established from the ir ν(CO) region since the ir-active ν(CO) mode (ν_5, t_{1u}) of $Cr(CO)_6$ is hidden under the strong e ν(CO) mode of $Cr(CO)_5(CX)$.

All ir spectra in the 4000-200 cm^{-1} region were recorded on a Perkin-Elmer model 521 grating spectrophotometer. The bands were calibrated against the vibrational-rotational spectra of gaseous CO, NH_3 and HCl, and water vapour[14] (accuracy ±0.5 cm^{-1}). Gas-phase ir spectra were obtained using a 10-cm gas-cell fitted with CsI windows and the CS_2, CH_2Cl_2 and CCl_4 solution spectra were obtained using matched 0.1- and 0.2-mm KBr solution cells. The binary and ternary ν(CO) regions of CS_2 solutions, contained in 1.0- and 5.0-cm matched quartz cells, were measured on a Cary 17 spectrophotometer.

The Raman spectra of the powdered solids and CH_2Cl_2 solutions (in sealed Pyrex capillaries) were recorded on a Jarrell-Ash model 25-300 Raman spectrophotometer using the yellow 568.1-nm line of a Coherent Radiation krypton-ion laser (model 52K) for excitation. The laser power at the samples was ca. 50-100 mW for the solids and 50 mW or less for the solutions. No decomposition of the thiocarbonyl solutions was evident during the period of observation while rapid decomposition of the selenocarbonyl solutions prevented recording of peaks other than the most intense ones. The sampling conditions employed are given in the figure captions. Whenever mentioned in the text, low temperature data were obtained using a closed-cycle helium cryogenic unit (Cryodyne Cryocooler, model 21, Cryogenic Technology Inc., Waltham, Mass.). All the Raman spectra were calibrated against the emission lines of a standard neon lamp and the band positions are generally accurate to ±0.5 cm^{-1}.

Chapter 5

Molecular Compliance Constants

5.1. Interpretation and Advantages of Compliance Constants (Compliants)

Characterization of the molecular potential function in terms of compliance constants was first suggested by Decius[15] and a computer program written by Ottinger[16] allows a least-squares estimate of compliants from vibrational frequencies. Some of the advantages of the use of these constants rather than the more familiar force constants are given in this section, together with their significance in discussions on bonding and electronic structure.

Jones and co-workers have determined compliance constants for several transition metal carbonyl complexes and because of the extensive use of isotopic substitution their results constitute the best estimates of metal carbonyl potential constants. Therefore, reliable data exist for the comparison and transfer of compliants as is frequently done with force constants. In Section 5.2, a survey of compliance-constant calculations for metal carbonyls will be presented.

Before discussing the significance and advantages of compliance constants, the derivation of the secular equation is outlined in "compliance constant" form. The following description is based on the treatise of Ottinger given in Ref. 16. Wilson's GF matrix system is the generally used method of analysis of molecular vibrations in polyatomic systems[17]. In the harmonic oscillator approximation, the potential and kinetic energies are

$$2V = S'FS \qquad (II.4)$$

$$2T = \dot{S}'G^{-1}\dot{S} \qquad (II.5)$$

where S is the vector of internal coordinate displacements, Δi; S' the transpose of S; and $\dot{S}$ the vector of the derivatives of Δi with respect to time. F and G^{-1} are the force constant and kinetic energy matrices, respectively. In terms of normal coordinates, Q, the potential and kinetic energies become

$$2V = Q'\Lambda Q \qquad (II.6)$$

$$2T = \dot{Q}'Q \qquad (II.7).$$

The term Λ is a diagonal matrix with elements $4\pi^2\nu_i^2$ where ν_i is the vibrational frequency of the i^{th} mode. The transformation from normal to internal coordinates is

$$S = LQ \tag{II.8}$$

And substitution of LQ for S in Eqs. II.4 and II.5 gives the following two equations:

$$L'FL = \Lambda \tag{II.9}$$

$$L'G^{-1}L = E \tag{II.10}$$

Simple matrix manipulation of Eqs. II.9 and II.10 yields two possible forms of the secular equation:

$$GFL = L\Lambda \tag{II.11}$$

$$FG(L^{-1})' = (L^{-1})'\Lambda \tag{II.12}$$

The solutions to II.11 and II.12 lead to two forms of the secular determinant:

$$|GF - E\Lambda| = 0 \tag{II.13}$$

$$|FG - E\Lambda| = 0 \tag{II.14}$$

However, the potential energy, V, can be written in an alternative manner. Let us define a generalized force vector $\mathcal{F}$[15] where

$$\mathcal{F} = -FS \tag{II.15}$$

$$\therefore \quad S = -F^{-1}\mathcal{F} = -C\mathcal{F} \tag{II.16}$$

Substitution of S and F in Eq. II.4 gives

$$2V = \mathcal{F}'C\mathcal{F} \tag{II.17}$$

Here C, which equals F^{-1}, is the compliance constant matrix. Equations II.9 and II.10 can be written as $L^{-1}F^{-1}(L^{-1})' = \Lambda^{-1}$ and $L^{-1}G(L^{-1})' = E$ and the corresponding secular equation is $G^{-1}F^{-1}(L^{-1})' = (L^{-1})'\Lambda^{-1}$. If $K = G^{-1}$, $C = F^{-1}$ and $\Phi = \Lambda^{-1}$, the secular equation takes the form

$$KC(L^{-1})' = (L^{-1})'\Phi \qquad (II.18)$$

and the secular determinant is

$$|KC - E\Phi| = 0 \qquad (II.19)$$

As Decius[15] previously pointed out, the compliance matrix $C = F^{-1}$ characterizes the molecule as completely as the force constant matrix F; there are exactly the same number of parameters in C as in F. Furthermore, C is not merely a mathematical tool since its elements have a perfectly legitimate physical interpretation[18,19]. Equation II.17 can be written as

$$2V = \sum_{i,j} C_{i,j}\mathcal{f}_i\mathcal{f}_j \qquad (II.20)$$

where $\mathcal{f}_i$ are the elements of the force vector, $\mathcal{F}$, and represent forces applied to the coordinates, i. If unit force is applied to i the displacement, Δi, is given by $C_{i,i}$ if all $\mathcal{f}_j$ ($j \neq i$) are zero, i.e., the molecule relaxes to a minimum potential energy with i displaced. Therefore, the primary compliance constant, $C_{i,i}$, is a measure of the <u>displacement</u> of coordinate i which takes place as a result of unit force applied to this coordinate while all other coordinates adjust themselves such that a minimum energy configuration is obtained with i displaced. A primary force constant, on the other hand, gives the force required to distort a coordinate a unit amount while holding all other coordinates fixed at their equilibrium configurations. The primary potential constants (force and compliance) thus give a measure of the strength of the bond (or bonds) involved in the internal coordinate.

The off-diagonal or interaction compliants, $C_{i,j}$, give information about changes in the electronic configuration as a given coordinate is distorted. $C_{i,j}$ is a measure of the displacement of coordinate j which results from unit displacement of coordinate i, while the remaining coordinates adjust or relax such that the potential energy is constrained to a minimum. The interaction force constant, $F_{i,j}$, is defined as the force experienced by coordinate j resulting from unit displacement of coordinate i while j and all other coordinates except i remain fixed at their equilibrium values.

One immediate advantage of the use of compliance constants is that they are more directly related to the physically significant interaction coordinates $(j)_i$ than force constants[18-20]. The interaction displacement coordinate $(j)_i$ is defined as the relative displacement of coordinate j required to minimize the potential energy when coordinate i is distorted a unit amount. In terms of compliance constants, the interaction coordinates can be expressed as

$$(j)_i = C_{i,j}/C_{i,i} \qquad \text{(II.21)}$$

No such direct relationship exists between force constants and interaction coordinates[18].

The importance of interaction coordinates is that they relate the potential constants to electronic structure. This has been done in a qualitative manner for the metal hexacarbonyls[9]. In $Cr(CO)_6$, for example, C_{CO}, C_{MC} and $C_{CO,MC}$ are 0.05900, 0.567 and -0.0229 A $mdyn^{-1}$, respectively; thus $(MC)_{CO} = -0.388$ and $(CO)_{MC} = -0.0404$. Stretching a CO bond lowers the energy of its antibonding π orbitals making them more available for metal-to-CO backbonding. This leads to a shortening of the adjacent MC bond, as predicted by the negative interaction constant. Stretching the MC bond, on the other hand, weakens this bond and reduces the π-backbonding to the adjacent CO group resulting in a stronger CO bond.

Although the negative value of the interaction compliant, $C_{CO,MC}$, indicates that if either bond is stretched the other will contract, it does not indicate the difference in the relative displacements of the two bonds, which vary by an order of magnitude depending on whether the CO or MC bond is stretched. Stretching a CO bond greatly increases the strength of the adjacent MC bond, whereas stretching the MC bond has little effect on the CO bond which, in fact, remains almost rigid. The $(j)_i$ values can, therefore, be considered a measure of the change in strength of bond j in the distorted molecule resulting from a weakening of bond i.

Another generally applicable advantage of compliance constants is that they are uniquely defined[15,20]. This is not so for force constants when redundant coordinates are employed since the symmetry force constants for the redundant coordinates are undefined[15,18,20]. An example of coordinates which form a redundant set are the twelve CMC angle increments of the $M(CO)_6$ molecules. Three redundant symmetry coordinates exist for this set[7] which means that three of the symmetry force constants are undefined. Thus, only linear combinations of the CMC valence force constants can be determined[7]. The symmetry compliants for redundant coordinates, on the other hand, are zero. This provides three additional equations which suffice to define all the CMC valence compliants[18]. Consequently, the primary and interaction CMC compliants can be transferred from the $M(CO)_6$ to the $M(CO)_5(CX)$ complexes under investigation in the present study, an impossible situation in the case of force constants.

Finally, unlike the elements of F, those of C are independent of the coordinate system chosen. A comparison of the two force fields derived for the $^{14}NO_2$ and $^{15}NO_2$ molecules[21] serves to illustrate this point. In the General Quadratic Valence Force Field (GQVFF), the internal coordinate set consists of the two NO stretches and the ONO bend, while in the General Quadratic Central Force Field (GQCFF) the third element of the set is the change in the O··O distance. The values obtained for the stretching force constants are, respectively, 10.88 and 1.99 mdyn A^{-1} for GQVFF and 15.51 and 6.6 mdyn A^{-1} for GQCFF. The difference in the force constants is a consequence of their dissimilar definitions; e.g., in a valence force field, F_{NO} is the force required to stretch one NO bond with the remaining NO bond and ONO angle fixed at their equilibrium values. If a central force field is assumed, F_{NO} is again the energy required to stretch one NO bond but with the second NO bond and the O-O distance fixed. C_{NO} and $C_{NO,NO'}$, on the other hand, are 0.1011 and -0.0181 A $mdyn^{-1}$, respectively, in both force fields[18].

Compliants are invariant to the coordinates defining the potential field because on displacement of a given coordinate the distorted molecule is allowed to relax to its potential energy minimum, V_{min}. At V_{min}, Eqs. II.20 and II.16 become, respectively, $2V_{min} = C_{i,i}\delta_i^2$, and $S_i = \Delta i = -C_{i,i}\delta_i$. Combination of these equations gives $2V_{min} = S_i^2/C_{i,i}$; since V_{min} is invariant from one coordinate set to the next, it follows that if S_i is the same in the two sets, then so is $C_{i,i}$. Similarly, $C_{i,j} = S_iS_j/2V_{min}$, so again, if a new set of coordinates is chosen such that S_i and S_j are unaltered, $C_{i,j}$ will be identical in the two systems.

5.2. Survey of Compliance Constant Data for Metal Carbonyl Complexes

One of the chief disadvantages of compliance constants is their unfamiliarity because potential constants for most molecules are reported as force rather than compliance constants. However, in the last decade, Jones and coworkers have advocated the use of compliants and have reported both types of potential constants for the metal carbonyls they have analyzed during this period. The molecules studied include species from each of the three structural types found in simple mononuclear carbonyls: $M(CO)_6$ (M=Cr,Mo,W)[7,9,18], octahedral (O_h); $Ni(CO)_4$[18,22], tetrahedral (T_d); and $Fe(CO)_5$[23], trigonal bipyramidal (D_{3h}). Also, two structurally related, monosubstituted derivatives have been examined: $Co(CO)_3(NO)$[24], tetrahedral (C_{3v}); and $Mn(CO)_5Br$[8], octahedral (C_{4v}). For all these molecules, isotopic substitution at both the carbon and oxygen of the carbonyl groups allowed the vibrational spectra of their isotopic species to be observed directly. Additional substitution at the nitrogen and oxygen of the nitrosyl group in $Co(CO)_3(NO)$ furnished vibrational data for a total of six isotopically-labelled derivatives.

In most complex molecules, the number of potential constants in a general quadratic potential field exceeds the number of fundamental frequencies from which they are determined, with the result that some simplifying approximations about the field must be made. Isotopically substituted molecules provide additional frequencies which serve to reduce, or in some simple cases totally eliminate, the number of approximations necessary. Therefore, the potential fields of the above compounds provide some of the best estimates of potential constants for metal carbonyl systems. An outline of the calculations carried out for these five systems will now be given.

5.2.1. Hexacarbonylmetal(0) Complexes, $M(CO)_6$ (M=Cr,Mo,W)

Compliance constants have been determined for the group VIB metal hexacarbonyls in the vapour phase and in solution[9,18]. The three isotopic species studied for each complex yielded more vibrational frequencies than the number of general-quadratic compliance constants. However, two of the compliants, $C_{CO,\alpha}$ and $C_{CO,\beta}$ (following the nomenclature of Ref. 18, α and β are the CMC and MCO bending modes, respectively), had to be constrained in the least-squares refinement of the compliant field because the frequencies were rather insensitive to these constants. A statistical analysis of the results showed that most of the constants are statistically the same at the 95% confidence level for the three molecules and the two phases. Thus, statistical averages and their standard deviations have been estimated for the compliants. Interaction coordinates for $M(CO)_6$ were determined from these average values. The suitability of the interaction compliants for transfer to other metal carbonyls was emphasized by the authors.

5.2.2. Tetracarbonylnickel(0), $Ni(CO)_4$

The compliants determined for $Ni(CO)_4$ in the gas-phase and in solution are listed in Ref. 18. As in the case of the hexacarbonyls, this problem was overdetermined with frequencies from three isotopic species being available, but again the $C_{CO,\alpha}$ and $C_{CO,\beta}$ interaction compliants had to be constrained since the observed frequencies were insensitive to these constants[22]. A comparison of the potential constants of $Ni(CO)_4$ and $M(CO)_6$ has been previously undertaken[18]. The values obtained for the primary stretching compliants reveal less M-CO π-bonding for the nickel complex but greater M-CO σ-bonding than for $Cr(CO)_6$ or $Mo(CO)_6$ but not $W(CO)_6$. The (CO,CO) interaction of $Ni(CO)_4$ is less than the cis interaction of $M(CO)_6$. This is consistent with the hypothesis that (CO,CO) interactions arise primarily from CO dipole-dipole interactions[7] which are greater at 90° than at 109.5°. The tetrahedral angle also accounts for the (MC,MC) interaction being closer to the cis (90°) rather than the trans (180°) interaction of $M(CO)_6$. Similarly, other primary and interaction constants showed differences explicable on the basis of molecular structure[18].

5.2.3. Pentacarbonyliron(0), $Fe(CO)_5$

The isotopic species examined for $Fe(CO)_5$ did not supply sufficient vibrational data to determine a unique potential field; in the E symmetry block, there are a total of 21 quadratic compliants while only 18 frequencies were observed. This necessitated the transferral of many interaction compliants from the hexacarbonyls. Compliants for 90° and 180° interactions were transferred directly while the 120°

interactions were estimated as $\frac{3}{4}$ of the cis and $\frac{1}{4}$ of the trans hexacarbonyl interactions. Agreement of the calculated values and those estimated from $M(CO)_6$ for constants not constrained is rather good, indicating the validity of transferring interaction constants.

A comparison of the equatorial and axial CO stretching compliants suggests that the Fe-CO π-backbonding is greater in the equatorial carbonyls than in the axial carbonyls. However, the values obtained for the FeC compliants indicate that the FeC bonds are of similar strength. These contradictory results make it difficult to conclude whether or not there is any difference in the equatorial and axial bonding.

5.2.4. Tricarbonyl(nitrosyl)cobalt(0), $Co(CO)_3(NO)$

This molecule has C_{3v} symmetry which gives rise to six a_1, one a_2 and seven e modes. The vibrational spectra of the six isotopic species examined furnish 36 a_1 and 42e frequencies for the evaluation of 21 A_1 and 28E potential constants. Owing to the large dimensions of the A_1 and E symmetry blocks, this system is relatively complex; it therefore presents an interesting problem since such systems are rarely overdetermined. However, despite the abundance of isotopic data, to achieve convergence it was necessary to constrain five and fourteen potential constants in the A_1 and E blocks, respectively. Again, constraints had to be applied to most of the stretch-bend interactions, and in most cases, the constrained values were estimated from the corresponding $Ni(CO)_4$ values. The final potential field indicates that the total backbonding for cobalt is greater than that for nickel, which, considering the smaller positive charge on the nucleus of cobalt, is not surprising. The (CO,CO), (MC,MC) and (MC,CO) interactions are about the same in the two complexes. The most interesting result, however, is the negligible interaction of MN and NO stretches despite the large amount of π-backbonding to the NO ligand. To account for this, changes in the σ-bonding as well as in π-backbonding were considered. Thus, when the NO bond is stretched, the 5σ and 2π orbitals decrease in energy leading to decreased M-N σ-overlap but increased M-N π-overlap. In $Co(CO)_3(NO)$, these two effects must cancel each other to a large extent resulting in negligible (MN,NO) interaction, whereas in the MCO moiety, changes in the π-overlap predominate and a moderately large (MC,CO) interaction is observed.

5.2.5. Bromopentacarbonylmanganese(I), $Mn(CO)_5Br$

$Mn(CO)_5Br$ (C_{4v}) is one of the most complex molecules for which a precise normal coordinate analysis has been attempted. Vibrational data, from the three isotopic species studied, give only $21a_1$ and 24e frequencies to solve for the $28A_1$ and 36E potential constants present in the two largest symmetry blocks. Thus, lowering the symmetry from O_h to C_{4v} in an octahedral complex results in such a large increase in the number of general quadratic potential constants that vibrational analysis would be impossible in the absence of suitable constraints.

In the A_1 block many of the interaction compliants were held fixed at the $M(CO)_6$ values, particularly the stretch-bend interactions. Extensive mixing of the CMC, CMBr and MCO bending modes prevented any refinement of the interaction constants, except for the (MC,CO) interaction, in the E block. Furthermore, it was found necessary to adjust manually the CMC and CMBr primaries to obtain a fit of the observed frequencies. Hence, correlating differences in bending potential constants between $Mn(CO)_5Br$ and $M(CO)_6$ with differences in molecular structure is pointless since the majority of relations defining these constants come from the rather inexact E symmetry block calculation. The primary stretching compliants, however, indicate an overall decrease in the π-backbonding in this system compared to $M(CO)_6$, while the axial CO bond strength is preferentially reduced on ligand substitution. The (CO,CO), (MC,CO) and (MC,C'O') interactions are similar to those found in the hexacarbonyls. As predicted[8], the large [MnBr, MnC(axial)] interaction is found to be the most significant interaction of the MnBr moiety.

The difficulties encountered in the refinement of the potential field of $Mn(CO)_5Br$ clearly indicate that unless suitable constraints can be estimated for a large number of potential constants a final converging field may never be obtained for molecules of this complexity. The equally complex $M(CO)_5(CX)$ (M=Cr,W; X=S,Se) systems studied in the next two chapters fully exploit the advantages of potential constant transferability between closely related systems.

Chapter 6

Compliance Constant Calculations

6.1. Outline of Computer Methods

A brief description of the programmed computations employed in solving the vibrational secular equation (Eq. II.18) and in the least-squares refinement of the compliant field to fit the observed fundamental frequencies will be presented in this chapter. For a detailed and comprehensive analysis of the operation of computer programs similar to those used here, Ref. 25 should be consulted. Figure II.9 shows a flow diagram of the procedure followed.

The use of symmetry coordinates rather than internal coordinates in Eqs. II.4 and II.5 results in the factorization of the C and G matrices into blocks of smaller matrices which can be treated separately as there are no

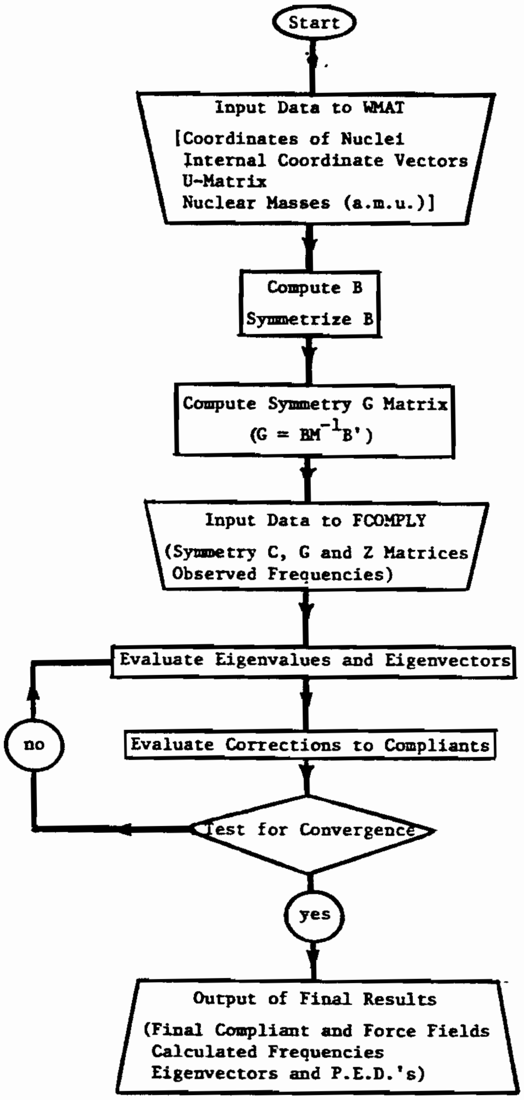

Figure II.9. Flow diagram of the computational procedure used in the normal co-ordinate analysis.

cross terms between the blocks[26]. This speeds up and simplifies the calculations considerably. Thus, for each symmetry block, a G and a C matrix must be determined.

The G matrix is a function of atomic distances and masses. The program, WMAT[27], computes G from the cartesian coordinates of the nuclei, the internal coordinate vectors, the U matrix (i.e., transformation from internal to symmetry coordinates) and the nuclear masses. WMAT first computes the B matrix, which is the transformation from cartesian to internal coordinates, for any of the six Wilson internal coordinates[26], and after symmetrization of this matrix, the symmetry G matrix is obtained from $G = BM^{-1}B$, where M is a diagonal matrix of the atomic masses.

A second program, FCOMPLY, is employed to solve the secular equation in compliance constant form (Eq. II.18) and to least-squares fit the initial compliant field to the observed frequencies (FCOMPLY is an abbreviated version of COMPLY[16] modified to accept frequency data only). The input to FCOMPLY includes the symmetry G and C matrices, the observed frequencies and the Z matrix. This latter matrix is a linear transformation such that

$$C_{k,l} = {}_{i}C'_{i}Z_{kl,i} \qquad \text{(II.22)}$$

where the C'_i are a set of independent compliants of which each $C_{k,l}$ is a linear combination. This kind of transformation is introduced in order to relate the elements of C to each other, thereby reducing the number of independent compliants.

FCOMPLY first solves Eq. II.18 using the input symmetry C and G matrices (K in Eq. II.18 is the inverse of G) to give the calculated eigenvalues, Φ_i^{calc} and the L matrix. A non-linear least-squares adjustment of the compliant field is then performed until the difference in the observed and calculated eigenvalues is acceptable. The changes to the compliance constants are given by

$$\Delta C' = JZ\Delta\Phi \qquad \text{(II.23)}$$

where $\Delta C'$ is a column vector of the corrections to the n independent compliance constants, C_i'; JZ is the Jacobian matrix whose elements form an array of partial derivatives, $(JZ)_{i,j} = \partial\Phi_i/\partial C_j'$; and $\Delta\Phi_i = \Phi_i^{obs} - \Phi_i^{calc}$. The elements of JZ are calculated from the eigenvectors as $\partial\Phi_i/\partial C_j = \sum_{kl} (L^{-1}_{k,i})'(L^{-1}_{l,i})'Z_{kl,j}$ [16]. Thus, once the solution to the secular equation is obtained, the corrections to the compliants may be determined from Eq. II.23. Using the corrected compliants, the process is repeated until convergence is obtained. The criterion used for convergence in the present calculations is that the correction for each compliant be equal to or less than 1% of that compliant.

The output from FCOMPLY includes the final compliant and force fields with estimated errors for the refined compliants, the JZ matrix, the eigenvectors and potential energy distribution.

6.2. Input

The cartesian coordinates of the nuclei were determined from the MC and CO bond lengths used by Jones *et al.*[7] for $Cr(CO)_6$ and $W(CO)_6$ with one exception. The value reported for CO in $Cr(CO)_6$ is 1.171 A[4(a)]. However, if this value is used to calculate the G matrix element for the t_{1g} frequency the corresponding force constant (obtained for all three isotopic species) does not agree with that published, the calculated and published values being 0.384 and 0.375±0.0001 mdyn A^{-1}, respectively. A more recent study[4(b)] reports a CO bond length of 1.141 A in $Cr(CO)_6$ (both values were corrected for thermal motion). If the average of these two values, 1.156 A, and the MC value reported by Jones *et al.*[7] are used to calculate the G matrix element, the resultant force constant equals 0.377 mdyn A^{-1} for all three isotopic frequencies observed for the t_{1g} mode. Furthermore, use of this average CO bond length and Jones' published compliant field[9] gives a better fit to the observed frequencies than that obtained using a

CO bond length of 1.171 A.

Bond lengths for the CX and MC(X) bonds in $M(CO)_5(CX)$ were estimated by multiplying the corresponding hexacarbonyl CO and MC bonds by the CX/CO and MC(X)/MC(O) ratios found in $(\eta^6\text{-}CH_3CO_2C_6H_5)Cr(CO)_2(CX)$ (X=O,S,Se)[28]. The actual bond lengths input into the calculations were: $Cr(CO)_5(CX)$, CO 1.156, CS 1.565, CSe 1.736, CrC(O) 1.916, CrC(S) 1.854, CrC(Se) 1.835; $W(CO)_5(CS)$, CO 1.148, CS 1.556, WC(O) 2.059, and WC(S) 1.996 A. The atomic masses used were those of the most abundant isotopes based on ^{12}C = 12.00000 a.m.u., viz., O = 15.99491, S = 31.97207, Cr = 83.76 and Se = 79.9165 a.m.u.

The internal and symmetry coordinates are the same as those previously published[1] and are shown here in Figure II.10 and Table II.9, respectively. A correction is made in Table II.9 to the β coordinate in the E block (S_{17a}) given in Ref. 1. The generating coordinate used ($\beta_2 + \beta_3$) is not "properly oriented" for the E_a block because it is not invariant under the same symmetry operations as the other generating coordinates in this block[26]. The correct generating coordinate is $\beta_2 - \beta_3$.

The symmetry compliant matrix elements were determined by the method described in Ref. 26 and are presented in Table II.10. The valence compliant labelling used here corresponds to that given for the internal coordinates in

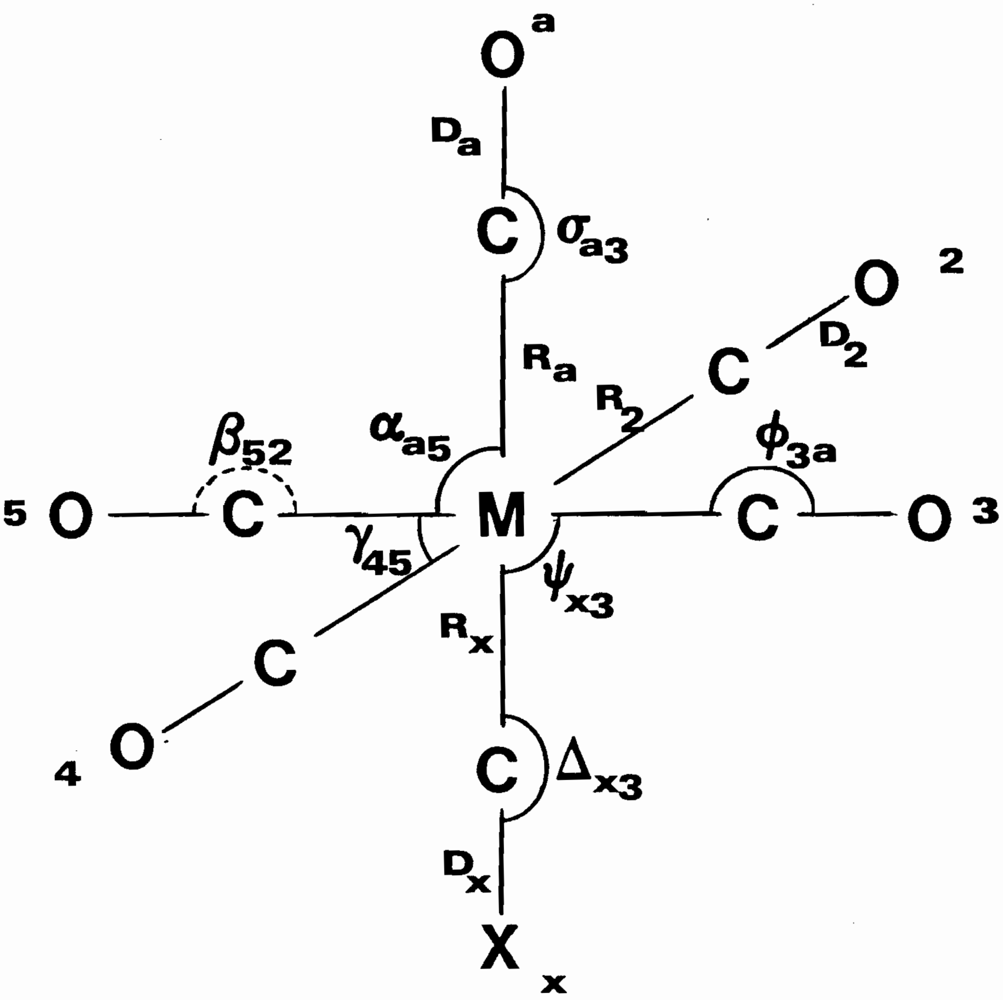

Figure II.10. Internal coordinates of the $M(CO)_5(CX)$ molecules.

TABLE II.9: Symmetry Coordinates for the $M(CO)_5(CX)$ Molecules[a]

A_1 Block

$S_1 = \frac{1}{2}(D_2 + D_3 + D_4 + D_5)$

$S_2 = D_a$

$S_3 = D_x$

$S_4 = \frac{1}{2}(\phi_{2a} + \phi_{3a} + \phi_{4a} + \phi_{5a})$

$S_5 = R_a$

$S_6 = \frac{1}{2}(R_2 + R_3 + R_4 + R_5)$

$S_7 = R_x$

$S_8 = \frac{1}{2}\sqrt{2}(\alpha_{a2} + \alpha_{a3} + \alpha_{a4} + \alpha_{a5}$
$\quad - \psi_{x2} - \psi_{x3} - \psi_{x4} - \psi_{x5})$

A_2 Block

$S_9 = \frac{1}{2}(\beta_{23} + \beta_{34} + \beta_{45} + \beta_{52})$

B_1 Block

$S_{10} = \frac{1}{2}(D_2 - D_3 + D_4 - D_5)$

$S_{11} = \frac{1}{2}(\phi_{2a} - \phi_{3a} + \phi_{4a} - \phi_{5a})$

$S_{12} = \frac{1}{2}(R_2 - R_3 + R_4 - R_5)$

$S_{13} = \frac{1}{2}\sqrt{2}(\alpha_{a2} - \alpha_{a3} + \alpha_{a4} - \alpha_{a5}$
$\quad - \psi_{x2} + \psi_{x3} - \psi_{x4} + \psi_{x5})$

B_2 Block

$S_{14} = \frac{1}{2}(\beta_{23} - \beta_{34} + \beta_{45} - \beta_{52})$

$S_{15} = \frac{1}{2}(\gamma_{23} - \gamma_{34} + \gamma_{45} - \gamma_{52})$

E_a Block

$S_{16a} = \frac{1}{2}(D_2 + D_3 - D_4 - D_5)$

$S_{17a} = \frac{1}{2}(\beta_{23} - \beta_{34} - \beta_{45} + \beta_{52})$

$S_{18a} = 1/\sqrt{2}(\sigma_{a2} + \sigma_{a3})$

$S_{19a} = 1/\sqrt{2}(\Delta_{x2} + \Delta_{x3})$

$S_{20a} = \frac{1}{2}(R_2 + R_3 - R_4 - R_5)$

$S_{21a} = \frac{1}{2}(\phi_{2a} + \phi_{3a} - \phi_{4a} - \phi_{5a})$

$S_{22a} = \frac{1}{2}(\alpha_{a2} + \alpha_{a3} - \alpha_{a4} - \alpha_{a5})$

$S_{23a} = 1/\sqrt{2}(\gamma_{23} - \gamma_{45})$

$S_{24a} = \frac{1}{2}(\psi_{x2} + \psi_{x3} - \psi_{x4} - \psi_{x5})$

---

[a] The internal coordinates and numbering of atoms are shown in Figure II.10.

Figure II.10. The superscripts, c and t, denote cis- and trans-interactions of the equatorial coordinates, respectively. The initial values for the symmetry compliants were calculated from the corresponding $M(CO)_6$ values[9] and the matrix elements listed in Table II.10; these initial estimates are given in Table II.11.

The observed frequencies input to the calculation are collected in Table II.12. Harmonic, vapour-phase frequencies were used in all cases for the ν(CO) and ν(CX) modes, and vapour phase data, when available, were used for the remaining frequencies. In FCOMPLY, the relative weighting of the frequencies is given by $\nu_i^6/(\sigma\nu_i)^2$, where $\sigma\nu_i$ is the standard deviation of ν_i. The weighting scheme used here was simply ν_i^6 as the $\sigma\nu_i$ were considered to be unity. However, certain frequencies, particularly amongst the CMC bending modes, were given zero weight by assigning them a value of zero.

6.3. Refinement of the Symmetry Compliants

For $M(CO)_5(CX)$, there are $36A_1$, $1A_2$, $10B_1$, $3B_2$ and 45E general quadratic compliance constants. The three isotopic species of $Cr(CO)_5(CS)$ yield $16a_1$ and 16e different frequencies while fewer frequencies exist for $Cr(CO)_5(CSe)$ and $W(CO)_5(CS)$ since only two isotopic species

TABLE II.10: Symmetry Compliants for the $M(CO)_5(CX)$ Molecules

---

A_1 Block[a]

$C_{1,1} = C_D + 2C^c_{DD} + C^t_{DD}$

$C_{2,2} = C_{D_a}$

$C_{3,3} = C_{D_x}$

$C_{4,4} = C_\phi + 2C^c_{\phi\phi} + C^t_{\phi\phi}$

$C_{5,5} = C_{R_a}$

$C_{6,6} = C_R + 2C^c_{RR} + C^t_{RR}$

$C_{7,7} = C_{R_x}$

$C_{8,8} = C_\alpha + 2^c_{\alpha\alpha} + C^t_{\alpha\alpha} - C_{\alpha\psi}$
$\quad - 2C^c_{\alpha\psi} - C^t_{\alpha\psi}$

$C_{1,2} = 2C_{DD_a}$

$C_{1,3} = 2C_{DD_x}$

$C_{1,4} = C_{D\phi} + 2C^c_{D\phi} + C^t_{D\phi}$

$C_{1,5} = 2C_{R_a D}$

$C_{1,6} = C_{RD} + 2C^c_{RD} + C^t_{RD}$

$C_{1,7} = 2C_{R_x D}$

$C_{1,8} = 1/\sqrt{2}(C_{D\alpha} + 2C^c_{D\alpha} + C^t_{D\alpha}$
$\quad -C_{D\psi} - 2C^c_{D\psi} - C^t_{D\psi})$

$C_{2,3} = C_{D_a D_x}$

$C_{2,4} = 2C_{D_a \phi}$

$C_{2,5} = C_{R_a D_a}$

$C_{2,6} = 2C_{RD_a}$

$C_{2,7} = C_{R_x D_a}$

$C_{2,8} = \sqrt{2}(C_{D_a \alpha} - C_{D_a \psi})$

$C_{3,4} = 2C_{D_x \phi}$

$C_{3,5} = C_{R_a D_x}$

$C_{3,6} = 2C_{RD_x}$

$C_{3,7} = 2C_{R_x D_x}$

$C_{3,8} = \sqrt{2}(C_{D_x \alpha} - C_{D_x \psi})$

$C_{4,5} = 2C_{R_a \phi}$

$C_{4,6} = C_{R\phi} + 2C^c_{R\phi} + C^t_{R\phi}$

$C_{4,7} = 2C_{R_x \phi}$

TABLE II.10: (cont'd)

$$C_{4,8} = 1/\sqrt{2}(C_{\phi\alpha} + 2C^{c}_{\phi\alpha} + C^{t}_{\phi\alpha} - C_{\phi\psi} - 2C^{c}_{\phi\psi} - C^{t}_{\phi\psi})$$

$$C_{5,6} = 2C_{R_a R}$$

$$C_{5,7} = C_{R_a R_x}$$

$$C_{5,8} = \sqrt{2}(C_{R_a\alpha} - C_{R_a\psi})$$

$$C_{6,7} = 2C_{RR_x}$$

$$C_{6,8} = 1/\sqrt{2}(C_{R\alpha} + 2C^{c}_{R\alpha} + C^{t}_{R\alpha} - C_{R\psi} - 2C^{c}_{R\psi} - C^{t}_{R\psi})$$

$$C_{7,8} = \sqrt{2}(C_{R_x\alpha} - C_{R_x\psi})$$

A_2 Block

$$C_{9,9} = C_{\beta} + 2C^{c}_{\beta\beta} + C^{t}_{\beta\beta}$$

B_1 Block

$$C_{10,10} = C_{D} - 2C^{c}_{DD} + C^{t}_{DD}$$

$$C_{11,11} = C_{\phi} - 2C^{c}_{\phi\phi} + C^{t}_{\phi\phi}$$

$$C_{12,12} = C_{R} - 2C^{c}_{RR} + C^{t}_{RR}$$

$$C_{13,13} = C_{\alpha} - 2C^{c}_{\alpha\alpha} + C^{t}_{\alpha\alpha} - C_{\alpha\psi} + 2C^{c}_{\alpha\psi} - C^{t}_{\alpha\psi}$$

$$C_{10,11} = C_{D\phi} - 2C^{c}_{D\phi} + C^{t}_{D\phi}$$

$$C_{10,12} = C_{RD} - 2C^{c}_{RD} + C^{t}_{RD}$$

$$C_{10,13} = 1/\sqrt{2}(C_{D\alpha} - 2C^{c}_{D\alpha} + C^{t}_{D\alpha} - C_{D\psi} + 2C^{c}_{D\psi} - C^{t}_{D\psi})$$

$$C_{11,12} = C_{R\phi} - 2C^{c}_{R\phi} + C^{t}_{R\phi}$$

$$C_{11,13} = 1/\sqrt{2}(C_{\phi\alpha} - 2C^{c}_{\phi\alpha} + C^{t}_{\phi\alpha} - C_{\phi\psi} + 2C^{c}_{\phi\psi} - C^{t}_{\phi\psi})$$

$$C_{12,13} = 1/\sqrt{2}(C_{R\alpha} - 2C^{c}_{R\alpha} + C^{t}_{R\alpha} - C_{R\psi} + 2C^{c}_{R\psi} - C^{t}_{R\psi})$$

B_2 Block

$$C_{14,14} = C_{\beta} - 2C^{c}_{\beta\beta} + C^{t}_{\beta\beta}$$

$$C_{15,15} = C_{\gamma} - 2C^{c}_{\gamma\gamma} + C^{t}_{\gamma\gamma}$$

$$C_{14,15} = 2(C_{\gamma\beta} + C^{c}_{\gamma\beta})$$

TABLE II.10: (cont'd)

E Block

$C_{16,16} = C_{D} - C^{t}_{DD}$

$C_{17,17} = C_{\beta} - C^{t}_{\beta\beta}$

$C_{18,18} = C_{\phi} - C^{t}_{\phi\phi}$

$C_{19,19} = C_{R} - C^{t}_{RR}$

$C_{20,20} = C_{\sigma}$

$C_{21,21} = C_{\Delta}$

$C_{22,22} = C_{\alpha} - C^{t}_{\alpha\alpha}$

$C_{23,23} = C_{\gamma} - C^{t}_{\gamma\gamma}$

$C_{24,24} = C_{\psi} - C^{t}_{\psi\psi}$

$C_{16,17} = C_{D\beta} + 2C^{c}_{D\beta} - C^{t}_{D\beta}$

$C_{16,18} = C_{D\phi} - C^{T}_{D\phi}$

$C_{16,19} = C_{RD} - C^{t}_{RD}$

$C_{16,20} = \sqrt{2}C_{D\sigma}$

$C_{16,21} = \sqrt{2}C_{D\Delta}$

$C_{16,22} = C_{D\alpha} - C^{t}_{D\alpha}$

$C_{16,23} = \sqrt{2}(C_{D\gamma} - C^{t}_{D\gamma})$

$C_{16,24} = C_{D\psi} - C^{t}_{D\psi}$

$C_{17,18} = C_{\beta\phi} - C^{t}_{\beta\phi}$

$C_{17,19} = C_{R\beta} + 2C^{c}_{R\beta} - C^{t}_{R\beta}$

$C_{17,20} = \sqrt{2}C_{\beta\sigma}$

$C_{17,21} = \sqrt{2}C_{\beta\Delta}$

$C_{17,22} = 2C^{c}_{\beta\alpha}$

$C_{17,23} = \sqrt{2}(C_{\gamma\beta} - C^{c}_{\gamma\beta})$

$C_{17,24} = 2C^{c}_{\beta\psi}$

$C_{18,19} = C_{R\phi} - C^{t}_{R\phi}$

$C_{18,20} = \sqrt{2}C_{\phi\sigma}$

$C_{18,21} = \sqrt{2}C_{\phi\Delta}$

$C_{18,22} = C_{\phi\alpha} - C^{t}_{\phi\alpha}$

$C_{18,23} = \sqrt{2}(C_{\phi\gamma} - C^{t}_{\phi\gamma})$

$C_{18,24} = C_{\phi\psi} - C^{t}_{\phi\psi}$

$C_{19,20} = \sqrt{2}C_{R\sigma}$

TABLE II.10: (cont'd)

$C_{19,21} = \sqrt{2}C_{R\Delta}$

$C_{19,22} = C_{R\alpha} - C^{t}_{R\alpha}$

$C_{19,23} = \sqrt{2}(C_{R\gamma} - C^{t}_{R\gamma})$

$C_{19,24} = C_{R\psi} - C^{t}_{R\psi}$

$C_{20,21} = C_{\sigma\Delta}$

$C_{20,22} = \sqrt{2}C_{\sigma\alpha}$

$C_{20,23} = 2C_{\sigma\gamma}$

$C_{20,24} = \sqrt{2}C_{\sigma\psi}$

$C_{21,22} = \sqrt{2}C_{\Delta\alpha}$

$C_{21,23} = 2C_{\Delta\gamma}$

$C_{21,24} = \sqrt{2}C_{\Delta\psi}$

$C_{22,23} = \sqrt{2}(C^{t}_{\alpha\gamma} - C_{\alpha\gamma})$

$C_{22,24} = C_{\alpha\psi} - C^{t}_{\alpha\psi}$

$C_{23,24} = \sqrt{2}(C_{\gamma\psi} - C^{t}_{\gamma\psi})$

---

[a] The subscripts, R, D, etc. refer to the internal coordinates shown in Figure II.10; the superscripts, c and t, represent *cis* and *trans* interactions, respectively, of the equatorial coordinates.

TABLE II.11: Initial Estimates of the Symmetry Compliants for the $M(CO)_5(CX)$ Molecules

$C_{i,j}$: Sym		$Cr(CO)_5(CX)$ (X=S,Se)	$W(CO)_5(CS)$	$C_{i,j}$: Sym		$Cr(CO)_5$ (CX) (X=S,Se)	$W(CO)_5(CS)$
$C_{1,1}$	A_1	0.05695	0.5707	$C_{1,7}$	A_1	0.0025	0.0037
$C_{2,2}$		0.05900	0.05928	$C_{1,8}$		0	0
$C_{3,3}$		0.05900	0.05928	$C_{2,3}$		-0.00051	-0.00053
$C_{4,4}$		2.29	3.22	$C_{2,4}$		-0.01	-0.01
$C_{5,5}$		0.568	0.450	$C_{2,5}$		-0.0229	-0.0221
$C_{6,6}$		0.407	0.335	$C_{2,6}$		0.002	0.004
$C_{7,7}$		0.568	0.450	$C_{2,7}$		0.009	0.008
$C_{8,8}$		1.68	1.61	$C_{2,8}$		-0.011	-0.011
$C_{1,2}$		-0.00154	-0.00168	$C_{3,4}$		0.010	-0.010
$C_{1,3}$		-0.00154	-0.00168	$C_{3,5}$		0.009	0.008
$C_{1,4}$		0	0	$C_{3,6}$		0.0025	0.0037
$C_{1,5}$		0.0025	0.0037	$C_{3,7}$		-0.023	-0.022
$C_{1,6}$		-0.011	-0.010	$C_{3,8}$		0.011	0.011

TABLE II.11: (cont'd)

$C_{i,j}$:	Sym	$Cr(CO)_5(CX)$ (X=S,Se)	$W(CO)_5(CS)$	$C_{i,j}$:	Sym	$Cr(CO)_5(CX)$ (X=S,Se)	$W(CO)_5(CS)$
$C_{4,5}$	A_1	0.28	-0.04	$C_{13,13}$	B_1	3.04	3.37
$C_{4,6}$		0	0	$C_{10,11}$		0	0
$C_{4,7}$		-0.28	0.04	$C_{10,12}$		-0.0161	-0.0176
$C_{4,8}$		0.86	1.30	$C_{10,13}$		0	0
$C_{5,6}$		0.005	-0.013	$C_{11,12}$		0	0
$C_{5,7}$		-0.166	-0.102	$C_{11,13}$		0.523	0.735
$C_{5,8}$		0.258	0.028	$C_{12,13}$		0	0
$C_{6,7}$		0.005	-0.013	$C_{14,14}$	B_2	3.11	2.78
$C_{6,8}$		0	0	$C_{15,15}$		2.04	2.78
$C_{7,8}$		-0.258	-0.028	$C_{14,15}$		0.94	0.92
$C_{9,9}$	A_2	2.66	2.58	$C_{16,16}$	E	0.05951	0.05981
$C_{10,10}$	B_1	0.06003	0.06043	$C_{17,17}$		2.03	2.48
$C_{11,11}$		1.77	1.74	$C_{18,18}$		2.89	2.68
$C_{12,12}$		0.397	0.361	$C_{19,19}$		0.734	0.552

TABLE II.11: (cont'd)

$C_{i,j}$:	Sym	$Cr(CO)_5(CX)$ (X=S,Se)	$W(CO)_5(CS)$	$C_{i,j}$:	Sym	$Cr(CO)_5(CX)$ (X=S,Se)	$W(CO)_5(CS)$
$C_{20,20}$	E	2.46	2.58	$C_{17,19}$	E	0.28	-0.04
$C_{21,21}$		2.46	2.58	$C_{17,20}$		0.184	0.523
$C_{22,22}$		2.20	2.64	$C_{17,21}$		0.184	0.523
$C_{23,23}$		2.36	2.49	$C_{17,22}$		0.12	0.20
$C_{24,24}$		2.20	2.64	$C_{17,23}$		0.693	1.018
$C_{16,17}$		-0.01	-0.01	$C_{17,24}$		0.12	0.20
$C_{16,18}$		0	0	$C_{18,19}$		0	0
$C_{16,19}$		-0.0322	-0.03	$C_{18,20}$		0.156	0.071
$C_{16,20}$		-0.0071	-0.0071	$C_{18,21}$		-0.156	-0.071
$C_{16,21}$		-0.0071	-0.0071	$C_{18,22}$		0.47	0.46
$C_{16,22}$		-0.008	-0.008	$C_{18,23}$		0	0
$C_{16,23}$		-0.0113	-0.0113	$C_{18,24}$		-0.47	-0.46
$C_{16,24}$		-0.008	-0.008	$C_{19,20}$		0.198	0.028
$C_{17,18}$		0	0	$C_{19,21}$		0.198	0.028

TABLE II.11: (cont'd)

$C_{i,j}$:	Sym	$Cr(CO)_5(CX)$ (X=S,Se)	$W(CO)_5(CS)$
$C_{19,22}$	E	0.183	0.02
$C_{19,23}$		0.258	0.028
$C_{19,24}$		0.182	0.02
$C_{20,21}$		-0.43	-0.10
$C_{20,22}$		0.68	0.83
$C_{20,23}$		0.12	0.20
$C_{20,24}$		0.014	0.184
$C_{21,22}$		0.014	0.184
$C_{21,23}$		0.12	0.20
$C_{21,24}$		0.68	0.834
$C_{22,23}$		-0.48	-0.62
$C_{22,24}$	E	0.16	-0.14
$C_{23,24}$		-0.48	-0.62

TABLE II.12: Wavenumbers Input to Compliant Calculations for the $M(CO)_5(CX)$ Molecules

ν_i		$Cr(CO)_5(CS)$	$Cr(CO)_5(^{13}CS)$	$Cr(^{13}CO)_5(CS)$	$Cr(CO)_5(CSe)$	$Cr(^{13}CO)_5(CSe)$	$W(CO)_5(CS)$[a]	trans-$W(CO)_4(^{13}CO)(CS)$
ν_1	(a_1)	2118.1	2117.9	2069.6	2116.0	2068.0	2123	2118
ν_2		2060.7	2060.8	2014.4	2064.6	2017.7	2045	2006
ν_3		1287.3	1247.4	1287.0	1101.1	1099.3	1294	1292
ν_4		650.4	649.6	639.6	643.1	631.4	569	
ν_5		421.2	421.0	415	406.4	400.4	426	425
ν_6		376.0	376.0	370	370.2	363.2	380	371
ν_7		346.6	345.9	343.7	280.1	278.4	346	345
ν_8		95			85		80	
ν_9	(a_2)	364	364	353	363	352		
ν_{10}	(b_1)	2052.4		2006.0	2054.3	2008.0	2054	2054
ν_{11}		511.0	510.0	495.6	505.5	490	518	
ν_{12}		390			389		412	
ν_{13}					68	67		
ν_{14}	(b_2)	525	526	507.6	528	508	479	

TABLE II.12: (cont'd)

ν_i	$Cr(CO)_5(CS)$	$Cr(CO)_5(^{13}CS)$	$Cr(^{13}CO)_5(CS)$	$Cr(CO)_5(CSe)$	$Cr(^{13}CO)_5(CSe)$	$W(CO)_5(CS)^a$	trans-$W(CO)_4(^{13}CO)(CS)$
ν_{15}	85			85	84		
ν_{16} (e)	2044.9	2044.8	1999.4	2044.6	1998.7	2039	2039
ν_{17}	650.4	649.6	639.6	643.1	631.4	569	
ν_{18}	525	526	507.6	528	508	491	483
ν_{19}	487.6	484.7	475.0	480.5	468.4	463	463
ν_{20}	424.6	423.2	417.8	419.8	413.9	375	
ν_{21}	340.7	335.3	335.8	328.3	323.8	332	331
ν_{22}	95			95			
ν_{23}							
ν_{24}	56			46		50	

[a] Data for tungsten complexes from Ref. 1.

were available for these compounds; therefore, a large number of constants must be constrained in the refinement. Most of the $M(CO)_6$ interaction constants should be directly transferable to $M(CO)_5(CX)$ owing to the isoelectronic nature of CO, CS and CSe. Furthermore, close agreement was found between the observed frequencies and those calculated from the initial values of the compliants in Table II.11 which indicates that the potential fields for the hexacarbonyls and the pentacarbonyl derivatives are quite similar. This prompted us to allow only the diagonal elements to vary, especially since the off-diagonal elements are so numerous.

6.3.1. A_1 Symmetry Compliants

Refinement of the primary compliants alone did not lead to a stable solution for this 8x8 block because the two CO modes, ν_1 and ν_2, could not be fit simultaneously using the input value for $C_{1,2}$. However, when $C_{1,1}$, $C_{2,2}$ and $C_{1,2}$ were refined together, the final values of these compliants varied considerably for the three complexes. Large changes in $C_{1,1}$ from its starting value are not expected since the effect of CX should be mainly *trans*-directed. Thus, a subsequent run, constraining $C_{1,1}$ to its initial value and refining $C_{2,2}$ and $C_{1,2}$, led to rapid convergence and a somewhat reduced value for $C_{1,2}$ for each system. Holding $C_{1,2}$ fixed at this new value and refining all the primaries gave values for $C_{1,1}$ which did not deviate significantly from the initial values. Furthermore, this final compliant set gives eigenvectors for ν_1 and ν_2 in which the relative amplitudes of the two CO symmetry coordinates correspond to the amplitudes predicted on the basis of the Raman polarization of these modes, as will be shown in Section 7.3.

Constraining all the off-diagonal elements (except $C_{1,2}$) requires that interactions such as (CO,CX) and [CX, MC(X)] are equal to the corresponding hexacarbonyl values. However, even with additional data from the isotopic species the (CO,CX) interaction constants remain ill-defined [as was observed previously for (CO,CS)[1]] since varying the (CO,CX) interaction compliant from its initial value to zero produces changes of less than 1 cm^{-1} in the calculated frequencies. The excellent agreement between the observed and calculated frequencies (Table II.14) means that any attempted refinement of the interaction constants, which are sensitive to the frequencies, will only lead to insignificant changes in their values. A substantial adjustment of the off-diagonal elements would necessitate a similar adjustment of the diagonal elements, and since the latter appear reasonable, there is no reason to adjust either.

6.3.2. A_2, B_1 and B_2 Symmetry Compliants

Values of 2.66 and 2.68 A mdyn^{-1} were calculated for the $Cr(CO)_5(CS)$ and $Cr(CO)_5(CSe)$ A_2 compliants, respectively, from the first overtone of the a_2 mode (ν_9) observed in the Raman spectra of the solids. These values are equivalent to the initial value of 2.66 A mdyn^{-1}. No Raman overtone was previously reported for ν_9 in the spectrum of $W(CO)_5(CS)$[1]; therefore, the final value of the A_2 compliant was considered equal to the initial value of 2.58 A mdyn^{-1}.

Rapid convergence of the B_1 and B_2 symmetry blocks was obtained by refining the primary constants only. This was anticipated because the initial field gave calculated frequencies almost identical to those observed for the b_1 and b_2 modes.

6.3.3. E Symmetry Compliants

Again, all interactions were constrained to their associated hexacarbonyl values and the field converged on refining the diagonal elements. The potential energy distributions reveal that most of the modes in this block are strongly mixed; thus, the ready convergence of such a complex problem to less than a wavenumber fit of the observed frequencies indicates that the hexacarbonyl compliant fields are very good, first approximations for the present systems. Ease of convergence in a least-square treatment of parameters generally indicates that the quantities being refined are close to their true values[29].

Chapter 7

Results and Discussion

7.1. Potential Constants

For ease of computation, the potential functions of $M(CO)_5(CX)$ were expressed in terms of symmetry coordinates. The final potential constants output from FCOMPLY are, therefore, the symmetry compliance and symmetry force constants. The physically more meaningful valence potential constants can be derived from these using the relationships given in Table II.10.

7.1.1. Final Symmetry Compliants

The final symmetry compliants and their standard deviations are listed in Table II.13. The latter are estimates of the errors or uncertainties associated with the compliants. These uncertainties are dependent upon the

TABLE II.13: Final Symmetry Compliants for the $M(CO)_5(CX)$ Molecules[a,b]

$C_{i,j}$	: Sym	$Cr(CO)_5(CS)$		$Cr(CO)_5(CSe)$		$W(CO)_5(CS)$	
$C_{1,1}$	(A_1)	0.05694	(3)[c]	0.05695	(4)	0.05751	(20)
$C_{2,2}$		0.05834	(3)	0.05815	(5)	0.05911	(20)
$C_{3,3}$		0.1314	(1)	0.1746	(6)	0.1358	(6)
$C_{4,4}$		2.48	(1)	2.50	(1)	3.22	(2)
$C_{5,5}$		0.581	(2)	0.617	(2)	0.509	(6)
$C_{6,6}$		0.424	(1)	0.438	(1)	0.329	(2)
$C_{7,7}$		0.487	(2)	0.452	(3)	0.328	(5)
$C_{8,8}$		1.65	(5)	1.63	(10)	1.76	(23)
$C_{1,2}$		-0.00101	(2)	-0.00091	(3)	-0.00087	(20)
$C_{9,9}$	(A_2)	2.66		2.68		2.58	
$C_{10,10}$	(B_1)	0.05960	(3)	0.05946	(2)	0.05944	(0)
$C_{11,11}$		1.77	(0)	1.81	(0)	1.75	(0)
$C_{12,12}$		0.397	(1)	0.399	(1)	0.358	(0)
$C_{13,13}$		[3.04]		[3.04]		[3.37]	
$C_{14,14}$	(B_2)	3.19	(1)	3.17	(3)	2.85	(0)
$C_{15,15}$		[2.04]		[2.04]		[2.78]	
$C_{16,16}$	(E)	0.05942	(2)	0.05944	(4)	0.05974	(5)
$C_{17,17}$		1.98	(4)	2.04	(15)	2.54	(31)
$C_{18,18}$		2.67	(10)	3.10	(42)	2.64	(25)
$C_{19,19}$		0.729	(17)	0.740	(6)	0.552	(4)
$C_{20,20}$		2.80	(15)	3.08	(73)	2.96	(47)
$C_{21,21}$		2.39	(7)	1.97	(18)	2.56	(35)

TABLE II.13: (cont'd)

$C_{i,j}$: Sym	$Cr(CO)_5(CS)$		$Cr(CO)_5(CSe)$		$W(CO)_5(CS)$	
$C_{22,22}$	2.44	(10)	1.93	(16)	2.31	(42)
$C_{23,23}$	2.35	(2)	2.56	(7)	2.68	(32)
$C_{24,24}$	2.32	(10)	2.63	(24)	2.66	(32)

---

[a] Units are A $mdyn^{-1}$ for stretching compliants and rad^2A^{-1} $mdyn^{-1}$ for bending compliants.

[b] All interaction compliants, except $C_{1,2}$ (A_1), were held fixed at the values given in Table II.11.

[c] Quantities in parentheses are the standard deviations in units of the last digit for the given compliants.

[d] Primary compliants in square brackets were not refined.

differences in the observed and calculated values of the eigenvalues[25]. The calculated values are the least-squares best estimates of the true values and are, in turn, dependent upon the physical "reasonableness" of the theoretical model of the molecular forces. Thus, if the theoretical model approximates the real molecules, the observed and calculated eigenvalues will be in good agreement and the uncertainties in the refined compliants small.

Examination of Table II.13 shows that the errors associated with the compliants for $Cr(CO)_5(CSe)$ are generally larger than those for $Cr(CO)_5(CS)$. This is in part due to the additional vibrational data available from $Cr(CO)_5(^{13}CS)$. Also, the hexacarbonyl field is probably more "transferable" to the thiocarbonyl than the selenocarbonyl complex since substitution of a CO group by CSe should perturb the remainder of the molecule to a greater extent than substitution by CS. The estimated deviations in the $W(CO)_5(CS)$ constants are also larger than those obtained for $Cr(CO)_5(CS)$; this can, once again, be attributed to the greater number of frequencies observed for the chromium complex.

The errors in the frequencies calculated from these final compliant fields are listed in Table II.14. Also

TABLE II.14: Wavenumber Errors for the Fundamental Modes of the $M(CO)_5(CX)$ Molecules (X=S,Se)[a,b]

	ν_i	$Cr(CO)_5(CS)$	$Cr(CO)_5(^{13}CS)$	$Cr(^{13}CO)_5(CS)$	$Cr(CO)_5(CSe)$	$Cr(^{13}CO)_5(CSe)$	$W(CO)_5(CS)$	trans-$W(CO)_4(^{13}CO)(CS)$
a_1	ν_1	-0.1	-0.2	0.6	-0.5	0.5	-0.8	0.8
	ν_2	-0.4	-0.3	0.4	-0.1	0.1	-0.8	0.8
	ν_3	0.0	0.0	-0.3	0.9	-0.9	1.0	-1.0
	ν_4	-0.4	-1.2	1.6	-0.8	0.9	0.0	568.9
	ν_5	-0.3	-0.3	0.7	-0.5	0.4	0.5	425.5
	ν_6	-0.1	0.0	0.0	0.4	-0.4	2.2	-2.6
	ν_7	-0.1	0.6	-0.4	-0.3	0.3	0.2	0.4
	ν_8	1.7	93.1	93.0	-1.0	85.8	0.3	79.7
a_2	ν_9	0.0	0.0	0.0	0.0	0.0	361.6	361.6
b_1	ν_{10}	-0.1	2052.5	1.0	-0.5	0.8	-0.2	-0.2
	ν_{11}	-0.1	-1.1	1.2	-0.6	0.4	0.0	518.0
	ν_{12}	0.0	390.0	383.5	0.0	382.6	0.0	412.0
	ν_{13}	67.8	67.8	67.4	0.2	-0.3	61.1	61.1

TABLE II.14: (cont'd)

	ν_i	$Cr(CO)_5(CS)$	$Cr(CO)_5(^{13}CS)$	$Cr(^{13}CO)_5(CS)$	$Cr(CO)_5(CSe)$	$Cr(^{13}CO)_5(CSe)$	$W(CO)_5(CS)$	trans-$W(CO)_4(^{13}CO)(CS)$
b_2	ν_{14}	-0.6	-0.6	1.0	0.6	-0.3	-0.1	479.1
	ν_{15}	89.0	89.0	88.7	-4.1	88.8	81.3	81.3
e	ν_{16}	-0.1	-0.2	0.3	0.0	0.0	0.0	0.0
	ν_{17}	-0.6	0.5	-0.2	0.2	-0.3	0.0	565.3
	ν_{18}	-0.3	-0.2	0.3	0.0	-0.2	-0.2	0.2
	ν_{19}	0.2	0.4	-0.5	1.0	-0.8	-0.2	0.3
	ν_{20}	-0.4	0.6	-0.2	-0.1	0.1	0.0	374.7
	ν_{21}	-0.4	0.0	0.5	-1.2	1.2	-0.9	0.8
	ν_{22}	1.7	93.2	92.8	0.6	94.0	83.2	83.1
	ν_{23}	79.1	79.1	78.7	77.1	76.7	70.4	70.4
	ν_{24}	-0.4	56.3	56.1	-0.4	46.1	-1.1	51.0

---

[a] Error in $\nu_i = \nu_i(\text{obs}) - \nu_i(\text{calc})$.

[b] Calculated frequencies are given for the ν_i not input to the refinement.

given are the calculated values for those modes which were assigned input values of zero.

7.1.2. Valence Potential Constants

The valence compliance and force constants calculated from the refined symmetry constants are presented in Table II.15. The estimated errors in the valence compliants were obtained from those of the symmetry compliants using the usual relations for the propagation of errors[30]. No errors were calculated for some of the CMC bending compliants since the corresponding symmetry compliants were constrained in the refinements. It should be emphasized, however, that a comparison of the errors estimated for the $M(CO)_6$ and $M(CO)_5(CX)$ molecules is meaningless. For example, larger errors were obtained for the $Cr(CO)_6$ compliants compared to those of $Cr(CO)_5(CS)$ because the number of degrees of freedom (m-n; m=number of observed frequencies, n=number of compliants refined)[25] in the refinement of the thiocarbonyl compliant field greatly exceeded that in the hexacarbonyl refinement as all off-diagonal elements were constrained in the former.

In terms of the valence constants, holding all off-diagonal symmetry compliants fixed means that only interactions within symmetry-equivalent sets of internal

TABLE II.15(a): Valence Compliance Constants for the $M(CO)_5(CX)$ Molecules and the $M(CO)_6$ Equivalents (X=S,Se; M=Cr,W)[a]

C^b	$Cr(CO)_6$[c,d]	$Cr(CO)_5(CS)$	$Cr(CO)_5(CSe)$	$W(CO)_6$[c]	$W(CO)_5(CS)$
C_D	0.05900 (8)	0.05885 (1)	0.05882 (2)	0.05928 (6)	0.05911 (6)
C_{D_a}	0.05900 (8)	0.05834 (3)	0.05815 (5)	0.05928 (6)	0.05901 (20)
C_{D_x}	-	0.1314 (1)	0.1756 (6)	-	0.1358 (6)
C_R	0.568 (37)	0.570 (8)	0.580 (3)	0.450 (4)	0.448 (3)
C_{R_a}	0.568 (37)	0.581 (2)	0.617 (2)	0.450 (4)	0.509 (6)
C_{R_x}	-	0.487 (2)	0.452 (3)	-	0.328 (5)
C^c_{DD}	-0.00077 (7)	-0.00066 (1)	-0.00063 (2)	-0.00084 (3)	-0.00048 (5)
C^t_{DD}	-0.00051 (8)	-0.00057 (1)	-0.00062 (2)	-0.00053 (6)	-0.00063 (6)
C_{DD_a}	-0.00077 (7)	-0.00051 (1)	-0.00045 (2)	-0.00084 (4)	-0.00059 (10)

TABLE II.15(a): (cont'd)

C^{b}	$Cr(CO)_6^{c,d}$	$Cr(CO)_5(CS)$	$Cr(CO)_5(CSe)$	$W(CO)_6^{c}$	$W(CO)_5(CS)$
C^{c}_{RR}	0.00256 (68)	0.00674 (0)	0.00955 (0)	-0.00633 (38)	-0.00713 (0)
C^{t}_{RR}	-0.166 (37)	-0.159 (8)	-0.161 (3)	-0.102 (4)	-0.104 (3)
C_{β}	2.46 (33)	2.45 (2)	2.49 (8)	2.58 (20)	2.63 (16)
C_{ϕ}	2.46 (33)	2.40 (5)	2.63 (21)	2.58 (20)	2.56 (12)
C_{σ}	2.46 (33)	2.80 (15)	3.08 (73)	2.58 (20)	2.96 (47)
C_{Δ}	-	2.39 (7)	1.97 (18)	-	2.57 (35)
$C^{c}_{\beta\beta}$	-0.11 (14)	-0.13 (0)	-0.12 (0)	-0.05 (0)	-0.05 (0)
$C^{t}_{\beta\beta}$	0.43 (33)	0.47 (2)	0.43 (8)	0.10 (20)	0.09 (16)
$C^{c}_{\phi\phi}$	0.13 (30)	0.18 (0)	0.17 (0)	0.37 (10)	0.37 (0)
$C^{t}_{\phi\phi}$	-0.43 (33)	-0.27 (5)	-0.47 (21)	-0.10 (20)	-0.08 (12)

TABLE II.15(a): (cont'd)

C^b	$Cr(CO)_6{}^{c,d}$		$Cr(CO)_5(CS)$		$Cr(CO)_5(CSe)$		$W(CO)_6{}^c$		$W(CO)_5(CS)$	
$C_\alpha - C^t_{\alpha\alpha}$	2.20	(41)	2.44	(10)	1.93	(16)	2.64	(25)	2.31	(42)
$C_\psi - C^t_{\psi\psi}$	2.20	(41)	2.32	(10)	2.63	(24)	2.64	(25)	2.66	(32)
$C_\gamma - C^t_{\gamma\gamma}$	2.36	(37)	2.35	(2)	2.56	(7)	2.49	(23)	2.68	(32)
$C_\alpha - C_{\alpha\psi}$	2.20	(41)	2.30	e	2.10		2.64	(25)	2.71	
$C^c_{\alpha\alpha} - C^c_{\alpha\psi}$	-0.34	(24)	-0.34		-0.34		-0.44	(10)	-0.40	
$C^t_{\alpha\alpha} - C^t_{\alpha\psi}$	0.16	(41)	0.16		0.16		0.14	(25)	0.13	

---

[a] Units are given in Footnote a, Table II.13.

[b] The subscripts and superscripts are explained in Footnote a, Table II.10.

[c] $M(CO)_6$ compliants from Ref. 9.

[d] See Footnote c, Table II.13.

[e] No errors were estimated for these constants, see text.

TABLE II.15(b): Valence Force Constants for the $M(CO)_5(CX)$ Molecules and the $M(CO)_6$ Equivalents (X=S,Se; M=Cr,W)[a]

F^b	$Cr(CO)_6$[c]	$Cr(CO)_5(CS)$[d]	$Cr(CO)_5(CSe)$	$W(CO)_6$[c]	$W(CO)_5(CS)$
F_D	17.24	17.28	17.28	17.22	17.28
F_{D_a}	17.24	17.42	17.47	17.22	17.24
F_{D_x}	-	7.677	5.768	-	7.455
F_R	2.08	2.04	2.00	2.36	2.41
F_{R_a}	2.08	2.03	1.90	2.36	2.13
F_{R_x}	-	2.45	2.66	-	3.31
F^c_{DD}	0.21	0.18	0.16	0.22	0.11
F^t_{DD}	0.02	0.04	0.05	0.00	0.02
F_{DD_a}	0.21	0.13	0.12	0.22	0.15

TABLE II.15(b): (cont'd)

F^b	$Cr(CO)_6{}^c$	$Cr(CO)_5(CS)^d$	$Cr(CO)_5(CSe)$	$W(CO)_6{}^c$	$W(CO)_5(CS)$
F^c_{RR}	-0.19	-0.04	-0.06	0.05	0.06
F^t_{RR}	0.44	0.42	0.41	0.56	0.54
F_β	0.48	0.48	0.47	0.48	0.46
F_ϕ	0.48	0.48	0.44	0.48	0.47
F_σ	0.48	0.41	0.38	0.48	0.41
F_Δ	-	0.48	0.60	-	0.47
$F^c_{\beta\beta}$	0.00	0.00	0.00	-0.01	0.00
$F^t_{\beta\beta}$	-0.09	-0.11	-0.10	-0.08	-0.07
$F^c_{\phi\phi}$	-0.01	-0.02	-0.02	-0.04	-0.05
$F^t_{\phi\phi}$	0.09	0.07	0.10	0.08	0.07

TABLE II.15(b): (cont'd)

F^b	$Cr(CO)_6$ [c]	$Cr(CO)_5(CS)$ [d]	$Cr(CO)_5(CSe)$	$W(CO)_6$ [c]	$W(CO)_5(CS)$
$F_\alpha - F^t_{\alpha\alpha}$	0.57	0.49	0.65	0.50	0.59
$F_\psi - F^t_{\psi\psi}$	0.57	0.53	0.46	0.50	0.50
$F_\gamma - F^t_{\gamma\gamma}$	0.67	0.56	0.50	0.63	0.57
$F_\alpha - F_{\alpha\psi}$	0.57	0.53	0.60	0.50	0.46
$F^c_{\alpha\alpha} - F^c_{\alpha\psi}$	0.08	0.10	0.11	0.14	0.12
$F^t_{\alpha\alpha} - F^t_{\alpha\psi}$	-0.02	0.03	-0.05	0.13	0.11

[a] Units are mdyn A^{-1} for stretching and mdyn A rad^{-2} for bending coordinates.

[b] See Footnote b, Table II.15(a).

[c] $M(CO)_6$ force constants (except CMC bending constants) from Ref. 7; CMC bending force constants from Ref. 1.

[d] No errors estimated for force constants in FCOMPLY.

coordinates were refined. These valence compliants are sometimes referred to as "on-diagonal" interaction constants as they appear in the expressions for the diagonal element of the symmetry C matrix. Likewise, the "off-diagonal" elements of this matrix are linear combinations of the "off-diagonal" interaction compliants which relate to internal coordinates of different symmetry-equivalent sets.

Stretch-Stretch Constants

From Table II.15, it can be seen that substitution of CX for CO in $M(CO)_6$ produces no significant difference in the equatorial CO and MC stretching constants. The main effect of CX is to reduce the axial MC(O) bond strength, as indicated by the larger axial MC(O) and the slightly smaller axial CO compliants in the chalcocarbonyls; this effect is greater in the selenocarbonyl complex than in the thiocarbonyl complex. The MC stretching constants of the substituted ligands show the reverse trend, i.e., $C_{MC(O)} > C_{MC(S)} > C_{MC(Se)}$, which supports the hypothesis that MC(X) π-backbonding increases as X descends the chalcogens[6]. Also, the largely <u>trans</u>-directing effect of the CX ligands is similar to that noted for Br in $Mn(CO)_5Br$[8]. In this complex, however, C_{MC}(axial) < C_{MC}(equatorial) since Br is a poorer π-acceptor than CO.

As mentioned above, constraining the "off-diagonal" interaction constants implies that interactions involving the CX and MC(X) coordinates are identical to the analogous CO and MC(O) interactions. However, it should be noted that constraining a given compliant is not equivalent to constraining the corresponding force constant, e.g., $F_{CX,MC(X)}$ = 0.68, 0.36 and 0.30 mdyn A^{-1} in $Cr(CO)_6$, $Cr(CO)_5(CS)$ and $Cr(CO)_5(CSe)$, respectively. Interactions involving the CX moiety are discussed in Section 7.2 and Part IV after the interaction displacement coordinates (which have greater physical significance) are presented.

The "diagonal" stretch-stretch interactions, which involve the equatorial MCO groups only, do not vary significantly from their corresponding $M(CO)_6$ values. This was partly anticipated as the equatorial system should be only weakly perturbed by the substitution of an axial ligand. Indeed, the transferability of the equatorial interaction compliants suggests that the final field is reliable.

Bend-Bend Constants

The valence potential constants for the bending modes of the $M(CO)_5(CX)$ species are also shown in Table II.15. The equatorial constants, C_β, C_ϕ and their interactions, all fall within the error limits of the corresponding hexacarbonyl values. Those constants which are defined solely in the E block, such as C_{Δ}, are more poorly determined than the rest owing to the complexity of this particular block. The uncertainties in C_{Δ} and C_{σ} [MCX and MCO(axial) linear bending compliants, respectively] indicate that these constants may differ considerably from their true values. Nevertheless, the relative magnitudes of these constants and the corresponding MC(O) and MC(X) constants are similar, as expected, since increasing the strength of the MC(X) bond should increase the rigidity of the MCX fragment.

As in the case of the equatorial linear bending constants, the values for the CMC compliants are all within the error limits of the corresponding $M(CO)_6$ values.

7.2. Interaction Coordinates

Compliance constants are directly related to the interaction displacement coordinates, $(j)_i$, as shown in Section 5.1 (Eq. II.21). The $(j)_i$ represent the relative displacement of coordinate j required to minimize the potential energy when coordinate i is distorted by a unit amount. Table II.16 lists the interaction coordinates for the stretching modes of $M(CO)_5(CX)$ and compares them with

TABLE II.16: Interaction Coordinates for the Stretching Modes of the $M(CO)_5(CX)$ (X=O,S,Se) Molecules[a]

$(j)_i = C_{i,j}/C_{i,i}$[c]	$M(CO)_6$[b]	$Cr(CO)_5(CS)$	$Cr(CO)_5(CSe)$	$W(CO)_5(CS)$
$(D)^c_D$	-0.0129	-0.0113	-0.0107	-0.0082
$(D)^t_D$	-0.0087	-0.0097	-0.0105	-0.0107
$(D)_{D_a} = (D_a)_D$	-0.0129	-0.0087	-0.0077	-0.0100
$(R)^c_R$	e	0.0118	0.0165	-0.0159
$(R)^t_R$	-0.228	-0.279	-0.278	-0.232
$(R)_{R_a}$	e	0.0044	0.0042	-0.0124
$(R)_{R_x}$	e	0.0053	0.0057	-0.0193
$(R_a)_R = (R_x)_R$	e	0.0045	0.0044	-0.0141
$(R_a)_{R_x}$	-0.228	-0.341	-0.367	-0.311
$(R_x)_{R_a}$	-0.228	-0.286	-0.269	-0.200
$(D)_R$	-0.0446	-0.0402	-0.0395	-0.0494
$(D)^c_R = (D_a)_R = (D_x)_R$	0.0040	0.0022	0.0022	0.0042
$(D)^t_R$	0.019	0.0163	0.0160	0.0183
$(D)_{R_a}$	0.0040	0.0022	0.0020	0.0036
$(D)_{R_x}$	0.0040	0.0026	0.0028	0.0057

TABLE II.16: (cont'd)

$(j)_i = C_{i,j}/C_{i,i}$ [c]	$M(CO)_6$ [b]	$Cr(CO)_5(CS)$	$Cr(CO)_5(CSe)$	$W(CO)_5(CS)$
$(D_a)_{R_a}$	-0.00446	-0.0394	-0.0371	-0.0434
$(D_a)_{R_x}$	0.019	0.019	0.020	0.025
$(D_x)_{R_x}$	-0.0446	-0.0470	-0.0501	0.0673
$(D_x)_{R_a}$	0.019	0.0160	0.0151	0.0161
$(R)_D = (R_a)_{D_a}$	-0.401	-0.390	-0.390	-0.374
$(R)_D^c$	0.037	0.022	0.022	0.032
$(R)_D^t = (R_x)_{D_a}$	0.164	0.158	0.158	0.139
$(R)_{D_a} = (R_a)_D = (R_x)_D$	0.037	0.038	0.038	0.030
$(R)_{D_x}$	0.037	0.010	0.007	0.014
$(R_a)_{D_x}$	0.164	0.071	0.053	0.060
$(R_x)_{D_x}$	-0.401	-0.174	-0.131	-0.163

[a] The $(j)_i$ are dimensionless for stretch-stretch interactions.

[b] $M(CO_6)$ (M = Cr, MO or W), values are taken from Ref. 9.

[c] The i and j refer to the interal coordinates given in Figure II.10; the superscripts, c and t, represent *cis* and *trans* interactions, respectively, of the equatorial coordinates.

[d] The MC *cis* interaction coordinates are not statistically equivalent in the three metal hexacarbonyls; this constant equals 0.0041 in the chromium complex and -0.0128 in the tungsten complex[9].

average values reported for the three metal hexacarbonyls[9]. Inspection of this table reveals that the coordinates involving the CX ligand, $(j)_{CX}$ [j = MC(X), MC(O)], vary considerably with X. For example, $[MC(O)]_{CO} = -0.401$ in $M(CO)_6$, $[MC(S)]_{CS} = -0.174$ in $Cr(CO)_5(CS)$ and $[MC(Se)]_{CSe} = -0.131$ in $Cr(CO)_5(CSe)$. The negative value for $[MC(O)]_{CO}$, as explained in Section 5.1, arises because stretching a CO bond lowers the energy of its π^* orbitals making them more available for bonding to the metal thereby causing a decrease in the MC bond length. The interaction coordinates show, however, that there is a significant reduction in the overall change in the MC(X) bond as CX is stretched when X = S or Se. The $(CX)_{MC(X)}$ interaction coordinates, on the other hand, indicate that as X descends the chalcogen group, the change in CX on stretching MC(X) increases.

Trends such as these are obviously a manifestation of the difference in bonding of the three chalcocarbonyl ligands. Thus, an understanding of the electronic structures of the complexes is necessary before a meaningful discussion of the interaction coordinates can be undertaken. In Part IV, the results of some molecular orbital calculations on these molecules are presented, so a detailed discussion of the interaction coordinates is postponed until then.

7.3. Normal Modes

Characterization of the normal modes of vibration of a molecule requires that the contribution of each coordinate (symmetry or internal) to the vibrations be known. The group frequency approximation, which assumes that only one type of coordinate changes during a vibration, is, in general, an over-simplification since a normal mode often involves the displacement of several different coordinates. There are two measures of the contributions of the given coordinates to the normal modes: (a) the relative amplitudes of displacement of each coordinate in the normal vibration (eigenvectors) and (b) the contribution of each coordinate to the total potential energy of the normal vibration [potential energy distribution (P.E.D.)].

The normal coordinates are obtained from the symmetry coordinates by the transformation, $S = LQ$, where S and Q are symmetry and normal coordinate vectors, respectively. Therefore, for an $n \times n$ symmetry block with n normal vibrations we have:

$$\begin{aligned} S_1 &= L_{1,1}Q_1 + L_{1,2}Q_2 \ . \ . \ . + L_{1,n}Q_n \\ S_2 &= L_{2,1}Q_1 + L_{2,2}Q_2 \ . \ . \ . + L_{2,n}Q_n \\ &\vdots \\ S_n &= L_{n,1}Q_1 + L_{n,2}Q_2 \ . \ . \ . + L_{n,n}Q_n . \end{aligned} \tag{II.24}$$

In the k^{th} normal mode, all n coordinates vibrate at the same frequency but with various amplitudes of displacement. The relative values of these amplitudes are given by

$$(S_1)_k/(S_2)_k/..../(S_n)_k = L_{1,k}/L_{2,k}/..../L_{n,k}. \quad \text{(II.25)}$$

The P.E.D. is determined as follows. From Eq. II.6, the total potential energy in terms of the normal coordinates equals $\frac{1}{2}\sum_i Q_i^2\lambda_i$ (all cross terms cancel since $Q_iQ_j=0$). The potential energy, V_k, of the k^{th} normal mode is, therefore, $\frac{1}{2}Q_k^2\lambda_k$. Putting $\lambda_k = \sum_{ij}\sum L_{i,k}L_{j,k}F_{i,j}$ (Eq. II.9) gives $V_k = \frac{1}{2}Q_k^2\sum_{ij}\sum L_{i,k}L_{j,k}F_{i.j}$ which for unit displacement of Q_k becomes

$$V_k = \frac{1}{2}\sum_{ij}\sum L_{i,k}L_{j,k}F_{i,j} \quad \text{(II.26)}$$

Similar equations can be written for the n normal modes, and if each term in the n summations is considered a separate element, an n x n matrix, V, is obtained whose elements are given by

$$V_{ij,k} = L_{i,k}L_{j,k}F_{i,j} \quad \text{(II.27)}$$

For i=j, $V_{ii,k}$ gives the potential energy contribution of symmetry coordinate S_i to the normal coordinate Q_k. For i≠j, $V_{ij,k}$ gives the contribution of the S_i,S_j coordinate interaction to Q_k. Terms with i=j are generally much larger, and if, for a given Q_k, $L_{i,k}^2F_{i,i}$ is the largest term, this frequency is called the characteristic frequency of coordinate i. If there are two or more terms of similar magnitude in the P.E.D. of a normal vibration, then it is said to be a strong mixture of the two or more coordinates involved.

The amplitudes (or eigenvectors) and the P.E.D. are both output from FCOMPLY. However, the P.E.D. is generally favoured over the eigenvectors as the standard method of classification of the normal modes. This is because this method is more often in accord with the empirical description of vibrations (as bond stretches, angle deformations, torsions, etc.) based on their frequencies[31]. Therefore, the P.E.D.'s of all the normal modes of the $M(CO)_5(CX)$ molecules are reported here, whereas only the eigenvectors of the a_1 modes are given. These are included because of their significance in the refinement of the A_1 symmetry block (Section 6.3.1).

7.3.1. Eigenvectors for the a_1 Modes of the $M(CO)_5(CX)$ Molecules

Examination of Table II.17, which lists the eigenvectors for the a_1 fundamental modes of the unlabelled species, shows that these vectors are very similar for all three

TABLE II.17: Eigenvectors of the a_1 Fundamentals of the $M(^{12}CO)_5(^{12}CX)$ Molecules

a_1	ν_k(obs)				$Cr(CO)_5(CS)$				
		L_{1k}	L_{2k}	L_{3k}	L_{4k}	L_{5k}	L_{6k}	L_{7k}	L_{8k}
ν_1	2118.1	0.34	0.17	0.01		-0.10	-0.20	-0.01	
ν_2	2060.7	-0.17	0.34			-0.20	0.10		
ν_3	1287.3	-0.01	-0.01	0.34	0.01	0.01		-0.27	-0.02
ν_4	650.4			-0.02	0.42	0.11		-0.09	-0.28
ν_5	421.2			-0.01	-0.19	0.18		-0.09	0.01
ν_6	376.0				-0.01	-0.01	0.18	-0.02	
ν_7	346.6			0.03	0.05	0.08	0.03	0.11	0.01
ν_8	93.3 (calc)				0.08	0.02		-0.02	0.08

TABLE II.17: (cont'd)

a_1	ν_k(obs)				$Cr(CO)_5(CSe)$				
		L_{1k}	L_{2k}	L_{3k}	L_{4k}	L_{5k}	L_{6k}	L_{7k}	L_{8k}
ν_1	2116.0	0.34	0.17	0.01		-0.10	-0.20	-0.01	
ν_2	2064.6	-0.17	0.34			-0.10	0.10		
ν_3	1101.1		-0.01	0.30	0.02	0.02		-0.29	-0.03
ν_4	643.1			-0.03	0.43	0.11		-0.07	-0.28
ν_5	406.4			-0.01	-0.18	0.19	-0.01	-0.07	
ν_6	370.2	0.01			-0.01		0.18	-0.01	
ν_7	280.1			0.04	0.07	0.06	0.01	0.08	0.03
ν_8	86.0 (calc)				-0.08	-0.02		0.02	-0.08

TABLE II.17: (cont'd)

				W(CO)$_5$(CS)					
a_1	ν_k(obs)	L_{1k}	L_{2k}	L_{3k}	L_{4k}	L_{5k}	L_{6k}	L_{7k}	L_{8k}
ν_1	2123	0.34	0.17	0.02		-0.10	-0.20	-0.01	
ν_2	2045	-0.17	0.34	0.01		-0.20	0.10		
ν_3	1294	-0.01	-0.01	0.33	0.02			-0.26	-0.01
ν_4	569			-0.02	0.43	0.04		-0.03	-0.21
ν_5	426	0.01		0.01		0.02	0.18	0.01	
ν_6	380			0.03	-0.02	0.16	-0.03	0.05	0.01
ν_7	346			-0.03	-0.10	0.11		-0.12	0.01
ν_8	80				0.09				0.08

L_{ik} is the relative amplitude of symmetry coordinate i in the normal mode k. The units of L_{ik} are length for i = 1,2,3,5,6 and 7 and angle bend for 4 and 8.

complexes. In particular, $L_{1,1}$, $L_{1,2}$ and $L_{2,2}$ are identical. Furthermore, their ratios ($-L_{1,2}/L_{1,1} = L_{2,1}/L_{2,2} = \frac{1}{2}$) have the values which, according to Bigorgne[2], should give rise to a highly polarized band for ν_1 and a depolarized band for ν_2. Thus, the Raman depolarization measurements reported for $W(CO)_5(CS)$[1] (Section 4.2) are not compatible with these results.

The only notable difference between the three compounds is the reversal of the order of the MC equatorial and axial stretching modes in the chromium and tungsten complexes.

Table II.17 also reveals some of the inconsistencies which occur when a given frequency is assigned to the coordinate with the largest displacement amplitude. For instance, in ν_5, which is clearly an MC stretching mode (Section 4.3), the linear bending coordinate (S_4) and the MC stretching coordinates (S_5) have almost equal amplitudes. In the P.E.D., however, ν_5 has its largest term in the MC stretching coordinate; this arises because, per unit displacement, the MC stretching coordinate contributes substantially more energy to the normal mode than does the linear bending coordinate.

7.3.2. Potential Energy Distributions for the $M(CO)_5(CX)$ Molecules

Table II.18 lists the contributions of the symmetry

TABLE II.18(a): Diagonal Elements of the Potential Energy Distribution for the Normal Isotopic Species of $Cr(CO)_5(CS)$[a,b,c,d]

a_1	ν_1	$0.78S_{\underline{1}}+0.18S_2$	b_2	ν_{14}	$0.44S_{\underline{14}}+0.29S_{15}$
	ν_2	$0.20S_1+0.82S_{\underline{2}}$		ν_{15}	$0.71S_{14}+0.86S_{\underline{15}}$
	ν_3	$0.89S_{\underline{3}}+0.18S_7$			
	ν_4	$0.37S_{\underline{4}}+0.11S_5+0.25S_8$	e	ν_{16}	$1.02S_{16}$
	ν_5	$0.18S_4+0.63S_{\underline{5}}+0.21S_7$		ν_{17}	$0.29S_{\underline{17}}+0.16S_{19}+0.11S_{23}$
	ν_6	$0.93S_6$		ν_{18}	$0.34S_{\underline{18}}+0.12S_{20}+0.15S_{22}+0.12S_{24}$
	ν_7	$0.10S_3+0.21S_5+0.46S_{\underline{7}}$		ν_{19}	$0.38S_{\underline{17}}+0.11S_{19}+0.13S_{20}+0.10S_{21}$
	ν_8	$0.69S_4+0.19S_5+0.25S_7+1.04S_{\underline{8}}$		ν_{20}	$0.56S_{\underline{19}}+0.16S_{20}$
				ν_{21}	$0.41S_{\underline{18}}+0.27S_{20}+0.39S_{21}$
b_1	ν_{10}	$1.00S_{10}$		ν_{22}	$0.36S_{17}+0.25S_{19}+0.24S_{20}+0.33S_{22}+0.47S_{\underline{23}}$
	ν_{11}	$0.78S_{11}$		ν_{23}	$0.12S_{17}+0.22S_{18}+0.15S_{20}+0.21S_{21}+0.47S_{\underline{22}}+0.34S_{23}+0.16S_{24}$
	ν_{12}	$0.96S_{12}$			
	ν_{13}	$0.26S_{11}+0.97S_{\underline{13}}$		ν_{24}	$0.30S_{21}+0.19S_{22}+0.35S_{23}+0.80S_{\underline{24}}$

TABLE II.18(a): (cont'd)

---

[a] The symmetry coordinates S_i are defined in Table II.9.

[b] The coefficients of S_i, $V_{ii,k}$, (Eq. II.27) give the contribution of S_i to the normal mode ν_k.

[c] Contributions less than 0.10 are omitted.

[d] The major contribution to a mixed mode is underlined.

TABLE II.18(b): Diagonal Elements of the Potential Energy Distribution for the Normal Isotopic Species of $Cr(CO)_5(CSe)$[a]

a_1	ν_1	$0.78S_{\underline{1}}+0.20S_2$	b_2	ν_{14}	$0.44S_{\underline{14}}+0.29S_{15}$
	ν_2	$0.21S_1+0.81S_{\underline{2}}$		ν_{15}	$0.71S_{14}+0.88S_{\underline{15}}$
	ν_3	$0.75S_{\underline{3}}+0.32S_7$			
	ν_4	$0.38S_{\underline{4}}+0.10S_5+0.25S_8$	e	ν_{16}	$1.02S_{16}$
	ν_5	$0.16S_4+0.72S_{\underline{5}}+0.12S_7$		ν_{17}	$0.23S_{\underline{17}}+0.17S_{19}$
	ν_6	$0.96S_6$		ν_{18}	$0.10S_{17}+0.22S_{\underline{18}}+0.14S_{20}+0.18S_{22}$
	ν_7	$0.21S_3+0.15S_5+0.39S_{\underline{7}}$		ν_{19}	$0.36S_{\underline{17}}+0.17S_{21}+0.11S_{24}$
	ν_8	$0.66S_4+0.17S_5+0.32S_7+1.02S_{\underline{8}}$		ν_{20}	$0.60S_{\underline{19}}+0.11S_{20}$
				ν_{21}	$0.48S_{\underline{18}}+0.32S_{20}+0.32S_{21}$
b_1	ν_{10}	$1.00S_{10}$		ν_{22}	$0.23S_{17}+0.12S_{18}+0.21S_{19}+0.36S_{20}+0.50S_{\underline{22}}$ $+0.27S_{23}$
	ν_{11}	$0.80S_{11}$			
	ν_{12}	$0.96S_{12}$		ν_{23}	$0.22S_{17}+0.14S_{18}+0.10S_{20}+0.15S_{21}+0.38S_{22}$ $+0.67S_{\underline{23}}$
	ν_{13}	$0.26S_{11}+0.96S_{\underline{13}}$			
				ν_{24}	$0.39S_{21}+0.10S_{22}+0.20S_{23}+0.90S_{\underline{24}}$

---

[a] See Footnotes to Table II.18(a).

TABLE II.18(c): Diagonal Elements of the Potential Energy Distribution for the Normal Species of $W(CO)_5(CS)$[a]

a_1	ν_1	$0.76\underline{S_1}+0.19S_2$	b_2	ν_{14}	$0.57\underline{S_{14}}+0.21S_{15}$
	ν_2	$0.21S_1+0.81\underline{S_2}$		ν_{15}	$0.55S_{14}+0.91\underline{S_{15}}$
	ν_3	$0.85\underline{S_3}+0.23S_7$			
	ν_4	$0.44\underline{S_4}+0.19S_8$	e	ν_{16}	$1.03S_{16}$
	ν_5	$0.92S_6$		ν_{17}	$0.33S_{17}$
	ν_6	$0.64\underline{S_5}+0.11S_7$		ν_{18}	$0.19S_{17}+0.13S_{18}+0.28\underline{S_{20}}+0.15S_{22}$
	ν_7	$0.37S_5+0.72\underline{S_7}$		ν_{19}	$0.28\underline{S_{18}}+0.20S_{21}+0.20S_{24}$
	ν_8	$0.93S_4+1.25\underline{S_8}$		ν_{20}	$0.94S_{19}$
				ν_{21}	$0.39S_{18}+0.30S_{20}+0.38S_{21}$
b_1	ν_{10}	$1.00S_{10}$		ν_{22}	$0.23S_{17}+0.16S_{18}+0.46S_{20}+0.78\underline{S_{22}}+0.13S_{23}$
	ν_{11}	$0.79S_{11}$		ν_{23}	$0.45S_{17}+0.24S_{21}+0.20S_{22}+0.85\underline{S_{23}}+0.15S_{24}$
	ν_{12}	$0.96S_{12}$		ν_{24}	$0.35S_{21}+0.16S_{22}+0.41S_{23}+0.89\underline{S_{24}}$
	ν_{13}	$0.31S_{11}+1.03\underline{S_{13}}$			

---

[a] See Footnotes to Table II.18(a).

coordinates ($V_{ij,k}$) to the potential energy of the normal modes of the $M(^{13}CO)_5(^{13}CX)$ molecules. A comparison of the P.E.D.'s of the $M(CO)_6$[7] (O_h) and $M(CO)_5(CX)$ (C_{4v}) molecules is possible by comparing the contributions from the coordinates in the A_1, B_1 and B_2 blocks of the C_{4v} systems with those of the analogous coordinates in the $A_{1g} + T_{1u}$, $E_g + T_{2u}$ and T_{2g} blocks, respectively, of the O_h systems. The various $V_{ij,k}$ for the two systems agree closely; in particular, the P.E.D.'s for the B_1 and B_2 blocks are almost identical to their $M(CO)_6$ equivalents since all the $C_{i,j}$ ($i \neq j$) in these blocks were constrained at their $M(CO)_6$ values. In the E block, however, there is so much mixing of coordinates forbidden under O_h symmetry, that many of the $V_{ij,k}$ do not have hexacarbonyl equivalents.

In the A_1 blocks, all the complexes show appreciable mixing between the equatorial and axial CO stretches but none between the CO and CX stretching modes. The mixing of $\nu(CX)$ and $\nu[MC(X)]$ increases progressively as O is replaced by S and Se. Also, $\nu[MC(O)]$ (axial) and $\nu[MC(X)]$ are extensively mixed, whereas the equatorial MC stretch is essentially uncoupled.

Strong mixing of the MCO and CMC bends is observed for all the blocks and, in the chromium complexes, these modes also show a significant amount of MC stretching. In the

E block, the linear bending modes are highly mixed, particularly the MCO and MCX axial bends and the equatorial out-of-plane bends. In fact, most of the modes in this block are so strongly coupled that only the ν(CO), ν(MC) and δ(CMC) (ν_{24}) can be assigned characteristic frequencies.

7.4. Energy-Factored Force Fields (EFFF)

Anharmonic energy-factored force fields were determined for the $M(CO)_5(CX)$ species as an aid to the assignment of the partially-labelled species and to determine the position of the ir-inactive ν(CO) b_1 mode, as discussed above (Section 4.1). The frequencies calculated by the anharmonic EFFF are given in Table II.1(a) for the vapour and CS_2 solution spectra of $Cr(CO)_5(CX)$ and the final force constants are given in Table II.19. Harmonic EFFF were obtained from the harmonic ν(CO) and ν(CX) frequencies for $Cr(CO)_5(CX)$ and $W(CO)_5(CS)$ to allow a comparison of the harmonic CO and CX energy-factored force constants with those obtained using the GQVFF. Again, these results are given in Table II.19.

All the EFFF were determined using FCOMPLY. The initial compliant fields were determined from $(F)^{-1}$ where F represents the appropriate energy-factored force constant

TABLE II.19: CO and CX Force Constants and (CO,CO) Interaction Constants for the $M(CO)_5(CX)$ Molecules for Some Approximate Force Fields

			$Cr(CO)_5(CS)$		
F^a	Solution[b] Anhar EF	Vapour Anhar EF	Vapour[c] Anhar GQ[d]	Vapour Har EF	Vapour Har GQ
F_D	16.46	16.68	16.71	17.19	17.28
F_{D_a}	16.63	16.91	17.01	17.30	17.42
F^c_{DD}	0.24	0.23	0.21	0.24	0.18
F^t_{DD}	0.47	0.39	0.21	0.30	0.04
F_{DD_a}	0.22	0.22	0.21	0.17	0.13
F_{D_x}	8.18	8.41	8.01	8.52	7.68

			$Cr(CO)_5(CSe)$	
	Solution Anhar EF	Vapour Anhar EF	Vapour Har EF	Vapour Har GQ
F_D	16.50	16.71	17.19	17.28
F_{D_a}	16.72	16.98	17.34	17.47
F^c_{DD}	0.23	0.23	0.22	0.16
F^t_{DD}	0.46	0.39	0.30	0.05
F_{DD_a}	0.20	0.20	0.16	0.12
F_{D_x}	7.13	7.38	7.42	5.77

TABLE II.19: (cont'd)

F^a	W(CO)$_5$(CS) Vapour Anhar EF	Vapour Anhar GQ[e]	Vapour Har EF	Vapour Har GQ
F_D	16.71	16.78	17.16	17.28
F_{D_a}	16.60	16.88	17.08	17.24
F^c_{DD}	0.27	0.16	0.25	0.11
F^t_{DD}	0.47	0.12	0.37	0.02
F_{DD_a}	0.21	0.16	0.21	0.15
F_{D_x}	8.50	8.17	8.61	0.46

[a] Subscripts and superscripts are explained in Footnote d Table II.15; Units: mdyn $Å^{-1}$.

[b] CS_2 solution; EF = energy-factored.

[c] The values calculated here for the interaction constants are considered more reasonable than those given previously[1].

[d] GQ = general quadratic.

[e] Force constants from Ref. 1.

matrix from $M(CO)_6$[7]. The C and G matrices were used in their non-symmetry reduced forms because some of the partially-labelled species have different molecular symmetries which give rise to different symmetry C and G matrices. No changes are required in C on substitution of ^{13}CO for ^{12}CO, while the G matrix, which is diagonal, simply requires a change in the $G_{i,i}$ element corresponding to a labelled CO group from $(\mu_{^{12}CO})^{-1}$ to $(\mu_{^{13}CO})^{-1}$, where μ is the reduced mass of CO. The energy-factored force constants were obtained from C^{-1} and only these are given in Table II.19 as energy-factored compliant constants have not been tabulated for any compounds. The CX force constants, which are also presented in Table II.19, were determined from the corresponding CX frequencies with all (CO,CX) interactions being set equal to zero.

As in the case of $M(CO)_6$[7], the neglect of anharmonicity corrections has a significant effect on the primary CO stretching force constants and the (CO,CO) *trans*-interaction constants, the *cis*-interaction constants changing to a lesser extent. CO-energy factoring, on the other hand, leads to large errors for all the interaction constants but again, the *trans*-(CO,CO) constant is the one most affected. Similar results were obtained for the CO-EFFF of the metal hexacarbonyls[7] and $Mn(CO)_5Br$[8].

A comparison of the CX energy-factored force constants and the corresponding general quadratic constants indicates that energy factoring is a poor approximation for the ν(CS) and ν(CSe) modes. If one examines the expression for the ν(CX) mode of an isolated MCX (X=O,S,Se) moiety, it becomes obvious why energy factoring is an increasingly poor approximation as O is replaced by S or Se (Table II.19).

Labelling the CX and MC(X) stretches, coordinates 1 and 2, respectively, the secular equation for this two-coordinate system (Eq. II.11) is given by

$$\begin{bmatrix} G_{1,1}F_{1,1}+G_{1,2}F_{1,2} & G_{1,1}F_{1,2}+G_{1,2}F_{2,2} \\ G_{1,2}F_{1,1}+G_{2,2}F_{1,2} & G_{1,2}F_{1,2}+G_{2,2}F_{2,2} \end{bmatrix} \begin{bmatrix} L_{1,1} & L_{1,2} \\ L_{2,1} & L_{2,2} \end{bmatrix} = \begin{bmatrix} L_{1,1} & L_{1,2} \\ L_{2,1} & L_{2,2} \end{bmatrix} \begin{bmatrix} \lambda_1 & \\ & \lambda_2 \end{bmatrix}$$

which yields the following expression for λ_1 after matrix multiplication:

$$\lambda_1 = G_{1,1}F_{1,1} + (G_{1,2}F_{1,2}) + (G_{1,1}F_{1,2}+G_{1,2}F_{2,2})L_{2,1}/L_{1,1} \quad \text{(II.28)}$$

For an isolated CX stretch, λ_1 is simply

$$\lambda_1 = G_{1,1}\ F_{1,1} \quad \text{(II.29)}$$

If typical values for $F_{2,2}$, $F_{1,2}$ and $L_{2,1}/L_{1,1}$ are substituted into Eq. II.28, a comparison of the energy-factored (Eq. II.29) and the general quadratic (Eq. II.28) $F_{1,1}$

values arising from a given λ_1 value is possible. From Table II.17, $L_{2,1}/L_{1,1}$ for $Cr(CO)_5(CS)$ and $Cr(CO)_5(CSe)$ were found to be -0.790 and -0.971, respectively, while a value of -0.581 was previously calculated for this ratio in an isolated MCO system[32]. Thus, bearing in mind that $F_{CO} < F_{CS} < F_{CSe}$, $F_{CO,MC} > F_{CS,MC} > F_{CSe,MC}$ [Table II.15(b)] and $G_{1,2} = -\mu_C$, it is evident that the terms, $(G_{1,2}F_{1,2})$ and $[(G_{1,1}F_{1,2}+G_{1,2}F_{2,2})L_{2,1}/L_{1,1})]$, of Eq. II.28 become less negative and more positive, respectively, upon descending the O, S, Se series. The relatively close agreement of the energy-factored and general quadratic force constants for CO stretching modes (Table II.19) is due to the fortuitous cancelling of the extra terms in Eq. II.28 for the carbonyl group. Thus, for the thio- and selenocarbonyls, the sum of these terms is greater than zero by increasing amounts and the general quadratic force constants decrease in value relative to the corresponding energy-factored constants.

The $L_{2,1}/L_{1,1}$ ratio gives the relative amplitudes of MC and CX bond displacements in the normal mode assigned to the CX stretch. Thus, the large increase in the absolute value of this ratio signifies a greater degree of coupling between these two motions as the atomic weight of X increases. Furthermore, the considerable effect of $L_{2,1}/L_{1,1}$

TABLE II.20: Harmonic Frequencies (cm^{-1}) and Harmonic Force Constants (mdyn A^{-1}) for Free and Coordinated CX (X=O,S,Se) Ligands

Ligand	Molecule[a]	F_{CX}	ω_e
CO	CO	19.017	2169.8
CO	$Cr(CO)_6$	17.24	2060.1[b]
CO	$W(CO)_6$	17.22	2056.9[b]
CS	CS	8.489	1285.1
CS	$Cr(CO)_5(CS)$	7.68	1287.3
CS	$W(CO)_5(CS)$	7.46	1294
CSe	CSe	6.587	1036.0
CSe	$Cr(CO)_5(CSe)$	5.77	1098

[a] Vapour phase data used for all molecules; $M(CO)_6$ and diatomic data from Refs. 7 and 18(a) (p. 185), respectively.

[b] Arithmetic mean of a_{1g}, e_g and t_{1u} $\nu(CO)$ frequencies weighted by their degeneracies.

on the size of the last term in Eq. II.28 explains how increased mixing prevents changes in the observed CX frequencies from accurately reflecting changes in the CX bond orders on coordination since both ν(CS) and ν(CSe) may increase in frequency relative to the free ligand while F_{CS} and F_{CSe} decrease. Table II.20, which lists force constants and wavenumbers for the coordinated and free chalcocarbonyl ligands, emphasizes this point.

References (Part II)

1. I.S. Butler, A. Garcia-Rodriguez, K.R. Plowman and C.F. Shaw III, Inorg. Chem., 15, 2602 (1976).

2. M. Bigorgne, Spectrochim. Acta, 32A, 1365 (1976).

3. W.F. Edgell, ibid., 31A, 1623 (1975).

4. (a) A. Whitaker and J.W. Jeffery, Acta Cryst., 23, 977 (1967); (b) A. Jost, B. Rees and W.B. Yelon, ibid., B31, 2649 (1975).

5. J.Y. Saillard and D. Grandjean, ibid., B34, 3318, (1978).

6. D.L. Lichtenberger and R.F. Fenske, Inorg. Chem., 15, 2015 (1976).

7. L.H. Jones, R.S. McDowell and M. Goldblatt, ibid., 8, 2349 (1969).

8. D.K. Ottesen, H.B. Gray, L.H. Jones and M. Goldblatt, ibid., 12, 1051 (1973).

9. L.H. Jones, J. Mol. Spectrosc., 36, 398 (1970).

10. L.H. Jones and J.M. Smith, ibid., 20, 248 (1966).

11. F.A. Cotton, A. Musco and G. Yagupsky, Inorg. Chem., 6, 1357 (1967).

12. (a) L.G. Bonner, Phys. Rev., 46, 458 (1934); (b) B.T. Darling and D.M. Dennison, ibid., 57, 128 (1940).

13. L.H. Jones, Inorg. Chem., 7, 1681 (1968).

14. IUPAC Commission on Molecular Structure and Spectroscopy, "Tables of Wavenumbers for the Calibration of Infrared Spectrometers", Butterworths, London, 1961.

15. J.C. Decius, J. Chem. Phys., 38, 241 (1963).

16. R. Ottinger, Ph.D. Thesis, Oregon State University, Corvallis, Oregon, USA, 1966.

17. E.B. Wilson Jr., J. Chem. Phys., 7, 1047 (1939).

18. L.H. Jones, "Inorganic Vibrational Spectroscopy", Marcel Dekker, New York, 1971.

19. L.H. Jones and B.I. Swanson, Accounts Chem. Res., 9, 128 (1976).

20. L.H. Jones and R.R. Ryan, J. Chem. Phys., 52, 2003 (1970).

21. S.J. Cyvin and N.B. Slater, Nature, 188, 485 (1960).

22. L.H. Jones, R.S. McDowell and M. Goldblatt, J. Chem. Phys., 48, 2663 (1968).

23. L.H. Jones, R.S. McDowell, M. Goldblatt and B.I. Swanson, ibid., 57, 2050 (1972).

24. L.H. Jones, R.S. McDowell and B.I. Swanson, ibid., 58, 3757 (1973).

25. Natural Sciences and Engineering Research Council Canada, Bulletin #15, "Computer Programs for Infrared Spectrophotometry", (R.N. Jones Editor) Ottawa, 1976.

26. E.B. Wilson, J.C. Decius and P.C. Cross, "Molecular Vibrations", McGraw-Hill, New York, 1955.

27. (a) G. Overend and J.R. Scherer, J. Chem. Phys., 32, 1289 (1960); (b) C.D. Needham, Ph.D. Thesis, University of Minnesota, Minneapolis, Minnesota, USA, 1965.

28. (a) J.Y. Saillard and D. Grandjean, Acta Cryst., B32, 2285 (1976); (b) J.Y. Saillard, G. Le Borgne and D. Grandjean, J. Organometal. Chem., 94, 409 (1975); (c) J.Y. Saillard and D. Grandjean, Acta Cryst., B34, 3772 (1978).

29. W.C. Hamilton, "Statistics in Physical Science", Ronald Press, New York, 1964.

30. P.R. Bevington, "Data Reduction and Error Analysis for the Physical Sciences", McGraw-Hill, New York, 1969.

31. Y. Morino and K. Kuchitsu, J. Chem. Phys., 20, 1809 (1952).

32. P.S. Braterman, "Metal Carbonyl Spectra", Academic Press, London, 1975.

PART III

NORMAL COORDINATE ANALYSES OF
(η^6-BENZENE)TRICARBONYLCHROMIUM(0),
(η^6-BENZENE)DICARBONYL(THIOCARBONYL)CHROMIUM(0) AND
(η^6-BENZENE)DICARBONYL(SELENOCARBONYL)CHROMIUM(0)

Chapter 8

Review of Normal Coordinate Analyses of Metal Chalcocarbonyl Complexes Containing π-Bonded Cyclic Polyenes

8.1. Introduction

The structures and properties of π-complexes of cyclic polyenes C_nH_n (n = 4-8) have received considerable attention during the last twenty-five years[1]. Their vibrational spectra have been closely studied mainly to determine the effects of coordination on the ring. Comprehensive reviews by Fritz[2] and Davidson[3] cover most of the early work on symmetrical "sandwich" type complexes such as ferrocene and dibenzenechromium. These reviewers also report studies on "mixed" π-complexes, $(\eta^n\text{-}C_nH_n)_2ML_x$ and $(\eta^n\text{-}C_nH_n)ML_x$, where L = CO, H, Cl, Br, NO, etc., and C_nH_n is mainly a six π-electron donor such as benzene or the cyclopentadienyl ion. Less detailed, but more updated, reviews of the spectra of a wide variety of organometallic complexes are contained in books by Nakamoto[4] and Maslowsky[5].

This review presents the results of normal coordinate analyses on complexes of the general formula, $(\eta^n\text{-}C_nH_n)ML_x$, where L is a chalcocarbonyl ligand. The few systems studied have x=3 and these are: $(\eta^6\text{-}C_6H_6)Cr(CO)_3$[6-9], $(\eta^6\text{-}CH_3CO_2C_6H_5)Cr(CO)_2(CX)$ (X=O,S,Se)[10] and $(\eta^4\text{-}C_4H_4)Fe(CO)_3$[11].

8.2. $(\eta^6\text{-}C_6H_6)Cr(CO)_3$

From the results given in Table III.1, it is obvious that the force fields determined for $BzCr(CO)_3$ vary considerably. This is, in part, due to the different approximations used. In the first analysis by Cataliotti *et al.*[6], the reported force field is that of $RCr(CO)_3$, where the benzene ring is approximated by a point mass, R, of 78 a.m.u. This model possesses a single metal-ring stretching coordinate which, under C_{3v} symmetry, gives rise to an a_1 vibration. The possibility, therefore, of coupling between the metal-ring and metal-carbonyl stretching vibrations is excluded in the E symmetry block. Further limitations of the model include the absence of coupling between any of the ring modes and the metal-ring stretching mode,

TABLE III.1: Literature Values for Some Force Constants for the $M(CO)_2(CX)$ Moiety in $(\eta^n-C_nH_n)M(CO)_2(CX)$ (X=O,S,Se)[a]

Force Constant[c]	$(\eta^6-C_6H_6)Cr(CO)_3(C_{3v})$[b]			$(\eta^4-C_4H_4)Fe(CO)_3(C_{3v})$
	Ref. 6	Ref. 8	Ref. 9	Ref. 11
CO	13.55	14.8	14.64	16.01
CO,CO	0.46		0.35	0.39
MC	2.97	1.6	3.88	2.98
MC,MC	0.12			
MC(R)	2.37	1.3	3.74	3.24
$MCO_\perp$	1.10	0.46	0.70	0.57
$MCO_\parallel$	1.00	0.33	0.79	0.75
CMC		0.1	0.34	0.55
CMC(R)		0.1	0.44	0.27

Force Constant[c,d]	$(\eta^6-CH_3CO_2C_6H_5)Cr(CO)_2(CX)$		
	X=O (C_s)	X=S (C_1)	X=Se(C_1)
	Ref. 10(a)	Ref. 10(b)	Ref. 10(c)
CO	14.98	15.45	15.65
CO,CO	0.25	0.25	0.25
CX		7.30	5.90
MC(O)	2.15	2.15	2.00
MC,MC	-0.02	-0.02	-0.02
MC(X)		2.30	2.70
MC(R)	0.75	0.75	0.65
$MCO_\perp$	0.84	0.84	0.84

TABLE III.1: (cont'd)

Force[c,d] Constant	$(\eta^6\text{-}CH_3CO_2C_6H_5)Cr(CO)_2(CX)$ X=O (C_s) Ref. 10(a)	X=S (C_1) Ref. 10(b)	X=Se (C_1) Ref. 10(c)
$MCO_{\parallel}$	0.84	0.84	0.84
$MCX_{\perp}$		0.92	0.84
$MCX_{\parallel}$		0.92	0.84
CMC(O)	0.40	0.40	0.40
CMC(X)		0.60	0.60
CMC(R)	0.20	0.20	0.20

[a] Units are mdyn A^{-1} for stretching and mdyn A rad^{-2} for bending force constants.

[b] Local symmetry of $M(CO)_2(CX)$ moiety.

[c] C(R) = carbon of arene ring, except for Refs. 6 and 11 C(R) = "point mass", see text; $MCO_{\perp}$ and $MCO_{\parallel}$ represent linear bending modes perpendicular and parallel to metal-ring axis, respectively.

[d] Average of values given in Ref. 10.

or between the ring and the carbonyl moiety. The latter coupling, however, should be less significant since no non-zero G matrix elements exist between the internal coordinates of the ring and $Cr(CO)_3$. In addition to the above limitations, the force field reported by these workers is rendered more questionable by a number of misassignments. Attributing the peaks at 676 and 532 cm^{-1} in the ir spectrum of the CCl_4 solution to $\delta(MCO)$ and $\nu(MC)$ modes, respectively, leads to an assignment which is not compatible with the isotopic behaviour of these peaks on ^{13}CO substitution (Table III.4). Thus, the values obtained for the MCO and MC force constants are not very meaningful.

In three subsequent calculations on $BzCr(CO)_3$[7-9], the molecule as a whole was considered. Data from the fully-deuterated species were also included in two of these studies[8,9]. The emphasis in the work of Brunvoll *et al.*[7] and Adams *et al.*[8] was mainly on differences in the force fields of free and coordinated benzene. However, the conclusions reached by the two teams are contradictory; Brunvoll's group maintains that kinematic coupling effects account for the observed wavenumber shifts on complexation, while Adams' group shows that considerable changes in the force field of free benzene are necessary to obtain a satisfactory fit of the frequencies observed for the complex.

Comparison of the actual force fields obtained by the two groups is not possible since Brunvoll _et_ _al_. report mean amplitudes of vibration only. Furthermore, the significance of the force constants reported for the tricarbonyl moiety by Adams _et_ _al_. is somewhat questionable as all interaction constants were set to zero and the frequency fit is not very satisfactory.

Bisby and coworkers[9] also used a complete set of internal coordinates to describe the molecule. The agreement here between the observed and calculated wavenumbers is much better than reported by Adams _et_ _al_. However, some of the force constants obtained by these workers seem unrealistically large when compared to those found in related molecules. For example, the metal-carbonyl stretching force constant calculated is 3.88 mdyn A^{-1} as opposed to 2.10 mdyn A^{-1} in $Cr(CO)_6$. The large value obtained for this constant stems partly from the assignment of the antisymmetric metal-carbonyl stretch to a band at 621 cm^{-1} while from Table III.4 it can be seen that this band exhibits the isotopic behaviour of a δ(MCO) mode. Similarly, the value obtained for the metal-ring force constant is greater than expected (3.74 mdyn A^{-1})*,

---

*Multiplication of the metal-ring force constant by six (since these workers used six metal-ring stretching coordinates) should give a rough indication of the strength of the metal-ring interaction. However, the value obtained (28.44 mdyn A^{-1}) suggests that dissociation of the ring but the sizable interaction constants calculated for these metal-ring stretching coordinates reduce the significance of the diagonal term.

8.3. $(\eta^6\text{-}CH_3CO_2C_6H_5)Cr(CO)_2(CX)$ (X=O,S,Se)

The first study[10(a)] in this series, dealing with the normal coordinate analysis of the tricarbonyl complex, appeared before we commenced work on the analogous series, $BzCr(CO)_2(CX)$ (X=O,S,Se). While our work was in progress, the remaining two analyses were published[10(b),(c)].

A complete set of internal coordinates was defined for the three molecules and the data input in each case were taken from the ir and Raman spectra of the solids. The initial valence force field for the tricarbonyl was estimated from previous normal coordinate analyses of the free arene ligand[13] and $Cr(CO)_6$[14]. Of the 119 non-zero force constants initially input, 96 were left unchanged. The metal-ring stretching constant was fixed at 0.75 mdyn $Å^{-1}$, a value estimated from the ν[CrC(R)] mode at 300 cm^{-1}. The perturbations of the initial force field signify overall electron-donation from the arene; the carbon-carbon stretching constants of the ring decrease as do the carbonyl stretching

---

would require considerably more energy than dissociation of the three carbonyl groups. The thermochemical data available for $BzCr(CO)_3$[12] show that the converse is true.

constants indicating a reduction in the carbon-carbon bond order and an increase in the π-backbonding to the CO groups, respectively.

To fit the tricarbonyl field to the frequencies observed for the thio- and selenocarbonyl complexes, adjustment of the force constants pertaining to the MCX grouping was necessary. As Table III.1 shows, the most significant changes are in the ν[MC(X)] and ν(CX) constants; substitution of O for S and Se gives stronger MC bonds and weaker CX bonds.

Although the final force fields obtained by Caillet for these chalcocarbonyl complexes seem reasonable on the basis of chemical intuition, they are in truth somewhat meaningless. When factors such as the complexity of the system, the many unobserved bands plus the poor wavenumber fit for some of those observed, and the use of solid-state data are all taken into account, the conclusions regarding structural properties and vibrational assignments are not particularly convincing. These results are discussed further, together with those for the benzene complexes, in Chapter 12.

8.4. $(\eta^4\text{-}C_4H_4)Fe(CO)_3$

A valence force field was calculated for this molecule using C_{4v} symmetry for the ring and C_{3v} symmetry for the $Fe(CO)_3$ moiety. The vibrational assignment was carried out using these "local symmetry" approximations and the number of observed and predicted frequencies are in agreement. The analysis was performed in two separate sections: the C_4H_4 ring was treated as an isolated C_{4v} system and the whole complex was analyzed as an eight-atom system, $RFe(CO)_3$, where R = 52 a.m.u. The potential constants obtained for the ring cannot be compared with those of the free ligand since no analysis of uncomplexed C_4H_4 (which exists only in frozen inert-gas matrices[15]) has been reported. However, the ν(CC) force constant is smaller than that obtained for free C_6H_6 or $C_5H_5^-$. This is consistent with increased p-character in the carbon-carbon bond as the ring size decreases because overlap of pure p orbitals give weaker bonds than overlap of sp^2 hybrids.

A comparison of the force fields of $Fe(CO)_5$[16] and $RFe(CO)_3$ indicates that there is increased π-backbonding in the tricarbonyl since the ν(MC) force constant is larger and the ν(CO) force constant is smaller than those of the pentacarbonyl. Also, the large value obtained for the Fe-R force constant (3.24 mdyn A^{-1}) suggests that the metal-ring interaction is quite strong. Recent molecular orbital studies on $(\eta^4\text{-}C_4H_4)Fe(CO)_3$[17] reveal that the molecule is best described as a $(\eta^4\text{-}C_4H_4)Fe$ fragment perturbed by the CO's rather than a $Fe(CO)_3$ fragment perturbed by the C_4H_4 ring. The metal-ring bonding gives rise to a benzene-like π-delocalization which serves to stabilize the complexed ring. This stabilization is termed "metallo-aromaticity" by the authors. The larger metal-ring and ν(CO) force constants obtained for $RFe(CO)_3$ compared to those of the chromium compounds given in Table III.1 support this picture of the complex.

Chapter 9

Representation of the Vibrations of the $(\eta^6\text{-}C_6H_6)Cr(CO)_2(CX)$ Molecules

9.1. Choice of Internal Coordinate Set

In the present analyses, the focus will be on the perturbation of the chalcocarbonyl groups by the substitution of a benzene for three carbonyl groups in $Cr(CO)_5(CX)$. Changes occurring in the ring itself on complexation will not be considered since such changes have been discussed in some detail previously[6-9,11].

In the absence of any approximations, 57 internal coordinates are necessary to describe the internal motion of $BzCr(CO)_2(CX)$, 30 of which are required for the ring; these have been given previously for the tricarbonyl complex[18]. Thus, the complete set of coordinates produces large F (or C) and G matrices even after symmetry factoring of the secular equation is performed. Refinement of the potential field is not only difficult but extremely costly when the potential-constant matrix is this large. A more approximate vibrational model requiring a significantly smaller number of internal coordinates would greatly simplify the calculations. As the potential constants of complexed benzene are not desired in this study, a set of coordinates which exclude those of the ring while remaining a reasonable vibrational model for the molecules would be appropriate.

The model chosen is that of an all-cis octahedron, $L_3M(CO)_2(CX)$, where the ring is approximated by three point masses L such that $L=C_2H_2$ (26 a.m.u.) and M=Cr. Twenty-seven internal coordinates are necessary to describe the internal motion of this octahedron as compared to 19 for the point ring approximation $[RCr(CO)_3]$ used by Cataliotti et al.[6] An octahedral geometry, however, is more compatible with the theoretical bonding model of chromium(0) where sp^3d^2 hybridization yields six octahedrally-directed hybrid orbitals. The crystal structure of $BzCr(CO)_3$, which has been studied by x-ray and neutron diffraction[19], shows an average OC-Cr-CO bond angle of 87.76°, a value close to the octahedral bond angle of 90°. Furthermore, at 78 K, the symmetry of the benzene ring is C_{3v} rather than C_{6v}

since two different bond lengths are observed for the carbon-carbon linkages. If the metal bonding is described in terms of octahedrally-directed localized orbitals, three of these will point towards the centers of the three shorter carbon-carbon bonds, placing these bonds trans to the carbonyl groups. The fact that some of the carbon-carbon bonds are found to be shorter is indicative of partial localization of the double bonds which in turn implies partial destruction of the aromaticity of the ring.

As mentioned above, one of the aims of this analysis is to determine the perturbation of the benzene ring on the potential field of the $Cr(CO)_2(CX)$ fragment. The most instructive comparison is, therefore, with the potential field calculated for $Cr(CO)_5(CX)$, but for this to be valid, the vibrational models representing the two systems should be as consistent as possible. Hence, given that chromium is formally in its zero oxidation state in both series, an octahedral geometry should be used in each case. Furthermore, this would allow the direct transfer of the interaction constants of $Cr(CO)_6$ to the arene complexes, as was done previously for $Cr(CO)_5(CX)$.

One of the most serious limitations of the $L_3M(CO)_3$

model is the exclusion of coupling between $\nu(CC)$ and $\tau(CCCC)$ of the ring and the metal-ring stretching modes. Use of different approximations for the ferrocene molecule showed that the interaction between the metal-ring stretch and the ring vibrations was significant[20]. However, employing three bonds to represent the metal-ring bonding does allow coupling between these stretches and those of the metal-carbonyls in the symmetry blocks containing the antisymmetric vibrations.

The internal and symmetry coordinates for $L_3M(CO)_2(CX)$ are given in the next sections, and the following chapters present the vibrational analyses of $BzCr(CO)_2(CX)$ using this model.

9.2. Internal and Symmetry Coordinates for $L_3M(CO)_2(CX)$

The internal coordinates for $BzCr(CO)_2(CX)$ in the $L_3\,M(CO)_2(CX)$ approximation are shown in Figure III.1. The corresponding symmetry coordinates are listed in Tables III.2 (X=O; C_{3v} symmetry) and III.3 (X=S,Se; C_s symmetry). The symmetry coordinates are linear combinations of the 27 internal coordinates given in Figure III.1. Since a ten-atom, nonlinear molecule possesses 24 vibrations, only 24 symmetry coordinates are needed; it is therefore necessary to construct three redundant symmetry coordinates.

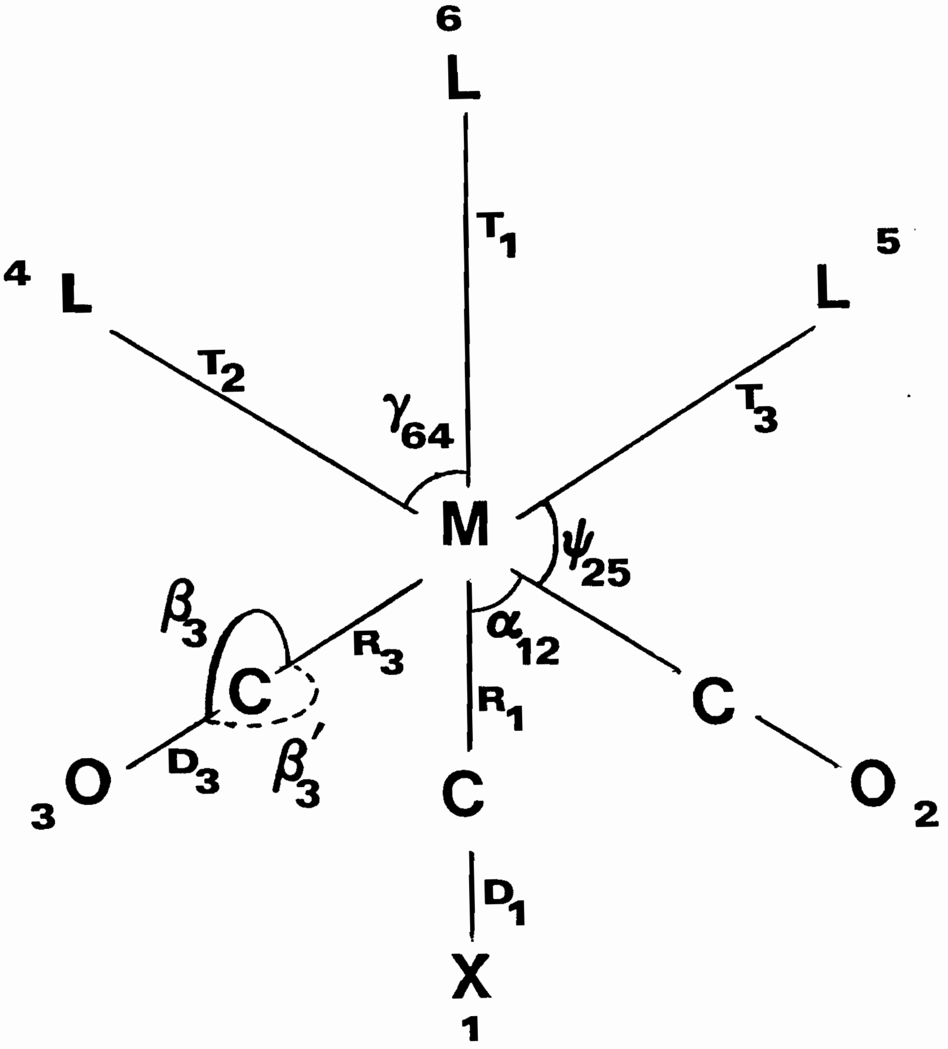

Figure III.1. Internal coordinates of the $L_3M(CO)_2(CX)$ (X=O,S,Se) molecules. For X=S,Se; $R_1=R_x$, $D_1=D_x$, $T_1=T_x$, $\beta_1=\phi$ and $\beta_1'=\phi'$.

TABLE III.2: Symmetry Coordinates for $L_3M(CO)_3$ (C_{3v} Symmetry)[a]

A_1 Block

$S_1 = 1/\sqrt{3}(D_1 + D_2 + D_3)$

$S_2 = 1/\sqrt{3}(\beta_1 + \beta_2 + \beta_3)$

$S_3 = 1/\sqrt{3}(R_1 + R_2 + R_3)$

$S_4 = 1/\sqrt{3}(T_1 + T_2 + T_3)$

$S_5 = 1/\sqrt{6}(\alpha_{23} + \alpha_{12} + \alpha_{13} - \gamma_{45} - \gamma_{64} - \gamma_{65})$

$$S_6 = 1/\sqrt{12}(\psi_{25} + \psi_{34} + \psi_{14} + \psi_{26} + \psi_{15} + \psi_{36} - \alpha_{23} - \alpha_{12} - \alpha_{13} - \gamma_{45} - \gamma_{64} - \gamma_{65})$$

$$S_{Red} = 1/\sqrt{12}(\psi_{25} + \psi_{34} + \psi_{14} + \psi_{26} + \psi_{15} + \psi_{36} + \alpha_{23} + \alpha_{12} + \alpha_{13} + \gamma_{45} + \gamma_{64} + \gamma_{65}) = 0$$

A_2 Block

$S_7 = 1/\sqrt{3}(\beta'_1 + \beta'_2 + \beta'_3)$

$S_8 = 1/\sqrt{6}(\psi_{14} - \psi_{15} + \psi_{25} - \psi_{26} + \psi_{36} + \psi_{34})$

E_a Block

$S_9 = 1/\sqrt{6}(2D_1 - D_2 - D_3)$

$S_{10} = 1/\sqrt{2}(\beta'_2 - \beta'_3)$

$S_{11} = 1/\sqrt{6}(2\beta_1 - \beta_2 - \beta_3)$

TABLE III.2: (cont'd)

E_a Block

$$S_{12} = 1/\sqrt{6}(2R_1 - R_2 - R_3)$$

$$S_{13} = 1/\sqrt{6}(2T_1 - T_2 - T_3)$$

$$S_{14} = 1/\sqrt{12}(2\alpha_{23} - \alpha_{12} - \alpha_{13} - 2\gamma_{45} + \gamma_{64} + \gamma_{65})$$

$$S_{15} = 1/\sqrt{24}(2\psi_{25} + 2\psi_{34} - \psi_{14} - \psi_{26} - \psi_{15} - \psi_{36} - 2\alpha_{23} + \alpha_{12} + \alpha_{13} - 2\gamma_{45} + \gamma_{64} + \gamma_{65})$$

$$S_{16} = \tfrac{1}{2}(\psi_{14} - \psi_{26} + \psi_{15} - \psi_{36})$$

$$S_{Red} = 1/\sqrt{24}(2\psi_{25} + \psi_{34} - \psi_{14} - \psi_{26} - \psi_{15} - \psi_{36} + 2\alpha_{23} - \alpha_{12} - \alpha_{13} + 2\gamma_{45} - \gamma_{64} - \gamma_{65}) = 0$$

---

[a] The internal coordinates and numbering of atoms are shown in Figure III.1, except for X=O, D_X, R_X and T_X = D_1, R_1 and T_1, respectively.

TABLE III.3: Symmetry Coordinates for $L_3M(CO)_2(CX)$ (C_s Symmetry)[a,b]

A' Block

$S_1 = 1/\sqrt{2}(D_2 + D_3)$

$S_2 = D_x$

$S_3 = 1/\sqrt{2}(\beta_2' - \beta_3')$

$S_4 = 1/\sqrt{2}(\beta_2 + \beta_3)$

$S_5 = \phi$

$S_6 = 1/\sqrt{2}(R_2 + R_3)$

$S_7 = R_x$

$S_8 = 1/\sqrt{2}(T_2 + T_3)$

$S_9 = T_x$

$S_{10} = \frac{1}{2}(\alpha_{23} - \psi_{34} + \gamma_{45} - \psi_{25})$

$S_{11} = 1/\sqrt{2}(\alpha_{23} - \gamma_{45})$

$S_{12} = \frac{1}{2}(\alpha_{12} + \alpha_{13} - \gamma_{64} - \gamma_{65})$

$S_{13} = \frac{1}{2}(\psi_{14} + \psi_{15} - \psi_{26} - \psi_{36})$

$S_{14} = 1/\sqrt{8}(\alpha_{12} + \alpha_{13} + \gamma_{64} + \gamma_{65} + \psi_{14} - \psi_{15} - \psi_{26} - \psi_{36})$

$S_{Red} = 1/\sqrt{8}(\alpha_{12} + \alpha_{13} + \gamma_{64} + \gamma_{65} + \psi_{14} + \psi_{15} + \psi_{26} + \psi_{36}) = 0$

$S_{Red} = \frac{1}{2}(\alpha_{23} + \psi_{34} + \gamma_{45} + \psi_{25}) = 0$

TABLE III.3: (cont'd)

A" Block

$S_{15} = 1/\sqrt{2}(D_2 - D_3)$

$S_{16} = 1/\sqrt{2}(\beta_2' + \beta_3')$

$S_{17} = 1/\sqrt{2}(\beta_2 - \beta_3)$

$S_{18} = \phi'$

$S_{19} = 1/\sqrt{2}(R_2 - R_3)$

$S_{20} = 1/\sqrt{2}(T_2 - T_3)$

$S_{21} = \frac{1}{2}(\alpha_{12} - \alpha_{13} - \gamma_{64} + \gamma_{65})$

$S_{22} = 1/\sqrt{2}(\psi_{25} - \psi_{34})$

$S_{23} = \frac{1}{2}(\psi_{14} - \psi_{15} - \psi_{26} + \psi_{36})$

$S_{24} = 1/\sqrt{8}(\alpha_{12} - \alpha_{13} + \gamma_{64} - \gamma_{65} - \psi_{14} + \psi_{15} - \psi_{26} + \psi_{36})$

$S_{Red} = 1/\sqrt{8}(\alpha_{12} - \alpha_{13} + \gamma_{64} - \gamma_{65} + \psi_{14} - \psi_{15} + \psi_{26} - \psi_{36}) = 0$

---

[a] See Footnote to Table III.2.

[b] Under C_s symmetry α, γ and ψ belong to seven symmetrically non-equivalent sets (see text). The notation used for C_{3v} symmetry is retained for the sake of simplicity. The symmetrically-equivalent valence angle bending modes can be readily deduced from Figure III.1.

The redundancies occur in the bending coordinates as only 2n-3 independent angles exist about a central atom bonded to n other atoms. Thus, for n=6 nine symmetry coordinates are required though the symmetrically equivalent sets of internal coordinates consist of a total of twelve angle increments. Under C_{3v} and C_s symmetry, the redundancies have $a_1 + e$ and $a' + 2a''$ symmetries, respectively. The redundancy condition is of the form, $S_{red} = 0$; thus, the redundant coordinates in Table III.2 and III.3 are those whose sums equal zero.

Chapter 10

Infrared and Raman Spectra of the $(\eta^6\text{-}C_6H_6)Cr(CO)_2(CX)$ (X=O,S,Se) Molecules

10.1. $(\eta^6\text{-}C_6H_6)Cr(CO)_3$

The vibrational spectra of $BzCr(CO)_3$ have been studied by various groups[6-9] and for the most part the assignments are satisfactory. For the calculations performed in this work, ir (CS_2 solution) and Raman (solid and C_6H_6 solution) data for the normal, perdeuterated and all-^{13}CO substituted species were obtained. The regions examined were limited to the CO fundamental and binary regions and the low-energy region from $\sim$800-40 cm^{-1}. These regions contain all the frequencies necessary for analyses using the model discussed in the last section.

The ir spectrum of the CS_2 solution and the Raman spectrum of the solid are shown in Figure III.2, while the

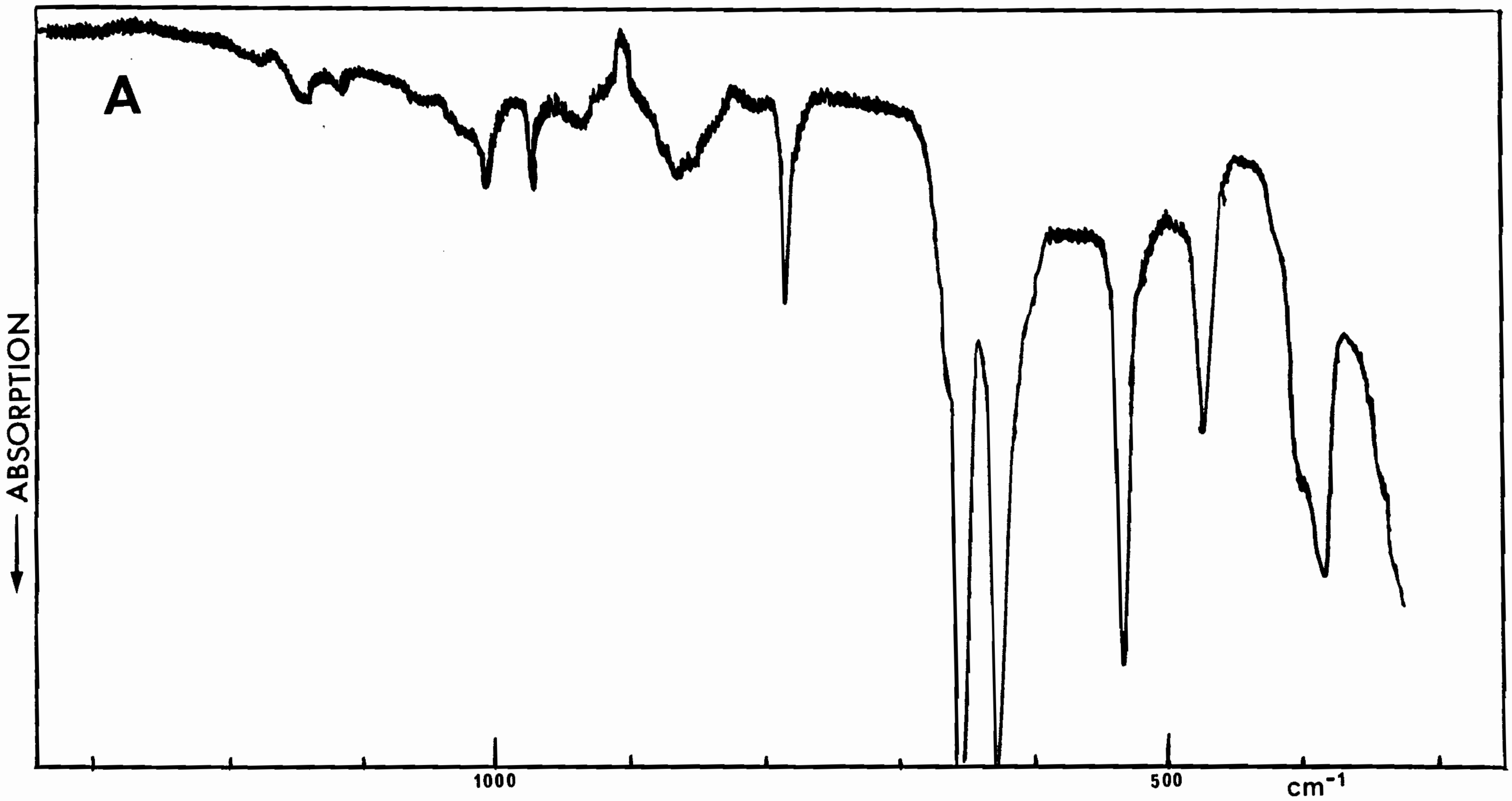

Figure III.2. Vibrational spectra of $BzCr(CO)_3$ in the region below 1500 cm^{-1}. (A) Infrared spectrum of the CS_2 solution; 0.2-mm solution cells.

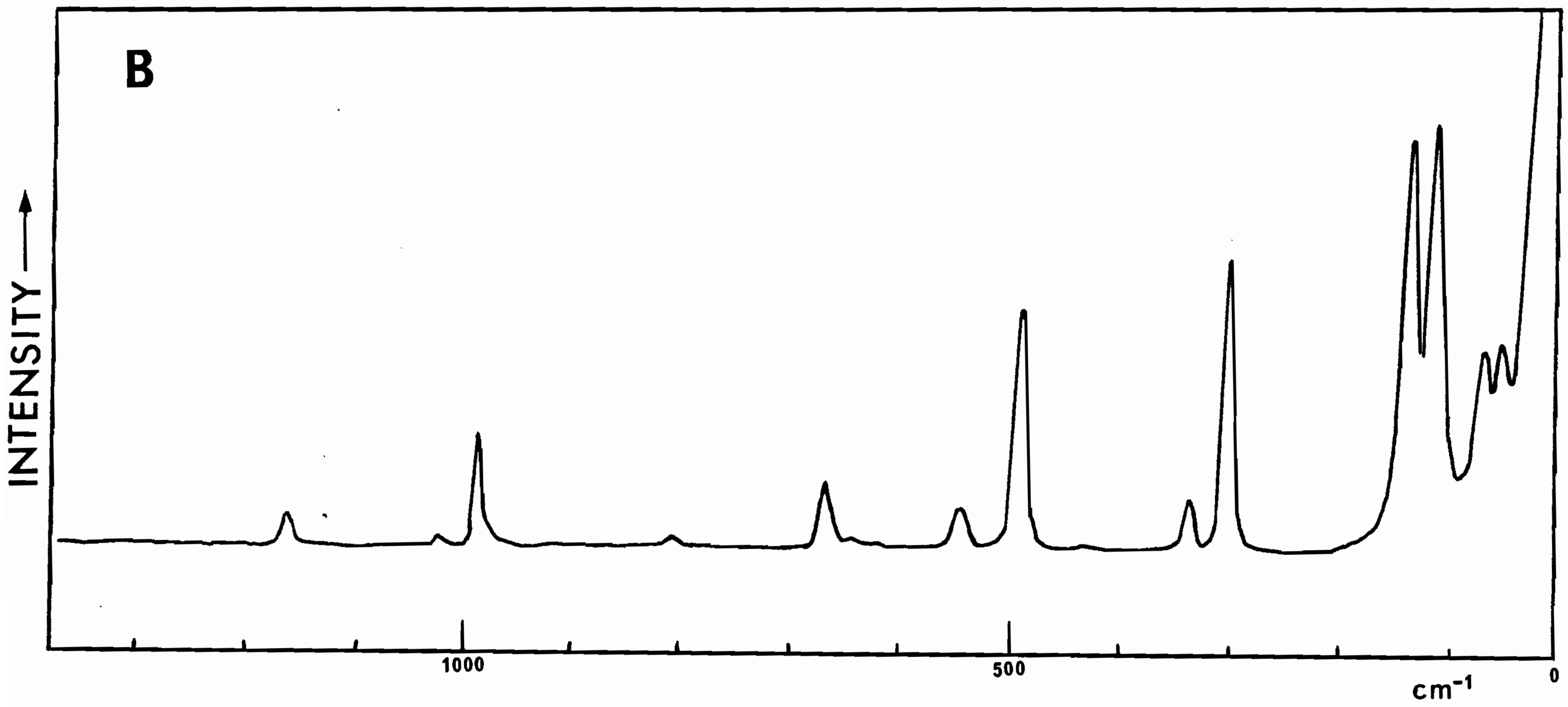

(B) Raman spectrum of the solid at ∿25°C. Conditions: sensitivity $2x10^4$ counts s^{-1}, slit widths 5 cm^{-1}, time constant 1 s, scan speed 50 cm^{-1} min^{-1}, Kr^+ 568.1 nm excitation, 25 mW.

TABLE III.4: Observed Wavenumbers in the ν(CO) Fundamental and Binary Combination Regions, and in the Low Energy Region of $(\eta^6\text{-}C_6H_6)Cr(CO)_3$[c]

BzCr(CO)$_3$[d]			$\text{B}\overset{D}{\text{z}}$Cr(CO)$_3$			BzCr(^{13}CO)$_3$			Assignments[a]
IR	Raman		IR	Raman		IR	Raman		
CS$_2$ Soln	Solid	C$_6$H$_6$ Soln	CS$_2$ Soln	Solid	C$_6$H$_6$ Soln	CS$_2$ Soln	Solid	C$_6$H$_6$ Soln	
3944 w			3944 w			3856 w			$2\nu_1$
3866 w			3865 w			3778 w			$\nu_1+\nu_2$
3798 w			3797 w			3711 w			$2\nu_2$
1976 s	1942 m	1970 p	1975 s	1942 ms	1974 p	1931 s	1897 s	1930 p	ν(CO) a_1 ν_1
1904 s	1886 ms	1893 dp	1904 s	1886 s	1897 p	1860 s	1843 s	1854 dp	ν(CO) e ν_9
	1863 s			1863 ms			1823 s		ν(CO)
647 w						647 w			
$\underline{653}$ ms	660 ms	658 p	671 ms	674 ms	678 p	640 ms	643 ms	641 p	$\delta(MCO)_\perp$ a_1 ν_2
$\underline{624}$ ms	636 w		622 ms	632 m		608 m			$\delta(MCO)_\parallel$ e ν_{10}
$\underline{615}$ sh	612 w		572 m			617 w,sh	614 w		α(CCC) e
				588 s	586 p				γ(CD) a_1
$\underline{532}$ m	537 m	536 dp	529 m	534 m	532 dp ?	517 m	522 m	518 dp ?	$\delta(MCO)_\perp$ e ν_{11}
	484 s	$\underline{478}$ p		484 s	477 p		476 s	470 p	ν(MC) a_1 ν_3
$\underline{471}$ mw			472 mw			465 mw			ν(MC) e ν_{12}
	423 w			384 m			425 w		τ(CCCC)
	328 ms	$\underline{335}$ dp		310 ms	313 dp		329 s	334 dp	ν(ML) e ν_{13}
	295 vs	$\underline{302}$ dp		284 vs	291 p		294 s	301 p	ν(ML) a_1 ν_4

TABLE III.4: (cont'd)

$BzCr(CO)_3$[d]			$B\overset{D}{z}Cr(CO)_3$			$BzCr(^{13}CO)_3$			Assignments[a]
IR	Raman		IR	Raman		IR	Raman		
CS_2 Soln	Solid	$C_6C_6H_6$ Soln	CS_2 Soln	Solid	C_6H_6 Soln	CS_2 Soln	Solid	C_6H_6 Soln	
	$\underline{270}$ w			266 m					
	$\underline{131}$ vs			130 vs			130 vs		b: a: ν_5, ν_6 e: ν_{14}, ν_{15} ν_{16}
	$\underline{108}$ vs			108 vs			108 vs		
	61 ms			60 s			62 s		
	46 ms			45 s			45 s		

[a] The spectra were analysed on the basis of the approximate model given in Section 9.1, therefore the observed bands (other than those which arise from ring vibrations) are assigned to the symmetry coordinates given in Table III.2.

[b] These peaks are due to vibrations involving strong mixtures of several different coordinates as can be seen from the P.E.D. given in Table III.15.

[c] The underlined frequencies of the normal species and those in the corresponding columns of the labelled species were input to the normal coordinate analysis.

[d] $Bz = (\eta^6-C_6H_6)$; $B\overset{D}{z} = (\eta^6-C_6D_6)$.

actual band positions and proposed assignments for all the various species are collected together in Table III.4. The assignment and numbering of the vibrations are based on the $L_3M(CO)_3$ model, thus the ring modes which appear in the low-energy region are not numbered. The predicted vibrational modes and their symmetries are: $\nu(CO)$ $(a_1 + e)$, $\delta(MCO)$ $(a_1 + a_2 + 2e)$, $\nu(MC)$ $(a_1 + e)$, $\nu(ML)$ $(a_1 + e)$ and $\delta(CMC) + \delta(LMC) + \delta(LML)$ $(2a_1 + a_2 + 3e)$. The assignments for the carbonyl fragment are in complete agreement with those of Adams et al.[8] The extra data from the all-^{13}CO substituted molecule confirm many of the previous assignments since the $\delta(MCO)$ and $\nu(MC)$ modes assigned by Adams et al. all exhibit the expected isotopic behaviour. However, one anomaly stands out; the wavenumber increase observed (here and previously[8,9]) on deuteration for the band assigned to the a_1 in-phase $\delta(MCO)$ mode suggests that either the normal mode description in the deuterated and undeuterated species is somewhat different or, that resonance interaction causes the frequency shift. Since the previous calculations on the complete molecule[8,9] gave a poor fit for this band in the deuterated molecule, the possibility of Fermi resonance was investigated. In benzene and deuterobenzene, the a_2 $\gamma(CH)$ and $\gamma(CD)$ modes are observed at 673 and 496 cm^{-1}, respectively[8]. On coordination, these modes show large wavenumber increases and are assigned to polarized bands at 791 and 588 cm^{-1} in the Raman spectra of the benzene solutions. However, the wavenumber shift on coordination is less in the deuterated complex since a comparable shift would give a band at 614 cm^{-1}. Furthermore, the δ(MCO) mode loses considerable intensity on deuteration whereas γ(CD) is almost twice as intense as γ(CH). Such observations are indicative of Fermi resonance which causes modes of the same symmetry and similar energies to diverge and share intensity[21]. A similar phenomenon was observed for CpMn(CO)$_3$ and its perdeuterated derivative[22].

In the assignment of the angle bending regions (150-40 cm^{-1}), the calculated values were relied upon heavily and, as will be seen in the next chapter, the experimental and calculated wavenumbers are in good agreement.

From the observed overtone and combinations bands (Table III.4), anharmonicity constants and harmonic frequencies were calculated for the two ν(CO) modes. The computational procedure was given in Part II and the harmonic frequencies and anharmonicity constants for all three chalcocarbonyl complexes are presented in Table III.7.

10.2. $(\eta^6\text{-}C_6H_6)Cr(CO)_2(CX)$ (X=S,Se)

Again, the normal, perdeuterated and all-^{13}CO isotopic species were examined. For the thiocarbonyl complex, the additional ^{13}CS-labelled molecule was available. The ir spectra of the CS_2 solutions and the Raman spectra of the solids were recorded for all species. Raman spectra of C_6H_6 solutions of only the thiocarbonyl complexes were obtained as the selenocarbonyl solutions decomposed rapidly in the laser beam.

The spectra were analysed in the ν(CO) and ν(CX) fundamental and binary regions, and from 800-40 cm^{-1}. Survey scans of the ir and Raman spectra of the normal species are shown in Figures III.3 and III.4, while the band positions and the proposed assignments are listed in Tables III.5 and III.6. As before, analysis of the spectra was based on the model given in Chapter 9. For $L_3M(CO)_2(CX)$ under C_s symmetry, the following modes are expected: ν(CO) (a' + a"), ν(CX) (a'), δ(MCO) (2a' + 2a"), δ(MCX) (a' + a"), ν[MC(O)] (a' + a"), ν[MC(X)] (a'), ν(ML) (a' + a"), ν(ML') (a') (ML and ML' are trans to the MCO and MCX groups, respectively) and nine valence-angle bending modes, (5a' + 4a").

The ν(CO) and ν(CX) fundamental and binary regions were readily assigned on the basis of C_s symmetry. The two

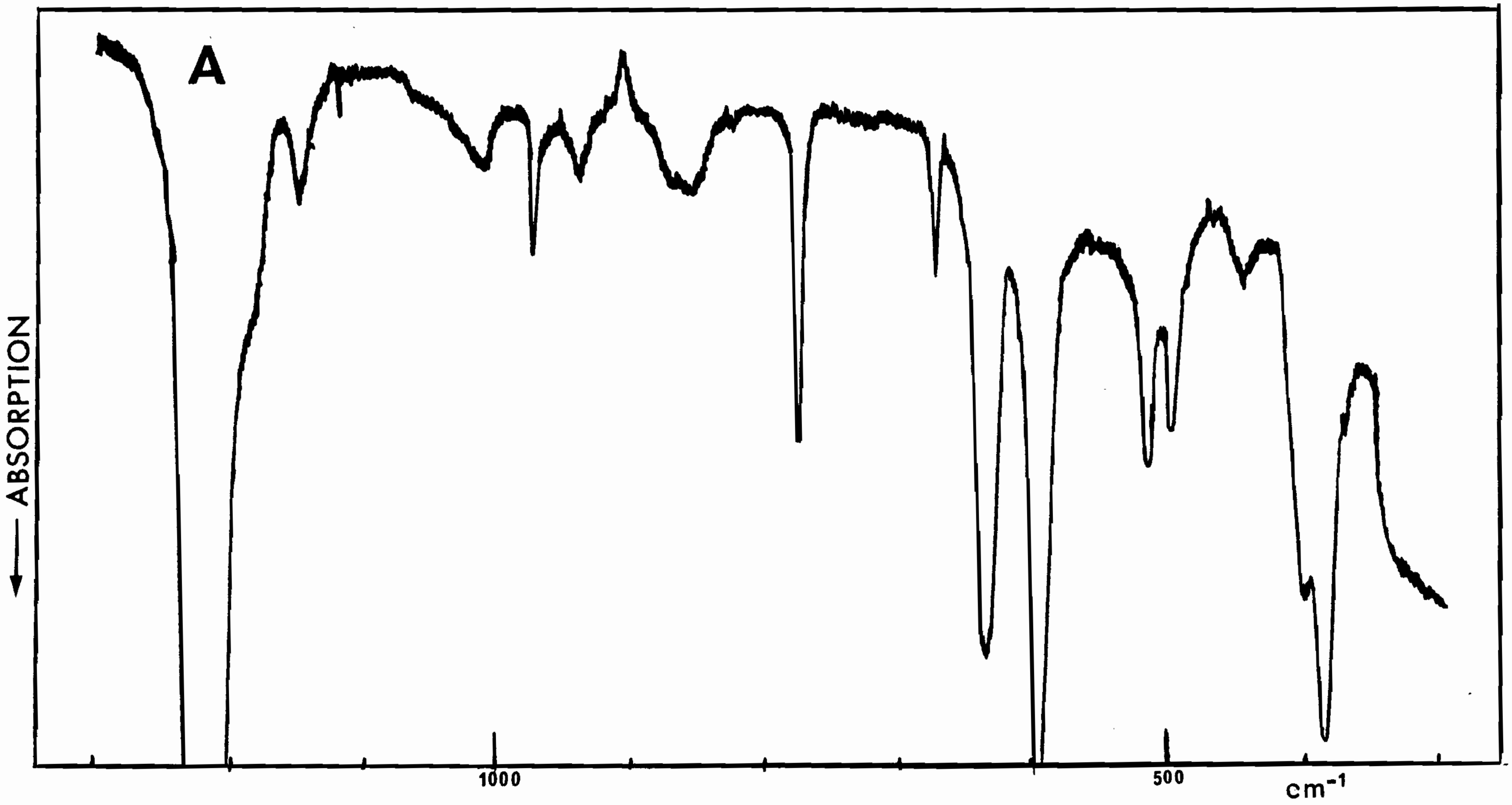

Figure III.3. Vibrational spectra of BzCr(CO)$_2$(CS) in the region below 1500 cm^{-1}. (A) Infrared spectrum of the CS$_2$ solution; 0.2-mm solution cells.

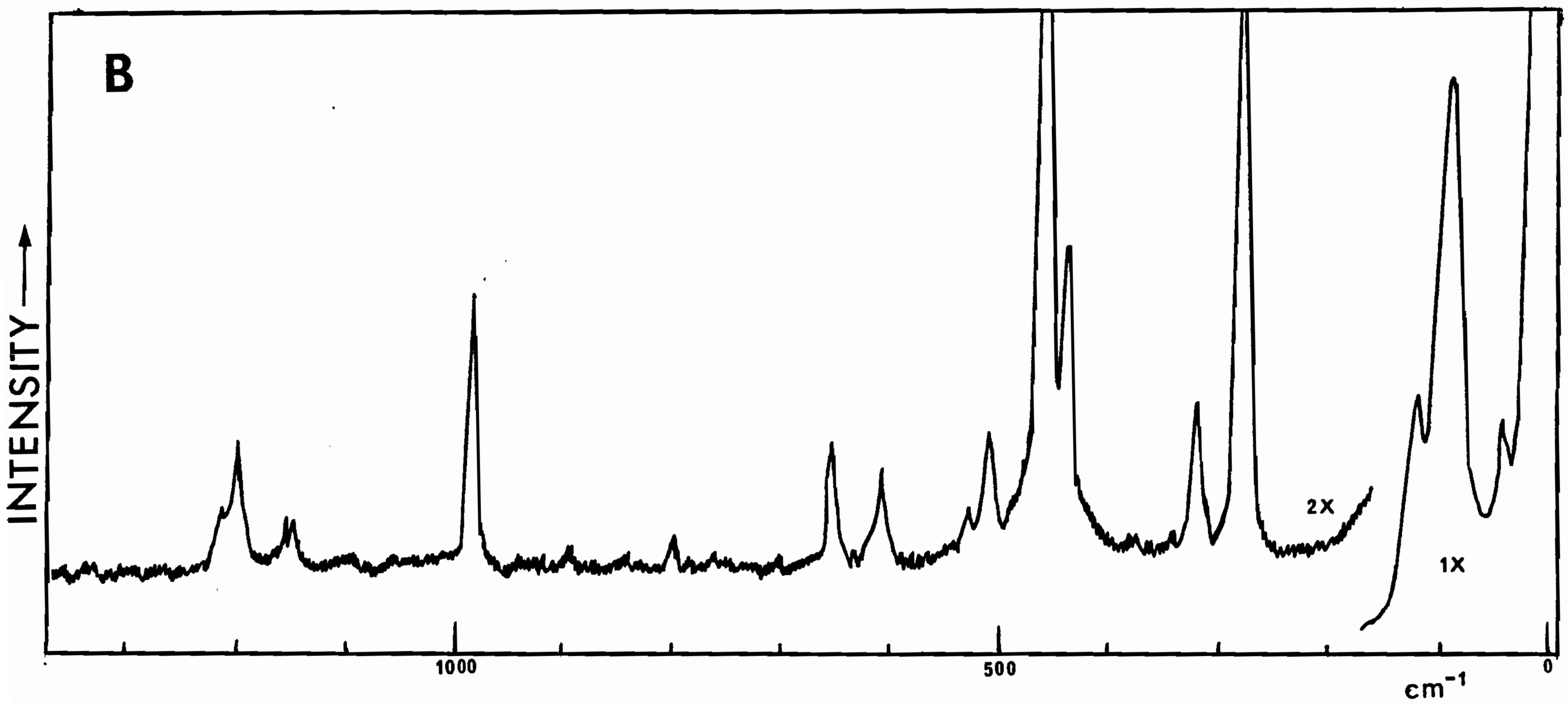

(B) Raman spectrum of the solid at ∿25°C. Conditions: sensitivity (2x) 5x10^{2} counts s^{-1}, slit widths 5 cm^{-1}, time constant 1 s, scan speed 50 cm^{-1} min^{-1}, Kr^{+} 568.1 nm excitation, 25 mW.

TABLE III.5: Observed Wavenumbers in the ν(CO) and ν(CS) Fundamental and Binary Combination Regions, and in the Low Energy Region of $(\eta^6\text{-}C_6H_6)Cr(CO)_2(CS)^c$

$BzCr(CO)_2(CS)^d$			$\overset{D}{B}zCr(CO)_2(CS)$			$BzCr(^{13}CO)_2(CS)$			$BzCr(CO)_2(^{13}CS)$			Assignments[a]
IR	Raman		IR	Raman		IR	Raman		IR	Raman		
CS_2 Soln	Solid	C_6H_6 Soln	CS_2 Soln	Solid	C_6H_6 Soln	CS_2 Soln	Solid	C_6H_6 Soln	CS_2 Soln	Solid	C_6H_6 Soln	
3925 w			3925 w						3926 w			$2\nu_1$
3867 w			3866 w						3866 w			$\nu_1+\nu_{15}$
3835 w			3834 w						3835 w			$2\nu_{15}$
2424 w			2423 w						2362 w			$2\nu_2$
1969 s	1977 m	1973 p	1969 s	1978 m	1969 p	1924 s	1910 w		1969 s			ν(CO) a' ν_1
1923 s	1953 m	1924 dp	1923 s	1963 w	1921 dp	1880 s	1849 w		1923 s			ν(CO) a" ν_{15}
	1892 m			1931 w								
1220 s	1207 w	1223 p	1220 s	1203 w	1221 p	1221 s	1208 w		1182 s	1175 w		ν(CS) a' ν_2
	1194 w			1188 w			1197 w			1132 w		
637 m	646 mw	645 p	648 m	656 mw	656 p	638 m	638 m		636 m	646 mw	643 p	$\delta(MCO)_\perp$ a' ν_3
600 m	603 mw		602 m	604 mw		589 m	590 m		599 m	602 mw		$\delta(MCO)_\perp$ a" ν_{16}
597 m,sh			598 m,sh			594 m,sh			589 m,sh			$\delta(MCO)_\parallel$ a' ν_4
				581 s	580 p							γ(CD)
			574 m									α(CCC)
517 mw	521 w		515 mw	521 w		510 mw						$\delta(MCS)_\parallel$ a' ν_5
517 mw						502 mw			516 mw			$\delta(MCO)_\parallel$ a" ν_{17}
499 mw	502 mw	502 ?	497 mw	502 mw	502 ?	492 mw	497 mw		495 mw	502 mw		$\delta(MCS)_\perp$ a" ν_{18}

TABLE III.5: (cont'd)

$\mathrm{BzCr(CO)_2(CS)}^d$			$\mathrm{BzCr(CO)_2(CS)}^b$			$\mathrm{BzCr(^{13}CO)_2(CS)}$			$\mathrm{BzCr(CO)_2(^{13}CS)}$			Assignments[a]
IR	Raman		IR	Raman		IR	Raman		IR	Raman		
CS_2 Soln	Solid	C_6H_6 Soln	CS_2 Soln	Solid	C_6H_6 Soln	CS_2 Soln	Solid	C_6H_6 Soln	CS_2 Soln	Solid	C_6H_6 Soln	
452 w,sh	452 vs	449 p	450 w,sh	450 vs	449 p	446 w,sh	448 vs	446 p	452 w,sh	450 s	449 p	ν[MC(O)] a' ν_6
443 w			443 w			439 w			442 w			ν[MC(O)] a" ν_{19}
	433 m		431 m			431 m			428 m			ν[MC(S)] a' ν_7
				372 m	380 dp							τ(CCCC)
	314 mw	321 dp		298 mw	302 dp		315 mw	322 dp		316 mw	319 dp	ν(ML) a" ν_{20}
	272 vs	273 p		265 vs	280 p		272 vs	275 p		272 vs	275 p	ν(ML) a' ν_8
	121 s,sh			121 s,sh			121 s,sh			121 s,sh		b a': ν_{10}, ν_{11}, ν_{12}
	112 s,sh			112 s,sh			112 s,sh			114 s,sh		ν_{13}, ν_{14}
	84 s			84 s			84 s			85 s		a": ν_{21}, ν_{22}, ν_{23}
	35 s			35 s			34 s			34 s		ν_{24}

[a,b,c,d] See Footnotes a,b,c and d, Table III.4.

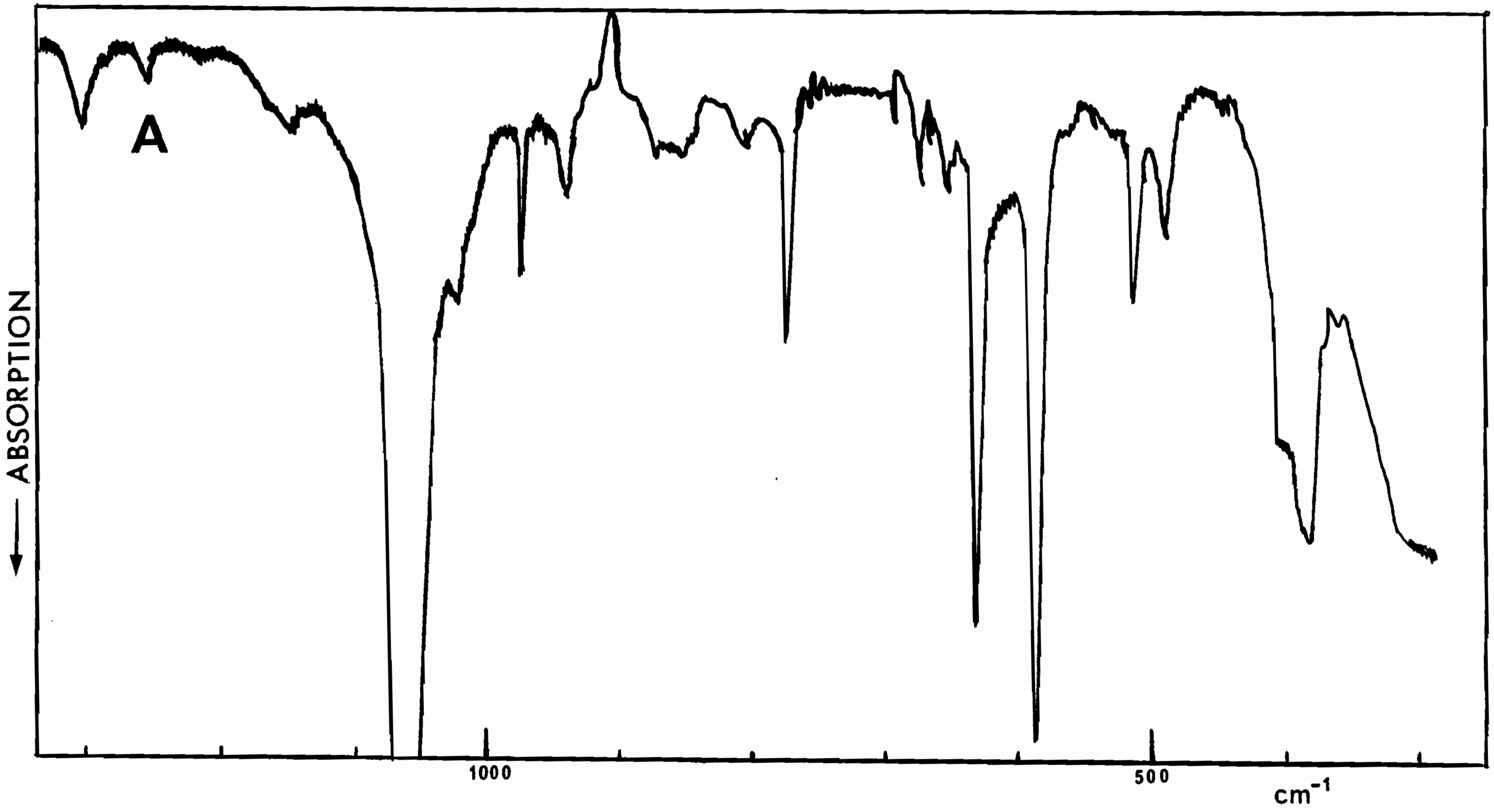

Figure III.4. Vibrational spectra of $BzCr(CO)_2(CSe)$ in the region below 1500 cm^{-1}. (A) Infrared spectrum of the CS_2 solution; 0.2-mm solution cells.

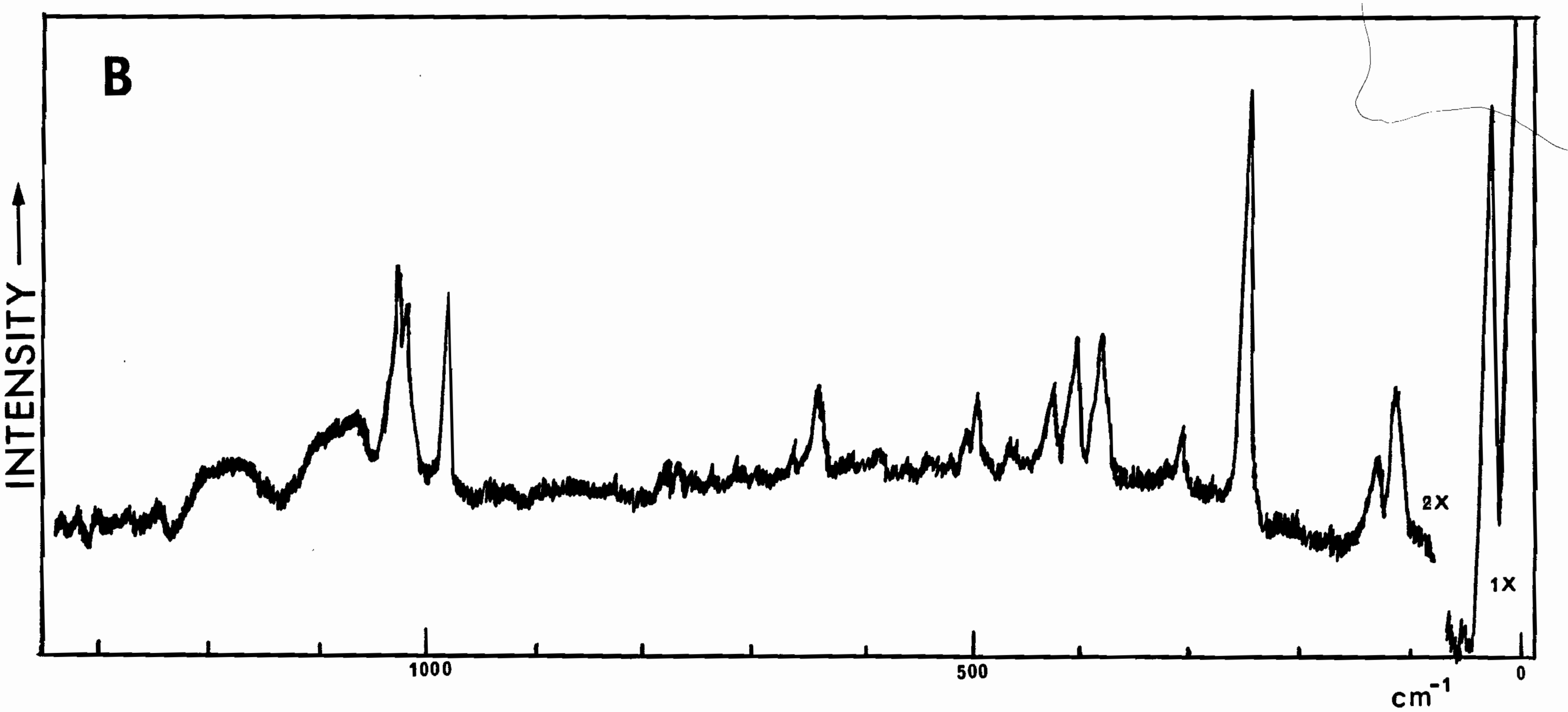

(B) Raman spectrum of the solid at ∿25°C. Conditions: sensitivity (2x) $5\text{x}10^2$ counts s^{-1}, slit widths 5 cm^{-1}, time constant 1 s, scan speed 50 cm^{-1} min^{-1}, Kr^+ 568.1 nm excitation, 15 mW.

TABLE III.6: Observed Wavenumbers in the $\nu(CO)$ and $\nu(CSe)$ Fundamental and Binary Combination Regions, and in the Low Energy Region of $(\eta^6\text{-}C_6H_6)Cr(CO)_2(CSe)^c$

$BzCr(CO)_2(CSe)^d$		$B\overset{D}{z}Cr(CO)_2(CSe)$		$BzCr(^{13}CO)_2(CSe)$		Assignments[a]
IR CS_2 Soln	Raman Solid	IR CS_2 Soln	Raman Solid	IR CS_2 Soln	Raman Solid	
3939 w						$2\nu_1$
3880 w						$\nu_1+\nu_{15}$
3851 w						$2\nu_{15}$
1975 s	1937 w	1975 s	1937 w	1930 s	1987 w	$\nu(CO)$ a' ν_1
1932 s	1912 w	1931 s	1911 w	1888 s	1872 w	$\nu(CO)$ a" ν_{15}
1061 s	1028 w	1062 s	1030 w	1061 s	1027 w	$\nu(CSe)$ a' ν_2
	1018 w				1018 w	
634 m	640 mw	643 m	647 m	624 m	630 m	$\delta(MCO)_\perp$ a' ν_3
613 w		570 m		613 w,sh		$\alpha(CCC)$
586 m		589 m		573 m		$\delta(MCO)_\parallel$ a' ν_4
586 m				582 m		$\delta(MCO)_\perp$ a" ν_{16}
			577 w			$\gamma(CD)$
513 mw		511 m		497 m		$\delta(MCO)_\parallel$ a" ν_{17}

TABLE III.6: (cont'd)

BzCr(CO)$_2$(CSe)^d		^{D}BzCr(CO)$_2$(CSe)		BzCr(^{13}CO)$_2$(CSe)		Assignments^a
IR CS$_2$ Soln	Raman Solid	IR CS$_2$ Soln	Raman Solid	IR CS$_2$ Soln	Raman Solid	
513 mw				504 m		$\delta(MCSe)_{\parallel}$ a' ν_5
491 mw	496 m	489 m	495 m	483 m	486 m	$\delta(MCSe)_{\perp}$ a" ν_{18}
450 vvw		450 vvw		441 vvw		ν_7+CMC
	429 m,br		420 m,br		426 m,br	ν[MC(O)] a', a" ν_6, ν_{19}
	407 m		377 m		407 m	τ(CCCC)
	383 m		381 m		381 m	ν[MC(Se)] a' ν_7
			300 w		319 w	ν_8+CMC
	306 mw		287 mw		304 mw	ν(ML) a" ν_{20}
	249 vs		238 vs		248 vs	ν(ML) a' ν_8
	131 s,sh				130 s,sh	b a': ν_{10}, ν_{11}, ν_{12} ν_{13}, ν_{14} a": ν_{21}, ν_{22}, ν_{23}, ν_{24}
	127 s,sh				125 s,sh	
	113 s		113 s		112 s	
	65 vs		65 vs		64 vs	

[a,b,c,d] See Footnotes a,b,c and d, Table III.4.

TABLE III.7: Harmonic Frequencies (cm^{-1}) and Anharmonicity Constants for the $\nu(CO)$ and $\nu(CX)$ Modes of the $(\eta^6-C_6H_6)Cr(CO)_2(CX)$ (X=O,S,Se) Molecules in CS_2 Solution[a]

ω_i and $X_{i,j}$	$BzCr(CO)_3$[b] ^{12}CO	^{13}CO	ω_i and $X_{i,j}$	$BzCr(CO)_2(CS)$ ^{12}CO	^{13}CO	^{13}CS	$BzCr(CO)_2(CSe)$ ^{12}CO	^{13}CO
ω_1 (a_1)	1998	1952	ω_1 a'	1995	1948	1995	2001	1955
ω_9 (e)	1927	1882	ω_{15} a"	1948	1903	1948	1957	1912
			ω_2 a'	1236	1237	1196	1073	1073
$X_{1,1}$	-3.8	-3.5	$X_{1,1}$	-6.8	-6.2	-6.3	-6.1	-5.8
$X_{9,9}$	-5.2	-5.0	$X_{15,15}$	-5.9	-5.5	-5.7	-6.0	-5.7
$X_{1,9}$	-14.2	-13.5	$X_{1,15}$	-26.2	-24.9	-26.3	-26.9	-25.7
			$X_{2,2}$	-8.0	-8.0	-7.4	-6.0	-6.0

[a] The $X_{i,j}$ for the ^{13}CO substituted thio- and selenocarbonyl complexes were determined from those of the normal species and Eq. II.2.

[b] $Bz=(\eta^6-C_6H_6)$.

ν(CO) fundamentals were attributed to the a' and a" modes in order of decreasing energy. As observed for the pentacarbonyl complexes, the ν(CS) and ν(CSe) fundamentals were found to be strongly ir-active and only weakly Raman-active.

The main difficulties arose in the assignment of the low-energy regions. Even with extra data available from the isotopic species, many alternative assignments of the ν(MC), δ(MCO) and δ(MCX) modes were possible. Bands exhibiting large shifts on ^{13}CO substitution occurred between 650 and 480 cm^{-1} while those with the smaller shifts typical of ν(MC) modes fell between 460 and 230 cm^{-1}. Also, the latter modes were relatively weak in the ir and strong in the Raman whereas the former exhibited the reverse pattern. Such intensity[23] and isotopic behaviour[14] suggest that the higher-energy bands should be assigned to linear bending modes and the lower-energy ones to metal-ligand stretches. The assignments given in Tables III.5 and III.6 are those considered to yield the most acceptable potential constants. However, since the potential energy distributions (Table III.15) show that many of the modes are strongly mixed, even these assignments represent an over-simplification. For example, the calculated mixing of δ(MCO) and δ(MCX) from the P.E.D.'s reveals that these modes are almost completely mixed; this explains the unexpected shift of δ(MCX) on ^{13}CO substitution and the shift of δ(MCO) on ^{13}CS substitution which complicate the low-energy assignments.

Strong and medium-intense bands observed in the Raman spectra of the thiocarbonyl solid (unlabelled) at 452 and 433 cm^{-1} are assigned to the ν[MC(O)] and ν[MC(S)] a' modes, respectively. A broad, asymmetric, polarized band, corresponding to these two solid-state bands, appears at 449 cm^{-1} in the Raman spectrum of the C_6H_6 solution. A weak ir band at 443 cm^{-1} is assigned to the ν[MC(O)] a" mode. The ν(ML) modes are readily assigned because of their large shifts on deuteration.

The lack of Raman spectra for the solutions of the selenocarbonyl complexes makes the detailed assignment of the metal-ligand stretching regions in these complexes more tentative. The two strong bands observed below 300 cm^{-1} are attributed to the a" and a' ν(ML) modes in order of decreasing energy. This leaves two medium-intense bands (at 407 and 383 cm^{-1} in the normal species and at 407 and 381 cm^{-1} in the ^{13}CO species) which are ascribed to the low-energy ring torsion mode, τ(CCCC), and the a' ν[MC(Se)] mode, respectively, since on deuteration the 407 cm^{-1} peak shifts to 377 cm^{-1} while the other remains at 381 cm^{-1}.

The a' and a" ν[MC(O)] modes are both assigned to a broad, medium-intense band at 429 cm^{-1} in the Raman spectrum of solid $BzCr(CO)_2(CSe)$ and a corresponding peak at 426 cm^{-1} for the ^{13}CO labelled species supports this assignment. In the deuterated species, however, a band is observed at 420 cm^{-1} which is similar in shape and intensity to that at 429 cm^{-1} in the normal species. Such a large shift on deuteration is not expected unless lattice or resonance interactions are perturbing the internal modes of this species.

A very weak band appears at 450 cm^{-1} in the ir spectra of the normal species which was initially assigned to the a" ν[MC(O)] mode. However, this resulted in a diverging field with unacceptable values for some of the potential constants while, in fact, the band can be easily accounted for by a combination of two fundamental modes (Table III.6).

10.3. Experimental

The complexes were prepared as described in Part I and were sublimed immediately prior to use. Spectrograde solvents (CS_2 and C_6H_6) were used without further purification. The infrared and Raman spectra were obtained as indicated in Section 4.6 for the pentacarbonyl complexes. The accuracy in the fundamental and binary ν(CO) and ν(CX) regions is ±0.5 cm^{-1} for all the complexes. In the 800-40 cm^{-1} regions of both the ir and Raman spectra, the band positions are accurate to ±1 cm^{-1} for the tricarbonyl, and to only ±2-3 cm^{-1} for the dicarbonyls due to the many weak and overlapping bands of these complexes. The procedures given in Section 4.6 were used to calibrate all spectra.

Chapter 11

Normal Coordinate Calculations

11.1. Input

The procedure followed in the normal coordinate analyses of the arene complexes is the same as that outlined in Part II.

The molecular dimensions used in the determination of the G matrix for $L_3M(CO)_3$ are those given in Ref. 19. The M - L distance was calculated from the C-C and Cr-C(C_6H_6) distances. Suitable bond lengths for $L_3M(CO)_2(CX)$ (X=S,Se) were estimated from those reported for the series, $(\eta^6\text{-}CH_3CO_2C_6H_5)Cr(CO)_2(CX)$ (X=O,S,Se)[24]. To allow for any differences caused by the presence of a different arene group, the lengths obtained for the benzoate chalcocarbonyls were multiplied by the ratio of the lengths of the corresponding bonds in $BzCr(CO)_3$ and $(\eta^6\text{-}CH_3CO_2C_6H_5)Cr(CO)_3$.

The actual values used in the calculations were: $BzCr(CO)_3$, CrC 1.845, CrL 2.118, CO 1.159; $BzCr(CO)_2(CS)$, CrC(O) 1.848, CrC(S) 1.792, CrL 2.127, CO 1.165, CS 1.584; $BzCr(CO)_2(CSe)$, CrC(O) 1.862, CrC(Se) 1.786, CrL 2.134, CO 1.156 and CSe 1.737 A. All bond angles were set equal to 90°. The atomic masses employed were the same as those given for the pentacarbonyls with the additional values for ^1H and ^2H of 1.007825 and 2.01410 a.m.u., respectively.

The internal and symmetry coordinates are given in Figure III.1 and Tables III.2 and III.3. The elements of the symmetry compliance constant matrices were constructed in the manner outlined for the pentacarbonyl complexes and the diagonal elements are given in Tables III.8 and III.9 for the tricarbonyl (C_{3v}) and the dicarbonyl (C_s) complexes, respectively. The labelling of the valence compliance constants in these Tables corresponds to that of the internal coordinates given in Figure III.1. In the C_s complexes, the valence-angle bending coordinates belong to seven different, symmetrically non-equivalent sets: (1) α_{23}; (2) α_{13}, α_{12}; (3) γ_{45}; (4) γ_{46}, γ_{56}; (5) ψ_{14}, ψ_{15}; (6) ψ_{26}, ψ_{36} and (7) ψ_{34}, ψ_{25}. Additional notation to distinguish each set was not introduced since these can be readily deduced from the numbering of the

TABLE III.8: Primary Symmetry Compliants for $(\eta^6\text{-}C_6H_6)Cr(CO)_3$ in the $L_3M(CO)_3$ Approximation

A_1 Block[a,b]	E Block
$C_{1,1} = C_D + 2C_{DD}$	$C_{9,9} = C_D - C_{DD}$
$C_{2,2} = C_\beta + 2C_{\beta\beta}$	$C_{10,10} = C_\beta - C_{\beta\beta}$
$C_{3,3} = C_R + 2C_{RR}$	$C_{11,11} = C_{\beta'} - C_{\beta'\beta'}$
$C_{4,4} = C_T + 2C_{TT}$	$C_{12,12} = C_R - C_{RR}$
$C_{5,5} = C_{\alpha\gamma} + 2C_{\alpha\gamma,\alpha\gamma}$	$C_{13,13} = C_T - C_{TT}$
$C_{6,6} = C_{\alpha\gamma\psi} + 2C_{\alpha\gamma\psi,\alpha\gamma\psi}$	$C_{14,14} = C_{\alpha\gamma} - C_{\alpha\gamma,\alpha\gamma}$
A_2 Block	$C_{15,15} = C_{\alpha\gamma\psi} - C_{\alpha\gamma\psi,\alpha\gamma\psi}$
$C_{7,7} = C_{\beta'} - 2C_{\beta'\beta'}$	$C_{16,16} = C_{\psi'} + C_{\psi'\psi'}$
$C_{8,8} = C_{\psi'} - 2C_{\psi'\psi'}$	

[a] The subcripts, D, R, T, β and β' refer to the internal coordinates shown in Figure III.1.

[b] The expressions for the angle-bending symmetry compliants were simplified as follows;

$C_{\alpha\gamma} = \frac{1}{2}(C_\alpha + C_\gamma - 2C''_{\alpha\gamma})$, $C_{\alpha\gamma,\alpha\gamma} = \frac{1}{2}(C'_{\alpha\alpha} + C'_{\gamma\gamma} - 2C'''_{\alpha\gamma})$,

$C_{\alpha\gamma\psi} = (\frac{1}{4}C_\alpha + \frac{1}{4}C_\gamma + \frac{1}{2}C_\psi + \frac{1}{2}C''_{\alpha\gamma} + \frac{1}{2}C''_{\psi\psi} - C''''_{\alpha\gamma} - C''''_{\gamma\psi})$,

$C_{\alpha\gamma\psi,\alpha\gamma\psi} = \frac{1}{2}(C'_{\alpha\alpha} + C'_{\gamma\gamma} + 2C'''_{\alpha\gamma})$,

$C_{\psi'} = (C_\psi - C''_{\psi\psi})$ and $C_{\psi'\psi'} = (2C'_{\psi\psi})$.

The quantities in brackets are the angle-bending valence compliants whose subscripts, α, γ, and ψ, refer to the bending coordinates in Figure III.1; the primes on the valence interaction compliants have the same meaning as in $M(CO)_6$, (Ref. 14).

TABLE III.9: Primary Symmetry Compliants for the $(\eta^6\text{-}C_6H_6)Cr(CO)_2(CX)$ Molecules in the $L_3M(CO)_2(CX)$ (X=S,Se) Approximation

A' Block[a,b,c,]	A" Block
$C_{1,1} = C_D + C_{DD}$	$C_{15,15} = C_D - C_{DD}$
$C_{2,2} = C_{D_x}$	$C_{16,16} = C_{\beta'} - C_{\beta'\beta'}$
$C_{3,3} = C_{\beta'} + C_{\beta'\beta'}$	$C_{17,17} = C_\beta - C_{\beta\beta}$
$C_{4,4} = C_\beta + C_{\beta\beta}$	$C_{18,18} = C_{\phi'}$
$C_{5,5} = C_\phi$	$C_{19,19} = C_R - C_{RR}$
$C_{6,6} = C_R + C_{RR}$	$C_{20,20} = C_T - C_{TT}$
$C_{7,7} = C_{R_x}$	$C_{21,21} = C_{\alpha\gamma} - C_{\alpha\gamma,\alpha\gamma}$
$C_{8,8} = C_T + C_{TT}$	$C_{22,22} = C^*_{\psi'}$
$C_{9,9} = C_{T_x}$	$C_{23,23} = C_{\psi'} - C_{\psi'\psi'}$
$C_{10,10} = C^*_{\alpha\gamma\psi}$	$C_{24,24} = C_{\alpha\gamma\psi} - C_{\alpha\gamma\psi,\alpha\gamma\psi}$
$C_{11,11} = C^*_{\alpha\gamma}$	
$C_{12,12} = C_{\alpha\gamma} + C_{\alpha\gamma,\alpha\gamma}$	
$C_{13,13} = C_{\psi'} + C_{\psi'\psi'}$	
$C_{14,14} = C_{\alpha\gamma\psi} + C_{\alpha\gamma\psi,\alpha\gamma\psi}$	

[a,b] See Footnotes a and b to Table III.8.

[c] An asterisk is used to denote the non-equivalence of certain linear combinations of valence compliants; e.g., the internal coordinates whose compliants are given in $C^*_{\alpha\gamma}$ ($C_{11,11}$) and those whose compliants appear in $C_{\alpha\gamma} + C_{\alpha\gamma,\alpha\gamma}$ ($C_{12,12}$) do not belong to the same sets (see Footnote b to Table III.3).

valence-angle coordinates.

11.2. Refinement of the $(\eta^6\text{-}C_6H_6)Cr(CO)_3$ Compliant Field

The band positions input for the normal species are underlined in Table III.4. The corresponding values were used for the perdeuterated and the all-^{13}CO substituted complexes. For ν(CO), the harmonic frequencies listed in Table III.7 were input. As in the case of the pentacarbonyls, the number of general quadratic compliance constants is far in excess of the number of observed frequencies. Numerous constants must, therefore, be constrained in the refinement. Many of the hexacarbonyl interaction constants should be reasonable approximations to those of the tricarbonyl moiety since the MCO groups are at approximately 90° to each other in both complexes. In the absence of suitable constraints from similar systems, the choice of interaction constants for the ML_3 moiety is somewhat arbitrary. This is also true of the interactions between the $M(CO)_3$ and ML_3 fragments.

For a complex system such as this, a diagonal potential is frequently used. However, the potential constants obtained with diagonal and non-diagonal potentials are usually quite different. This means that if the potential constants of the tricarbonyl and hexacarbonyl are to reflect differences in the electronic structures of the two complexes, rather than differences in the values assumed for the interaction constants, a non-diagonal potential should also be used for the tricarbonyl. Thus, as a first approximation, all diagonal and off-diagonal constants of $L_3M(CO)_3$ were set equal to $Cr(CO)_6$ equivalents. This initial field was then used to calculate the tricarbonyl frequencies. To observe the effect of setting all interactions equal to zero, the frequencies were also calculated using only the diagonal compliants. However, owing to the much closer frequency fit obtained with the non-diagonal field, this was judged to be a better initial estimate of the tricarbonyl potential and was allowed to refine. The ready convergence of this field to within ±1 cm^{-1} of the observed band positions on refinement of the primary constants only (Table III.12) was rather unexpected, but indicates, nonetheless, that the initial interaction constants are reasonable estimates of the tricarbonyl values. Furthermore, the changes in the primary constants from their initial, or $Cr(CO)_6$, values, were acceptable on the basis of chemical intuition. Such a close fit on refinement of the primary constants alone usually means that any subsequent refinement of the interaction constants leads to very small changes in these

TABLE III.10: Initial and Final Symmetry Compliants for $(\eta^6\text{-}C_6H_6)Cr(CO)_3$ in the $L_3M(CO)_3$ Approximation[a,d]

$C_{i,j}$	Initial Value	Final[b,c] Value	$C_{i,j}$	Initial Value	Final Value
	A_1 Block			E Block	
$C_{1,1}$	0.05837	0.06345 (7)	$C_{9,9}$	0.06044	0.06737 (6)
$C_{2,2}$	2.63	1.84 (9)	$C_{10,10}$	2.52	1.37 (6)
$C_{3,3}$	0.570	0.385 (12)	$C_{11,11}$	2.32	1.95 (6)
$C_{4,4}$	0.570	1.10 (1)	$C_{12,12}$	0.566	0.554 (12)
$C_{5,5}$	1.5	2.9 (2)	$C_{13,13}$	0.566	0.864 (8)
$C_{6,6}$	2.0	3.2 (2)	$C_{14,14}$	2.64	4.7 (8)
$C_{1,2}$	0.007		$C_{15,15}$	2.04	3.6 (2)
$C_{1,3}$	-0.019		$C_{16,16}$	1.88	2.0 (1)
$C_{1,4}$	0.014		$C_{9,10}$	0.006	
$C_{1,5}$	-0.011		$C_{9,11}$	-0.004	
$C_{1,6}$	0		$C_{9,12}$	-0.026	
$C_{2,3}$	-0.198		$C_{9,13}$	0.008	
$C_{2,4}$	0.198		$C_{9,14}$	0.006	
$C_{2,5}$	-0.48		$C_{9,15}$	0	
$C_{2,6}$	0.68		$C_{9,16}$	-0.01	
$C_{3,4}$	-0.168		$C_{10,11}$	0	
$C_{3,5}$	0.26		$C_{10,12}$	-0.171	
$C_{3,6}$	0		$C_{10,13}$	0.171	
$C_{4,5}$	-0.26		$C_{10,14}$	0.36	
$C_{4,6}$	0		$C_{10,15}$	-0.42	
$C_{5,6}$	0		$C_{10,16}$	-0.03	

TABLE III.10: (cont'd)

$C_{i,j}$	Initial Value
	E Block
$C_{11,12}$	0.10
$C_{11,13}$	-0.10
$C_{11,14}$	1.1
$C_{11,15}$	-0.34
$C_{11,16}$	0.36
$C_{12,13}$	-0.18
$C_{12,14}$	-0.13
$C_{12,15}$	0
$C_{12,16}$	0.22
$C_{13,14}$	0.13
$C_{13,15}$	0
$C_{13,16}$	-0.22
$C_{14,15}$	0
$C_{14,16}$	0.66
$C_{15,16}$	0

---

[a] Units are A $mdyn^{-1}$ for stretching compliants and $rad^2 A^{-1}$ $mdyn^{-1}$ for bending compliants.

[b] Quantities in parentheses are the standard deviations in units of the last digit for the given compliant.

[c] All non-diagonal elements were held fixed as discussed in the text.

[d] The initial values for the A_2 compliants are: $C_{7,7} = 2.21$, $C_{8,8} = 3.02$ and $C_{7,8} = -0.36$ A $mdyn^{-1}$. This block was not refined since the a_2 modes are inactive.

constants. Attempts to refine the (MC,CO) interaction together with the MC primary gave a converging field with negligible changes in the constants. A similar result was obtained when refinement of the (ML,MC) interaction with either the ML or MC primary was undertaken.

Thus, on the basis of the good wavenumber fit and the "reasonable" values obtained for the refined compliants, this solution is considered to be a good estimate of the tricarbonyl compliant field. Moreover, it should allow a fairly valid comparison of the tricarbonyl and hexacarbonyl compliance (or force) constants.

The initial and refined symmetry compliants are given in Table III.10. The valence compliance and force constants are listed in Table III.13. Only those valence constants which were elements of the "on-diagonal" symmetry constants are listed since all "off-diagonal" symmetry constants were constrained to the values of their $Cr(CO)_6$ equivalents. The significance of the estimated errors, which are also given in Table III.13 for the refined constants, was explained in Part II.

11.3. Refinement of the $(\eta^6-C_6H_6)Cr(CO)_2(CX)$ (X=S,Se) Compliant Fields

The low symmetry of these complexes leads to a large increase in the number of potential constants. The A' block contains 14 primary and 91 interaction constants and the A" block 10 primary and 45 interaction constants. Thus, only refinement of the diagonal elements was attempted for these systems. The initial fields were estimated from the tricarbonyl data except for the MCX grouping. The initial values for the ν(CX) and ν[MC(X)] constants were taken from the pentacarbonyl complexes. The diagonal elements of the symmetry compliant matrix for $L_3M(CO)_2(CX)$ are given in Table III.9. The input wavenumbers for the normal species are underlined in Tables III.5 and III.6. Again, the corresponding values were input for the deuterated and ^{13}CO-labelled species, together with the harmonic frequencies for the ν(CO) and ν(CX) modes listed in Table III.7.

Refinement was attempted for several alternative frequency assignments of the linear bending and metal-ligand stretching vibrations. For each complex, two or three of these alternative assignments resulted in converging fields. The set of potential constants finally selected in each case was that which yielded both a good fit of the observed frequencies and reasonable values for the valence constants when compared with those of $BzCr(CO)_3$ and $Cr(CO)_5(CX)$.

TABLE III.11: Initial and Final Symmetry Compliants for the $(\eta^6\text{-}C_6H_6)Cr(CO)_2(CX)$ Molecules in the $L_3M(CO)_2(CX)$ (X=S,Se) Approximation[a,b]

$C_{i,j}$[c]	$BzCr(CO)_2(CX)$[d] Initial Value	$BzCr(CO)_2(CS)$ Final Value	$BzCr(CO)_2(CSe)$ Final Value
	A' Block		
$C_{1,1}$	0.06476	0.06309 (9)	0.06262 (14)
$C_{2,2}$	0.1314; 0.1746	0.1547 (48)	0.2119 (144)
$C_{3,3}$	1.37	1.60 (1)	1.59 (1)
$C_{4,4}$	1.88	1.84 (3)	1.98 (16)
$C_{5,5}$	1.88	1.62 (7)	1.42 (13)
$C_{6,6}$	0.441	0.530 (24)	0.561 (14)
$C_{7,7}$	0.473	0.371 (36)	0.353 (30)
$C_{8,8}$	1.02	1.20 (2)	1.44 (5)
$C_{9,9}$	0.943	1.00	1.10
$C_{10,10}$	3.0	3.0	3.0
$C_{11,11}$	4.1	4.1	4.1
$C_{12,12}$	3.5	3.5	3.5
$C_{13,13}$	2.0	2.0	2.0
$C_{14,14}$	2.4	2.4	2.4
	A" Block		
$C_{15,15}$	0.06738	0.06589 (14)	0.06320 (12)
$C_{16,16}$	1.37	1.60 (10)	1.65 (2)
$C_{17,17}$	1.95	1.88 (5)	2.14 (4)

TABLE III.11: (cont'd)

$C_{i,j}$[c]	$BzCr(CO)_2(CX)$[d] Initial Value	$BzCr(CO)_2(CS)$ Final Value		$BzCr(CO)_2(CSe)$ Final Value	
	A" Block				
$C_{18,18}$	1.37	1.23	(6)	1.09	(1)
$C_{19,19}$	0.554	0.545	(10)	0.556	(11)
$C_{20,20}$	0.864	0.936	(13)	1.03	(1)
$C_{21,21}$	4.7	4.7		4.7	
$C_{22,22}$	2.4	2.4		2.4	
$C_{23,23}$	2.8	2.8		2.8	
$C_{24,24}$	3.6	3.6		3.6	

[a,b] See corresponding Footnotes, Table III.10.

[c] All off-diagonal elements were constrained.

[d] $Bz=(\eta^6-C_6H_6)$.

[e] Initial values for $C_{22}(C_{D_x})$ were taken from $Cr(CO)_5(CX)$ (X=S,Se) data, Table II.15.

TABLE III.12: Wavenumber Errors for the Fundamental Modes of the $(\eta^6\text{-}C_6H_6)Cr(CO)_2(CX)$ (X=O,S,Se) Molecules[a,b]

	ν_i	$BzCr(CO)_3$[c]				ν_i	$BzCr(CO)_2(CS)$				$BzCr(CO)_2(CSe)$		
		N	D	C-13			N	D	C(S)-13	C-13	N	D	C-13
a_1	ν_1	0	1	1	a'	ν_1	0	0	0	-1	0	0	1
	ν_2	1	652	0		ν_2	2	2	2	2	-5	-4	-5
	ν_3	0	0	0		ν_3	-1	638	-1	3	-4	637	5
	ν_4	1	2	1		ν_4	-1	0	0	4	-3	1	-5
	ν_5	0	127	131		ν_5	-3	-5	514	-7	7	4	4
	ν_6	87	87	87		ν_6	0	0	-2	0	-3	430	-2
						ν_7	2	1	4	4	0	0	-2
a_2	ν_7	541	541	524		ν_8	311	303	311	311	269	262	268
	ν_8	82	80	82		ν_9	-1	-2	1	2	2	-2	2
						ν_{10}	134	130	134	134	133	128	133
e	ν_9	0	0	0		ν_{11}	122	119	122	122	118	114	118
	ν_{10}	-1	-2	3		ν_{12}	110	108	110	110	104	102	104
	ν_{11}	2	-1	0		ν_{13}	79	79	79	79	76	75	76

TABLE III.12: (cont'd)

		$BzCr(CO)_3$[c]					$BzCr(CO)_2(CS)$				$BzCr(CO)_2(CSe)$		
	ν_i	N	D	C-13		ν_i	N	D	C(S)-13	C-13	N	D	C-13
e	ν_{12}	0	0	0	a'	ν_{14}	57	57	57	57	50	49	50
	ν_{13}	0	327	0									
	ν_{14}	0	128	131	a"	ν_{15}	0	0	0	0	1	1	1
	ν_{15}	0	105	108		ν_{16}	-3	-1	-5	2	0	1	0
	ν_{16}	61	60	61		ν_{17}	0	2	1	1	-3	-3	-6
						ν_{18}	2	0	6	4	-2	-1	2
						ν_{19}	1	1	1	4	-2	429	3
						ν_{20}	2	-8	0	4	4	-8	2
						ν_{21}	125	122	125	125	125	121	124
						ν_{22}	98	96	98	98	96	94	96
						ν_{23}	78	76	78	78	77	75	77
						ν_{24}	55	54	55	55	48	47	47

TABLE III.12: (cont'd)

---

[a] Error in $\nu_i = \nu_i(\text{obs}) - \nu_i(\text{calc})$.

[b] Calculated frequencies are given for those ν_i not input to the refinement.

[c] Bz = (η^6-C_6H_6), N = normal isotope, D = deuterated ring, C-13 = ^{13}CO derivative and C(S)-13 = ^{13}CS derivative.

The initial and final symmetry compliants are given in Table III.11 and the errors in the calculated wavenumbers are listed in Table III.12. The poorer overall fit obtained for the dicarbonyls compared to the tricarbonyl is partly due to the greater difficulty in estimating the maxima of the weak and overlapping peaks in the spectra of the former. Furthermore, the criterion of convergence in the C_s calculations was that no calculated compliant correction exceeded by more than 5% the value of the compliant, whereas in the tricarbonyl (and pentacarbonyls) the corrections were $\leq 1\%$ of the compliants. The calculated wavenumbers are given for modes which were not observed, or which were given zero weight due to large uncertainties in their peak positions. All valence-angle bending modes were set to zero in the C_s complexes and the corresponding compliants were constrained to their tricarbonyl values. Also, since no frequency was assigned to the unique chromium-ring stretch (ML'), a suitable constraint was estimated for the ML' compliant from the tricarbonyl equivalent.

The valence force and compliance constants as well as the P.E.D.'s for all three arene complexes are presented and discussed in the next chapter.

Chapter 12

Results and Discussion

12.1. Valence Potential Constants

The valence compliance and force constants for $BzCr(CO)_2(CX)$ (X=O,S,Se) are listed in Tables III.13(a) and (b) together with the equivalent values for $Cr(CO)_6$ and $Cr(CO)_5(CX)$. The force constants were obtained from the inverse compliance constant matrix, $F = C^{-1}$. Only those compliants (and the corresponding force constants) which were allowed to refine are given here. The remaining compliants have the same value as their $Cr(CO)_6$ counterparts.

A comparison of the hexacarbonyl and tricarbonyl data in Table III.13 reveals that substitution of three carbonyl groups in $Cr(CO)_6$ leads to a considerable increase

TABLE III.13(a): Valence Compliance Constants for the $(\eta^6\text{-}C_6H_6)Cr(CO)_2(CX)$ (X=O,S,Se) Molecules and the $Cr(CO)_6$ Equivalents[a]

C[b]	$BzCr(CO)_3$[c,d,e]	$BzCr(CO)_2(CS)$	$BzCr(CO)_2(CSe)$	$Cr(CO)_6$[f,g]
C_D	0.06606 (5)	0.06449 (8)	0.06291 (9)	0.05975 (4)
C_{D_x}		0.1547 (48)	0.2119 (144)	0.1314 (1); 0.1746 (6)
C_R	0.498 (9)	0.538 (13)	0.559 (9)	0.568 (23)
C_{R_x}		0.371 (36)	0.353 (30)	0.487 (2); 0.452 (3)
C_T	0.943 (6)	1.07 (1)	1.24 (2)	
C_{T_x}		[1.00]	[1.10]	
C_{DD}	-0.00131 (3)	-0.00139 (8)	-0.00029 (9)	-0.00069 (3)
C_{RR}	-0.0056 (6)	-0.007 (13)	0.0025 (9)	0.00228 (31)
C_{TT}	0.0796 (4)	0.132 (12)	0.204 (2)	

TABLE III.13(a): (cont'd)

C[b]	$BzCr(CO)_3$[c,d,e]		$BzCr(CO)_2(CS)$	$Bz(Cr(CO)_2(CSe)$	$Cr(CO)_6$[f,g]	
$C^*_{\alpha\gamma\psi}$			[3.0]	[3.0]		
$C^*_{\psi'}$			[2.4]	[2.4]		
$C_{\alpha\gamma,\alpha\gamma}$	-0.60	(27)	[-0.60]	[-0.60]	-0.40	(22)
$C_{\alpha\gamma\psi,\alpha\gamma\psi}$	-0.63	(9)	[-0.63]	[-0.63]	0.00	(22)
$C_{\psi'\psi'}$	[-0.40]		[-0.40]	[-0.40]	-0.40	(22)

---

[a] Units are given in Footnote a, Table III.10.

[b] For explanation of subscripts and asterisks see Footnote a, Table III.8 and Footnote c, Table III.9, respectively.

[c] $Bz=(\eta^6-C_6H_6)$.

[d] Numbers in square brackets were not refined.

[e] See Footnote b, Table III.10.

[f] From Ref. 26.

[g] Values for D_x, R_x and ϕ from $Cr(CO)_5(CX)$ (X=S,Se) data, Table II.15.

TABLE III.13(a): (cont'd)

C^b	$BzCr(CO)_3{}^{c,d,e}$	$BzCr(CO)_2(CS)$	$BzCr(CO)_2(CSe)$	$Cr(CO)_6{}^{f,g}$
C_β	1.91 (5)	1.86 (3)	2.06 (8)	2.42 (26)
$C_{\beta'}$	1.37	1.60 (5)	1.62 (1)	2.42 (26)
C_ϕ		1.62 (7)	1.42 (13)	2.39 (7); 1.97 (18)
$C_{\phi'}$		1.23 (6)	1.09 (10)	2.39 (7); 1.97 (18)
$C_{\beta\beta}$	-0.034 (36)	-0.02 (3)	-0.08 (8)	0.10 (13)
$C_{\beta'\beta'}$	[0]	-0.004 (50)	-0.032 (11)	-0.10 (13)
$C_{\alpha\gamma}$	4.1 (5)	[4.1]	[4.1]	2.2 (3)
$C_{\alpha\gamma\psi}$	3.0 (2)	[3.0]	[3.0]	2.0 (6)
$C_{\psi'}$	2.4	[2.4]	[2.4]	2.2 (3)
$C^*_{\alpha\gamma}$		[4.1]	[4.1]	

TABLE III.13(b): Valence Force Constants for the (η^6-C_6H_6) $Cr(CO)_2(CX)$ (X=O,S,Se) Molecules and the $Cr(CO)_6$ Equivalents[a]

$F^{b,c}$	$BzCr(CO)_3$[d,e]	$BzCr(CO)_2(CS)$	$BzCr(CO)_2(CSe)$	$Cr(CO)_6$[f,g]
F_D	15.41	15.77	15.89	17.04
F_{D_x}		6.528	4.757	7.677; 5.768
F_R	2.40	2.14	2.04	2.10
F_{R_x}		3.26	3.44	2.45; 2.66
F_T	1.19	1.04	0.897	
F_{T_x}		1.12	1.01	
F_{DD}	0.3021	0.314	0.305	0.169
F_{RR}	0.285	0.005	-0.045	-0.020
F_{TT}	-0.096	-0.138	-0.159	
F_β	0.627	0.597	0.537	0.460
$F_{\beta'}$	0.813	0.705	0.699	0.460
F_ϕ		0.706	0.816	0.48; 0.60
$F_{\phi'}$		0.939	1.08	
$F_{\beta\beta}$	0.00	0.03	0.044	0.00
$F_{\beta'\beta'}$	0.00	0.04	0.053	0.00

TABLE III.13(b): (cont'd)

$F^{b,c}$	$BzCr(CO)_3{}^{d,e}$	$BzCr(CO)_2(CS)$	$BzCr(CO)_2(CSe)$	$Cr(CO)_6{}^{f,g}$
$F_{\alpha\gamma}$	0.31	0.28	0.28	0.55[h]
$F_{\alpha\gamma\psi}$	0.31	0.39	0.39	0.59
$F_{\psi'}$	0.47	0.51	0.51	0.55
$F^*_{\alpha\gamma}$		0.27	0.27	
$F^*_{\alpha\gamma\psi}$		0.37	0.36	
$F^*_{\psi'}$		0.50	0.50	
$F_{\alpha\gamma,\alpha\gamma}$	0.04	0.04	0.04	0.08
$F_{\alpha\gamma\psi,\alpha\gamma\psi}$	0.31	-0.09	-0.09	0.08
$F_{\psi'\psi'}$	0.10	0.10	0.10	0.16

[a] Units are mdyn A^{-1} for stretching and mdyn A rad^{-2} for bending force constants. Values for F from C^{-1}.

[b,c,d,g] See corresponding Footnotes, Table III.13.

[f] Values from Ref. 14.

[h] Angle bending constants from Ref. 27.

in the ν(CO) compliant and a reduction in the ν(MC) compliant. Such changes indicate a substantial increase in the amount of π-backbonding to the π^* orbitals of the ligands; this in turn implies that there is less competition for the metal $d\pi$ electrons in the arene compound compared to that in the hexacarbonyl. The large decrease in the δ(MCO) compliant can also be attributed to an increase in π-backbonding since a stronger MC bond should increase the rigidity of the MCO group.

In the thio- and selenocarbonyls, the ν(CO) and ν[MC(O)] compliants become progressively smaller and larger, respectively, than those of the tricarbonyl. Also, the δ(MCO) compliants increase from the tri- to the dicarbonyls; the averages of β and β' going down the series are 1.64, 1.78 and 1.84 A mdyn^{-1}. On the other hand, the constants for δ(MCX), as well as those for ν(CX) and ν[MC(X)] exhibit the reverse trend as X varies from O to S to Se. By comparing these constants to the corresponding values for $Cr(CO)_5(CX)$, it is apparent that the arene complexes possess much stronger MC(X) bonds and much weaker CX bonds. Thus, the π-acceptance of CX is significantly greater in $BzCr(CO)_2(CX)$ than in $Cr(CO)_5(CX)$. Furthermore, the presence of CX in the benzene compounds causes a reduction in the π-backbonding to the remaining carbonyls as indicated by the decrease in the ν(CO) compliants. These findings are compatible with the "charge buffering effect" of CS postulated by Andrews[25], who concluded after comparing the ν(CO) and ν(CS) frequencies of various complexes that the π-acceptor/σ-donor ratio for coordinated CS can be either smaller or larger than for coordinated CO, inferring a greater adaptability of CS to its environment. The soft CSe group should also be able to withstand greater variations in charge density than the harder CO group as the results here imply.

In contrast, the results obtained for $(\eta^6\text{-}CH_3CO_2C_6H_5)Cr(CO)_2(CX)$ (Table III.1) when compared to those for $Cr(CO)_5(CX)$ indicate that the π-backbonding to CS and CSe is comparable in the two series. This is an unlikely result since the π-backdonation to the benzoate ring is not expected to be equal to that donated to three carbonyl groups. Results such as these demonstrate the worthlessness of obtaining potential constants for complex molecules when those of related molecules are not available to ascertain whether the values obtained are reasonable or not.

The values obtained for the metal-ring compliants (C_T) for the three benzene complexes show that the metal-ring interaction becomes progressively weaker on substitution of CO by CS and then CSe. This is reflected in the relative ease of removal of the ring in the thio- and selenocarbonyls compared to the tricarbonyl, as discussed in Part I. However, comparing this constant with those obtained previously (Table III.1) is not very meaningful because the metal-ring bonding was approximated by a metal-"point mass" interaction in one model[6] and by six metal-carbon bonds in the other[7-9,10]. Nevertheless, the relative magnitudes of the ν(ML) and ν[MC(O)] compliants agree with the theoretical picture of bonding in $BzCr(CO)_3$[17]. This complex is viewed as a $Cr(CO)_3$ fragment perturbed by a benzene ring rather than a BzCr fragment perturbed by three carbonyls, which implies that the metal-carbonyl interaction dominates the bonding.

Further discussion of the potential constants is delayed until the electronic sturctures of these complexes are presented in more detail in Part IV of this thesis.

12.2. Potential Energy Distributions for the $BzCr(CO)_2(CX)$ Molecules

The contributions of the symmetry coordinates ($V_{ii,k}$) to the potential energy of the normal modes are listed in Tables III.14 and III.15. The P.E.D. for the tricarbonyl is similar to that observed for $Cr(CO)_6$. This is partly

TABLE III.14: Diagonal Elements of the Potential Energy Distribution for the Normal Isotopic Species of $(\eta^6\text{-}C_6H_6)Cr(CO)_3$[a,b,c,d]

a_1	ν_1	$0.99S_1$	e	ν_9	$1.00S_9$
	ν_2	$0.40S_{\underline{2}}+0.23S_3$		ν_{10}	$0.68S_{10}$
	ν_3	$0.27S_2+0.69S_{\underline{3}}$		ν_{11}	$0.10S_{10}+0.62S_{\underline{11}}+0.12S_{12}+0.15S_{16}$
	ν_4	$0.89S_4$		ν_{12}	$0.11S_{11}+0.60S_{\underline{12}}+0.13S_{13}$
	ν_5	$0.52S_5+0.53S_6$		ν_{13}	$0.14S_{12}+0.70S_{\underline{13}}$
	ν_6	$0.48S_2+0.48S_5+0.48S_6$		ν_{14}	$0.23S_{12}+0.21S_{13}+0.10S_{14}+0.10S_{15}+0.61S_{\underline{16}}$
a_2	ν_7	$0.90S_7$		ν_{15}	$0.81S_{\underline{15}}+0.18S_{16}$
	ν_8	$0.13S_7+0.99S_{\underline{8}}$		ν_{16}	$0.10S_{10}+0.34S_{\underline{11}}+1.04S_{14}+0.18S_{16}$

[a] The symmetry coordinates, S_i, are defined in Table III.2.

[b] The coefficients of S_i, $V_{ii,k}$, (see Eq. II.27) give the contribution of S_i to the potential energy of the normal mode, ν_k.

[c] Contributions less than 0.10 are omitted.

[d] The major contribution to a mixed mode is underlined.

TABLE III.15: Diagonal Elements of the Potential Energy Distribution for the Normal Isotopic Species of the $(\eta^6\text{-}C_6H_6)Cr(CO)_2(CX)$ (X=S,Se) Molecules[a,b,c,d]

	ν_k	$(\eta^6\text{-}C_6H_6)Cr(CO)_2(CS)$	$(\eta^6\text{-}C_6H_6)Cr(CO)_2(CSe)$
a'	ν_1	$1.00S_1$	$1.00S_1$
	ν_2	$0.81S_{\underline{2}}+0.28S_7$	$0.63S_{\underline{2}}+0.47S_7$
	ν_3	$0.58S_3$	$0.62S_3$
	ν_4	$0.43S_{\underline{4}}+0.11S_5$	$0.37S_{\underline{4}}+0.17S_5$
	ν_5	$0.11S_4+0.24S_{\underline{5}}+0.12S_6+0.12S_7+0.12S_{13}$	$0.22S_4+0.28S_{\underline{5}}+0.11S_6+0.13S_{13}$
	ν_6	$0.50S_{\underline{6}}+0.28S_7$	$0.73S_6$
	ν_7	$0.12S_4+0.27S_{\underline{5}}+0.23S_6+0.17S_7$	$0.18S_2+0.10S_5+0.27S_7+0.27S_9$
	ν_8	$0.15S_8+0.58S_{\underline{9}}$	$0.33S_8+0.31S_9$
	ν_9	$0.70S_{\underline{8}}+0.23S_9$	$0.50S_{\underline{8}}+0.36S_9$
	ν_{10}	$0.10S_{10}+0.28S_{12}+0.54S_{\underline{14}}$	$0.14S_{10}+0.10S_{11}+0.22S_{12}+0.50S_{\underline{14}}$
	ν_{11}	$0.11S_5+0.10S_7+0.40S_{\underline{10}}+0.14S_{11}+0.10S_{12}+0.21S_{13}$	$0.58S_{\underline{10}}+0.14S_{11}+0.11S_{12}+0.20S_{14}$
	ν_{12}	$0.37S_3+0.13S_7+0.33S_{10}+0.56S_{\underline{13}}$	$0.30S_3+0.27S_7+0.12S_{10}+0.69S_{\underline{13}}$

TABLE III.15: (cont'd)

	ν_k	$(\eta^6\text{-}C_6H_6)Cr(CO)_2(CS)$	$(\eta^6\text{-}C_6H_6)Cr(CO)_2(CSe)$
a'	ν_{13}	$0.31S_4+0.13S_5+0.17S_{10}+0.44S_{\underline{11}}+0.11S_{12}$ $+0.17S_{14}$	$0.30S_4+0.17S_{10}+0.57S_{\underline{11}}+0.12S_{14}$
	ν_{14}	$0.22S_5+0.38S_{11}+0.52S_{\underline{12}}+0.24S_{13}+0.13S_{14}$	$0.31S_5+0.24S_{11}+0.57S_{\underline{12}}+0.24S_{13}+0.19S_{14}$
a"	ν_{15}	$1.01S_{15}$	$1.01S_{15}$
	ν_{16}	$0.24S_{16}+0.33S_{\underline{18}}$	$0.16S_{16}+0.42S_{\underline{18}}$
	ν_{17}	$0.55S_{\underline{17}}+0.10S_{16}+0.10S_{19}$	$0.64S_{\underline{16}}+0.20S_{18}$
	ν_{18}	$0.50S_{\underline{16}}+0.36S_{18}$	$0.48S_{\underline{17}}+0.16S_{19}$
	ν_{19}	$0.18S_{17}+0.68S_{\underline{19}}$	$0.27S_{17}+0.60S_{\underline{19}}$
	ν_{20}	$0.85S_{20}$	$0.86S_{20}$
	ν_{21}	$0.19S_{17}+0.18S_{19}+0.10S_{20}+0.10S_{21}+0.32S_{\underline{22}}$ $+0.10S_{23}+0.23S_{24}$	$0.19S_{17}+0.17S_{19}+0.10S_{20}+0.10S_{21}+0.31S_{\underline{22}}$ $+0.26S_{24}$
	ν_{22}	$0.10S_{16}+0.13S_{18}+0.13S_{21}+0.37S_{22}+0.58S_{\underline{24}}$	$0.11S_{16}+0.12S_{18}+0.15S_{21}+0.47S_{22}+0.50S_{\underline{24}}$
	ν_{23}	$0.25S_{22}+0.95S_{\underline{23}}$	$0.16S_{21}+0.16S_{22}+0.95S_{\underline{22}}$
	ν_{24}	$0.20S_{18}+0.75S_{\underline{21}}+0.12S_{22}+0.20S_{24}$	$0.29S_{18}+0.65S_{\underline{21}}+0.16S_{22}+0.25S_{24}$

[a] S_i defined in Table III.3.

[b,c,d] See Footnotes b,c and d of previous table.

due to the starting values for the $C_{i,j}$ and the constraints imposed on them in the calculation. As in the hexacarbonyl[14], the ν(MC) and δ(MCO) modes are strongly coupled in the bands appearing at ca. 650-400 cm^{-1}. The angle bending modes are also highly mixed and contain some δ(MCO), ν(MC) and ν(ML) character as well. Little mixing of the MC and ML stretches is indicated but, given that the calculated degree of mixing depends to a large extent on the value assumed for the (MC,ML) interaction constant which was somewhat arbitrarily set equal to the (MC,MC) interaction of $Cr(CO)_6$, some doubt must remain about the mixing of these modes.

The P.E.D.'s of $BzCr(CO)_2(CX)$ compared to those of $Cr(CO)_5(CX)$ reveal a large increase in mixing of the CX and MC(X) modes in the arene complexes. Since this means that the CS and CSe stretching modes contain an even greater amount of MC(X) stretching than the corresponding modes of $Cr(CO)_5(CX)$, energy-factoring is expected to be an even worse approximation here. The CO and CS or CSe stretches do not mix, which was also observed to be the case for $Cr(CO)_5(CX)$. On the other hand, $\delta(MCO)_{\parallel}$ and $\delta(MCX)_{\parallel}$ are almost completely mixed in the A' block and the same holds true for $\delta(MCO)_{\perp}$ and $\delta(MCX)_{\perp}$ in the A" block. As discussed above, this is reflected in the isotopic behaviour of these linear bending modes. It should also be noted that the MC and ML stretches again show little mixing in either the thio- or selenocarbonyl compounds. This is not surprising since the (MC,ML) interaction compliant was not adjusted in the C_s calculations.

12.3. Energy-Factored Force Fields (EFFF)

The harmonic and anharmonic ν(CO) and ν(CX) frequencies given in Tables III.4-III.7 were used to determine EFFF for the $BzCr(CO)_2(CX)$ molecules. The procedure followed is the same as that outlined in Part II and the results are given in Table III.16. The effects of CO-energy factoring and the neglect of anharmonicity on the primary CO and the (CO,CO) interaction constants are the same as those found for $Cr(CO)_5(CX)$. The (CO,CO) interaction here is equivalent to the cis constant of $Cr(CO)_5(CX)$.

It is clear from a comparison of the CX stretching force constants for the various approximations that an even greater difference exists between the general quadratic and energy-factored values for $BzCr(CO)_2(CX)$ than for $Cr(CO)_5(CX)$. This is especially true for the selenocarbonyls where ΔF (energy-factored - general quadratic) is 1.65 and 2.305 mdyn A^{-1} for $Cr(CO)_5(CSe)$ and $BzCr(CO)_2(CSe)$, respectively. Such variation certainly shows that energy-

TABLE III.16: CO and CX Force Constants and (CO,CO) Interaction Constants for the $(\eta^6\text{-}C_6H_6)Cr(CO)_2(CX)$ (X=O,S,Se) Molecules for Some Approximate Force Fields[a,b]

F[c]	Anhar EF[d]	Har EF	Har GQ[e]
		$BzCr(CO)_3$	
F_D	15.01	15.36	15.41
F_{DD}	0.378	0.374	0.3021
		$BzCr(CO)_2(CS)$	
F_D	15.30	15.69	15.77
F_{DD}	0.356	0.372	0.314
F_{D_x}	7.647	7.849	6.528
		$BzCr(CO)_2(CSe)$	
F_D	15.41	15.81	15.89
F_{DD}	0.344	0.350	0.305
F_{D_x}	6.905	7.062	4.757

[a] Units in mdyn A^{-1}.

[b] ν(CO) and ν(CX) frequencies from CS_2 solution data, Tables III.4-7.

[c] D=CO, D_x=CX.

[d] EF=energy-factored.

[e] GQ=general quadratic.

factored force constants for the ν(CX) modes of coordinated CS and CSe do not form a valid basis for comparison between different molecules as is possible in the case of CO. Furthermore, attempts to correlate other parameters (e.g., nmr chemical shifts) with either the observed CX stretching vibrations or the CX energy-factored force constants are rather pointless, although some fortuitous trends may well be observed.

References (Part III)

1. (a) G.E. Coates, M.L.H. Green and K. Wade, "Organometallic Compounds", Vol. II, Methuen, London, 1968; (b) K.F. Purcell and J.C. Kotz, "Inorganic Chemistry", Saunders, Philadelphia, 1977, and references therein.

2. H.P. Fritz, Advan. Organometal. Chem., 1, 239 (1964).

3. G. Davidson, Organometal. Chem. Rev. A, 8, 303 (1972).

4. K. Nakamoto, "Infrared and Raman Spectra of Inorganic and Coordination Compounds", 3rd ed., Wiley, New York, 1978.

5. E. Maslowsky Jr., "Vibrational Spectra of Organometallic Compounds", Wiley, New York, 1977.

6. R. Cataliotti, A. Poletti and A. Santucci, J. Mol. Struct., 5, 215 (1970).

7. J. Brunvoll, S.J. Cyvin and L. Schäfer, J. Organometal. Chem., 36, 143 (1972).

8. D.M. Adams, R.E. Christopher and D.C. Stevens, Inorg. Chem., 14, 1562 (1975).

9. E.M. Bisby, G. Davidson and D.A. Duce, J. Mol. Struct., 48, 93 (1978).

10. (a) P. Caillet, J. Organometal. Chem., 102, 481 (1975);
    (b) P. Caillet, C.R. Acad. Sc. Sér. C. 281, 1057 (1975);
    (c) P. Caillet, J. Organometal Chem., 164, 329 (1979).

11. D.C. Andrews and G. Davidson, ibid., 76, 373 (1974).

12. D.A. Connor, Topics in Current Chem., 71, 71 (1977).

13. P. Caillet and M.T. Forel, J. Chim. Phys., 522 (1975).

14. L.H. Jones, R.S. McDowell and M. Goldblatt, Inorg. Chem., 8, 2349 (1969).

15. G. Maier, Angew. Chem., Int. Ed. Engl., 13, 425 (1974).

16. L.H. Jones, R.S. McDowell, M. Goldblatt and B.I. Swanson, J. Chem. Phys., 48, 2663 (1968).

17. B.E. Bursten and R.F. Fenske, Inorg. Chem., 18, 1760 (1979).

18. S. Kjelstrup, S.J. Cyvin and J. Brunvoll, J. Organometal. Chem., 36, 137 (1972).

19. B. Rees and P. Coppers, Acta Cryst., B29, 2515 (1973).

20. I.J. Hyams, Chem. Phys. Letts., 15, 88 (1972).

21. E.B. Wilson, J.C. Decius and P.C. Cross, "Molecular Vibrations", McGraw-Hill, New York, 1955.

22. D.J. Parker, J. Chem. Soc. Dalton Trans., 155 (1974).

23. (a) G. Davidson, Inorg. Chim. Acta, 3, 596 (1969); (b) D.M. Adams and A. Squire, J. Chem. Soc. A, 814 (1970).

24. (a) J.Y. Saillard and D. Grandjean, Acta Cryst., B32, 2285 (1976); (b) J.Y. Saillard, G. Le Borgne and D. Grandjean, J. Organometal. Chem., 94, 409 (1975); (c) J.Y. Saillard and D. Grandjean, B34, 3772 (1978).

25. M.A. Andrews, Inorg. Chem., 16, 496 (1977).

26. L.H. Jones, J. Mol. Spectrosc., 36, 398 (1970).

27. I.S. Butler, A. Garcia-Rodriguez, K.R. Plowman and C.F. Shaw III, Inorg. Chem., 15, 2602 (1976).

PART IV

CORRELATION OF THE POTENTIAL CONSTANTS OF GROUP VIB METAL CHALCOCARBONYLS WITH SOME NON-VIBRATIONAL DATA

Chapter 13

Introduction

The success of vibrational spectroscopy in the elucidation of the structure of metal chalcocarbonyls has led to a predominance of vibrational data over other types of spectroscopic data for these compounds in the literature. However, the molecular frequencies, potential constants, interaction coordinates and dipole moment derivatives which can be obtained from the vibrational spectra are not direct manifestations of the electronic structure. Furthermore, their relationship to electronic structure is difficult to establish. The *ab initio* calculation of potential constants and molecular frequencies involves the theoretical determination of the potential-energy function of the molecule instead of simply assuming that the nuclear motion obeys Hooke's law, which is the basis of the general quadratic potential function approximation. Force constants and molecular frequencies have been determined non-empirically for some diatomic and simple polyatomic molecules[1].

For metal carbonyls, however, potential constants have only been calculated from observed vibrational frequencies. The electronic structures of these complexes have also been investigated using more direct methods such as photoelectron (pe) and electronic spectroscopy and molecular orbital (mo) calculations. Efforts have been made to correlate variations in the potential constants among different complexes with the bonding information obtained from these direct studies. The interpretation of some metal carbonyl potential constants from such correlations will be discussed in the following chapters and a similar interpretation of the MCS and MCSe constants will be attempted.

Other types of experimental evidence relevant to the theoretical conclusions on bonding in metal chalcocarbonyls will also be presented to ascertain whether the results of the vibrational studies are compatible with some of the other physicochemical properties of these complexes. The non-vibrational data to be discussed include the ^{13}C and ^{17}O nmr spectra, mass spectra, chemical reactivities and molecular structures from x-ray measurements.

Chapter 14

Electronic Structure and Physicochemical Properties of the $M(CO)_5(CX)$ Molecules

14.1. Introduction

Since the $M(CO)_5(CX)$ molecules have the simpler structure of the two series studied in Parts II and III, we will first attempt to correlate their electronic structure with other properties.

The electronic structure of the metal hexacarbonyls has received considerable attention. Theoretical calculations combined with pe and electronic spectra have led to a satisfactory determination of the energy levels in these complexes[2]. The He(I) pe spectra of $Cr(CO)_5(CS)$ and $W(CO)_5(CS)$[3] have also been measured and mo calculations were performed for the chromium complex to substantiate the pe assignments. Likewise, the energy levels of the free CS ligand were determined from pe measurements and mo calculations, and the mo diagrams for CO and CS are compared in Figure IV.1. Unlike CO and CS, the diatomic CSe species has never been isolated even at very low temperatures[4], so the pe spectrum of the free ligand has not been obtained and no mo calculations have been reported for this species. For these reasons, the He(I) pe spectrum of $Cr(CO)_5(CSe)$ was measured and the observed ionization potentials (ip's) were compared with those of the related complexes, $Cr(CO)_6$ and $Cr(CO)_5(CS)$. These results will be discussed before correlating the vibrational data with the electronic structures as some conclusions can be reached about the bonding in the selenocarbonyl complex from its pe spectrum.

14.2. Photoelectron Spectrum of $Cr(CO)_5(CSe)$

The He(I) pe spectrum of $Cr(CO)_5(CSe)$ is shown in Figure IV.2 and the measured ip's are listed in Table IV.1 together with the literature ionization data for $Cr(CO)_6$[2] and $Cr(CO)_5(CS)$[3]. Except for small shifts to lower binding energies in the selenocarbonyl complex, the spectra of the two pentacarbonyls are identical. The bands associated with the σ-donor and π-acceptor levels (regions B and C,

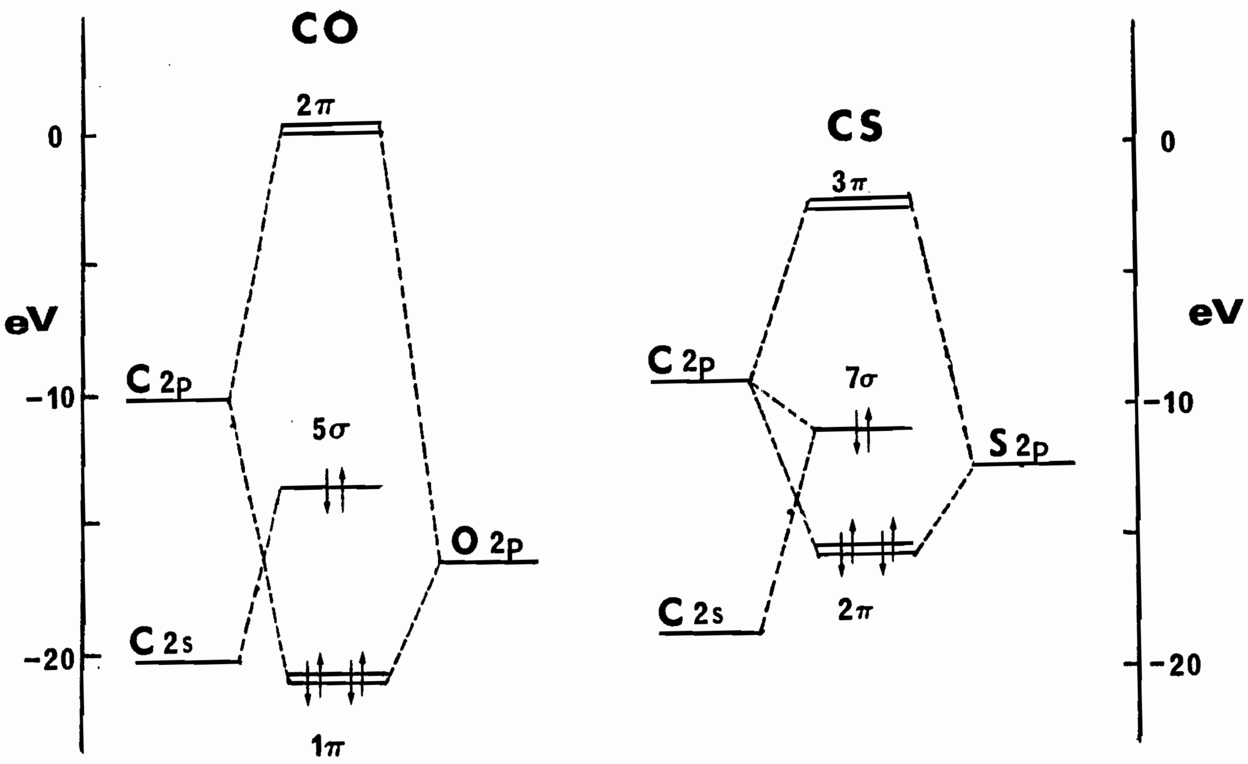

Figure IV.1. Molecular orbital diagrams of CO and CS. From Ref. 3.

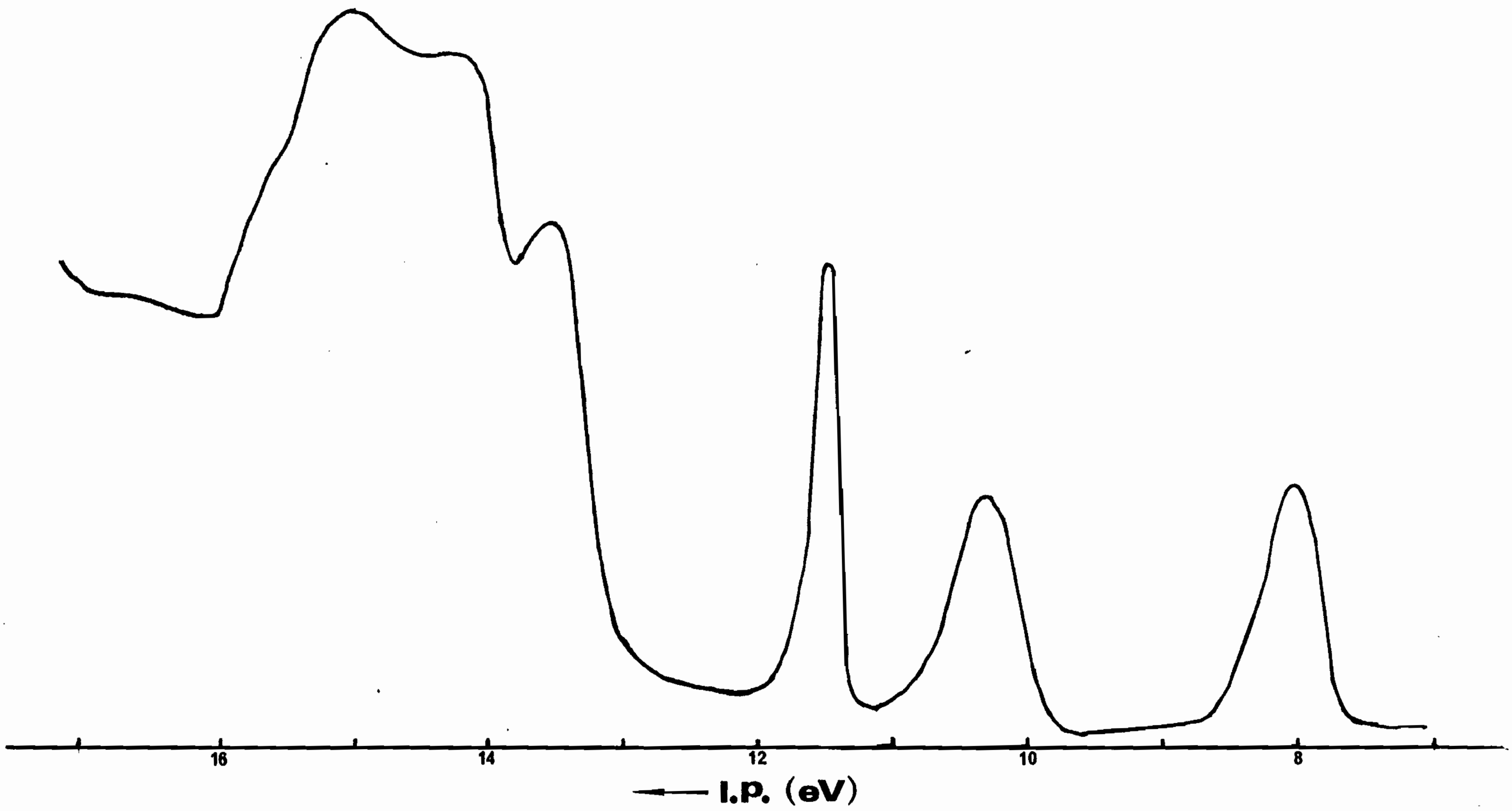

Figure IV.2. He(I) pe spectrum of $Cr(CO)_5(CSe)$ in the 7.0-16.5 eV range. Sample pressure 3.2×10^{-5} torr, scan time 1×10^{-3} s.

TABLE IV.1: Ionization Potentials (eV) for the $Cr(CO)_5(CX)$ (X=O,S,Se) Molecules

Region	$Cr(CO)_6$ [a,b]	$Cr(CO)_5(CS)$ [c]	$Cr(CO)_5(CSe)$
A	8.40 (t_{2g}) 3d; π*, CO	8.16 (b_2+e) 3d; π*, CO CS	8.03 (b_2+e) 3d; π*, CO CSe
B		10.93 (a_1) 7σ, CS	10.26 (a_1) 9σ, CSe
C		11.88 12.08 (e) 2π, CS 12.17	11.42 (e) 3π, CSe
D	13.38 (t_{1u}) 5σ, CO 14.21 (t_{1g}) 14.40 (t_{2u}) CO core 15.12 (t_{1u})		13.46 (e) 5σ, CO 14.12 CO core 15.04

[a] From Ref. 2.

[b] The symmetries of the mo's of the complexes are given in parentheses and the metal and ligand orbitals are listed in order of decreasing population as calculated for $Cr(CO)_6$ and $Cr(CO)_5(CS)$, and as projected for $Cr(CO)_5(CSe)$, see text.

[c] From Ref. 3.

respectively, in Table IV.1) of CSe are well separated for the other bands and appear in the 10-11.5 eV range, i.e., between the bands for the metal 3d levels (region A) and the carbonyl ligands (region D). In $Cr(CO)_6$, the predominantly metal 3d level, which is the highest filled mo (HOMO), has t_{2g} symmetry, and since exchanging a CO group for CS or CSe lowers the molecular symmetry from O_h to C_{4v}, the t_{2g} level should split into a b_2 + e set. No splitting of this peak was observed for the thiocarbonyl complexes and, as Figure IV.2 reveals, this is true for $Cr(CO)_5(CSe)$ also. The assignment of the bands in regions B and C of the pe spectrum of $Cr(CO)_5(CSe)$ to the mo's associated primarily with the highest filled σ and π (7σ, 2π) orbitals of CSe is based on that given previously for $Cr(CO)_5(CS)$ since these bands possess similar shapes and intensities in both complexes. The ionizations in region D are attributed to the highest occupied σ and π (5σ, 1π) levels and the core mo's of the CO groups in $Cr(CO)_5(CSe)$, again by comparison with the pe spectra of $Cr(CO)_6$ and $Cr(CO)_5(CS)$.

It seems reasonable to conclude from the similarities in their pe spectra that the electronic structures of the two pentacarbonyl complexes are quite similar. Furthermore, the mo levels calculated for $Cr(CO)_5(CS)$ should be a good approximation for those of $Cr(CO)_5(CSe)$ since in the thiocarbonyl the ordering of the occupied levels obtained from the mo calculations and pe spectrum are identical[3].

14.3. Electronic Structure of the Metal Chalcocarbonyls

The mo diagrams for $Cr(CO)_6$ and $Cr(CO)_5(CS)$ are given in Figure IV.3. The electronic structure of the thiocarbonyl will be discussed briefly here and much of the discussion is expected to apply to the selenocarbonyl as well because of the similarities in the pe spectra of the two complexes.

One of the surprising features of the pe spectrum of $Cr(CO)_5(CS)$ [and $Cr(CO)_5(CSe)$] is that, despite the differences in the electronic structures of CO and CS (Figure IV.1), the degeneracy of the $2t_{2g}$ ionizations of $Cr(CO)_6$ is not lifted. Since CS is a better π-acceptor than CO (the CS π^* orbital accepts 0.60 electron compared to 0.51 electron accepted by CO[3]), the metal e orbitals (d_{xz}, d_{yz}), which overlap with CS, are expected to be lower in energy than the b_2 (d_{xy}) orbital, which overlaps with CO only. The mo calculations[3], however, indicate that the e and b_2 levels of $Cr(CO)_5(CS)$ are separated by only 0.1 eV. Destabilization of the e level, despite increased interaction with the CS π^* level, is a consequence of increased metal

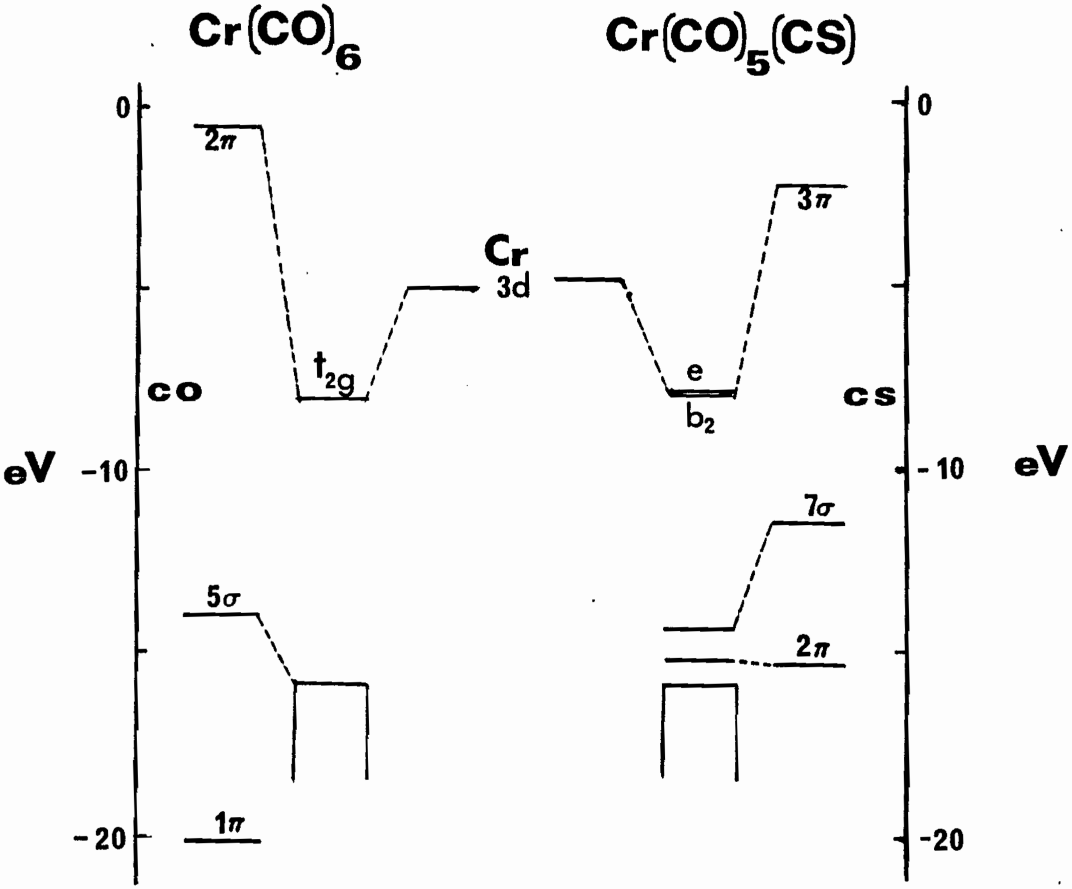

Figure IV.3. Molecular orbital diagrams of the Cr(CO)$_6$ and Cr(CO)$_5$(CS) molecules. From Ref. 3.

interaction with the CS occupied π bonds (the 2π level in Figure IV.1), which is less stable than the CO occupied 1π level. The greater interaction of the CS π levels with the metal compared to CO results in a strong MC bond and a weak CS bond.

The calculations also indicate that the CS group is a slightly better σ-donor, as expected, since the 7σ level of CS is higher in energy than the 5σ level of CO. This increased σ-donation reduces some of the additional charge on the carbon center due to the large π-acceptance of CS, and the smaller electronegativity of sulphur compared to oxygen.

Although there are significant differences in bonding to the CS ligand, the changes in the electronic structure of the remaining metal carbonyl fragment are small. The reduction in the electron density at the metal caused by the CS group results in slightly weaker MC(O) bonds since the MC overlap population in $Cr(CO)_6$ is 0.680, while the cis and trans values in $Cr(CO)_5(CS)$ are 0.652 and 0.618, respectively[3].

In light of the above discussion on the electronic structure of $Cr(CO)_5(CS)$, and the expected similarities of $Cr(CO)_5(CSe)$ and $W(CO)_5(CS)$, an effort will now be made to correlate the results obtained in Part II of this thesis with electronic structure.

14.4. Potential Constants, Interaction Coordinates and Electronic Structure of the $M(CO)_5(CX)$ Molecules

In an attempt to quantify the relationship between CO stretching force constants and bonding in metal carbonyls, the Cotton-Kraihanzel force constants (k)[5] and the occupancies of the 5σ and 2π orbitals of CO (from approximate mo calculations) were compared[6]. The complexes studied were a series of d^6 metal carbonyl halides and dihalides of general formula, $M(CO)_{6-x}L_x$ (M=Cr,Mn,Fe; L=Cl,Br,I; x=1,2). The results indicate that changes in both the degree of backbonding to the 2π orbital and the degree of σ-donation from the 5σ orbital contribute to the value of k. Furthermore, a linear relationship between k and the occupancies of the 5σ and 2π levels was obtained: $k = a(5\sigma) + b(2\pi_x + 2\pi_y)$, where a/b = 0.405. Both a and b are negative indicating that k decreases as the 5σ and 2π populations increase. The negative value of a is a consequence of the slightly antibonding nature of the 5σ orbital[6].

One of the most obvious effects of the halogen atoms in these complexes is the preferential reduction in the force constant of the _trans_-CO group (i.e., _trans_ to L), e.g., in $Cr(CO)_5Cl^-$, k(trans) = 14.07 and k(cis) = 15.58 mdyn A^{-1}. This reduction is attributed to an increase in the occupancy of the 2π levels of the trans CO, although enhanced donation from the 5σ level opposes this effect. Since the halogen atom is essentially a σ-donor, the difference in the cis and trans k values is due to redistribution of electron density on replacement of a CO group by a species with little or no π-acceptor ability.

In the thio- and selenocarbonyl complexes, on the other hand, the CO groups are replaced by ligands possessing greater π-acceptor ability. However, the values obtained for the cis- and trans-CO force constants differ by only 0.2 mdyn A^{-1} or less. The cis- and trans-CrC(O) force (and compliance) constants also show little variation, both values being similar to that of $Cr(CO)_6$ [Tables II.15(a) and (b)]. These changes are in accordance with the small differences calculated for the CrC(O) overlap populations in $Cr(CO)_5(CS)$ and $Cr(CO)_6$[3]. In $W(CO)_5(CS)$, a more substantial difference exists between the cis- and trans-WC(O) force constants, which have values of 2.41 and 2.13 mdyn A^{-1}, respectively. The smaller trans value can be ascribed to the increased metal-CS interaction in $W(CO)_5(CS)$ as indicated by the larger WC(S) and smaller CS force constants in this complex compared to $Cr(CO)_5(CS)$ [Table II.15(b)]. However, the trans-CO stretching force constant is not very different from the cis value or that of $W(CO)_6$, suggesting that the reduction in π-backbonding is accompanied by a decrease in σ-donation.

As mentioned previously, interaction coordinates are closely related to electronic structure and to the changes in electronic configuration which occur when a coordinate is displaced. The interaction coordinates for the stretch-stretch interactions of the $M(CO)_5(CX)$ molecules are given in Table II.16. On substituting O by S or Se, the most dramatic change occurs in the $[MC(X)]_{CX}$ coordinate which represents the relative displacement of MC(X) required to minimize the potential energy when CX is stretched a unit amount. The values obtained for this coordinate for X=O,S,Se are -0.401 [$M(CO)_6$, i.e., statistical average for M=Cr,Mo,W], -0.174 [$Cr(CO)_5(CS)$] and -0.131 [$Cr(CO)_5(CSe)$].

In an MCO group, the MC and CO interactions are usually interpreted in terms of π-backbonding only[7]; as the CO bond is stretched, its π^* orbitals are more available for overlap with the metal $d\pi$ electrons which results in a decrease in the MC bond length. Similar considerations predict interaction coordinates of the same magnitude, or even greater, for MCS and MCSe. The smaller values obtained for these groups suggest the involvement of two or more effects which partly cancel each other. It was noted above that the main difference between the CO and CS ligands is the relative instability of the occupied 7σ and 2π levels (Figure IV.1) of CS. Both these levels were found to interact considerably with the metal center in $Cr(CO)_5(CS)$. Stretching the CS bond stabilizes the 7σ level and increases the energy separation between this level and the σ-bonding orbitals of the metal, leading to reduced MC overlap. The 2π levels, on the other hand, are destabilized as the CS bond is stretched and their carbon character reduced, which again decreases the MC overlap.

In MCS, these effects apparently cancel to some extent the effect of increased MC π-overlap. Thus, the overall change in the MC bond order is reduced, and the interaction coordinate is decreased from its value in MCO. Such arguments should also apply to the MCSe group, and the small difference in the $[MC(X)]_{CX}$ value for $Cr(CO)_5(CS)$ and $Cr(CO)_5(CSe)$ indicates, in accordance with the pe spectra, that the bonding in the CS and CSe ligands is quite similar.

The $(CX)_{MC(X)}$ coordinates show the opposite trend as

X is changed from O to S and then to Se. The values calculated in this case are -0.0403, -0.0470 and -0.0507 for $Cr(CO)_6$, $Cr(CO)_5(CS)$ and $Cr(CO)_5(CSe)$, respectively. Here again, the negative values of the coordinates are consistent with a simple dπ-pπ* bonding model; as the MC(X) bond is stretched, π-backbonding from the metal is reduced and the adjacent CX bond decreases in length. The greater reduction predicted for the CS and CSe bond lengths is reasonable considering that the π* orbitals of these ligands accept more electron density than those of CO.

It is also worth mentioning here that the weak Raman activity of the CS stretching mode has been accounted for by the mutual interactions of the CS π and π* levels with the metal[3]. Stretching the CS bond increases the interaction of the π* orbitals with the metal and also increases their carbon character. Conversely, the CS π levels are destabilized when the CS bond is stretched and they acquire less carbon character, thereby decreasing their interaction with the metal. These two competing effects reduce the change in polarizability of the CS group during its stretching vibration and weaken its Raman activity. The equally weak activity of the ν(CSe) mode is further support for the similarity of the CS and CSe ligands.

14.5. ^{13}C and ^{17}O NMR Spectra of the $M(CO)_5(CX)$ Molecules

The carbon chemical shifts in closely related series have been correlated with various molecular parameters, the most common correlation being $\delta(^{13}CO)$ *vs*. k or $\nu(CO)$, where $\delta(^{13}CO)$ is the chemical shift and k the Cotton-Kraihanzel force constant. The $\delta(^{13}CO)$ and k values are given in Table IV.2 for a series of $W(CO)_5L$ complexes and an examination of this table indicates that both $\delta(^{13}CO)$ and k are directly related to the donor ability of L. Substitution of CO in $W(CO)_6$ by L leads to a decrease in k and an increase in $\delta(^{13}CO)$ for all L except CS. Furthermore, $\delta(^{13}CO$, *trans*) is greater than $\delta(^{13}CO$, *cis*) except for L = CS, in which the relative magnitudes are reversed. Thus, the replacement of CO by a monodentate ligand (L), which has a smaller π-acceptor/σ-donor ratio than CO causes an increase in the downfield ^{13}C chemical shift of coordinated CO, whereas replacement by CS produces an upfield shift. Again, this observation is consistent with the force constant and mo calculations which show that CS has an even greater electron-withdrawing power than CO.

The complete set of chemical shifts [$\delta(^{13}CO)$, $\delta(^{13}CX)$ and $\delta(C^{17}O)$] measured in this laboratory for $Cr(CO)_5(CX)$ (X=O,S,Se) and $W(CO)_5(CX)$ (X=O,S)[9] are collected in Table IV.3. The trends in $\delta(^{13}CO)$ are in accord with those in

TABLE IV.2: CO Energy-Factored Force Constants and $\delta(^{13}CO)$ for Some $W(CO)_5L$ Molecules[a]

L	$\delta(^{13}CO)^b$ trans	$\delta(^{13}CO)^b$ cis	k^c mdyn $Å^{-1}$ trans	k^c mdyn $Å^{-1}$ cis
CS	187.3	192.4	16.60	16.71
CO	192.1		16.41	
$P(OPh)_3$	197.0	194.5	15.88	16.08
$P(OEt)_3$	199.6	197.2	15.73	15.91
$AsPh_3$	199.7	197.5	15.53	15.90
PBu_3	200.4	198.6	15.45	15.75
$NH_2C_6H_{11}$	201.9	199.1	15.12	15.76

[a] Data for all complexes, except $W(CO)_5(CS)$, from Ref. 8; $\delta(^{13}CO)$ for $W(CO)_5CS$ from Ref. 9 and k from Table II.19.

[b] ± 0.3 ppm positive downfield relative to internal TMS.

[c] Cotton-Kraihanzel approximation used in determination of k for all complexes except $W(CO)_5CS$.

TABLE IV.3: CO and CX General Quadratic Force Constants and $\delta(^{13}\mathrm{CO})$, $\delta(^{13}\mathrm{CX})$ and $\delta(\mathrm{C}^{17}\mathrm{O})$ for the $M(CO)_5(CX)$ (X=O,S,Se; M=Cr,W) Molecules[a]

Complex	$\delta(^{13}\mathrm{CO})$[b]		$\delta(^{13}\mathrm{CX})$[b]	$\delta(\mathrm{C}^{17}\mathrm{O})$[c]		F_{CO} (mdyn A^{-1})		F_{CX} (mdyn A^{-1})
	trans	cis		trans	cis	trans	cis	
$Cr(CO)_6$	212.2		-	376.2		17.24		-
$Cr(CO)_5(CS)$	209.4	212.4	332.2	-	373.0	17.42	17.28	7.677
$Cr(CO)_5(CSe)$	208.1	211.7	360.7	385.3	373.4	17.47	17.28	5.768
$W(CO)_6$	192.1		-	335.5		17.22		-
$W(CO)_5(CS)$	189.3	192.4	298.7	364.4	357.0	17.24	17.28	7.455

[a] NMR data from Ref. 9; force constants from Table II.15(b).

[b] ± 0.1 ppm positive downfield relative to internal TMS.

[c] ± 0.15 ppm positive downfield relative to $H_2{}^{17}O$.

the force constants given in Table II.15(b); this can also be said for $\delta(C^{17}O)$ since the electronic effects which result in an upfield shift in $\delta(^{13}CO)$ produce a concomitant downfield shift in $\delta(C^{17}O)^9$. The greater electron-withdrawing capacity of CS and CSe compared to CO is reflected in the large downfield ^{13}C shift of the CS and CSe resonances from that of CO. Moreover, the order is the same as that predicted by the force constants, viz., CO<CS<CSe.

The ^{13}C and ^{17}O chemical shifts are thought to be dominated by the paramagnetic contribution to the screening tensor[10], which is given by

$$\sigma_p = -K(\Delta E_{av})^{-1}\langle r^{-3}\rangle_{2p}[Q_{AA} + \Sigma Q_{AB}]$$

Here, K is a constant, ΔE_{av} an average electronic excitation energy and $\langle r^{-3}\rangle_{2p}$ the mean inverse cube radius for the 2p orbitals; Q_{AA} and Q_{AB} depend on the atomic charge density and molecular bond order matrix elements. The relative importance of the various terms in σ_p is still a matter of some controversy. Brown and coworkers[11] calculated σ_p for the ^{13}C nuclei in the series $AM(CO)_3$ [AM = $(\eta^6\text{-}C_6H_6)Cr$, $(\eta^5\text{-}C_5H_5)Mn$, $(\eta^4\text{-}C_4H_4)Fe$, $(\eta^3\text{-}C_3H_5)Co$ and $(\eta^2\text{-}C_2H_5)Ni$] and found that the chemical shifts of the CO groups are dominated by the $(\Delta E_{av})^{-1}$ term, which was approximated by the energy separation of the complexes' HOMO's and LUMO's (lowest unoccupied mo's). In $Cr(CO)_5(CS)$, the HOMO's and LUMO's are the b_2 + e and CS π^* levels, respectively[3]. Thus, a transition from the HOMO's to the CS π^* orbitals has a smaller ΔE and a larger $(\Delta E)^{-1}$ than a corresponding transition to the CO π^* level. If $(\Delta E)^{-1} \equiv (\Delta E_{av})^{-1}$ is the most important term in σ_p, a larger chemical shift is predicted for $\delta(^{13}CS)$ compared to $\delta(^{13}CO)$, in agreement with the experimental results.

14.6. Substitution Reactions of the $M(CO)_5(CX)$ Molecules

These compounds undergo thermal substitution of one CO group by monodentate ligands such as PPh_3, C_5H_5N, Cl^- and Br^- to yield derivatives of the form, $M(CO)_5(CX)L$. In the case of $W(CO)_5(CS)$[12], the product is chiefly *trans*-$W(CO)_5(CS)(L)$, while statistical mixtures of the *cis*- and *trans*-isomers are obtained for $Cr(CO)_5(CX)$ (X=S,Se)[13]. The pronounced labilization of the *trans*-CO group of $W(CO)_5(CS)$ is reflected in the larger decrease in the *trans*-WC(O) force constant from that in $W(CO)_6$ [Table II.15(b)]. In $Cr(CO)_5(CS)$ and $Cr(CO)_5(CSe)$, neither the *cis*- nor the *trans*-CrC(O) force constants are significantly different from the $Cr(CO)_6$ value, which is reflected in the 4/1 *cis*/*trans* mixtures produced in the substitution reactions of $Cr(CO)_5(CX)$[13].

Kinetic studies have also been reported for some of the substitution reactions of $W(CO)_5(CS)$[12]. These studies clearly indicate that the CS ligand accelerates the rate of CO substitution in $W(CO)_5(CS)$ compared to that observed for $W(CO)_6$. Both dissociative (S_N1) and associative (S_N2) pathways occur for substitution by PPh_3, and the ratio of these pathways are 75 and 250 times faster, respectively, than the corresponding rates for $W(CO)_6$ under the same conditions. The reaction with I^-, which occurs by an associative mechanism only, is 1000 times faster in $W(CO)_5(CS)$ than in $W(CO)_6$. The increased reactivity of the trans-CO group towards nucleophiles is yet another indication of the electron withdrawing capacity of the CS. Presumably, similar kinetic behaviour will be exhibited by $Cr(CO)_5(CS)$ and $Cr(CO)_5(CSe)$, but on the basis of the vibrational data, a smaller rate enhancement is expected as CS and CSe are less effective in removing charge density from the chromium atom compared to CS in $W(CO)_5(CS)$.

Chapter 15

Electronic Structure and Physicochemical Properties of the $(\eta^6\text{-}C_6H_6)Cr(CO)_2(CX)$ Molecules

15.1. Electronic Structure of $(\eta^6\text{-}C_6H_6)Cr(CO)_3$

The electronic structure of this π-arene complex has been the subject of many semi-empirical molecular orbital calculations. Self-consistent, semi-empirical calculations have been reported by Brown and Rawlinson[14] and by Carroll and McGlynn[15]. Using both self-consistent[16] and CNDO[17] approaches, Fitzpatrick and coworkers have performed a comparative study on a series of $(Ring)M(CO)_3$ complexes including $BzCr(CO)_3$. Guest et al.[18] have reported ab initio SCF mo calculations and the low-energy pe spectra of both $BzCr(CO)_3$ and Bz_2Cr. In addition, the x-ray pe spectrum of $BzCr(CO)_3$ has been published[19].

Before correlating the vibrational data with any of the above results,the qualitative features of bonding in $BzCr(CO)_3$ will be outlined. The electronic structure of the $Cr(CO)_3$ moiety will be discussed first since the metal-carbonyl interaction is thought to dominate the metal-ring bonding[20]. The important CO orbitals are the symmetry-adapted linear combinations of the 5σ (σ-donor) and 2π (π-acceptor) orbitals which, under C_{3v} symmetry, form $a_1 + e$ and $a_1 + a_2 + 2e$ combinations, respectively. The metal 3d orbitals transform as $a_1(d_{z^2}) + 2e(d_{x^2-y^2}, d_{xy}; d_{xz}, d_{yz})$. If the z-axis is chosen so that it is coincident with the C_3-axis, the lower e combination of the 2π orbitals will interact primarily with the metal $e(d_{x^2-y^2}, d_{xy})$ level, and the second metal $e(d_{xz}, d_{yz})$ level will interact mainly with the 5σ orbitals of the same symmetry. The a_1 2π combination of CO interacts strongly with the metal d_{z^2} orbital while the a_1 5σ combination is only slightly perturbed by the metal center.

The interaction diagram for the construction of the orbitals of $Cr(CO)_3$ is shown in Figure IV.4. The HOMO's are predominantly metal $d_{x^2-y^2}$, d_{xy} and d_{z^2} in character. The small difference in energy between these $a_1 + e$ levels is due to the weak interaction of adjacent carbonyl 2π orbitals. In contrast, the splitting of the 5σ ($a_1 + e$)

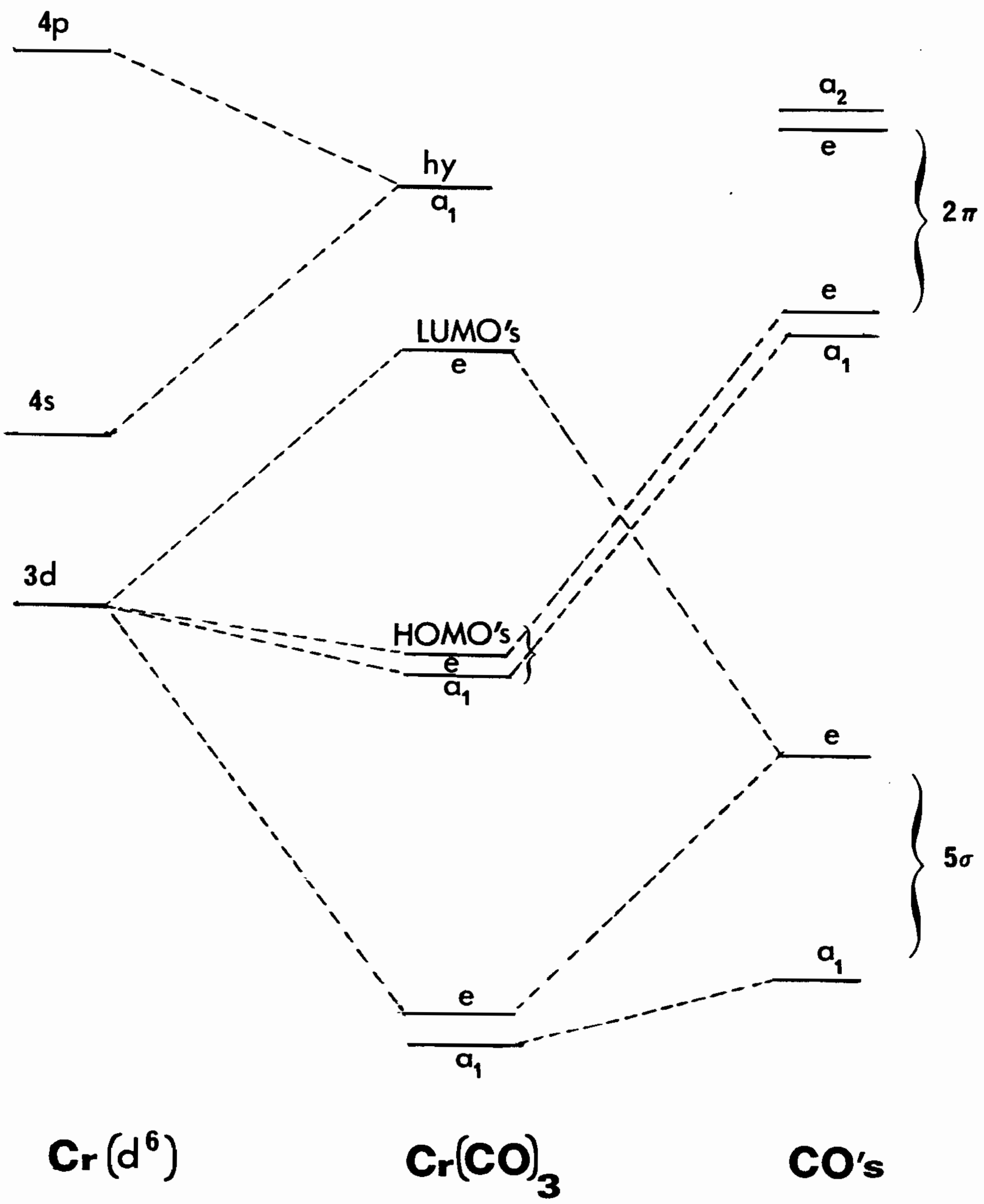

Figure IV.4. Qualitative molecular orbital diagram of the interaction of Cr with three CO groups (HOMO's, LUMO's and hy = highest occupied, lowest unoccupied and sp-hybrid molecular orbitals, respectively).

combinations by the strong σ-σ interactions of the ligands is much greater. The 5σ e combination interacts strongly with the metal whereas the a_1 does not. This gives rise to LUMO's which are mainly metal d_{xz} and d_{yz} in character. The orbital labelled "hy" (in accordance with Hoffmann and coworkers[21]) is the a_1 metal sp hybrid orbital.

A set of three low-lying acceptor orbitals of a_1 + e symmetries are therefore available for interaction with the six-electron π system of the ring. Since the arene-metal interaction is largely of the π-type, only the pπ orbitals of the ring are considered in the bonding[22]. Under the C_{6v} symmetry of the metal ring fragment, the π orbitals of C_6H_6 transform as $a_1 + e_1 + e_2 + b_1$, and the diagram for the interactions between these orbitals and the HOMO's and LUMO's of $Cr(CO)_3$ is shown in Figure IV.5. The most important interactions involve ligand-to-metal donation from the filled a_1 + e orbitals of benzene to the LUMO's of $Cr(CO)_3$, and metal-to-ligand donation from the HOMO's of $Cr(CO)_3$ to the empty $b_1 + e_2$ antibonding orbitals of benzene. One of the obvious consequences of this synergic bonding is the transfer of some π-electron density from the bonding to the antibonding orbitals of benzene. Therefore, even if the total π-electron density of the ring remains the same the aromatic nature of benzene is expected

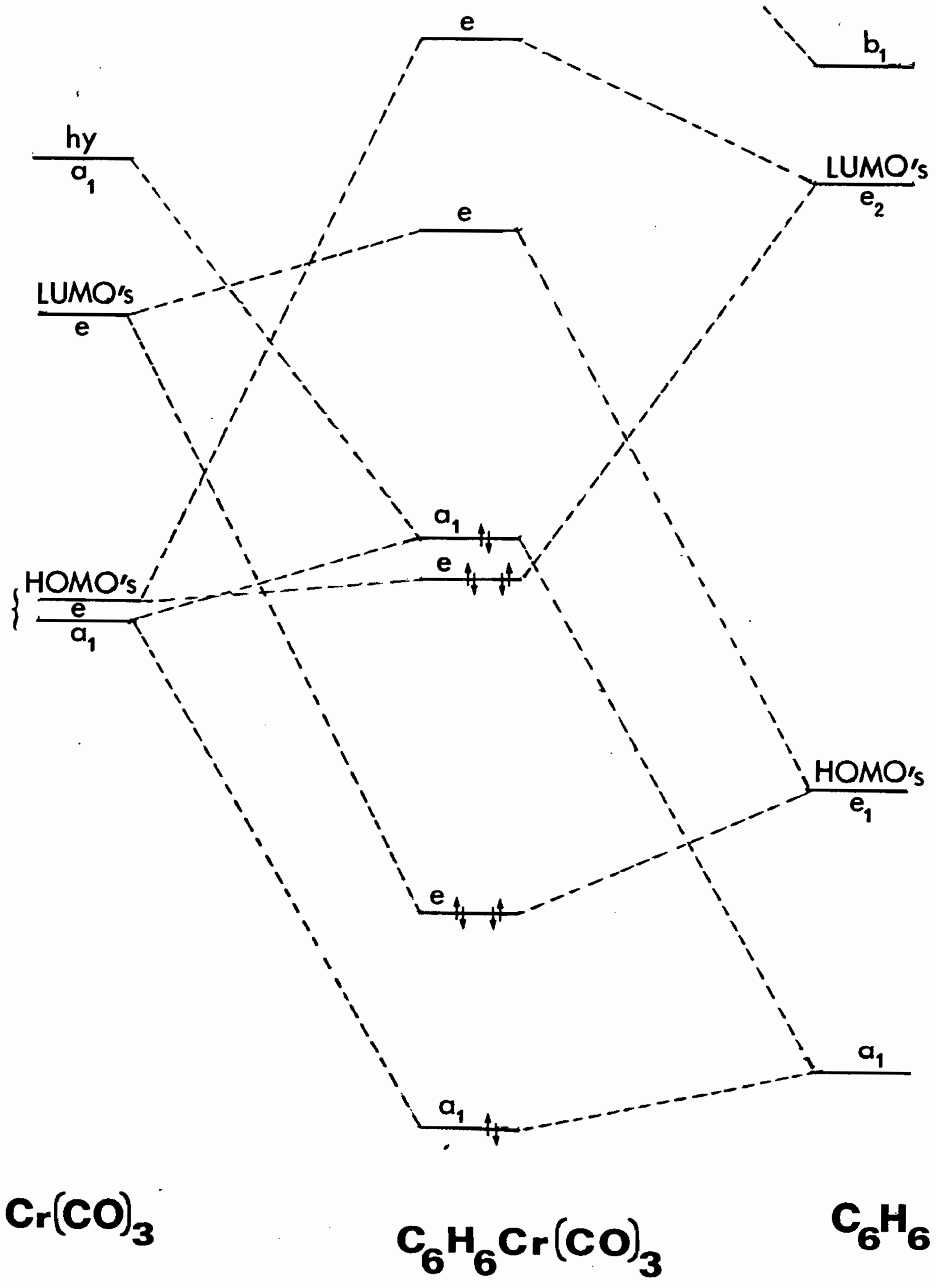

Figure IV.5. Qualitative molecular orbital diagram of the $Cr(CO)_3$ and C_6H_6 interaction (HOMO's and LUMO's = highest occupied and lowest unoccupied molecular orbitals, respectively).

to be somewhat altered on complexation.

15.2. Electronic Structure of the $(\eta^6\text{-}C_6H_6)Cr(CO)_2(CX)$ (X=S,Se) Molecules

Lichtenberger and Fenske have reported the pe spectra of $CpMn(CO)_3$[20] and $CpMn(CO)_2(CS)$[3] and assigned the ionization peaks with the aid of mo calculations. From their results, the complexes appear to have similar structures. The predominantly metal levels ($d_{x^2-y^2}$, d_{xy} and d_{z^2}) remain essentially degenerate in both complexes. A lower binding energy is found for the predominantly ring e_1'' level (e_1 in C_6H_6) in the thiocarbonyl despite the greater positive charge at the metal. However, the calculations reveal that the greater electron density on the carbon atom of CS destabilizes both the orbitals of the ring and those of the metal. Thus, substitution of CS for one CO group in $CpMn(CO)_3$ has a similar effect to that found on the introduction of CS into $M(CO)_6$ to give $M(CO)_5(CS)$.

To determine if similar trends occur for the $BzCr(CO)_2(CX)$ (X=O,S,Se) molecules, an attempt was made to record the pe spectra of the series. Unfortunately, only the first ip's were obtained since the compounds decomposed under typical operating conditions of the spectrometer. On descending the chalcocarbonyl series, the observed binding energies of the electrons in the HOMO's are 7.29, 7.32 and 7.36 eV. Once again, no splitting is observed in these predominantly metal 3d levels on lowering the local symmetry of the carbonyl fragments from C_{3v} to C_s. But, contrary to the trends in both the $CpMn(CO)_2(CX)$ and $Cr(CO)_5(CX)$ molecules, a small increase in binding energy is observed on descending the chalcogen group. Furthermore, a comparison of the binding energies obtained here with those in region A of Table IV.1 reveals a decrease of approximately 1 eV in the first ip's of the arene complexes. This destabilization is a consequence of the increased electron density on the metal in $BzCr(CO)_3$ compared to $Cr(CO)_6$[14,15].

15.3. Potential Constants, Interaction Coordinates and Electronic Structure of the $(\eta^6-C_6H_6)Cr(CO)_2(CX)$ (X=O,S,Se) Molecules

The chief purpose of the vibrational analysis of the $BzCr(CO)_2(CX)$ series was to probe the effects of the benzene ring on the chalcocarbonyl fragments. Hence, a correlation of the differences in the electronic structures of $Cr(CO)_5(CX)$ and $BzCr(CO)_2(CX)$ with differences in their potential constants is appropriate.

The results of the several approximate mo calculations for $BzCr(CO)_3$ mentioned earlier lead to different interpretations of the nature of the bonding in this complex. Thus, for a valid comparison of the electronic structures of $BzCr(CO)_3$ and $Cr(CO)_6$, the calculations have to be carried out using a method which is consistent in its application to both molecules. Fortunately, Brown and Rawlinson[14,23], as well as Carroll and McGlynn[15], have reported comparative studies on both complexes using self-consistent semi-empirical methods. Although the results obtained by the two groups differ in some respects, the same general features emerge. Both calculations reveal a net positive charge on the ring. Also, in $BzCr(CO)_3$,the metal has a smaller positive charge and the CO groups a greater negative charge than in $Cr(CO)_6$. Thus,net donation of charge from the ring to the tricarbonyl fragment is suggested. This is further supported by the x-ray pe investigations; the ls binding energy of the carbonyl carbon is lower in $BzCr(CO)_3$ compared to $Cr(CO)_6$ while the ls binding energies of the benzene carbons increase on complexation[19]. Since a decrease in core binding energy corresponds to an increase in the atomic electron density, the inference again is that a flow of charge from the ring to the CO groups takes place.

In addition to charge donation from the ring, the replacement of three CO groups in $Cr(CO)_6$ should substantially reduce the competition for $d\pi$ electron density among the remaining CO's. This expectation is borne out by the relative populations of the carbonyl π^* orbitals calculated by Brown and Rawlinson[14,23] who obtained values of 0.107 and 0.142 for $Cr(CO)_6$ and $BzCr(CO)_3$, respectively. By comparison, the populations of the 5σ donor orbitals are essentially unchanged, the values obtained being 1.99 for $Cr(CO)_6$ and 1.98 for $BzCr(CO)_3$. Consequently, the large difference in the general quadratic CO force constants of the two complexes [15.41 and 17.04 mdyn A^{-1} for $BzCr(CO)_3$ and $Cr(CO)_6$, respectively] can be ascribed to the relative occupancies of the CO π^* orbitals in these molecules.

MC and CO overlap populations have also been reported for both $Cr(CO)_6$ and $BzCr(CO)_3$. Brown and Rawlinson[14,23] calculated MC overlap populations of 0.4978 and 0.7232 for $BzCr(CO)_3$ and $Cr(CO)_6$, respectively, implying a weaker MC stretching force constant for the benzene complex. The vibrational analyses, however, yielded a value of 2.10 mdyn A^{-1} for the MC force constant in $Cr(CO)_6$ <u>vs</u>. 2.40 mdyn A^{-1} for $BzCr(CO)_3$. Furthermore, although the small difference in the CO overlap populations [1.678, $Cr(CO)_6$ and 1.630, $BzCr(CO)_3$] obtained by these workers is in the right direction, it does not reflect the substantial difference in the CO stretching force constants of the two complexes.

The overlap populations determined by Carroll and McGlynn[15] correlate much better with the force constants. For $Cr(CO)_6$, the MC and CO overlap populations are 0.415 and 1.317, respectively, while the corresponding values for $BzCr(CO)_3$ are 0.537 and 1.216. The contradictory results obtained by Brown and Rawlinson are probably due to their choice of overlap integrals, since the overlap populations are products of both these integrals and the mo populations[23].

Substitution of one CO group in $BzCr(CO)_3$ by either CS or CSe has results similar to those observed for the $Cr(CO)_6 \rightarrow Cr(CO)_5(CX)$ system. However, the effects of CX substitution are more pronounced here because larger differences are found for the remaining CO potential constants [Table III.13(a) and (b)]. For example, the CO stretching force constant varies from 15.41 mdyn A^{-1} in the tricarbonyl to 15.89 mdyn A^{-1} in the selenocarbonyl; the thiocarbonyl has an intermediate value of 15.77 mdyn A^{-1}. The corresponding range in the MC(O) stretching constants is 2.40 to 2.04 mdyn A^{-1}.

The effects of benzene substitution on the MCS and MCSe groupings are even greater than its effects on the

MCO grouping. In the thiocarbonyl complexes, for example, F_{R_X} increases from 2.45 mdyn A^{-1} in $Cr(CO)_5(CS)$ to 3.26 mdyn A^{-1} in $BzCr(CO)_2(CS)$, while F_{D_X} decreases from 7.677 to 6.528 mdyn A^{-1}. The changes obtained for the MCSe force constants are even greater. These results clearly indicate a substantial enhancement of the π-acceptor capacity of CS and CSe on the substitution of benzene for three carbonyl ligands. The larger π-acceptor/σ-donor ratio of CS and CSe in the benzene complexes is another indicator of the greater charge density on the metal in these compounds compared to the pentacarbonyls. Furthermore, the large variation in this ratio, as reflected in the substantial changes in the force constants of the two series, demonstrates the "charge buffering effect" of CS and CSe, as discussed in Section 12.1. The enhanced π-acceptor ability of CS relative to CO in the benzene complexes can be attributed to the stability of the π* orbitals of CS which permits greater overlap between these orbitals and the filled metal dπ orbitals, allowing a greater amount of charge to be transferred to the CS group. The π-acceptor ability of CSe is expected to arise from the same factors because of the similarity of the two ligands.

The introduction of a CS or CSe group into $BzCr(CO)_3$ causes a large decrease in the metal-ring stretching constant (F_T), which varies from 1.19 mdyn A^{-1} in the tricarbonyl to 0.897 mdyn A^{-1} in the selenocarbonyl. This weakening of the metal-ring interaction is probably due to a decrease in the backbonding to e_2 orbitals (antibonding) of benzene (Figure IV.5), as these orbitals are not expected to compete favourably with the low-lying π* orbitals of the CS or CSe ligands for the dπ electrons of the metal.

The $[MC(X)]_{CX}$ and $(CX)_{MC(X)}$ interaction coordinates show the same trends as their $Cr(CO)_5(CX)$ counterparts. However, owing to changes in the primary compliants, the values for $[MC(X)]_{CX}$ are somewhat reduced from their corresponding $Cr(CO)_5(CX)$ values, whereas the $(CX)_{MC(X)}$ values are larger (Table IV.4). The increase in $(CX)_{MC(X)}$ implies a greater reduction in the CX bond length in the $BzCr(CO)_2(CX)$ molecules compared to the $Cr(CO)_5(CX)$ molecules as the adjacent MC(X) bond is stretched (Section 14.4). This is consistent with the greater dπ-pπ* overlap in the benzene series, since a decrease in this overlap, which is responsible for the shortening of the CX bond, should be proportional to its magnitude in the first place.

The factors which contribute to the reduction in the $[MC(X)]_{CX}$ values for the benzene series are less apparent. An obvious suggestion is that the various compensatory

TABLE IV.4: Comparison of the $[MC(X)]_{CX}$ and $(CX)_{MC(X)}$ Interaction Coordinates for the $BzCr(CO)_2(CX)$ and $Cr(CO)_5(CX)$ (X=O,S,Se) Molecules[a,b]

Complex	$[MC(X)]_{CX}$	$(CX)_{MC(X)}$
$Cr(CO)_6$	-0.401	-0.0446
$Cr(CO)_5(CS)$	-0.174	-0.0470
$Cr(CO)_5(CSe)$	-0.131	-0.0501
$BzCr(CO)_3$	-0.354	-0.0470
$BzCr(CO)_2(CS)$	-0.151	-0.0631
$BzCr(CO)_2(CSe)$	-0.110	-0.0663

[a] $Cr(CO)_5(CX)$ data from Table II.16.

[b] The interaction coordinates are dimensionless for stretch-stretch interactions.

effects (Section 14.4) cancel each other to a greater extent in the BzCr$(CO)_2$(CX) molecules. However, rationalization of these effects in mo terms will not be possible until the energy levels in both series are known in more detail.

15.4. ^{13}C and ^{17}O NMR Spectra of the $(\eta^6-C_6H_6)Cr(CO)_2(CX)$ (X=O,S,Se) Molecules

The ^{13}C and ^{17}O chemical shifts of the BzCr$(CO)_2$(CX) molecules are listed in Table IV.5. A comparison of the $\delta(^{13}CX)$ values given here and those of Table IV.3 indicates a significant increase in π-backbonding to CX in the benzene complexes since the ^{13}C chemical shifts of the CX ligands are proportional to the extent of π-backbonding (Section 14.5). As X descends the chalcogen family, the ^{13}C chemical shifts of the remaining CO groups in the BzCr$(CO)_2$(CX) molecules show a progressive upfield shift while the ^{17}O resonances move downfield. The overall larger shifts on chalcogen substitution relative to those of the Cr$(CO)_5$(CX) series are consistent with the greater variation in the CO force constants in the BzCr$(CO)_2$(CX) series.

Another interesting feature of the nmr spectra of the benzene complexes is the large downfield shift (∿6 ppm) of the ring carbons on replacement of a CO group by CS or CSe[24].

TABLE IV.5: CO, CX and ML General Quadratic Force Constants and ^{13}C and ^{17}O Chemical Shifts for the BzCr(CO)$_2$(CX) (X=O,S,Se) Molecules[a,b]

δ and F	BzCr(CO)$_3$	BzCr(CO)$_2$(CS)	BzCr(CO)$_2$(CSe)
$\delta(^{13}CO)$	233.4	231.5	229.0
$\delta(^{13}CX)$	-	346.4	363.7
$\delta(^{13}C_6H_6)$	93.7	99.3	100.9
$\delta(C^{17}O)$	370.7	374.1	375.7
F_{CO}	15.41	15.77	15.89
F_{CX}	-	6.528	4.757
F_{ML}	1.19	1.04	0.897

---

[a] ^{13}C nmr data from Ref. 24 and ^{17}O nmr data from Ref. 9; CO, CX and ML (metal-ring) force constants from Table III.13(b).

[b] Units as given in Table IV.3.

Previous ^{13}C nmr studies on a series of $CpMn(CO)_2L$ complexes[25] reveal that increasing the electron density at the manganese atom causes an upfield shift of the ring carbon resonances. Thus, the shifts listed in Table IV.5 [and those of $CpMn(CO)_2(CX)$ (X=O,S,Se)[24]] indicate a reduction in the electron density at the metal center in the thio- and selenocarbonyls. This, again, concurs with the decrease in the metal-ring force constant on the substitution of CO by CS and CSe, since a decrease in the electron availability at the chromium atom should reduce the π-backbonding to the ring. Replacement of CO by PPh_3, on the other hand, produces an upfield shift (∿4 ppm) of the benzene carbons[26] reflecting the greater σ-donor capacity of the PPh_3 group compared to CO.

15.5. X-Ray Studies

Changes in the bond order of CX and MC bonds should be evidenced by proportional changes in their bond lengths. However, CO bond lengths are found to be relatively insensitive to bond order in the range (2-3) found in metal carbonyls[27] and very few CS and CSe bond lengths have been measured[28,29]. MC distances, on the other hand, are estimated to vary ∿0.3-0.4 A per unit of bond order in the 1-2 range[27]. The average CrC bond distances are 1.916 and

1.845 A in $Cr(CO)_6$[30] and $BzCr(CO)_3$[31], respectively, suggesting that MC bond order is about 1/3 of a unit higher in the arene complex compared to the hexacarbonyl.

No x-ray investigations have been reported for either $BzCr(CO)_2(CS)$ or $BzCr(CO)_2(CSe)$, but data for the structurally similar $(\eta^6\text{-}CH_3CO_2C_6H_5)Cr(CO)_2(CX)$[29] series are available. The CrC(X) distances are 1.842(3), 1.792(2) and 1.786(11) A for X=O,S,Se, respectively. Again, the smaller CrC(S) and CrC(Se) distances reveal the greater strength of the metal-CS and metal-CSe interactions relative to the metal-CO interaction. Furthermore, the greater difference between the CrC(O) and CrC(S) bond lengths compared to that between CrC(S) and CrC(Se) is reflected in the variation of F_{R_X} in the benzene series: 2.40 CrC(O), 3.26 CrC(S) and 3.44 CrC(Se) mdyn A^{-1}.

15.6. Mass Spectra

Mass spectral studies on some chalcocarbonyls provide further experimental data which support the theoretical interpretation of bonding in these complexes. Fragmentation schemes together with details of the fragment ions and their relative intensities have been reported for some $ArCr(CO)_2(CX)$ (Ar = η^6-Arene) complexes[32]. The cracking patterns of these molecules are quite straight-forward; successive loss of two CO groups from the parent ion occurs for all complexes to give $ArCr(CX)^+$, which dissociates as follows:

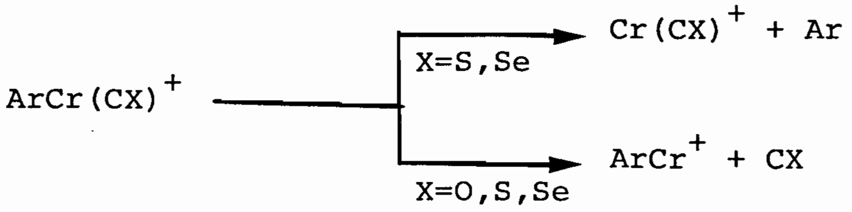

The absence of the $Cr(CO)^+$ fragment may be taken as an indication that the CrC(O) bond is weaker than the ArCr bond, whereas the observation of $Cr(CS)^+$ and $Cr(CSe)^+$ peaks can be ascribed to the weakening of the ArCr interaction on chalcogen substitution. Furthermore, in the benzoate series, $(\eta^6\text{-}CH_3CO_2C_6H_5)Cr(CO)_2(CX)$[32], the relative abundance of the $Cr(CSe)^+$ ion in the spectrum of the selenocarbonyl is greater than the corresponding value for the $Cr(CS)^+$ ion in the thiocarbonyl. One can presume on the basis of these results that the strength of the CrC bond increases in the order CrC(O) < CrC(S) < CrC(Se), and that the ArCr interaction decreases when chalcogen substitution in $ArCr(CO)_2(CX)$ follows the same order. Thus, the vibrational and mass spectral data lead to the same conclusions.

15.7. Substitution Reactions

The only substitution reaction of all three complexes in the $BzCr(CO)_2(CX)$ series reported to date is the displacement of the ring with CO under pressure, as described in Part I of this thesis. The agreement of the relative reactivities with the vibrational data was discussed earlier.

In the absence of any kinetic studies on the benzene series, the one reported for the similar series, $CpMn(CO)(CX)(C_8H_{14})$ (X=O,S)[33], is worth mentioning. Substitution of the cis-cyclooctene by PPh_3 follows an S_N1 (dissociative) mechanism in both $CpMn(CO)(CX)(C_8H_{14})$ complexes, but the rate constant for the thiocarbonyl is four times greater than that for $CpMn(CO)_2(C_8H_{14})$ under the same conditions. By comparison, the replacement of CO by PPh_3 in $W(CO)_5(CS)$ via an S_N1 pathway is 75 times faster than the corresponding reaction in $W(CO)_6$ (Section 14.6). The poor π-acceptor capacity of the ring[20], which reduces the competition among the remaining ligands for the π-electrons of the metal, is probably the factor most responsible for depressing the activating effect of the CS ligand in the manganese complex. Also, the cis-cyclooctene is being lost from a position cis to CS while in $W(CO)_5(CS)$ CO loss occurs from a position trans to CS. Finally, it seems reasonable to predict that the outcome of similar kinetic investigations on the chromium series will parallel that of the manganese complexes since the equally poor π-acceptor ability of benzene should oppose the rate accelerating effect of CX.

15.8. Experimental

The $BzCr(CO)_2(CX)$ (X=O,S,Se) and $Cr(CO)_5(CSe)$ complexes were prepared as described in Part I. The pe spectra were recorded on a Vacuum Generators UVG3 electron spectrometer with He(I) excitation. The samples were introduced into the spectrometer via a variable temperature inlet system and measurements were made at or slightly above room temperature. The measured ip's are considered accurate to ±0.04 eV.

References (Part IV)

1. C.J.H. Schutte, Struct. and Bonding, 9, 213 (1971).
2. D.R. Higginson, D.R. Lloyd, P. Burroughs, D.M. Gibson and A.F. Orchard, J. Chem. Soc., Faraday Trans. II, 69, 1659 (1973) and references therein.
3. D.L. Lichtenberger and R.F. Fenske, Inorg. Chem., 15, 2015 (1976).
4. R. Steudel, Angew. Chem., Int. Ed. Engl., 6, 635 (1976).
5. F.A. Cotton and C.S. Kraihanzel, J. Amer. Chem. Soc., 84, 4432 (1962).
6. M.B. Hall and R.F. Fenske, Inorg. Chem., 11, 1619 (1972).
7. L.H. Jones, "Inorganic Vibrational Spectroscopy", Marcel Dekker, New York, 1971.
8. P.S. Braterman, D.W. Milne, E.W. Randall and E. Rosenberg, J. Chem. Soc., Dalton Trans., 1027 (1973) and references therein.
9. J.P. Hickey, I.M. Baibich, I.S. Butler and L.J. Todd, Spectrosc. Letts., 11, 671 (1978).
10. (a) J.A. Pople, Mol. Phys., 7, 301 (1964); (b) K.A.K. Ebraheem and G.A. Webb, J. Magn. Res., 25, 399 (1977).
11. D.A. Brown, J.P. Chester, N.J. Fitzpatrick and J.J. King, Inorg. Chem., 16, 2497 (1977) and references therein.
12. B.D. Dombek and R.J. Angelici, J. Amer. Chem. Soc., 98, 4110 (1976).
13. I.M. Baibich, I.S. Butler, A.M. English, J.P. Hickey and G. Jaouen, to be published.
14. D.A. Brown and R.M. Rawlinson, J. Chem. Soc. A, 1534 (1968).
15. D.G. Carroll and S.P. McGlynn, Inorg. Chem., 7, 1285 (1968).

16. D.A. Brown, N.J. Fitzpatrick and N.J. Mathews, J. Organometal. Chem., 88, C27 (1975).

17. N.J. Fitzpatrick, J.M. Savariault and J.M.R. Labarre, ibid., 127, 325 (1977).

18. M.F. Guest, I.H. Hillier, B.R. Higginson and D.R. Lloyd, Mol. Phys. 29, 113 (1975).

19. S. Pignataro, A. Foffani and G. Distefano, Chem. Phys. Letts., 20, 350 (1973).

20. D.L. Lichtenberger and R.F. Fenske, J. Amer. Chem. Soc., 98, 50 (1976).

21. M. Elian, M.M.L. Chen, D.M.P. Mingos and R. Hoffman, Inorg. Chem., 15, 1148 (1976).

22. D.A. Brown, "Transition Metal Chemistry" Vol. 3 (R.L. Carlin, Ed.), Arnold, London, 1966.

23. D.A. Brown and R.M. Rawlinson, J. Chem. Soc. A, 1530 (1969).

24. D. Cozak, I.S. Butler and I.M. Baibich, J. Organometal. Chem., 169, 381 (1979).

25. A.G. Ginzburg, L.A. Fedorov, P.V. Petrovskii, E.I. Fedin, V.N. Setkina and D.N. Kursanov, ibid., 73, 77 (1974).

26. L.A. Fedorov, P.V. Petrovskii, E.I. Fedin, N.K. Baranetskaya, V.I. Zdanovich, V.N. Setkina and D.N. Kursanov, Dokl. Akad. Nauk. SSSR Phys. Chem., 209, 266 (1973).

27. F.A. Cotton and R.M. Wing, Inorg. Chem., 4, 314 (1965).

28. (a) G.R. Clark, K.R. Grundy, R.O. Harris, S.M. James and W.R. Roper, J. Organometal. Chem., 90, C37 (1975); (b) S.S. Woodward, R.A. Jacobson and R.J. Angelici, ibid., 117, C75 (1976), and references therein.

29. (a) J.Y. Saillard and D. Grandjean, Acta Cryst., B32, 2285 (1976); (b) J.Y. Saillard, G. Le Borgne and D. Grandjean, J. Organometal. Chem., 94, 409 (1975); (c) J.Y. Saillard and D. Grandjean, Acta Cryst., B34, 3772 (1978).

30. A. Jost, B. Rees and W.B. Yelon, ibid., B31, 2649 (1975).

31. B. Rees and P. Coppens, ibid., B29, 2515 (1973).

32. D. Cozak, Ph.D. Thesis, McGill University, Montreal, Quebec, Canada, 1977.

33. I.S. Butler and A.E. Fenster, Inorg. Chim. Acta, 7, 79 (1973).

SUMMARY AND CONTRIBUTIONS TO KNOWLEDGE

1. A new, facile route to $Cr(CO)_5(CX)$, involving the displacement of the arene ligand from $BzCr(CO)_2(CX)$ (X=S,Se) with CO under pressure, has been developed. The selenocarbonyl complex, $Cr(CO)_5(CSe)$, and its precursor, $BzCr(CO)_2(CSe)$, have been synthesized for the first time.

2. A new, multistep procedure for the photochemically-induced exchange of the three CO groups in $BzCr(CO)_3$ with ^{13}CO to yield $BzCr(^{13}CO)_3$ with 90 atom % ^{13}C-enrichment has been described. Other isotopically-labelled species which have been synthesized for the first time are: $Bz^DCr(CO)_2(CX)$ ($Bz^D=\eta^6-C_6D_6$), $BzCr(^{13}CO)_2(CX)$, $BzCr(CO)_2(^{13}CS)$, $Cr(^{13}CO)_5(CX)$ and $Cr(CO)_5(^{13}CS)$.

3. Detailed investigations of the ir and Raman spectra of all the complexes mentioned in 1 and 2 above have been completed. Prior to this work, only the spectra of $BzCr(CO)_3$, $Bz^DCr(CO)_3$ and $Cr(CO)_5(CS)$ had been assigned.

4. Anharmonicity corrections to the $\nu(CO)$, $\nu(CS)$ and $\nu(CSe)$ fundamentals have been determined from the bands observed

in the binary and ternary overtone and combination spectra of the complexes. On the basis of these results, it appears that it should be possible to transfer CO anharmonicity corrections between molecules of similar structures. The anharmonicity corrections obtained for the ν(CS) and ν(CSe) modes are the first ever to be reported.

5. General quadratic compliance and force constants have been calculated for the $Cr(CO)_5(CX)$, $W(CO)_5(CS)$, $BzCr(CO)_2(CX)$ and $BzCr(CO)_3$ molecules. The proposed vibrational assignments have been verified and the observed and calculated band positions agree to within ±1 cm^{-1}. Furthermore, the transferability of interaction constants between metal carbonyls of similar geometries has been clearly demonstrated in this study.

6. CO and CX energy-factored force constants have been determined for all the complexes and, while the CO values are closely similar to the corresponding general quadratic force constants, the CS and CSe values differ considerably. This is largely due to extensive mixing of the CX and MC(X) modes and implies that CX bond orders are not reflected accurately by the observed frequencies.

7. The He(I) photoelectron spectra of $Cr(CO)_5(CSe)$ and

$BzCr(CO)_2(CX)$ have been measured for the first time and the results indicate that the electronic structure and bonding of the CS and CSe ligands are very similar.

8. The trends in certain of the potential constants [e.g., CX and MC(X)] and interaction coordinates have been correlated with differences in the bonding behaviour of the CO, CS and CSe ligands. For example, the fact that the MC bond strength increases in the order MC(O) < MC(S) < MC(Se) is attributed to the greater interaction of the π and π^* levels of CS and CSe with the metal center compared to those of CO.

9. Finally, the results of the vibrational analyses have been compared with data available from other sources (e.g. mass spectra, chemical reactivities, ^{17}O and ^{13}C nmr spectra, etc.). The overall good agreement leads to a consistent description of the electronic structure and bonding in these complexes.

LIST OF PUBLICATIONS

1. I.S. Butler and A.M. English, "Laser Raman Spectra of Thiophosgene", Spectrochim. Acta, 33A, 545 (1977).

2. A.M. English, K.R. Plowman, I.S. Butler, G. Jaouen, P. LeMaux and J.-Y. Thépot, "A Facile Route to $Cr(CO)_5(CX)$ (X = S,Se) Complexes", J. Organometal. Chem., 132, Cl (1977).

3. E.L. Varetti, A. Müller, A.M. English, K.R. Plowman and I.S. Butler, "Photolysis of Pentacarbonyl(selenocarbonyl)chromium(0), $Cr(CO)_5(CSe)$, in an Argon Matrix at 20K", Z. Anorg. Allg. Chem., 446, 17 (1978).

4. A.M. English, K.R. Plowman, I.S. Butler, E. Diemann and A. Müller, "He(I) Photoelectron Spectra of Pentacarbonyl(selenocarbonyl)chromium(0) and Related Complexes", Inorg. Chim. Acta, 32, 113 (1979).

5. I.S. Butler, A.M. English, and K.R. Plowman, "Dicarbonyl(η^6-benzene)(selenocarbonyl)chromium(0) and Pentacarbonyl(selenocarbonyl)chromium(0)", Inorg. Syn., in press.

6. A.M. English, K.R. Plowman and I.S. Butler, "Synthesis of ^{13}C-Labelled Chromium(0) Chalcocarbonyl Complexes", J. Lab. Comp. Radiopharm, in press.